TEMPER EMBRITTLEMENT IN STEEL

A symposium
presented at a meeting of
Committee A-1 on Steel
AMERICAN SOCIETY FOR
TESTING AND MATERIALS
Philadelphia, Pa., 3–4 Oct., 1967

ASTM SPECIAL TECHNICAL PUBLICATION NO. 407

List price $21.00; 20 per cent discount to members

published by the
AMERICAN SOCIETY FOR TESTING AND MATERIALS
1916 Race Street, Philadelphia, Pa. 19103

Library of Congress Catalog Card Number: 68-19914

NOTE

Printed in Baltimore, Md.
August, 1968

Related ASTM Publications

Advances in the Technology of Stainless Steels and Related Alloys, STP 369 (1965), $21.50

Structures and Properties of Ultrahigh-Strength Steels, STP 370 (1965), $11.00

Effects of Residual Elements on Properties of Austenitic Stainless Steels, STP 418 (1967), $7.25

This page intentionally left blank

Contents

Introduction

Temper embrittlement has been one of the perennial problems of physical metallurgy, accompanying the use of alloy steels for a number of decades. Practical solutions have been found for particular problems involving embrittlement, better methods of measuring temper embrittlement have been developed, and a great deal has been learned about this complex problem, but real understanding of the fundamental mechanisms involved has been elusive.

Current trends in the design of heavy structural components, such as large pressure vessels and turbine-generator rotors, require increased size, more massive sections, higher stresses, and, in some cases, increased operating temperatures. At the same time, advances in understanding of fracture mechanics tend to require concurrent improvement in fracture toughness. Steels with higher hardenability are needed to attain the required through-section fracture toughness at the higher yield strengths needed for such components. However, temper embrittlement is assuming increasing importance as an obstacle inhibiting progress in the design of such heavy components.

The higher-alloy steels required for through-section hardenability and toughness tend to be much more susceptible to temper embrittlement than the lower-alloy pearlitic steels. Larger ingots imply greater segregation of alloying and embrittling elements, and more massive sections must be cooled more slowly through the temperature range of embrittlement. Susceptible steels operated for long times within the temperature range of embrittlement, 350 to 575 C, may embrittle to a surprising degree; the notch toughness transition temperature may increase by hundreds of degrees. The possibility of such embrittlement must be considered in every phase of design, heat treatment, and operation if unexpected deficiencies or losses in fracture toughness are to be avoided. The technical and economic value of effective control of temper embrittlement in high hardenability steel is very great.

The purpose of this symposium is to provide a better understanding of causes, mechanisms, and methods of control of temper embrittlement in steel, both that which is produced during heat treatment and that which is produced by operation within the temperature range of susceptibility.

The 11 papers which are presented and discussed include several on mechanisms, on phenomenology of embrittlement during heat treatment, and during operation in the temperature range of embrittlement, statistical analysis of factors affecting embrittlement, chemical analysis for embrittling residual elements, and others. Information presented in the papers, the extensive discussion of them during the first three sessions, and by the Panel in the last session, indicate the importance of the problem and the interest which it has attracted.

Considerable progress is reported in control of temper embrittlement during heat treatment, but control of long time isothermal embrittlement remains elusive at this time, as does an understanding of the basic mechanisms. However, promising models or hypotheses are discussed which suggest several critical experiments. A need for basic information, such as the solubilities and diffusivities of impurity elements in iron and the effects on these of alloying elements, is evident in the discussion. Both the measurement and control of impurities such as arsenic, antimony, and tin at the levels which may be required to avoid embrittlement are acknowledged to be formidable technical problems.

The updating of knowledge and experience about temper embrittlement, the interest shown, and the interaction among those performing research and those concerned with design and production of heavy sections forged and fabricated components will, it is hoped, provide guidance and support for the further work which is needed to understand and surmount the obstacles presented by temper embrittlement.

D. L. Newhouse
Manager, Forgings Development, General
Electric Co., Schenectady,
N. Y.; symposium chairman.

J. M. Capus[1]

The Mechanism of Temper Brittleness

REFERENCE: Capus, J. M., "**The Mechanism of Temper Brittleness,**" *Temper Embrittlement in Steel, ASTM STP 407,* American Society for Testing and Materials, 1968, pp. 3–19.

ABSTRACT: Recent experimental work with steels of carefully controlled purity has allowed the phenomenon of temper brittleness to be defined more closely. It is now seen as a reversible embrittlement to which alloy steels of commercial purity are subject if exposed for prolonged periods in the temperature range 400 to 600 C. It does not occur in alloy steels synthesized from high-purity elements; neither does it occur in carbon steels even of commercial purity. A detailed consideration of the equilibrium segregation theory of grain-boundary embrittlement, as well as some associated mechanisms advanced in recent years, has shown them all to be inadequate as explanations of the peculiar conditions under which temper-brittleness can arise.

A modified theory of "double segregation" is proposed to explain the influence of major alloying elements on the incidence of embrittlement by impurity elements. In this theory, grain-boundary enrichment with alloying elements such as manganese, chromium, and molybdenum during austenitizing can lead to enhanced segregation of the embrittlement elements such as phosphorus, arsenic, antimony, or tin by chemical interaction. Only the latter elements cause the shifts in transition temperature and the changeover from cleavage to intergranular brittle fracture which are characteristic of temper brittleness. They do this by lowering the intergranular fracture energy γ_I. On the basis of the theory the specific nature of the temper-brittleness phenomenon, as well as the relative influences of individual major alloying elements, can be explained.

KEY WORDS: temper embrittlement, alloy steels, embrittlement, impurities, elements, equilibrium segregation, segregation (metallographic), austenite, grain boundary, intergranular fracture, brittle fracture, evaluation

The phenomenon of temper brittleness is remarkable in two respects: firstly, it is a metallurgical phenomenon confined as far as is known to tempered alloy steels [*1–5*][2]; secondly, despite having been known for more than 50 years, it has so far defied all attempts at a complete and satisfactory explanation.

[1] Head, Metallurgy Group, Gillette Research Laboratory, Reading, England.

[2] The italic numbers in brackets refer to the list of references appended to this paper.

As is well known, the brittleness is shown up most strongly when the steels are in the martensitic condition, after conventional tempering at or above 600 C. If the steels are rapidly cooled, for example, by water quenching, from this tempering treatment then no damage ensues. If on the other hand, a susceptible steel is slowly cooled from above 600 C, or re-heated for a prolonged period in the temperature range 400 to 600 C, then embrittlement will result. The latter may be manifested in three ways:

(*a*) The ductile/brittle fracture energy and fracture appearance transitions are raised to higher temperatures.

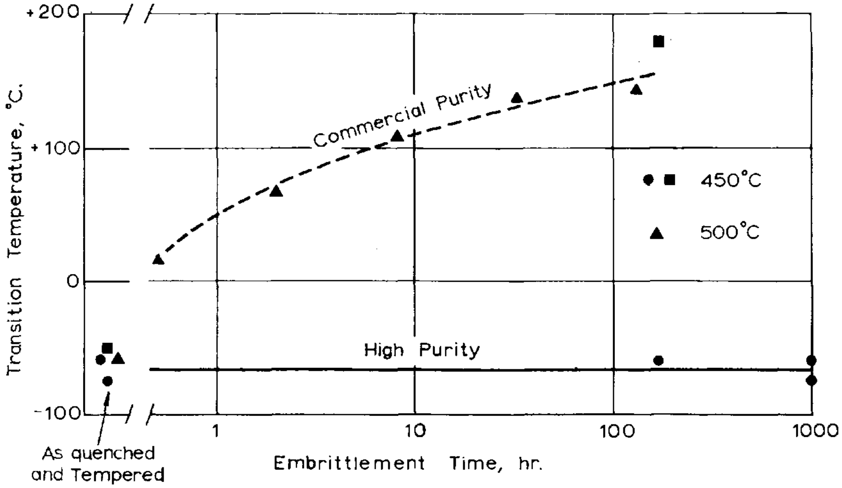

FIG. 1—*Influence of steel purity on embrittlement: effect of reheating on impact transition temperatures of commerical and high-purity nickel-chromium steels* (*Refs* 1 *and* 8).

(*b*) Brittle fractures tend to follow the path of the boundaries of prior austenite grains.

(*c*) A grain boundary etching effect may be shown in which the outline of the former austenite grain boundaries are selectively attacked after the embrittling heat treatment. Embrittlement is closely concerned with the austenite grain boundaries since higher transition temperatures are obtained with increased intergranular fracture.

The embrittlement is at least partly reversible by reheating the steel at a tempering temperature above 600 C.

In the laboratory, embrittlement is most easily demonstrated by impact testing to determine the transition curve, but, if conducted at sufficiently low temperatures, static tension tests show reduced fracture stress and reduction of area[3] [*1*,*6*].

---

[3] If the steel is severely embrittled, some effect may be shown in room-temperature tension tests [*6*].

Hollomon [*4*] and Woodfine [*1*] have reviewed the work on this subject up to 1953, and the present paper will generally be concerned only with subsequent investigations.

A turning point in the understanding of temper brittleness was the demonstration by Steven, Balajiva, and colleagues [*7,8*] that it was a phenomenon peculiar to commercial steels, that is it was only possible if certain impurity elements were present. They made steels by synthesis from high-purity elements in combinations corresponding with well-known alloy steel types that would normally be susceptible to embrittlement. They tested the high-purity steels for embrittlement by slow cooling after tempering as well as by prolonged reheating at the temperature of maximum sensitivity. Transition temperatures remained unchanged, and brittle fractures were transgranular (Fig. 1). They concluded that embrittlement in commercial alloy steels was due to the

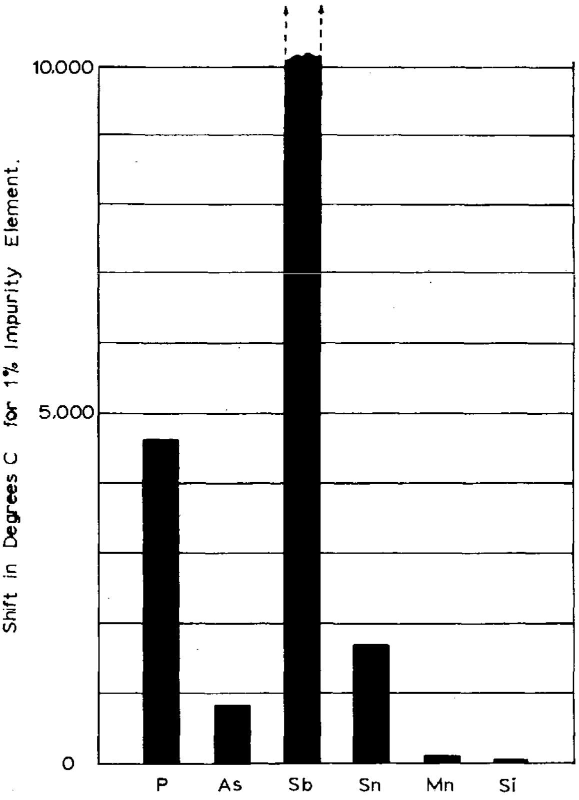

FIG. 2—*Relative intensity of embrittlement by impurity elements in nickel-chromium steels: shift of impact transition temperature* (*deg C*) *per 1 per cent of element, produced by reheating for 1000 h at 450 C* (*Ref* 8).

presence of deleterious trace elements, and proceeded to study the effects of all the likely elements, adding each in turn to vacuum melts of high-purity steels. They adopted an extremely critical test to determine the influence of added elements, firstly, by ensuring that all the alloys were in the martensitic condition, and, secondly, by measuring transition temperatures and examining fracture appearance both before and after reheating the steels for up to 1000 h at 450 C. It was found that the presence of any one of a group of metalloid elements that occur in steels of commercial manufacture could induce temper brittleness. The most strongly embrittling elements were antimony, phosphorus, tin, and arsenic (Fig. 2). These needed to be present in trace quantities only. The deoxidizing elements, silicon and manganese, were also found to have a slight embrittling effect.

This work settled much previous speculation about the elements in alloy steels that were really responsible for embrittlement. In the light of this work it is also possible to see at least a qualitative explanation of the often conflicting results of previous investigations in which commercial purity steels were compared. Thus, without control of the embrittling impurity elements it is really impossible to do satisfactory comparative tests.

The preferential etching effect at austenite grain boundaries has also recently been shown to have a specific chemical explanation. Examination of high-purity-base nickel-chromium steels embrittled by phosphorus and tin, respectively, showed that the grain-boundary etching effect could be obtained if phosphorus was present in the steel but not if tin was the embrittling element [*9*].

Current Theories

A frequently expressed view is that temper brittleness is just another example of an intergranular embrittlement suffered by an alloy as the result of equilibrium solute segregation [*10*]. If this be the case, then we must conclude from the work just cited that the segregating solute atoms are those of the impurity elements in the steels. There is possibly general agreement thus far among current theories; the four theories of intergranular brittleness outlined below differ from one another regarding the effects arising from the segregation.

In the first theory the increase in solute concentration at the grain boundary is considered to have a drastic effect on the interfacial surface energy; consequently, when the steel is being fractured, a smaller net increase in interfacial energy is involved if the fracture follows the grain boundaries instead of running along cleavage planes. Intergranular fracture and increased brittleness are thereby associated with segregation. In support of this, there is direct experimental evidence that at least one of the deleterious impurity elements, namely, phosphorus, can segregate at grain boundaries in pure iron [*11*].

The second mechanism is one that was originally advanced in connection with the segregation of sulfur at grain boundaries in pure iron [*12*]. This is that substitutional impurity atoms diffusing towards a grain boundary would be accompanied by an opposing flow of vacancies away from the boundary. The vacancy flow results in the multiplication of nearby dislocations by the process of "down-climb," thereby embrittling the grain boundaries through localized hardening [*13*]. Brammar and Honeycombe have implied that this could also be a mechanism for temper embrittlement [*14*].

A third suggestion has been made specifically in connection with the grain boundary embrittlement of intermetallic compounds such as silver-magnesium [*15,16*] but appears equally applicable to the embrittlement of steels. In this theory it is proposed that the solute atoms segregated at grain boundaries cause local embrittlement simply by solid solution hardening, and this has in fact been observed directly in intermetallic compounds by microhardness measurements.

Finally the most recent suggestion by Hill and Martin [*17*] is that in temper-brittle steels the segregation of impurity elements to grain boundaries leads to the growth there of enlarged lath-like carbide precipitates. These promote intergranular fracture and brittleness by further enrichment of the segregate around each particle, reducing the surface energy of the fracture facets.

Although each of these ideas has some plausibility, they are all inadequate in so far as they fail to explain one crucial point. This is that temper brittleness is a phenomenon of *alloy* steels, and that the same impurity elements do not result in similar grain boundary embrittlement in plain carbon steels. There are other difficulties in accepting any of the theories that have just been discussed, such as why the austenite grain boundaries should be involved in an effect occurring in the ferritic state, and why the tempered martensite structure gives the greatest sensitivity to embrittlement; but these points are of minor importance compared with the question about alloying elements.

Furthermore, when we examine these proposed mechanisms in detail we find that they are not really supported by much experimental evidence. Thus there have been no reported measurements of grain boundary energy for steels, although Hondros [*18*] has shown that phosphorus reduces the surface energy of pure iron.

No thin-foil transmission electron microscopy has been published on temper-embrittled steels, so that we have no direct evidence about the possible formation of dislocation tangles at grain boundaries. There is some indirect evidence (although negative) from microhardness meas-

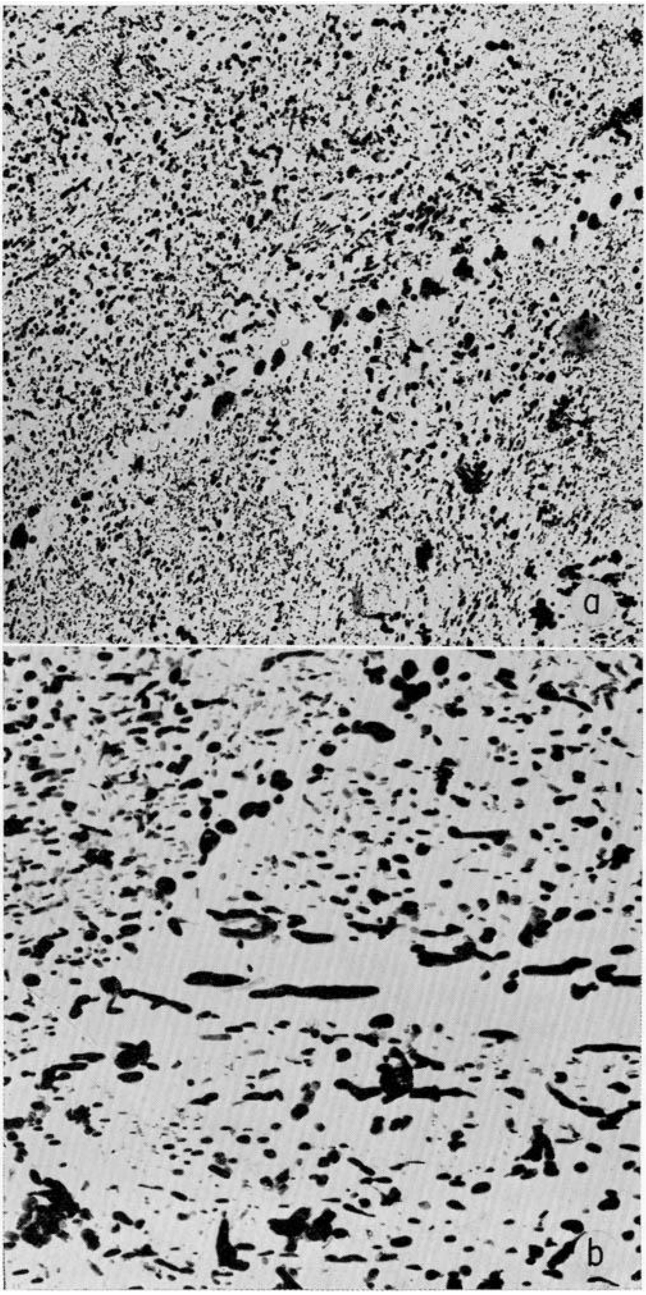

(*a*) Spheroidal particles (×6,000).
(*b*) Lath-like particles (×15,000).

FIG. 3—*Electron micrographs of extraction replicas from a susceptible nickel-chromium steel containing 0.023 per cent phosphorus (Ref 9). Illustrating enlarged carbides in the prior austenite grain boundaries.*

urements made in connection with the third mechanism—solid solution hardening at grain boundaries. In an attempt to test Westbrook's mechanism in a temper-brittle steel, microhardness measurements were made by the present author across a number of prior austenite grain boundaries in steels of Ref *9*. No change in hardness could be detected near the grain boundaries. It must be concluded that if there is grain boundary hardening, either by formation of dislocation tangles or solid solution strengthening, then it is not very significant.

The most attractive mechanism, in that pictorial evidence was produced for it, is that of Hill and Martin. Their claim that intergranular precipitates of thin cementite laths were associated with brittleness is analogous to observations of intergranular films of sulfides in steels embrittled by overheating and in cast alloy steels [*13,14*]. However, again the importance of comparing temper-brittle steels with steels of controlled purity should be emphasized. In tempered martensitic steels of the type under discussion, larger carbide particles will be seen in the grain boundaries in any case on account of the enhanced diffusion there.

In order to look further into this last question, an examination was made of the carbide distribution in a nonsusceptible nickel-chromium steel, as well as similar steels containing embrittling additions of phosphorus and tin. Figure 3 shows electron micrographs of extraction replicas taken from the phosphorus-containing steel used in Ref *9*. It emerged that enlarged spheroidal as well as lath-like carbide particles could be found in the prior austenite grain boundaries of pure and impure steels alike, both before and after embrittling treatments. It is concluded that the observations of Hill and Martin cannot be used to support a theory of embrittlement associated with the growth of grain-boundary carbide films.

Before proposing an alternative theory, it seems worthwhile to go back to the basic idea of equilibrium segregation and see how well it fits the case of temper embrittlement.

Equilibrium Segregation of Impurity Elements

The possibility, favored by Hollomon [*4*], of grain boundary precipitation as opposed to solute segregation was long ago dismissed by some work of McLean [*20*] and subsequently by many other investigators. He examined by electron microscopy the changes at austenite grain boundaries in nickel-chromium steel after prolonged embrittling treatments. The grain boundary etching obtained with an ether solution of picric acid was shown to be a grooving effect, and it did not change with time of embrittlement up to 2400 h at 500 C, whereas carbides in the structure coarsened considerably. If there had been a fine grain-boundary precipitate during the early stages of embrittlement, then one would have expected this also to coarsen.

If the embrittlement process is to be described in terms of equilibrium solute segregation, then the driving force will presumably be supplied by the misfit strain of the impurity atoms in the lattice of the solvent. The embrittling temperature range is determined by the lowest temperature for adequate solute diffusion, on the one hand, and the temperature above which solute atoms are "boiled off" the grain boundaries, on the other.

The questions to be examined are:

1. Whether the embrittling elements found by Steven and Balajiva differ significantly in atomic radii from iron.
2. Whether the diffusion rates of the impurity elements would permit equilibrium segregation at the observed temperatures.
3. Whether the minute concentrations of these elements found to be deleterious could lead to significant degrees of segregation at the austenite grain boundaries.

TABLE 1—*Comparison of activation energies for diffusion of impurity elements in iron and that for temper embrittlement of steel.*

Impurity Element	Activation Energy for Diffusion in α-Fe, kcal/mole	"Activation Energy" Derived from Embrittlement Data, kcal/mole
Phosphorus	~55 Ref *21* 52.3 Ref *22* 56 (Fe-Cr alloy) Ref *22*	42 to 50 Ref *24*
Tin	~46 (γ-Fe) Ref *23*	
Self diffusion of α-Fe	~60	

Atomic Radii

Goldschmidt atomic radii (for a coordination number of 12) of the major embrittling elements have been given as:

Phosphorus:	[1.09][4]
Arsenic:	[1.25][4]
Antinony:	1.61
Tin:	1.58

compared with the value of 1.28 kX for iron. These values indicate considerable misfit strain for phosphorus, antimony, and tin.

Diffusion Rates

Diffusion rate data for impurity elements such as phosphorus in alloy steels are apparently nonexistent, and even in iron are extremely scanty.

---

[4] One half of smallest interatomic distance (Smithells, C. J., *Metals Reference Book*, 3rd edition, Butterworths, London, 1967).

The diffusion constant required is for lattice diffusion of the impurity element in α-Fe. The experimentally determined activation energies for diffusion of phosphorus in pure iron [*21*] and Fe-1.3Cr alloy [*22*] are shown in Table 1. The only other embrittling element for which there is a value is tin, but the approximate figure of 46 kcal/mole is for diffusion in austenite [*23*].

TABLE 2—*Thickness of grain-boundary layers of segregated impurity elements in nickel-chromium steels for an assumed 10 per cent segregation.*

Impurity Element and Type of Steel	Impurity Concentration, %	Austenite Grain Dia, mm	Thickness x of Grain Boundary Layer for 10% Segregate^a Atomic Layers	Observed Maximum Embrittlement 1000 h at 450 C
Phosphorus:				
High-purity steel Ref *9*...	0.042	0.013	1	106^b
		1.25	40	138^b
Tin:				
High-purity steel Ref *9*...	0.035	0.014	1	58^b
		0.50	20	120^b
Phosphorus:				
High-purity steel Ref *8*...	0.009	0.013 to 0.014	~¼	45
	0.072	0.013 to 0.014	~2	110
Antimony:				
High-purity steel Ref *8*...	0.00046	0.013 to 0.014	1/50	210
Tin:				
High-purity steel Ref *8*...	0.032	0.013 to 0.014	~1	110
	0.052	0.013 to 0.014	~2	110
Arsenic:				
High-purity steel Ref *8*...	0.082	0.013 to 0.014	3 to 4	100
Commercial purity steel:				
(Steel K of Ref *1*) P as major impurity.........	0.066	estimated: 0.014	~2	204^c

[a] Calculated from thickness $x = (N_x V_x)/A)$ (where N_x = number of X atoms segregating per cm^3; V_x = atomic volume of X, assuming that impurity atoms occupy the same space in the lattice as iron atoms; A = grain boundary area per cm.^{3}

[b] 168 h at 450 C.

[c] 128 h at 500 C.

There is apparently only one set of experiments in the literature on the time-temperature relationship for embrittlement from which an "activation energy" can be derived. This is the investigation of a commercial purity 1¼ per cent nickel-chromium steel by Jaffe and Buffum [*24*]. They found reasonably consistent activation energy values between 42 and 50 kcal/mole. From Table 1 it is seen that there is fair agreement with the activation energy for diffusion of phosphorus and possibly tin. If the other embrittling elements present in a commercial steel diffused more slowly than these, then we could expect the presence of either of these elements to determine the temperature range and rate at which the steel was embrittled.

Available Concentration of Impurity Elements

We can further assess the effectiveness of the small concentrations of impurity elements available in steels for embrittlement by segregation: this we can do by seeing how thick a layer of impurity atoms could be produced on the austenite grain boundaries of some well-documented steels by an arbitrarily chosen 10 per cent degree of segregation. (That is, assuming 10 per cent of the impurity element in a steel moves to the austenite grain boundaries.) From Table 2 we see that even with fine-grained steels (which have the highest grain-boundary surface/volume ratios) there is generally sufficient impurity element to produce a complete saturation of the grain boundaries. With coarse-grained specimens there is much more solute available than needed to saturate the grain boundaries.

There is one further comparison that may be made between equilibrium segregation theory and the experimental data. This is to calculate segregation times for specific elements.

McLean [*25*] has considered the problem of the approach to equilibrium of grain-boundary segregation, deriving expressions for the particular case of isothermal treatment of an alloy at a temperature T_2, after quenching to T_2 from a higher temperature T_1. As expected, the grain-boundary concentration of the segregating solute builds up relatively rapidly at first, but the ultimate approach to equilibrium is a very much slower process. The time $t_{1/2}$ to reach a grain-boundary concentration equal to one half of the ultimate equilibrium value was found to be given by:

$$t_{1/2} = \frac{9a^2d^2}{64D} \quad \ldots\ldots\ldots\ldots\ldots\ldots\ldots (1)$$

where:

a = ratio of equilibrium grain-boundary concentration at T_2 to the concentration of solute in the interior of the grains (assumed constant),
d = thickness of the grain-boundary, and
D = (lattice) diffusion coefficient of the solute at T_2.

For the solutes with which we are concerned in temper brittleness, it seems reasonable to assume that Eq 1 is also applicable to the case where the specimen is quenched to a third (lower) temperature T_3 before reheating at T_2. For temper embrittlement, T_3, is usually room temperature.

The theory also assumes that the grain-boundary thickness $\ll$ the grain diameter and that the initial grain-boundary concentration $\ll$ the equilibrium grain-boundary concentration.

To obtain suitable values of *a*, an appropriate equilibrium grain-boundary concentration has to be chosen. Recent work with the field ion microscope [*26*] has confirmed the belief that high-angle grain boundaries are, at most, a few atom planes wide. If a grain boundary is considered as a layer three atoms thick, then a monatomic layer of segregated solute element would represent a limiting grain-boundary concentration of about 30 at per cent.

Again, the *D* values chosen should be for lattice diffusion, or at least bulk diffusion values from a temperature range where grain-boundary diffusion is minimized. As indicated in Table 1, we only have data for phosphorus and tin. Evaluating Eq 1 for the phosphorus and tin containing steels of Ref *9* gave values ranging from 100 to 1800 h (Table 3), apparently of the right order of magnitude for $t_{1/2}$ for isothermal embrittlement at 450 C.

TABLE 3—*Equilibrium segregation data for phosphorus and tin at 450 C.*

Element and Reference for Diffusion Data	Diffusion Coefficient D, cm^2/s^a	$t_{1/2}$ (time for half equilibrium segregation), h	Embrittlement Behavior in Ni-Cr Steel (Ref *8*)
Phosphorus:			
Ref *21* (in pure Fe)...	2.9 exp (−55,000/RT)	~1800	70% of shift in ITT for 1000 h occurs in first 168 h
Ref *22* (in pure Fe)...	1.6 exp (−52,300/RT)	500	
Ref *22* (in Fe-1.3Cr alloy).............	7.6 exp (−56,000/RT)	~1400	
Tin:			
Ref *23* (in γ-Fe)......	0.16 exp (−46,000/RT)	~100^b	50% of shift in ITT for 1000 h occurs in first 168 h

^{a} R = gas constant, T = temperature in degrees kelvin.

^{b} This figure is very much reduced (to about ½ h) if an attempt is made to correct the D_{Sn} value to that for ferrite using the factor: (D α-Fe)/(D γ-Fe), that is, the ratio of self diffusion of iron in α and γ forms.

However, while equilibrium solute segregation would appear to give a suitable account of the rate and temperature range of the embrittlement process, and, even if we had all the necessary diffusion data about the various impurity elements, it would still leave a number of difficult questions unanswered. Thus, equilibrium segregation is a general theory applicable to any alloy system. Why, therefore, are there so many unique features in the temper-brittleness case? Why does it occur only in alloy steels? Why do impurity elements choose to concentrate at the prior austenite grain boundaries when they must diffuse past ferrite grain boundaries to get there? Having segregated there, what is it that makes them modify the transition temperature and change the mode of brittle fracture etc.?

The difficulty of providing a theory for temper brittleness is the complex of experimental facts which must be explained. This tends to suggest that the mechanism is not likely to be a simple one like equilibrium segregation, either alone or in conjunction with grain-boundary dislocation tangles, carbide films, etc.

Proposed Modification of the Segregation Theory

It is now suggested that the major driving force for the segregation of impurity elements, like phosphorus, to prior austenite grain boundaries (which undoubtedly takes place in the ferritic state) is chemical interaction with major alloying elements which have previously concentrated at grain boundaries during austenitizing or in the earlier history of the steel.

A "double segregation" theory of this kind is supported by many experimental results unconnected with temper brittleness. Philibert et al [*27,28*] have confirmed by means of electron-probe microanalysis that even pure binary alloys of iron are subject to segregation during solidification—segregation which is enhanced by the presence of carbon (in ternary Fe-X-C alloys).

It is well known that such segregation persists in alloy steels as "banding" even after much processing and heat treatment.

How this affects temper brittleness is proposed as follows.

During austenitizing, accelerated diffusion along austenite grain boundaries would carry alloying element atoms from the enriched regions of the segregation to all parts of the grain-boundary network, even in regions impoverished in alloying elements. These elements do not diffuse away from the grain boundaries because they diffuse too slowly through the lattice. This is evident in the persistence of banding. Thus an overall enrichment of alloying elements can be formed at the austenite grain boundaries. (Some segregation of impurity atoms in the austenite phase is not excluded, but they can disperse very much faster because of their diffusion rates.)

The tendency of the common alloying elements to segregate in low-alloy steels has been found to lie in the following order:

Mo > Cr > Mn > Ni

$\frac{C_M}{C_m}$[5]: 1.8/2.2 $\sim$1.5 1.3 1.1 . . . . [Ref *29*]

This is also the order of decreasing tendency to form stable carbides and has therefore some chemical significance. Alloying elements therefore

---

[5] C_M, C_m are maximum and minimum concentrations, respectively.

appear to segregate in order of increasing affinity for carbon. This is probably also their order of increasing chemical affinity for the metalloid elements phosphorus, arsenic, antimony, and tin even when all are in solution in iron. Thus, it is proposed that presegregated chromium atoms, for example, would attract diffusing phosphorus atoms, and if the chromium segregation were at the prior austenite boundaries in a tempered steel then a significantly enhanced segregation of phosphorus would take place also at a suitable temperature.

Thus at a single stroke we have overcome two major objections to the equilibrium segregation theory: the importance of major alloying elements and the bypassing of ferrite grain boundaries by the segregating impurity atoms. Despite the presence of impurities we would not expect quenched-and-tempered plain carbon steels to be subject to temper brittleness. Reversibility of embrittlement can easily be understood on the present scheme in terms of the different diffusion rates for impurity elements and major alloying elements. Thus reheating the steel above the embrittling range allows the segregated impurity elements to be dispersed whereas the alloying elements remain at the grain boundaries.

TABLE 4—*Relative susceptibilities of steels with different combinations of alloying elements.*

Reference and Embrittlement Treatment	Impurity Element	Shift in Transition Temperature with Various Steel Types for 0.001% of Impurity Element, deg C			
		3% Ni	3% Cr	3% Ni-Cr	3% Ni-Cr-Mo
Woodfine [1]—commercial-purity steels reheated 24 h at 500 C	P, presumed major impurity	0.7[a]	5.4[a,d]	5.1[a]	...
Steven and Balajiva [8] —high-purity-base steels reheated, 1000 h at 450 C	P	...	...	4[c]	2.2[c]
	As	...	...	0.8[b]	0.1[c]
	Sb	...	...	210[a]	15[a]
	Sn	...	...	1.7[c]	0.5[c]

[a] Single steels.
[b] Average of two steels.
[c] Average of three or more steels.
[d] Reheated 24 h at 525 C.

In the past, many investigators have studied the influence of major alloying elements on the sensitivity of steels to temper brittleness. Unfortunately almost all the work prior to that of Balajiva [8], and even much subsequent work, gives a most confusing picture since the importance of using impurity-free raw materials has not generally been appreciated. Hence there is little published data from which a critical comparison of the influence of alloying elements can be made to test some of the predictions of the present theory.

Woodfine has recalled that plain nickel steels were not normally considered to be susceptible and confirmed this by experiment. On the other hand, steels containing any two of the elements, chromium, manganese, nickel, were highly susceptible [*1*]. Adding molybdenum to highly susceptible nickel-chromium steels has been known for a long time to reduce the tendency to embrittlement without actually eliminating it. The values given in Table 4 are taken from the papers of Woodfine [*1*] and Steven and Balajiva [*8*], in an attempt to compare the relative susceptibilities of steels with differing combinations of alloying elements. Plain nickel steel is seen to be very slightly susceptible compared with plain chromium and nickel-chromium steels. Molybdenum is seen to reduce drastically the effects of each embrittling element in nickel-chromium-molybdenum steels.

There is some further unpublished data on high-purity-base steels that is relevant here.[6] This showed that a nonsusceptible high-purity plain nickel steel could be made slightly embrittling by an addition of 0.02 per cent phosphorus, a concentration that would make 3 per cent nickel-chromium steel highly susceptible (Table 4). Furthermore an addition of 0.6 per cent manganese to the high-purity nickel steel did not produce embrittlement, but the combination of the same amount of manganese with 0.02 per cent phosphorus considerably magnified the embrittling effect of the latter element.

Such effects, as well as the data of Table 4, can be understood quite well in terms of the present theory. Thus, nickel itself is known to segregate only very slightly in steels [*27,29*], whereas manganese and chromium segregate significantly and the latter element quite markedly. The degree to which impurity elements such as phosphorus can cause embrittlement is thus controlled by the combination of major alloying elements present in the steel.

The influence of molybdenum would seem to be the major anomally in the present theory. Molybdenum decreases the rate of embrittlement considerably, whereas, as a strongly segregating element and strong carbide-former, the present theory would have predicted an enhancement of embrittlement. However, two further complicating factors may have an over-riding influence in this case.

Firstly, molybdenum appears to retard the diffusion of impurity elements (for example, 0.47 per cent molybdenum raises the activation energy for diffusion of phosphorus in iron to about 62 kcal/mole compared with 52 kcal/mole in pure iron [*22*]). Secondly, it has a more marked effect than nickel, manganese, or chromium on the tempering characteristics of martensite [*30*]. Thus, with molybdenum present in the steel even at the 0.5 per cent level, less recovery would occur during tempering at about 650 C *before* embrittling treatment at a lower temperature, and the matrix would still be largely martensitic with a high dislocation density. It is conceivable that a larger density of dislocations

---

[6] Capus, J. M., unpublished work.

in molybdenum-containing steels would provide alternative sites for the trapping of segregating impurity atoms, resulting in a further slowing down of the embrittlement process. This suggestion fits in well with some observations of Keh and Porr [*31*] on the influence of cold-working on the intensity of embrittlement: straining of 1 per cent chromium-manganese steel specimen by 35 per cent after tempering at 650 C suppressed embrittlement that would have resulted from subsequent heat treatment.

Little has been said so far about the mechanism of fracture and why segregation of one sort (major alloying elements) does not affect the ductile/brittle transition, whereas segregation of certain impurity elements has a very drastic effect both on the temperature of the transition as well as the mode of brittle failure.

Since no direct measurements have been made in relevant steels we can only repeat what has already been proposed elsewhere that the segregation of certain elements to the austenite grain boundaries affects the fracture transition by reducing the integranular fracture surface energy γ_I in the Griffiths equation:

$$\sigma_P = \left[\frac{2E\,\gamma_I}{\pi C}\right]^{1/2} \dots\dots\dots\dots\dots\dots\dots (2)$$

lowering the applied stress σ_p to propagate intergranular brittle fracture. The intergranular fracture surface energy term γ_I is given by: $\gamma_I = 2\gamma_s - \gamma_b$, where γ_b is the grain-boundary energy and γ_s is the surface energy.

As mentioned in a previous section, there is now direct evidence that phosphorus at least can considerably reduce γ_s and hence γ_I in iron [*18*].

Conclusions

A review of recent experimental work on temper brittleness has highlighted two important features: the embrittlement is essentially a phenomenon of alloy steels and is brought about by the presence of certain specific impurity elements. Thus it does *not* occur in alloy steels containing nickel, chromium, and molybdenum if made from high-purity ingredients.

A detailed consideration of the theory of equilibrium solute segregation, as well as some mechanisms that have been put forward in association with it, has shown that they all fail to explain why the embrittlement is peculiar to alloy steels.

A modified theory of double segregation has been proposed to explain the influence of major alloying elements. In this theory, grain-boundary enrichment with alloying elements such as manganese, chromium, and molybdenum during austenitizing can lead to enhanced segregation of the embrittling elements phosphorus, tin, antimony, or arsenic by chemical interaction. Supporting evidence has been found for the segregation of alloying elements that also helps to explain why steels containing chromium, manganese, or molybdenum are more prone to embrittlement than plain nickel steels. The theory also explains why the prior austenite grain boundaries are embrittled rather than the ferrite grain boundaries. The intergranular mode of brittle failure is seen as a consequence of decreased surface energy accompanying segregation, as in earlier models.

Acknowledgment

This paper is published by permission of the Director, Gillette Research Laboratory, Reading, England. Some of the ideas expressed and the supporting results were obtained when the author was with International Nickel Ltd., Birmingham, England.

References

[*1*] Woodfine, B. C., "Temper-Brittleness: A Critical Review of the Literature," *Journal of the Iron and Steel Institute*, Vol. 173, 1953, pp. 229–240; "Some Aspects of Temper-Brittleness," *Journal of the Iron and Steel Institute*, Vol. 173, 1953, pp. 240–255.

[*2*] Preece, A. and Carter, R. D., "Temper-Brittleness in High-Purity Iron-Base Alloys," *Journal of the Iron and Steel Institute*, Vol. 173, 1953, pp. 387–398.

[*3*] Greaves, R. H. and Jones, J. A., "Temper-Brittleness of Steel: Susceptibility to Temper-Brittleness in Relation to Chemical Composition," *Journal of the Iron and Steel Institute*, Vol. 111, 1925, pp. 231–255.

[*4*] Hollomon, J. H., "Temper-Brittleness," *Transactions*, American Society for Metals, Vol. 36, 1946, pp. 473–540.

[*5*] Entwisle, A. R. and Smith, G. C., (in discussion), *Transactions*, American Society for Metals, Vol. 43, 1951, pp. 751–753.

[*6*] Austin, E. W., Entwisle, A. R., and Smith, G. C., "Effect of Arsenic and Antimony on Temper-Brittleness," *Journal of the Iron and Steel Institute*, Vol. 173, 1953, pp. 376–386.

[*7*] Balajiva, K., Cook, R. M., and Worn, D. K., "Effects of Trace Elements on Embrittlement of Steels," *Nature*, Vol. 178, 1956, p. 433.

[*8*] Steven, W. and Balajiva, K., "The Influence of Minor Elements on the Isothermal Embrittlement of Steels," *Journal of the Iron and Steel Institute*, Vol. 193, 1959, pp. 141–147.

[*9*] Capus, J. M., "Austenite Grain Size and Temper-Brittleness," *Journal of the Iron and Steel Institute*, Vol. 200, 1962, pp. 922–927.

[*10*] McLean, D. and Northcott, L., "Micro-Examination and Electrode Potential Measurements of Temper-Brittle Steels," *Journal of the Iron and Steel Institute*, Vol. 158, 1948, pp. 169–177.

[*11*] Inman, M. C. and Tipler, H. R., "Grain-Boundary Segregation of Phosphorus in an Iron-Phosphorus Alloy and the Effect Upon Mechanical Properties," *Acta Metallurgica*, Vol. 6, 1958, pp. 73–84.

[*12*] Ainslie, N. G., Phillips, V. A., and Turnbull, D., "Sulfur Segregation at Alpha-Iron Grain-Boundaries.—II," *Acta Metallurgica*, Vol. 8, 1960, pp. 528–538.

[*13*] Brammar, I. S., "A New Examination of the Phenomena of Overheating and Burning of Steels," *Journal of the Iron and Steel Institute*, Vol. 201, 1963, pp. 752–761.

[*14*] Brammar, I. S. and Honeycombe, R. W. K., "Formation of Sulphides at Grain-Boundaries in Some Pure Iron Alloys," *Journal of the Iron and Steel Institute*, Vol. 202, 1964, pp. 335–342.

[*15*] Westbrook, J. H. and Wood, D. L., "Embrittlement of Grain Boundaries by Equilibrium Segregation," *Nature,* Vol. 192, 1961, pp. 1280–1281.

[*16*] Westbrook, J. H. and Wood, D. L., "A Source of Grain-Boundary Embrittlement in Intermetallics," *Journal of the Institute of Metals,* Vol. 91, 1963, pp. 174–182.

[*17*] Hill, R. G. C. and Martin, J. W., "A Fractographic Study of Some Temper-Brittle Steels," *Metal Treatment,* Vol. 29, 1962, pp. 301–306, 310.

[*18*] Hondros, E. D., "The Influence of Phosphorus in Dilute Solid Solution on the Absolute Surface and Grain Boundary Energies of Iron," *Proceedings of the Royal Society,* Vol. 286, 1965, Series A, pp. 479–498.

[*19*] Brammar, I. S. and Honeycombe, R. W. K., "Intergranular Brittleness of Cast Chromium-Nickel Steels," *Journal of the Iron and Steel Institute,* Vol. 200, 1962, pp. 1060–1067.

[*20*] McLean, D., (in discussion of Refs *1, 2,* and *6*), *Journal of the Iron and Steel Institute,* Vol. 174, 1953, pp. 360–361.

[*21*] Seibel, G., "Diffusion of Phosphorus in Iron," *Comptes Rendus,* Vol. 256, 27 May 1963, pp. 4661–4664.

[*22*] Gruzin, P. L. and Mural, V. V., "Effect of Alloying on the Diffusion of Phosphorus in Ferrite," *Fizika Metallov Metallovedenie,* Vol. 17, No. 3, 1964, pp. 384–389.

[*23*] Bannister, C. O. and Jones, W. D. J., "The Diffusion of Tin into Iron with Special Reference to the Formation of Columnar Crystals," *Journal of the Iron and Steel Institute,* Vol. 124, 1931, pp. 71–93.

[*24*] Jaffe, L. D. and Buffum, D. C., "Isothermal Temper Embrittlement" *Transactions,* American Society for Metals, Vol. 42, 1950, pp. 604–614.

[*25*] McLean, D., *Grain Boundaries in Metals,* Clarendon, Oxford, 1957.

[*26*] Cottrell, A. H., "Metallography at the Atomic Level," *Journal of the Institute of Metals,* Vol. 90, 1961–1962, pp. 449–456.

[*27*] Philibert, J., "The Castaing 'Microsonde' in Metallurgical and Mineralogical Research," *Journal of the Institute of Metals,* Vol. 90, 1961–1962, pp, 241–252.

[*28*] Philibert, J. and de Beaulieu, C., "Quantitative Investigation of Dendritic Segregation in Some Iron Alloys," *Revue Metallurgie,* Vol. 56, 1959, pp. 171–178.

[*29*] Clayton, D. B., Smith, T. B., and Brown, J. R., "The Application of Electron-Probe Microanalysis to the Study of Microsegregation in a Low-Alloy Steel," *Journal of the Institute of Metals,* Vol. 90, 1961–1962, pp. 224–228.

[*30*] Irvine, K. J., Pickering, F. B., and Garstonė, J. E., "Effect of Composition on the Structure and Properties of Martensite," *Journal of the Iron and Steel Institute,* Vol. 196, 1960, pp. 66–81.

[*31*] Keh, A. S. and Porr, W. C., "Effect of Cold Work on Temper-Brittleness," *Transactions,* American Society for Metals, Vol. 52, 1960, pp. 81–93.

L. F. Porter,[1] *G. C. Carter,*[1] *and S. J. Manganello*[1]

A Study of Temper Embrittlement During Stress Relieving of 5Ni-Cr-Mo-V Steels

---

REFERENCE: Porter, L. F., Carter, G. C., and Manganello, S. J., "**A Study of Temper Embrittlement During Stress Relieving of 5Ni-Cr-Mo-V Steels,**" *Temper Embrittlement in Steel, ASTM STP 407,* American Society for Testing and Materials, 1968, pp. 20–45.

ABSTRACT: Extensive studies of the effect of alloying elements and residual elements on the susceptibility of Ni-Cr-Mo-V steels to temper embrittlement have led to the selection and evaluation of a preferred composition for a weldable quenched and tempered plate steel that is resistant to temper embrittlement during stress relieving. The embrittling effects of carbon, manganese, nickel, chromium, and molybdenum were determined in a statistically selected series of 27 composition modifications of a 5Ni-Cr-Mo-V steel. In addition, the effects of vanadium contents up to 0.19 per cent were investigated. The results of these studies showed that manganese and molybdenum were alloying elements primarily responsible for temper embrittlement in the steel. The effect of the residual elements phosphorus, aluminum, nitrogen, and oxygen on the susceptibility of 5Ni-Cr-Mo-V steel to temper embrittlement was determined. This study showed that although oxygen was detrimental to the notch toughness of the steels, only phosphorus contributed to temper embrittlement.

On the basis of the preceding studies, a quenched and tempered plate steel with minimum susceptibility to temper embrittlement was selected; this composition exhibited good weldability and sufficient hardenability for 4-in.-thick plates. An 80-ton heat of this composition was produced, and the susceptibility of this steel to embrittlement during stress-relieving treatments was compared with that of a standard-composition 5Ni-Cr-Mo-V steel. The two steels were compared with and without 1 per cent prestrain. The modified-composition 5Ni-Cr-Mo-V steel exhibited about half the embrittlement of the standard composition. Embrittlement increased as the stress-relieving time increased and as the cooling rate from the stress-relieving temperature decreased. Prestraining produced no significant changes in the response of the steels to embrittlement.

KEY WORDS: alloy steels, temper embrittlement, stress relieving, submarine hull steels, weldability, heat treatment, notch toughness, transition temperature, mechanical properties, cold working, compositions, quenching (cooling), tempering, pressure vessels, trace elements, straining (metallurgical), evaluation

---

[1] Section supervisor, research engineer, and associate research consultant, respectively, applied Research Laboratory, United States Steel Corp., Monroeville, Pa. Dr. Porter is a personal member ASTM.

TABLE 1—*Chemical compositions of steels investigated—per cent (check analyses).*

Steel Code	Heat No.	C	Mn	P	S	Si	Ni	Cr	Mo	V	Al[a]	N[b]
A	T5505-1	0.12	0.52	0.004	0.005	0.26	5.01	0.52	0.50	0.069	0.028	0.005
B	T5506-1	0.10	0.75	0.004	0.004	0.23	4.95	0.49	0.27	0.070	0.028	0.005
C[c]	T5507-1	0.10	0.51	0.005	0.004	0.24	5.50	0.51	0.74	0.070	0.027	0.005
D	T5508-1	0.12	0.26	0.003	0.004	0.24	5.45	0.48	0.50	0.065	0.026	0.005
E	T5509-1	0.11	0.75	0.003	0.004	0.24	4.95	0.28	0.49	0.066	0.023	0.005
F	T5510-1	0.12	0.52	0.004	0.004	0.25	4.52	0.50	0.26	0.070	0.021	0.006
G	T5511-1	0.13	0.50	0.003	0.004	0.25	5.45	0.27	0.49	0.066	0.025	0.006
H	T5512-1	0.11	0.25	0.003	0.004	0.25	4.55	0.50	0.50	0.065	0.022	0.005
I	T5513-1	0.12	0.49	0.003	0.004	0.24	4.95	0.51	0.50	0.066	0.022	0.006
J[c]	T5514-1	0.13	0.26	0.003	0.004	0.23	4.95	0.74	0.51	0.071	0.030	0.006
K	T5515-1	0.12	0.25	0.003	0.004	0.24	5.05	0.26	0.49	0.067	0.025	0.006
L	T5516-1	0.12	0.75	0.003	0.004	0.24	5.00	0.50	0.75	0.074	0.027	0.006
M	T5517-1	0.12	0.51	0.004	0.004	0.25	5.00	0.27	0.76	0.068	0.020	0.006
N	T5518-1	0.12	0.50	0.003	0.004	0.24	4.52	0.25	0.51	0.066	0.024	0.006
O	T5519-1	0.11	0.75	0.003	0.006	0.24	4.48	0.51	0.51	0.070	0.030	0.005
P	T5520-1	0.11	0.51	0.003	0.004	0.25	4.97	0.27	0.26	0.066	0.028	0.006
Q	T5521-1	0.11	0.25	0.004	0.005	0.24	5.04	0.49	0.74	0.069	0.025	0.005
R	T5522-1	0.12	0.51	0.003	0.004	0.25	5.05	0.51	0.50	0.067	0.029	0.005
S[c]	T5523-1	0.11	0.75	0.007	0.006	0.25	5.01	0.74	0.51	0.068	0.028	0.007
T	T5524-1	0.10	0.50	0.003	0.005	0.25	4.50	0.74	0.50	0.070	0.026	0.006
U	T5525-1	0.10	0.74	0.004	0.005	0.26	5.50	0.51	0.50	0.070	0.029	0.006
V	T5526-1	0.096	0.50	0.003	0.004	0.25	4.52	0.50	0.75	0.068	0.026	0.007
W	T5527-1	0.10	0.51	0.004	0.005	0.27	4.95	0.74	0.76	0.070	0.029	0.006
X	T5528-1	0.096	0.52	0.003	0.004	0.25	5.05	0.72	0.26	0.067	0.028	0.006
Y	T5529-1	0.096	0.50	0.004	0.005	0.25	4.94	0.50	0.26	0.068	0.029	0.006
Z[c]	T5530-1	0.10	0.26	0.003	0.004	0.24	5.03	0.50	0.25	0.066	0.029	0.007
AA	T5531-1	0.088	0.49	0.004	0.005	0.25	5.32	0.71	0.50	0.064	0.028	0.006
BA	T5532-1	0.096	0.50	0.003	0.004	0.24	4.90	0.49	0.48	0.035	0.026	0.006
CA	T5533-1	0.10	0.50	0.004	0.005	0.25	4.97	0.28	0.26	0.036	0.026	0.005
DA[c]	T5534-1	0.096	0.50	0.003	0.004	0.24	5.03	0.74	0.75	0.038	0.026	0.006

[a] Acid soluble.

[b] Kjeldahl determination.

[c] Analysis of residual (tramp) elements made (see Table 2).

Weldable quenched and tempered alloy plate steels exhibiting excellent notch toughness and weldability at yield strengths of 130 to 150 ksi have been developed for ultraservice applications such as hydrospace vehicle hulls and solid-propellant missile motor cases. To provide dimensional stability to plates that have been cold worked and to relieve high stresses resulting from welding, these steels are occasionally subjected to stress-relieving treatments. Because the steels are generally tempered in the range 1050 to 1150 F, stress-relieving treatments are conducted at slightly lower temperatures, usually in or near the range where temper embrittlement occurs (900 to 1050 F). In addition, the steels are normally slow cooled from the stress-relieving temperature; thus, further embrittlement can occur during cooling through the temper-embrittling range.

The aforementioned considerations have resulted in extensive evaluations of the effects of alloying elements, residual elements, prestraining (cold working), and variations in stress-relieving heat treatments on the susceptibility of the steels to temper embrittlement. This paper describes the results of these studies on 5Ni-Cr-Mo-V steels designed to exhibit a minimum yield strength of 130 ksi in sections through 4 in. in thickness.

TABLE 2—*Results of special chemical analyses for residual (tramp) elements—per cent.*

Steel	B	As	Sn	Pb	Sb[a]
C	<0.0001	<0.01	<0.01	<0.005	0.0006
J	<0.0001	<0.01	<0.01	<0.005	0.0007
S	<0.0001	<0.01	<0.01	<0.005	0.0009
Z	<0.0001	<0.01	<0.01	<0.005	0.0009
DA	<0.0001	<0.01	<0.01	<0.005	0.0012

[a] Higher precision was requested for the antimony analysis.

Statistically Designed Experiment

In this study, a statistical experiment was designed as a three-level incomplete factorial, which permitted estimation of the coefficients in a second-degree polynomial response surface equation [*1*].[2] A selected series of 27 composition modifications of the 5Ni-Cr-Mo-V steel (Table 1) was evaluated to determine the effect of manganese (0.25 to 0.75 per cent), nickel (4.5 to 5.5 per cent), chromium (0.25 to 0.75 per cent), and molybdenum (0.25 to 0.75 per cent) on the susceptibility of ½-in. and of simulated 4½-in.-thick plates (water quenched and tempered at 1100 F) to embrittlement after holding for 125 h at temperatures of 1000 F followed by slow cooling (in Sil-O-Cel). The effect of reducing vanadium

---

[2] The italic numbers in brackets refer to the list of references appended to this paper.

from 0.07 to 0.035 was investigated in three additional heats (Table 1). Although carbon was to be constant at 0.11 per cent in all heats, the actual range of carbon values was wide enough to necessitate including carbon as a variable in the analysis.

TABLE 3—*Full equations for predicting the effect of prolonged stress relief on the mechanical properties of quenched and tempered 5Ni-Cr-Mo-V steel.*

½-IN.-THICK PLATES (AS-QUENCHED AND TEMPERED)

Yield strength (0.2% offset), ksi

$$
\begin{aligned}
&= 114.56 + 81.737\,(\%\,\mathrm{C}) + 3.3103\,(\%\,\mathrm{Ni}) + 15.309\,(\%\,\mathrm{Cr}) + 5.9186\,(\%\,\mathrm{Mo}) \\
&\quad - 0.70118\,(\%\,\mathrm{Ni})^2 + 8.8690\,(\%\,\mathrm{Ni})\,(\%\,\mathrm{Mo}) - 41.635\,(\%\,\mathrm{Cr})\,(\%\,\mathrm{Mo})
\end{aligned}
$$

Charpy V-notch energy absorption at 0 F, ft·lb

$$
\begin{aligned}
&= -131.10 - 38.923\,(\%\,\mathrm{Mn}) + 106.34\,(\%\,\mathrm{Ni}) - 33.769\,(\%\,\mathrm{Cr}) - 38.970\,(\%\,\mathrm{Mo}) \\
&\quad -10.806\,(\%\,\mathrm{Ni})^2 + 29.988\,(\%\,\mathrm{Cr})^2
\end{aligned}
$$

Fracture-appearance (50% shear) transition temperature, F

$$
\begin{aligned}
&= -306.32 + 521.54\,(\%\,\mathrm{Mn}) - 31.265\,(\%\,\mathrm{Ni}) - 169.23\,(\%\,\mathrm{Cr}) - 525.82\,(\%\,\mathrm{Mo}) \\
&\quad - 128.00\,(E) + 155.93\,(\%\,\mathrm{Mn})^2 - 103.62\,(\%\,\mathrm{Mn})\,(\%\,\mathrm{Ni}) \\
&\quad + 123.76\,(\%\,\mathrm{Ni})\,(\%\,\mathrm{Mo}) + 144.84\,(\%\,\mathrm{Cr})^2 + 209.86\,(\%\,\mathrm{Cr})\,(\%\,\mathrm{Mo}) \\
&\quad - 35.79\,(E)\,(\%\,\mathrm{Mn}) + 21.792\,(E)\,(\%\,\mathrm{Ni}) - 117.28\,(E)\,(\%\,\mathrm{Cr}) \\
&\quad + 93.112\,(E)\,(\%\,\mathrm{Mo}) + 152.83\,(E)\,(\%\,\mathrm{Mn})^2 + 161.48\,(E)\,(\%\,\mathrm{Cr})^2 \\
&\qquad \text{where } E = -1
\end{aligned}
$$

½-IN.-THICK PLATES (AFTER PROLONGED STRESS RELIEF)[a]

Yield strength (0.2% offset), ksi

$$
\begin{aligned}
&= 48.752 + 112.69\,(\%\,\mathrm{C}) + 132.34\,(\%\,\mathrm{Mn}) + 10.667\,(\%\,\mathrm{Ni}) + 7.8141\,(\%\,\mathrm{Cr}) \\
&\quad + 73.343\,(\%\,\mathrm{Mo}) - 20.416\,(\%\,\mathrm{Mn})\,(\%\,\mathrm{Ni}) - 33.849\,(\%\,\mathrm{Mn})\,(\%\,\mathrm{Cr}) \\
&\quad - 41.509\,(\%\,\mathrm{Mn})\,(\%\,\mathrm{Mo}) - 33.425\,(\%\,\mathrm{Mo})^2
\end{aligned}
$$

Charpy V-notch energy absorption at 0 F, ft·lb

$$
\begin{aligned}
&= 858.95 + 296.19\,(\%\,\mathrm{C}) - 148.17\,(\%\,\mathrm{Mn}) - 283.17\,(\%\,\mathrm{Ni}) - 17.476\,(\%\,\mathrm{Cr}) \\
&\quad - 107.66\,(\%\,\mathrm{Mo}) + 96.575\,(\%\,\mathrm{Mn})^2 - 108.12\,(\%\,\mathrm{Mn})\,(\%\,\mathrm{Mo}) \\
&\quad + 28.116\,(\%\,\mathrm{Ni})^2 + 105.10\,(\%\,\mathrm{Cr})^2 - 208.00\,(\%\,\mathrm{Cr})\,(\%\,\mathrm{Mo}) + 155.97\,(\%\,\mathrm{Mo})^2
\end{aligned}
$$

Fracture-appearance (50% shear) transition temperature, F

$$
\begin{aligned}
&= -306.32 + 521.54\,(\%\,\mathrm{Mn}) - 31.265\,(\%\,\mathrm{Ni}) - 169.23\,(\%\,\mathrm{Cr}) - 525.82\,(\%\,\mathrm{Mo}) \\
&\quad - 128.00\,(E) + 155.93\,(\%\,\mathrm{Mn})^2 - 103.62\,(\%\,\mathrm{Mn})\,(\%\,\mathrm{Ni}) \\
&\quad + 123.76\,(\%\,\mathrm{Ni})\,(\%\,\mathrm{Mo}) + 144.84\,(\%\,\mathrm{Cr})^2 + 209.86\,(\%\,\mathrm{Cr})\,(\%\,\mathrm{Mo}) \\
&\quad - 35.79\,(E)\,(\%\,\mathrm{Mn}) + 21.792\,(E)\,(\%\,\mathrm{Ni}) - 117.28\,(E)\,(\%\,\mathrm{Cr}) \\
&\quad + 93.112\,(E)\,(\%\,\mathrm{Mo}) + 152.83\,(E)\,(\%\,\mathrm{Mn})^2 + 161.48\,(E)\,(\%\,\mathrm{Cr})^2 \\
&\qquad \text{where } E = +1
\end{aligned}
$$

---

[a] 125 h at 1000 F followed by slow-cooling (in Sil-O-Cel).

Because the study was designed to determine the effect of the major alloying elements on temper embrittlement, it was important to be sure that the residual (tramp) elements that promote temper embrittlement were maintained at constant levels. To this end, a special lot of steel scrap was used in producing the heats. Table 2 lists the results of special chemical analyses for certain residual elements that reportedly could promote temper embrittlement [*2*,*3*]. These analyses were conducted on only five steels (Steels C, J, S, Z, and DA), but the steels were selected so that the source (alloying addition) of any residual elements detected could be determined. The results indicate that the five steels contained about the same amounts of boron, arsenic, tin, and lead. The five steels also contained 0.0006 to 0.0012 per cent of antimony. An attempt to correlate variations in the residual elements with variations in alloy additions led to the conclusion that the residuals did not contribute significantly to the variations in the degree of embrittlement observed.

For each steel studied, ½-in.-thick cross-rolled plates (rolling ratio 1.2 to 1) were produced from 5 by 12 by 17-in. ingots that were cast

TABLE 4—*Full equations for predicting the effect of prolonged stress relief on the mechanical properties of quenched and tempered 5Ni-Cr-Mo-V steel.*

4½-IN.-THICK PLATES (AS-QUENCHED AND TEMPERED)

Yield strength (0.2% offset), ksi

$$\begin{aligned} &= -388.41 + 2231.0\,(\%\,\mathrm{C}) + 246.85\,(\%\,\mathrm{Mn}) + 56.047\,(\%\,\mathrm{Ni}) + 292.72\,(\%\,\mathrm{Cr}) \\ &\quad + 177.42\,(\%\,\mathrm{Mo}) - 9128.2\,(\%\,\mathrm{C})^2 - 38.352\,(\%\,\mathrm{Mn})\,(\%\,\mathrm{Ni}) \\ &\quad - 64.080\,(\%\,\mathrm{Mn})\,(\%\,\mathrm{Cr}) - 40.387\,(\%\,\mathrm{Ni})\,(\%\,\mathrm{Cr}) - 86.256\,(\%\,\mathrm{Cr})\,(\%\,\mathrm{Mo}) \\ &\quad - 81.905\,(\%\,\mathrm{Mo})^2 \end{aligned}$$

Charpy V-notch energy absorption at 0 F, ft·lb

$$\begin{aligned} &= -277.45 - 194.64\,(\%\,\mathrm{C}) - 115.95\,(\%\,\mathrm{Mn}) + 170.76\,(\%\,\mathrm{Ni}) - 17.516\,(\%\,\mathrm{Cr}) \\ &\quad + 55.381\,(\%\,\mathrm{Mo}) + 75.635\,(\%\,\mathrm{Mn})^2 - 16.119\,(\%\,\mathrm{Ni})^2 - 17.227\,(\%\,\mathrm{Ni})\,(\%\,\mathrm{Mo}) \end{aligned}$$

Fracture-appearance (50% shear) transition temperature, F

$$\begin{aligned} &= 1503.3 - 1540.7\,(\%\,\mathrm{Mn}) - 267.37\,(\%\,\mathrm{Ni}) - 336.36\,(\%\,\mathrm{Cr}) - 871.58\,(\%\,\mathrm{Mo}) \\ &\quad + 669.72\,(E) + 253.35\,(\%\,\mathrm{Mn})\,(\%\,\mathrm{Ni}) + 261.30\,(\%\,\mathrm{Mn})\,(\%\,\mathrm{Cr}) \\ &\quad + 268.65\,(\%\,\mathrm{Mn})\,(\%\,\mathrm{Mo}) + 106.19\,(\%\,\mathrm{Ni})\,(\%\,\mathrm{Mo}) + 294.45\,(\%\,\mathrm{Cr})\,(\%\,\mathrm{Mo}) \\ &\quad + 58.664\,(\%\,\mathrm{Mo})^2 - 702.78\,(E)\,(\%\,\mathrm{Mn}) - 127.00\,(E)\,(\%\,\mathrm{Ni}) \\ &\quad - 146.65\,(E)\,(\%\,\mathrm{Cr}) - 802.19\,(E)\,(\%\,\mathrm{Mo}) + 125.95\,(E)\,(\%\,\mathrm{Mn})\,(\%\,\mathrm{Ni}) \\ &\quad + 313.54\,(E)\,(\%\,\mathrm{Mn})\,(\%\,\mathrm{Mo}) + 162.74\,(E)\,(\%\,\mathrm{Ni})\,(\%\,\mathrm{Mo}) \\ &\quad + 319.83\,(E)\,(\%\,\mathrm{Cr})\,(\%\,\mathrm{Mo}) - 241.20\,(E)\,(\%\,\mathrm{Mo})^2 \end{aligned}$$

where $E = -1$

4½-IN.-THICK PLATES (AFTER PROLONGED STRESS RELIEF)[a]

Yield strength (0.2% offset), ksi

$$\begin{aligned} &= -328.22 + 229.64\,(\%\,\mathrm{Mn}) + 72.723\,(\%\,\mathrm{Ni}) + 267.52\,(\%\,\mathrm{Cr}) + 436.67\,(\%\,\mathrm{Mo}) \\ &\quad - 36.399\,(\%\,\mathrm{Mn})\,(\%\,\mathrm{Ni}) - 69.012\,(\%\,\mathrm{Mn})\,(\%\,\mathrm{Cr}) - 34.998\,(\%\,\mathrm{Ni})\,(\%\,\mathrm{Cr}) \\ &\quad - 49.208\,(\%\,\mathrm{Ni})\,(\%\,\mathrm{Mo}) - 96.949\,(\%\,\mathrm{Cr})\,(\%\,\mathrm{Mo}) - 94.373\,(\%\,\mathrm{Mo})^2 \end{aligned}$$

Charpy V-notch energy absorption at 0 F, ft·lb

$$\begin{aligned} &= -98.223 - 87.001\,(\%\,\mathrm{Mn}) + 51.414\,(\%\,\mathrm{Ni}) + 391.80\,(\%\,\mathrm{Mo}) - 93.391\,(\%\,\mathrm{Ni}) \\ &\quad (\%\,\mathrm{Mo}) \end{aligned}$$

Fracture-appearance (50% shear) transition temperature, F

$$\begin{aligned} &= 1503.3 - 1540.7\,(\%\,\mathrm{Mn}) - 267.37\,(\%\,\mathrm{Ni}) - 336.36\,(\%\,\mathrm{Cr}) - 871.58\,(\%\,\mathrm{Mo}) \\ &\quad + 669.72\,(E) + 253.35\,(\%\,\mathrm{Mn})\,(\%\,\mathrm{Ni}) + 261.30\,(\%\,\mathrm{Mn})\,(\%\,\mathrm{Cr}) \\ &\quad + 268.65\,(\%\,\mathrm{Mn})\,(\%\,\mathrm{Mo}) + 106.19\,(\%\,\mathrm{Ni})\,(\%\,\mathrm{Mo}) + 294.45\,(\%\,\mathrm{Cr})\,(\%\,\mathrm{Mo}) \\ &\quad + 58.664\,(\%\,\mathrm{Mo})^2 - 702.78\,(E)\,(\%\,\mathrm{Mn}) - 127.00\,(E)\,(\%\,\mathrm{Ni}) \\ &\quad - 146.65\,(E)\,(\%\,\mathrm{Cr}) - 802.19\,(E)\,(\%\,\mathrm{Mo}) + 125.95\,(E)\,(\%\,\mathrm{Mn})\,(\%\,\mathrm{Ni}) \\ &\quad + 313.54\,(E)\,(\%\,\mathrm{Mn})\,(\%\,\mathrm{Mo}) + 162.74\,(E)\,(\%\,\mathrm{Ni})\,(\%\,\mathrm{Mo}) \\ &\quad + 319.83\,(E)\,(\%\,\mathrm{Cr})\,(\%\,\mathrm{Mo}) - 241.20\,(E)\,(\%\,\mathrm{Mo})^2 \end{aligned}$$

where $E = +1$

---

[a] 125 h at 1000 F followed by slow-cooling (in Sil-O-Cel).

from 300-lb vacuum-induction-melted heats. Plate specimens were heat-treated according to standard procedures for ½-in.-thick plates of 5Ni-Cr-Mo-V steel (austenitized 30 min at 1500 F, water-quenched, tempered for 30 min at 1100 F, and water-quenched), and to simulate 4½-in.-thick plate (austenitized for 2 h at 1500 F and blower-cooled in a wind channel that cools ½-in.-thick plates at a rate similar to that at the midthickness of a water-quenched 4½-in.-thick plate, tempered for 2 h at 1100 F, and blower cooled). By simulating the thermal cycles that occur during the heat treatment of a 4½-in.-thick plate, ½-in.-thick plates could be used to evaluate the effect of plate thickness on the temper-embrittlement susceptibility of the 30 experimental steels.[3]

TABLE 5—*Full equations for predicting the change in mechanical properties of quenched and tempered plates of 5Ni-Cr-Mo-V steel effected by prolonged stress relief.*[a]

½-IN.-THICK PLATES

Change in yield strength (0.2% offset), ksi

$$\begin{aligned}&= -65.809 + 30.948\,(\%\,\mathrm{C}) + 132.34\,(\%\,\mathrm{Mn}) + 7.3569\,(\%\,\mathrm{Ni}) - 7.4945\,(\%\,\mathrm{Cr})\\&\quad + 67.424\,(\%\,\mathrm{Mo}) - 20.416\,(\%\,\mathrm{Mn})\,(\%\,\mathrm{Ni}) - 33.849\,(\%\,\mathrm{Mn})\,(\%\,\mathrm{Cr})\\&\quad -41.509\,(\%\,\mathrm{Mn})\,(\%\,\mathrm{Mo}) + 0.70118\,(\%\,\mathrm{Ni})^2 - 8.8690\,(\%\,\mathrm{Ni})\,(\%\,\mathrm{Mo})\\&\quad + 41.635\,(\%\,\mathrm{Cr})\,(\%\,\mathrm{Mo}) - 33.425\,(\%\,\mathrm{Mo})^2\end{aligned}$$

Change in Charpy V-notch energy absorption at 0 F, ft·lb

$$\begin{aligned}&= +990.05 + 29.619\,(\%\,\mathrm{C}) - 109.25\,(\%\,\mathrm{Mn}) - 389.51\,(\%\,\mathrm{Ni}) + 16.293\,(\%\,\mathrm{Cr})\\&\quad -78.689\,(\%\,\mathrm{Mo}) + 96.575\,(\%\,\mathrm{Mn})^2 - 108.12\,(\%\,\mathrm{Mn})\,(\%\,\mathrm{Mo})\\&\quad + 38.922\,(\%\,\mathrm{Ni})^2 + 75.108\,(\%\,\mathrm{Cr})^2 - 208.00\,(\%\,\mathrm{Cr})\,(\%\,\mathrm{Mo}) + 155.97\,(\%\,\mathrm{Mo})^2\end{aligned}$$

Change in fracture-appearance (50% shear) transition temperature, F

$$\begin{aligned}&= -256.00 - 71.580\,(\%\,\mathrm{Mn}) + 43.584\,(\%\,\mathrm{Ni}) - 234.56\,(\%\,\mathrm{Cr}) + 186.22\,(\%\,\mathrm{Mo})\\&\quad + 305.66\,(\%\,\mathrm{Mn})^2 + 322.96\,(\%\,\mathrm{Cr})^2\end{aligned}$$

4½-IN.-THICK PLATES

Change in yield strength (0.2% offset), ksi

$$\begin{aligned}&= +60.186 - 2231.0\,(\%\,\mathrm{C}) - 17.209\,(\%\,\mathrm{Mn}) + 16.676\,(\%\,\mathrm{Ni}) - 25.197\,(\%\,\mathrm{Cr})\\&\quad + 259.25\,(\%\,\mathrm{Mo}) + 9128.2\,(\%\,\mathrm{C})^2 + 1.9523\,(\%\,\mathrm{Mn})\,(\%\,\mathrm{Ni})\\&\quad - 4.9321\,(\%\,\mathrm{Mn})\,(\%\,\mathrm{Cr}) + 5.3887\,(\%\,\mathrm{Ni})\,(\%\,\mathrm{Cr}) - 49.208\,(\%\,\mathrm{Ni})\,(\%\,\mathrm{Mo})\\&\quad - 10.693\,(\%\,\mathrm{Cr})\,(\%\,\mathrm{Mo}) - 12.468\,(\%\,\mathrm{Mo})^2\end{aligned}$$

Change in Charpy V-notch energy absorption at 0 F, ft·lb

$$\begin{aligned}&= +179.23 + 194.64\,(\%\,\mathrm{C}) + 28.951\,(\%\,\mathrm{Mn}) - 119.35\,(\%\,\mathrm{Ni}) + 17.516\,(\%\,\mathrm{Cr})\\&\quad + 336.42\,(\%\,\mathrm{Mo}) - 75.635\,(\%\,\mathrm{Mn})^2 + 16.119\,(\%\,\mathrm{Ni})^2 - 76.165\,(\%\,\mathrm{Ni})\,(\%\,\mathrm{Mo})\end{aligned}$$

Change in fracture-appearance (50% shear) transition temperature, F

$$\begin{aligned}&= 1339.4 - 1405.6\,(\%\,\mathrm{Mn}) - 254.00\,(\%\,\mathrm{Ni}) - 293.30\,(\%\,\mathrm{Cr}) - 1604.4\,(\%\,\mathrm{Mo})\\&\quad + 251.90\,(\%\,\mathrm{Mn})\,(\%\,\mathrm{Ni}) + 627.08\,(\%\,\mathrm{Mn})\,(\%\,\mathrm{Mo}) + 325.48\,(\%\,\mathrm{Ni})\,(\%\,\mathrm{Mo})\\&\quad + 639.66\,(\%\,\mathrm{Cr})\,(\%\,\mathrm{Mo}) - 482.40\,(\%\,\mathrm{Mo})^2\end{aligned}$$

[a] 125 h at 1000 F followed by slow-cooling (in Sil-O-Cel).

---

[3] Because the 5Ni-Cr-Mo-V steel was not designed for use at elevated temperatures it can embrittle only during the initial heat treatment, during stress-relieving treatments within the temper-embrittling region, or during slow cooling from the tempering and stress-relieving temperatures.

To evaluate the susceptibility to temper embrittlement during prolonged stress relieving, the ½-in.-thick plate specimens, heat treated by water quenching and tempering and also by blower cooling and tempering, were stress relieved for 125 h at 1000 F and slow cooled in Sil-O-Cel (an average cooling rate of about 500 F/h in the temperature range of 1000 to 700 F).

Two longitudinal 0.252-in.-diameter tension-test specimens and eight longitudinal Charpy V-notch impact-test specimens were machined from each plate specimen. The tension specimens were tested at room temperature, and the impact specimens were tested in the range +150 to −160 F. The steels were tested in both the quenched-and-tempered and the stress-relieved condition.

The results of the tension and impact tests were used to develop equations for predicting the yield strength, energy absorption, and fracture appearance transition temperature (FATT) of the steels prior to and after prolonged stress relief. An analysis of variance was performed first on each set of measurements to determine which effects of the alloying elements appeared to be significant. In these analyses, the intended percentages of manganese, nickel, chromium, and molybdenum were used, and carbon was used as a covariate. These effects were further tested in a regression analysis in which the actual percentages of the alloying elements were used. The final prediction equations include those effects judged to be significant at a confidence level of approximately 95 per cent.

Equations were also developed to predict the change in mechanical properties following prolonged stress relief. These equations were obtained by subtracting the prediction equation for quenched and tempered plates from the prediction equation for stress-relieved plates. Equations for the fracture-appearance transition temperature include susceptibility to temper embrittlement as a variable.

Equations for predicting the properties of ½ and 4½-in.-thick plates—quenched and tempered and after prolonged stress relief—are shown in Tables 3 and 4. Table 5 lists the equations for predicting changes in yield strength, Charpy V-notch energy absorption at 0 F,[4] and fracture-appearance (50 per cent shear) transition temperature (FATT) that were obtained by subtracting the equation for the quenched and tempered plates from those for the stress-relieved plates.

In general, the equations in Table 5 indicate that increases in manganese or molybdenum content most markedly impaired the toughness of

---

[4] Changes in Charpy V-notch energy at 0 F can be misleading because these results are greatly affected when the ductile-to-brittle transition of the embrittled steel occurs at 0 F and above. The change in FATT is probably the most generally accepted measure of embrittlement, but it is subject to inaccuracy because fracture appearance is determined by visual examination and estimation and is difficult to judge in high-strength steels such as those studied.

½ and 4½-in.-thick plates after prolonged stress relief; in other words, increases in manganese or molybdenum content or both promoted temper embrittlement. In addition, there was one notable interaction between chromium and molybdenum in which increases in these elements markedly impaired the energy absorption at 0 F of ½-in.-thick plates. The equations show that the effects of the elements studied are different for ½-in.-thick plate where the microstructures are completely martensitic than they are for 4½-in.-thick plate where the structures are about 50 per cent bainitic and 50 per cent martensitic.

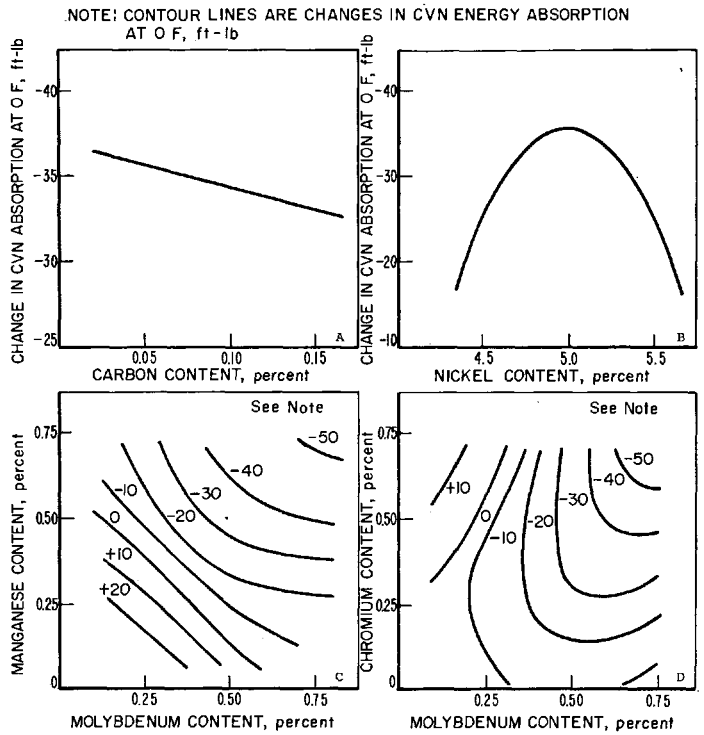

FIG. 1—*Effect of composition on change in Charpy V-notch energy absorption in ½-in.-thick plates held at 1000 F for 125 h and slow cooled.*

The full equations for predicting the changes in mechanical properties after prolonged stress relief are fairly simple. The equations for changes in yield strength appear to be most complicated, but calculation of the effects indicate that the changes in yield strength are minor, usually less than about 9 ksi *decrease* for ½-in.-thick plate and less than about 11 ksi *increase* for the simulated 4½-in.-thick plate. The increase in yield strength during long-time heat treatment at 1000 F is believed due to a delayed secondary-hardening reaction in the bainitic microstructures of

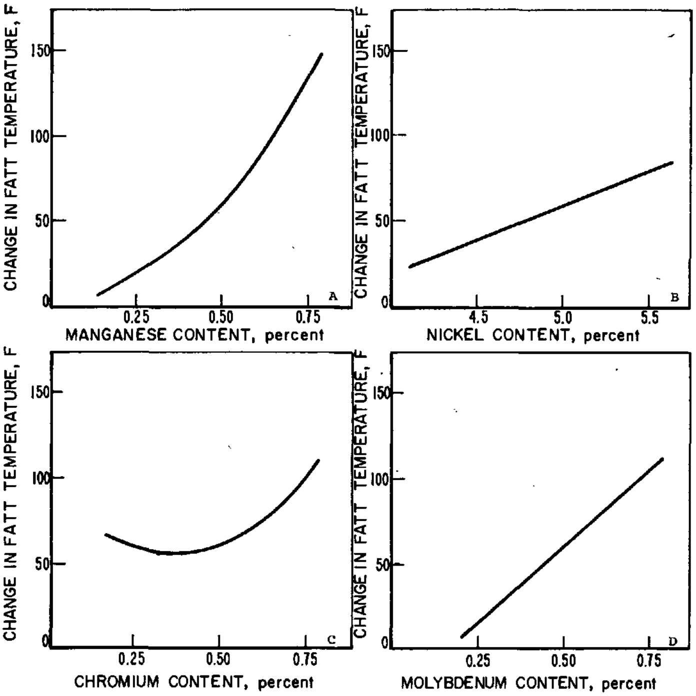

FIG. 2—*Effect of composition on the change in FATT temperature of ½-in.-thick plates held at 1000 F for 125 h and slow cooled.*

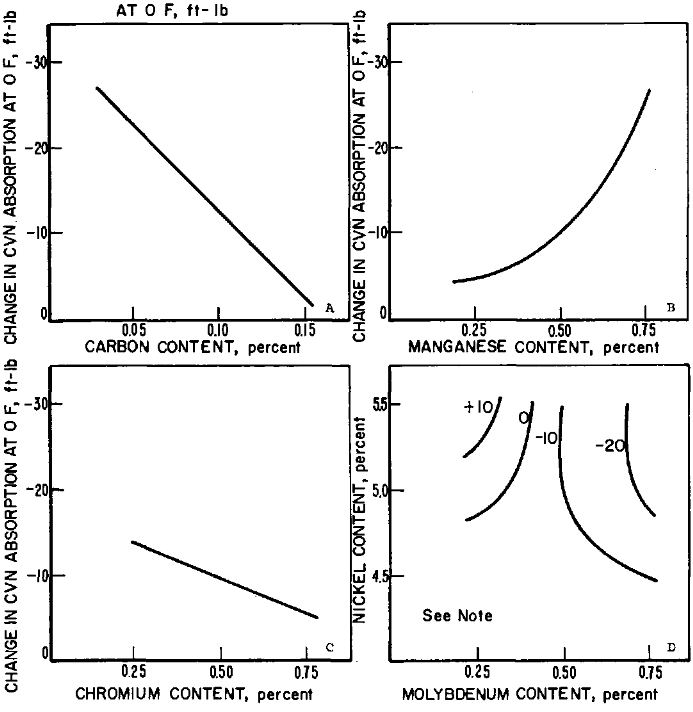
NOTE: CONTOUR LINES ARE CHANGES IN CVN ENERGY ABSORPTION AT O F, ft-lb

FIG. 3—*Effect of composition on the change in Charpy V-notch energy absorption of 4½-in.-thick plate held at 1000 F for 125 h and slow cooled.*

the simulated heavy-section plates. The presence of vanadium is believed to inhibit softening of ½-in.-thick martensitic plates during the long-time treatments at 1000 F.

The effects of the elements on the change in Charpy V-notch energy absorption at 0 F after temper embrittlement are best shown in a series of plots, Figs. 1 through 4. Where there are only linear and second-order effects, the weight per cent of the element is plotted against the change in energy absorption; where interactions occur, a contour map is used in which lines of constant changes in energy absorption or FATT are shown by plotting one element against the other. In all cases, the elements not involved in the plot are maintained at their center-point composition (0.10 per cent carbon, 0.50 per cent manganese, 5.0 per cent nickel, 0.50 per cent chromium, 0.50 per cent molybdenum). The same types of plots are used for showing effects of the elements on changes in fracture-appearance transition temperature.

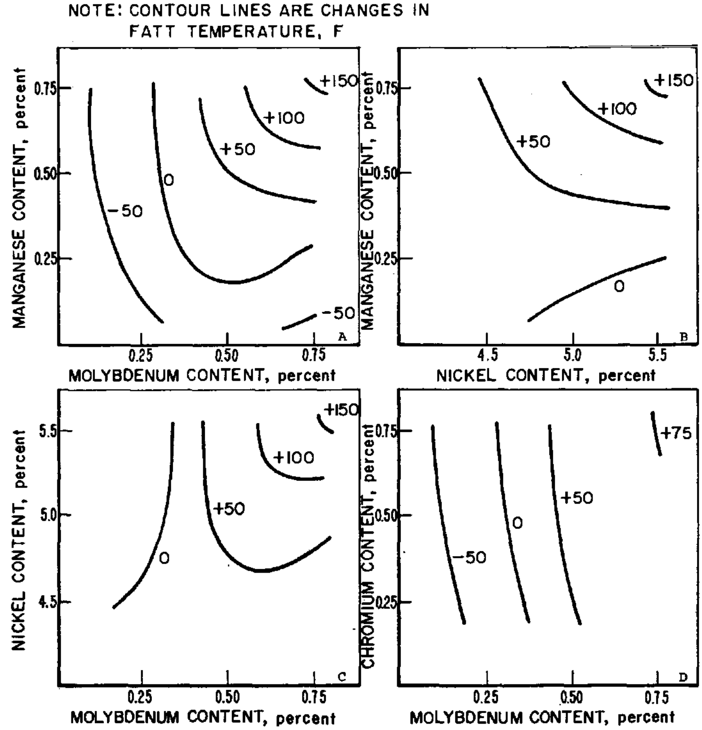

FIG. 4—*Effect of composition on changes in FATT temperature of 4½-in.-thick plates held at 1000 F for 125 h and slow cooled.*

Figure 1 shows the plots for the change in Charpy V-notch energy absorption at 0 F in ½-in.-thick plate. Increasing carbon causes a minor increase in energy absorption after the embrittling treatment. Embrittlement from nickel reaches a maximum at 5.0 per cent nickel and decreases when nickel is either increased or decreased, Fig. 1*b*. The interaction between manganese and molybdenum indicates that no embrittlement will occur if both manganese and molybdenum are kept below 0.30 per cent, Fig. 1*c*. If such compositions are not desirable because of hardenability or temperability considerations, it would be possible to minimize temper embrittlement by increasing one of the two elements and keeping the other at a very low level. The interaction between chromium and molybdenum indicates that chromium can be increased to 0.75 per cent provided that molybdenum is held below about 0.30 per cent, Fig. 1*d*. An optimum composition, therefore, would be a steel containing 0.30 per cent manganese, 0.30 per cent molybdenum, 0.75 per cent chromium, and 4.5 to 5.5 per cent nickel. If it is required that molybdenum be kept high for temperability, then chromium and manganese should be kept below 0.25 per cent.

Similar examination of the effect of the elements on the change in FATT for ½-in.-thick plate, Fig. 2, indicates again that manganese and molybdenum should be kept low, and, if a choice must be made between manganese and molybdenum, it is preferable to increase the molybdenum content rather than the manganese content. Increasing nickel causes a modest increase in embrittlement, but, because increasing nickel lowers the transition temperature of the unembrittled steel, the net effect is that, in the embrittled condition, there is no change in FATT with increased nickel content. Effects of varying chromium are small, particularly at chromium contents up to about 0.60 per cent.

The effects of the elements on the notch toughness of the 4½-in.-thick plates, Fig. 3, are similar to those for the ½-in.-thick plate in that manganese and molybdenum are the elements contributing most to the embrittlement. Increasing chromium and carbon decrease the amount of embrittlement, but, because increasing amounts of these elements decrease the toughness of the steel in the unembrittled condition, the net effect is that increasing amounts of chromium and carbon cause no change in the notch toughness of the embrittled steels.

Figure 4 shows that interactions among manganese, molybdenum, nickel, and chromium were found when evaluating FATT data. However, the interactions are relatively small, and increases in manganese and molybdenum are again found to produce the largest increases in transition temperature. It appears that if either manganese or molybdenum is maintained at about 0.25 per cent, little embrittlement (increase in FATT) will be noted on prolonged stress relief at 1000 F followed by slow cooling.

Effect of Vanadium

The three steels with low (0.036 per cent) vanadium (Steels BA, CA, and DA) were not part of the statistically designed program; therefore, their properties were compared directly with the properties of their high (0.068 per cent) vanadium counterparts (Steels A, I, R, P, and W). The mechanical properties of these steels are summarized in Table 6.

The changes in yield strength and Charpy V-notch energy absorption at 0 F or −80 F between the quenched and tempered and the stress-relieved ½ and 4½-in.-thick plates were about the same for both the high-vanadium and the low-vanadium steels. However, the fracture-appearance (50 per cent shear) transition temperatures of the 0.068 per cent vanadium steels averaged 15 to 43 F higher than those of the 0.036 per cent vanadium steels. Thus, increases in vanadium content in the range studied did not significantly affect the energy absorption at 0 F or −80 F, but did slightly increase the transition temperature.

TABLE 6—*Effect of vanadium content on mechanical properties after stress relieving.*

	Steel	Yield Strength, ksi	Charpy V-Notch Energy Absorption, ft·lb		FATT, deg F
			0 F	−80 F	
CHANGE IN INDICATED MECHANICAL PROPERTY (½-IN.-THICK PLATES)[a]					
0.068% V steels	A, I, R[b]	0	−30	−48	+70
	P	+3	−4	−11	+25
	W	−3	−62	−47	+155
Average change		0	−32	−35	+83
Corresponding 0.036% V steels	BA	−2	−31	−45	+75
	CA	0	−4	−6	+5
	DA	−10	−67	−67	+125
Average change		−4	−34	−39	+68
CHANGE IN INDICATED MECHANICAL PROPERTY (4½-IN.-THICK PLATES)[a]					
0.068% V steels	A, I, R[b]	+4	−9	−21	+65
	P	+6	−16	+1	+10
	W	+7	−34	−39	+120
Average change		+6	−20	−20	+65
Corresponding 0.036% V steels	BA	+8	−12	−37	+5
	CA	+7	−3	+6	+15
	DA	+3	−41	−49	+45
Average change		+6	−19	−27	+22

[a] Change in mechanical properties between quenched and tempered and prolonged-stress-relieved plates.

[b] Values shown are the average of three values (that is for Steels A, I, and R).

The preceding studies (excluding the data on the effect of composition on the FATT of 4½-in.-thick plate) indicate that manganese and molyb-

TABLE 7—*Summary of temper embrittlement studies of effect of vanadium on water-quenched and tempered ½-in.-thick plates of 5Ni-Cr-Mo-V steel.*

Steel	Vanadium, %	Yield Strength (0.2% offset), ksi		Charpy V-Notch Energy Absorption, at 0 F, ft·lb		Charpy V-Notch Energy Absorption, at −80 F, ft·lb		Fracture-Appearance (50% shear) Transition Temperature, deg F		15-Mil Lateral Expansion Transition Temperature, deg F	
		Unembrittled[a]	Embrittled[b]	Unembrittled	Embrittled	Unembrittled	Embrittled	Unembrittled	Embrittled	Unembrittled	Embrittled
Vanadium Series:											
AB	0.007	134	118	120	128	115	88	−185	−120	−230	−190[c]
BB	0.029	143	136	112	96	99	71	−145	−80	−160	−155
CB	0.063	147	145	105	118	94	106	−140	−170	−200	−230
DB	0.065	149	145	106	110	93	87	−140	−120	−210	−160
EB	0.071	150	149	103	90	95	68	−155	−90	−210	−140
FB	0.097[d]	150	152	90	107	76	84	−130	−130	−170	−180[c]
GB	0.130	155	151	92	114	80	87	−130	−125	−165	−170[c]
HB	0.190	150	145	98	125	37	94	−45	−120	−85	−160

[a] Plate specimens (½-in.-thick) were austenitized for 30 min at 1500 F, water quenched, tempered for 30 min at 1100 F, and water quenched.

[b] Quenched and tempered (at 1100 F) plate specimens were stress relieved for 125 h at 1000 F and slow cooled (in Sil-O-Cel).

[c] Estimated by extrapolation.

[d] Steel FB contained only 0.062 per cent carbon.

denum should be kept at about 0.25 to 0.35 per cent, chromium content may be increased to 0.75 per cent, nickel content can be increased to 5.5 per cent or over, and the 0.10 per cent carbon and 0.07 per cent vanadium levels are satisfactory. The data on FATT for 4½-in.-thick plate would suggest that manganese could be increased to 0.75 per cent if molybdenum is kept at 0.25 per cent. Because for all other conditions high manganese is somewhat more detrimental than high molybdenum, the use of a high-manganese composition was eliminated from consideration.

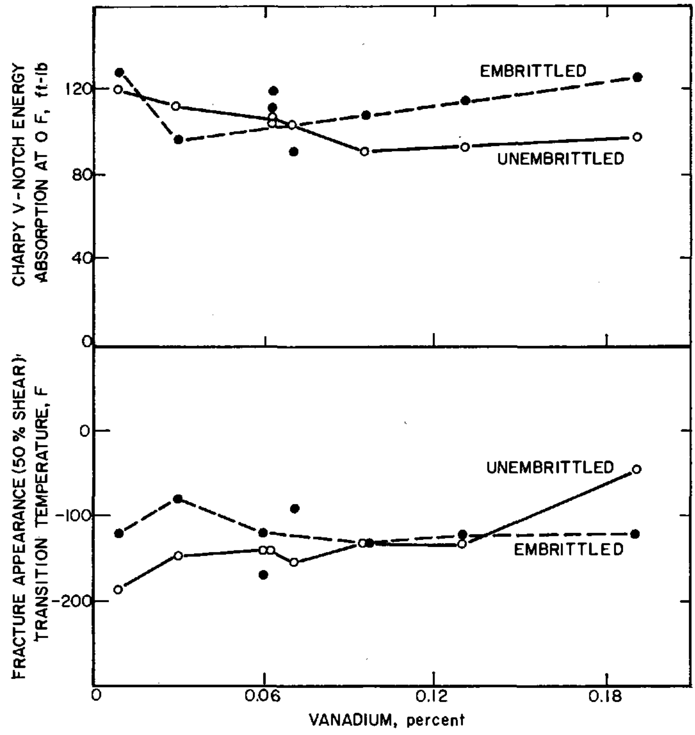

FIG. 5—*Effect of vanadium content on notch toughness of ½-in.-thick plates of 5Ni-Cr-Mo-V steel before and after 1000 F embrittling treatment.*

Therefore, the preferred composition, in per cent, based solely on the embrittling effects, was chosen as:

C	Mn	Ni	Cr	Mo	V
0.10..........	0.25	5.75	0.75	0.35	0.07

However, consideration of hardenability and temperability dictated that

TABLE 8—*Summary of stress-relieving studies on water-quenched and tempered ½-in.-thick plates.*

Steel	Varying Element, %	Yield Strength (0.2% offset), ksi		Charpy V-Notch Energy Absorption, at 0 F, ft·lb		Charpy V-Notch Energy Absorption, at −80 F, ft·lb		Fracture-Appearance (50% shear) Transition Temperature, deg F		15-Mil Lateral Expansion Transition Temperature, deg F	
		Unem-brittled[a]	Em-brittled[b]	Unem-brittled	Em-brittled	Unem-brittled	Em-brittled	Unem-brittled	Em-brittled	Unem-brittled	Em-brittled
Phosphorus Series:											
AC	0.003	147	145	105	118	94	106	−140	−170	−200	−230
BC	0.006	150	149	103	90	95	68	−155	−90	−210	−140
CC	0.006	147	146	108	117	98	89	−130	−120	−160	−160
DC	0.006	149	145	106	110	93	87	−140	−120	−210	−160
EC	0.017	149	147	106	83	89	50	−130	−50	−175	−100
FC	0.030	149	145	106	36	92	17	−130	+125	−160	+15
Nitrogen Series:											
GC	0.002	145	146	90	95	67	75	−85	−120	−145	−150
AC	0.006	147	145	105	118	94	106	−140	−170	−200	−230
BC	0.008	150	149	103	90	95	68	−155	−90	−210	−140
HC	0.008	149	145	106	110	93	87	−140	−120	−210	−160
IC	0.011[d]	145	137	93	99	86	89	−165	−185	−220	−200[c]
JC	0.012	149	139	111	121	103	92	−170	−120	−210	−170
KC	0.016[d]	142	128	105	120	104	112	−180	−165	−220	−220[c]
LC	0.018	150	131	123	136	114	116	−195	−130	−220	−210[c]
Aluminum Series (Vacuum-Melted):											
CC	0.004[e]	147	146	108	117	98	89	−130	−120	−160	−160
BC	0.010	150	149	103	90	95	68	−155	−90	−210	−140
HC	0.016	149	145	106	110	93	87	−140	−120	−210	−160
AC	0.025	147	145	105	118	94	106	−140	−170	−200	−230
MC	0.040	150	141	114	122	101	98	−160	−125	−190	−170[c]

Aluminum Series (Air-Melted):											
NC	0.005[e]	148	146	72	85	68	71	−130	−120	−140	−160
OC	0.006[f]	147	141	53	66	49	65	−135	−130	−120	−170[c]
PC	0.020[g]	154	144	73	52	62	36	−115	−40	−170	−80
QC	0.023	150	147	84	98	69	91	−120	−120	−150	−160
RC	0.045	150	151	83	91	74	71	−130	−130	−150	−155
Oxygen Series:											
KC	0.0020[d]	142	128	105	120	104	112	−180	−165	−220	−220[c]
JC	0.0026	149	139	111	121	103	92	−170	−120	−210	−170
CC	0.0034	147	146	108	117	98	89	−130	−120	−160	−160
NC	0.0068	148	146	72	85	68	71	−130	−120	−140	−160
OC	0.0177	147	141	53	66	49	65	−135	−130	−120	−170[c]

[a] Plate specimens (½-in.-thick) were austenitized for 30 min at 1500 F, water quenched, tempered for 30 min at 1100 F, and water quenched.

[b] Quenched and tempered (at 1100 F) plate specimens were stress relieved for 125 h at 1000 F and slow cooled (in Sil-O-Cel).

[c] Estimated by extrapolation.

[d] Steels IC and KC contained only 0.04 per cent silicon.

[e] Total.

[f] Steel OC contained 177 ppm of oxygen.

[g] Steel PC contained slightly higher manganese, silicon, nickel, and vanadium content than the remainder of the aluminum series.

the chromium should be lowered somewhat and the molybdenum raised. As a result, the composition, in per cent, chosen for further study was:

C	Mn	Ni	Cr	Mo	V
0.10..........	0.25	5.75	0.55	0.50	0.07

Because the original vanadium study was very limited and because there is evidence that vanadium promotes temper embrittlement in other steels [*2*], additional studies of the effect of vanadium were conducted on the low-manganese modification of the 5Ni-Cr-Mo-V steel. The vanadium content of the base steel was progressively varied in eight vacuum-melted 300-lb heats from 0.007 per cent vanadium (residual) to 0.190 per cent vanadium. The ½-in.-thick cross-rolled plates from the heats were all given a standard austenitizing and tempering treatment (1500 F austenitizing for 30 min, water quenched, 1100 F temper for 30 min, and water quenched), and a portion of each plate was subsequently subjected to a

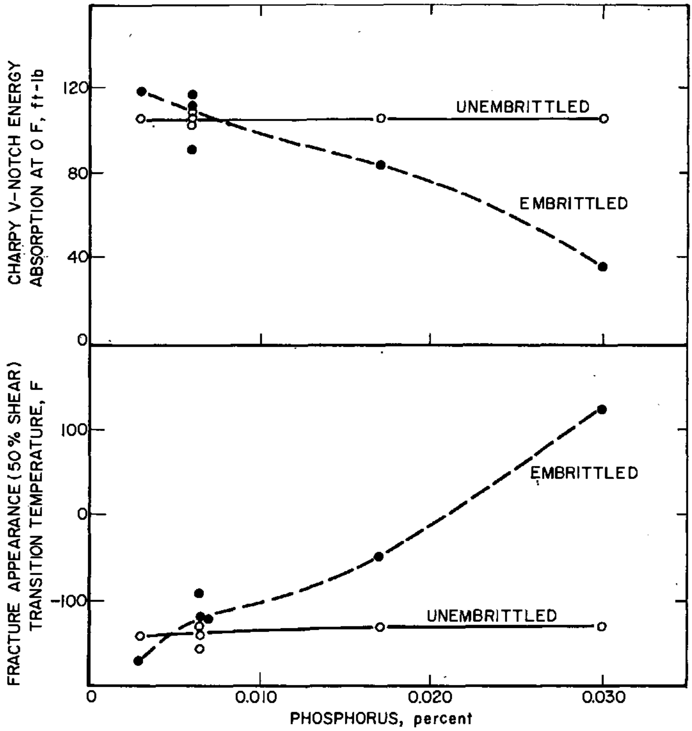

FIG. 6—*Effect of phosphorus content on the notch toughness of ½-in.-thick plates of 5Ni-Cr-Mo-V steel before and after 1000 F embrittling treatment.*

temper-embrittling treatment by holding at 1000 F for 125 h and slow-cooling (in Sil-O-Cel).

The effects of the conventional heat treatment and the temper-embrittling treatment on the mechanical properties are given in Table 7, and the data are summarized in Fig. 5. Except for the low-vanadium steel (Steel AB), none of the steels exhibited a loss in yield strength greater than 7 ksi after stress relieving. In the case of the low-vanadium steel, the 16 ksi loss in yield strength undoubtedly occurred because insufficient vanadium was present to promote secondary hardening and resistance to spheroidization of the carbides.

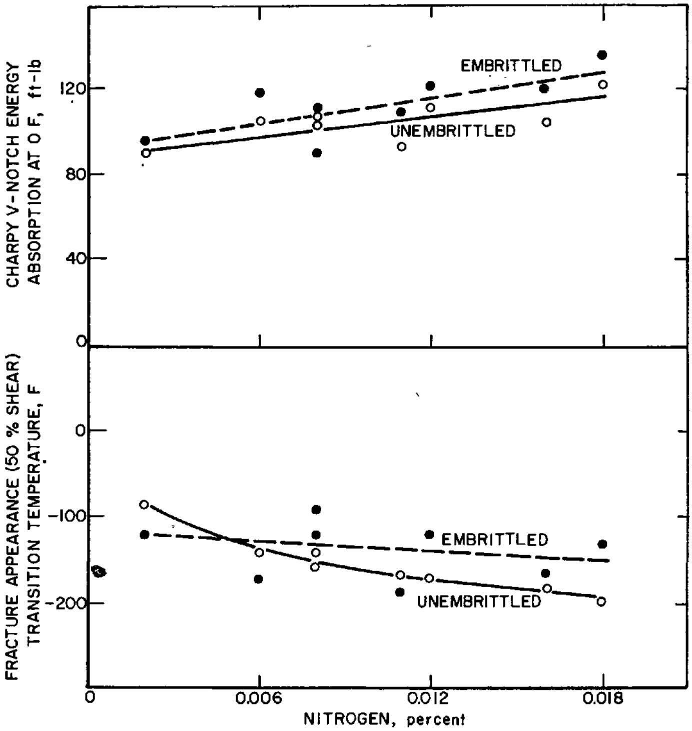

FIG. 7—*Effect of nitrogen content on notch toughness of ½-in.-thick plates of 5Ni-Cr-Mo-V steel before and after 1000 F embrittling treatment.*

Figure 5 shows that increases in vanadium content from 0.007 to 0.19 per cent had little or no effect on the notch toughness of the quenched and tempered plates up to about 0.13 per cent vanadium, but that further increases in vanadium content (0.19 per cent) slightly increased FATT. Similarly, the increases in vanadium content had little if any effect on the notch toughness of the plates after a prolonged temper-embrittling treatment. In fact, the toughness of the stress-relieved high-vanadium steels was somewhat better than that of the quenched and tempered steels. Thus, vanadium did not appear to contribute to temper embrittlement in any respect in this study. It was believed that variations in vanadium content might have caused variations in austenite grain size, which in turn might have influenced susceptibility to temper embrittlement. However, the prior-austenite grain size of the steels (including steels with wide variations in aluminum content) ranged only from ASTM No. 5¾ to 7.

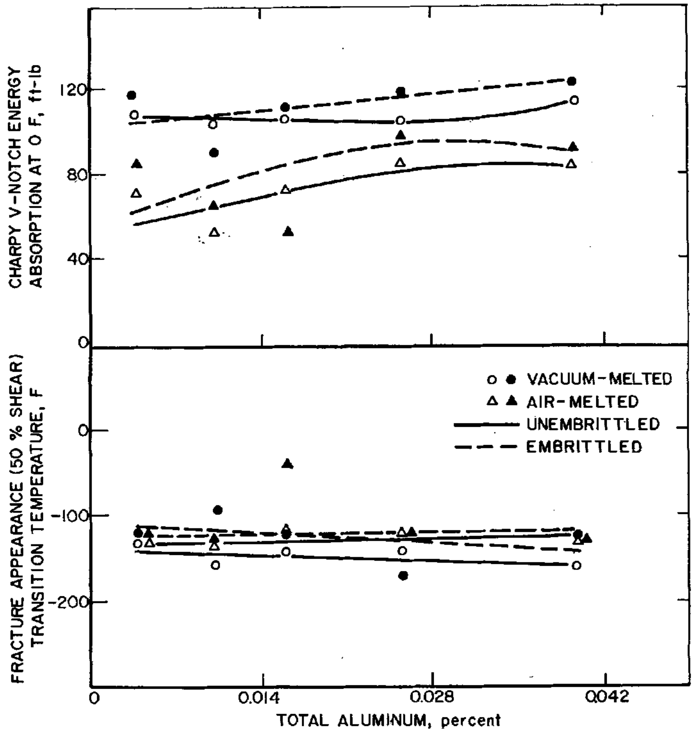

FIG. 8—*Effect of aluminum content on notch toughness of ½-in.-thick plates of 5Ni-Cr-Mo-V steel before and after 1000 F embrittling treatment.*

Effect of Residual Elements

In a manner similar to that described for the study of the effects of vanadium on temper embrittlement, several series of low-manganese steels were vacuum-induction-melted (except for an air-melted series of five steels with varied aluminum contents and two heats in a series of steels with varied oxygen contents). The steels were heat treated (quenched and tempered) and temper embrittled to evaluate the effects of phosphorus, nitrogen, aluminum, and oxygen content on temper embrittlement. A summary of the mechanical properties (yield strength and notch toughness) before and after embrittlement is shown in Table 8, and the notch toughness data are further summarized in Figs. 6–9.

Examination of the tables and figures shows that, for the elements and ranges studied, only phosphorus promoted temper embrittlement when the 5Ni-Cr-Mo-V steel was held for long periods at 1000 F and slow cooled. At phosphorus contents of 0.006 per cent and below, there was no indication of temper embrittlement, but above 0.006 per cent the embrittling treatment caused a loss in toughness and a rise in transition temperature that were directly dependent on the phosphorus content, Fig. 6. At 0.03 per cent phosphorus, the embrittling treatment reduces the energy absorption to one third its original value at 0 F and causes a 255 F increase in FATT. Within the ranges studied, phosphorus had no significant effect on the yield strength of the steel in either the unembrittled or the embrittled condition and no significant effect on the notch toughness of the steel in the unembrittled condition.

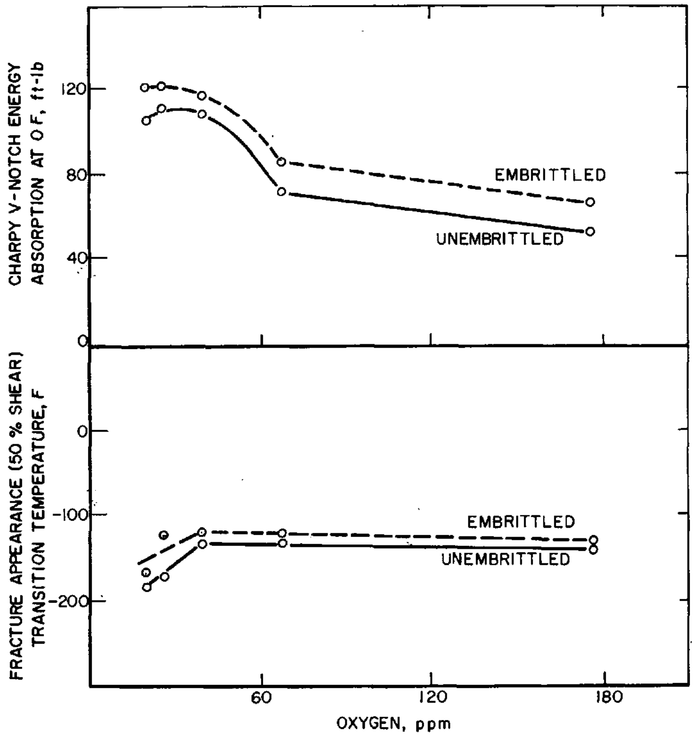

FIG. 9—*Effect of oxygen content on notch toughness of ½-in.-thick plates of 5Ni-Cr-Mo-V steel before and after 1000 F embrittling treatment.*

Increasing nitrogen content appeared to have a slight beneficial effect on notch toughness and showed no signs of promoting temper embrittlement, Fig. 7. At high-nitrogen contents, the yield strength of the steel was lowered significantly by the long-time heat treatment at 1000 F. Thus, it appears that nitrogen can alter the tempering response of the 5Ni-Cr-Mo-V steel, possibly by reacting with vanadium when the aluminum content is low.

Increasing aluminum content had no significant effect on the yield strength and notch toughness of the steel either in the unembrittled or embrittled condition, and did not contribute to temper embrittlement within the aluminum ranges studied, Fig. 8.

Increasing oxygen content markedly decreased the notch toughness of the steel, particularly when the oxygen content was raised to over 50 ppm. The loss in toughness with increased oxygen content would be expected because of the increase in nonmetallic oxide content, particularly alumina, of these aluminum-containing steels. Variations in oxygen content did not affect the yield strength of the steel or the tendency of the steel to temper embrittle after long-time holding at 1000 F and slow cooling, Fig. 9.

TABLE 9—*Chemical composition of steels investigated—per cent (check analyses).*

Steel Code	Heat No.	C	Mn	P	S	Si	Ni	Cr	Mo	V	Al[a]	N[b]
A..........	X53588	0.12	0.91	0.008	0.004	0.22	5.26	0.62	0.59	0.056	0.013	0.011
B..........	5PO719	0.10	0.35	0.007	0.004	0.23	5.33	0.49	0.57	0.064	0.020	0.012

[a] Total.
[b] Kjeldahl determination.

TABLE 10—*Results of special chemical analyses for residual (tramp) elements—per cent.*

Steel Code	Heat No.	B	As	Sn	Pb	Sb[a]
A...........	X53588	<0.0001	<0.01	0.003	<0.001	0.0003
B...........	5PO719	<0.0005	<0.01	0.006	<0.001	0.0003

[a] Higher precision was requested for the antimony analysis.

Embrittlement in Production Heats

To determine the effectiveness of the modified composition in reducing temper embrittlement in the 5Ni-Cr-Mo-V steel, an 80-ton electric furnace heat of the low-manganese composition was melted and processed to plate. The embrittling characteristics of the steel were determined on a ⅝-in.-thick plate by comparing the effects of 25-h stress relieving treatments at 1000 and 1050 F followed by slow cooling at 200 F/h with similar treatments on a ½-in.-thick plate of a standard-composition (high-manganese) 5Ni-Cr-Mo-V steel. In addition, studies were conducted to determine the influence of 1 per cent cold deformation in ten-

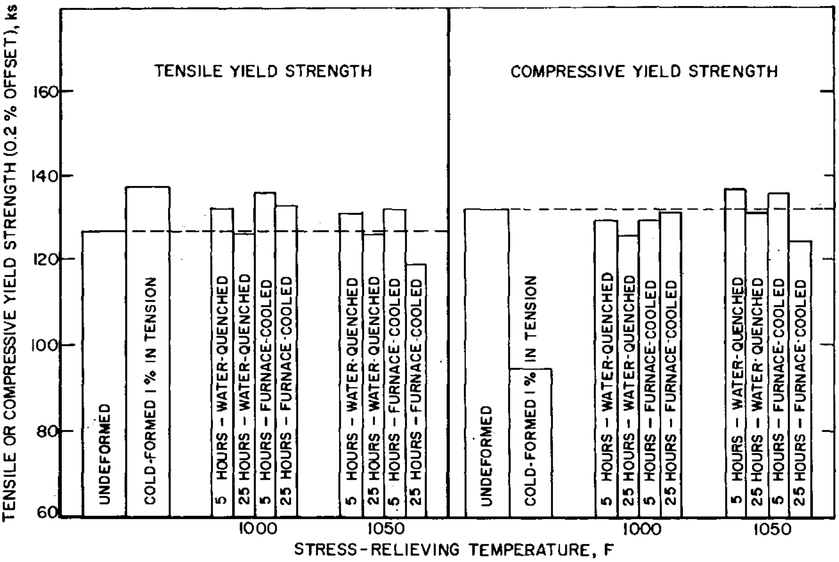

FIG. 10—*Effect of stress relieving on the yield strength of standard-manganese, 5Ni-Cr-Mo-V steel.*

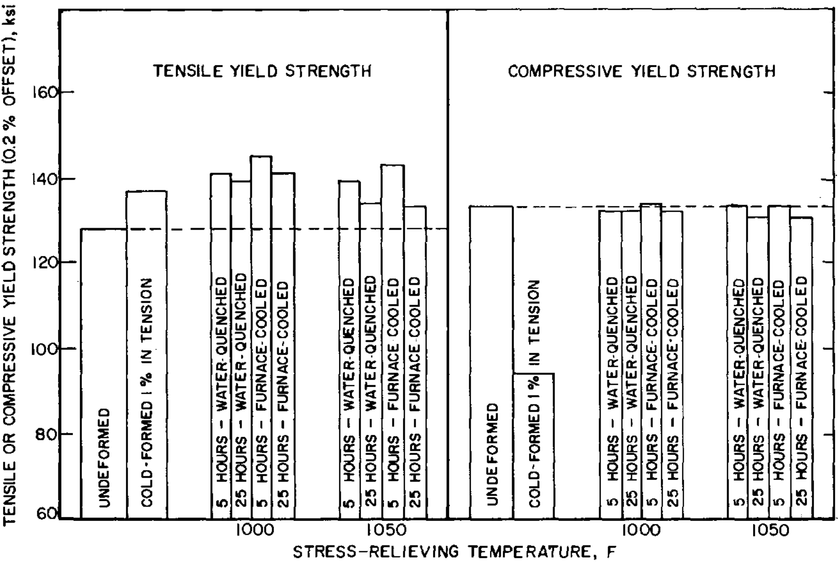

FIG. 11—*Effect of stress-relieving on the yield strength of low-manganese 5Ni-Cr-Mo-V steel.*

sion on the properties of the steels and on the subsequent embrittlement during stress relieving.

The chemical compositions of the two steels are shown in Table 9. The low-manganese steel had somewhat higher manganese and lower chromium and nickel than would be considered optimum on the basis of the statistical study. The steels were analyzed for the tramp elements (antimony, lead, tin, arsenic, and boron) that are known to contribute to temper embrittlement. The results shown in Table 10 indicate that the smaller-than-predicted degree of improvement obtained with the low-manganese composition cannot be ascribed to the presence of undesirable tramp elements.

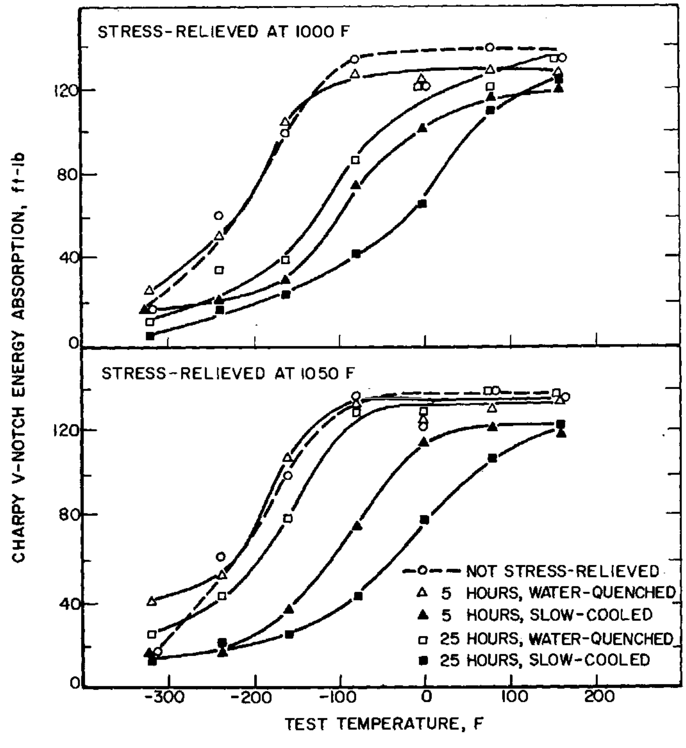

FIG. 12—*Effect of stress relieving treatments on the transition curves of standard-manganese 5Ni-Cr-Mo-V steel.*

The regression equation for determining the change in FATT for an embrittling treatment of 125 h at 1000 F indicates that the standard steel would be expected to exhibit an increase in FATT of 250 F, and the low-manganese steel would be expected to exhibit an increase in FATT of 57 F, or about one fourth of the embrittlement of the standard-manganese steel.

The tensile and compressive yield strength for the two steels before and after straining and stress relieving are summarized in Figs. 10 and 11. For both steels, the increase in tensile yield strength as a result of the prior straining was not removed even after stress relieving for 25 h at 1050 F. Specimens of both steels tested in compression exhibited the conventional Bauschinger effect (marked lowering of yield strength) when tested before stress relieving, but the yield strength was restored to its undeformed value on stress relieving at 1000 F.

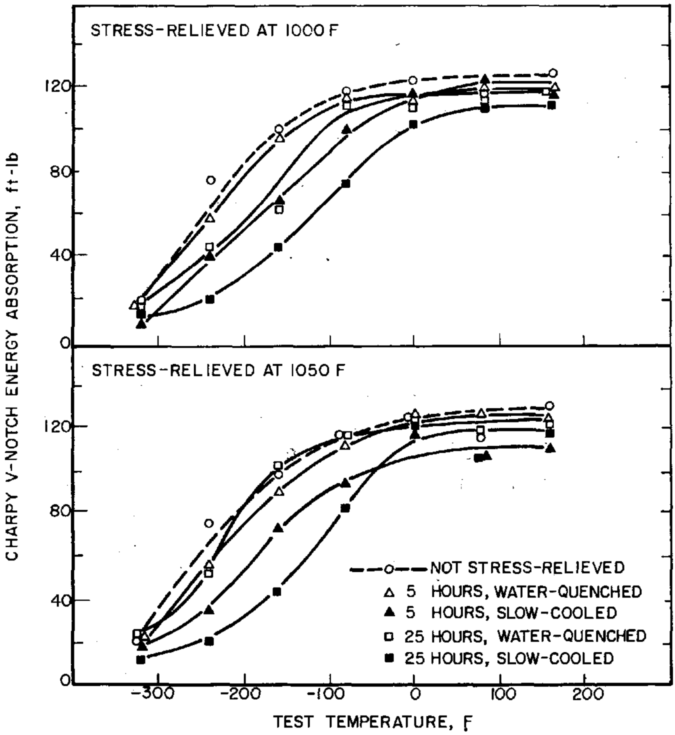

FIG. 13—*Effect of stress-relieving treatments on the transition curves of low-manganese 5Ni-Cr-Mo-V steel.*

The effects of the 1000 and 1050 F temperature treatments on the transition curves for the two steels in the undeformed condition are shown in Figs. 12 and 13. The transition curves for the steels water-quenched from the stress-relieving temperature show that embrittlement occurred in both steels during holding for 25 h at 1000 F. No embrittlement occurred during holding for only 5 h at 1000 F or at 1050 F. Additional marked embrittlement occurred during slow cooling (200 F/h) from the stress-relieving temperature. This additional embrittlement is evident both for the steels held at 1000 F and the steels held at 1050 F.

In addition to the shift in transition temperature, there was a small drop in the shelf energy of the embrittled steels.

When the steels were held for 25 h at 1000 F and water quenched, the standard-manganese steel exhibited an increase in transition temperature (measured at a toughness level of half the shelf energy) of about 120 F, and the low-manganese steel exhibited an increase in transition temperature of about 80 F. The reduction in shelf energy after the above embrittling treatment was negligible.

The effect of slow cooling was to produce additional embrittlement. The data inidcate that, on the average, slow cooling increased the transition temperature of the standard-manganese steel an additional 140 F and the transition temperature of the low-manganese steel an additional 60 F. The shelf energy was also lowered about 15 ft·lb as a result of the slow-cooling treatment. Prestraining caused a small increase in the transition temperature of the unembrittled steel, but somewhat reduced the additional increase in transition temperature resulting from subsequent stress-relieving treatments. The combined effect of prestraining and stress relieving was thus equivalent to the effect of stress relieving unstrained material.

Because the steels described in this paper would normally be welded and would most likely be stress-relieved in the welded condition, other temper-embrittlement studies have been conducted on weld metals of matching yield strength and on the weld-heat-affected zones of welded plate [*5*]. These studies indicate that high-manganese weld metals (2.0 per cent) are more susceptible to embrittlement than low-manganese weld metals (0.75 per cent manganese), and that weld metals of matching composition to the base plate are less susceptible to embrittlement than the base plate. The grain-coarsened region of the heat-affected zone is much more susceptible to embrittlement than the fine-grained region and the unaffected base plate.

The results for the production steels indicate that the change in composition did not produce as great an improvement in the resistance of the steels to embrittlement as that predicted by the statistical analysis. However, the improvement was substantial; embrittlement was reduced to about half that of the standard-manganese steel. Still further reduction would be expected if the composition of the low-manganese steel were adjusted to the optimum composition by lowering the manganese to 0.25 per cent and raising the nickel and chromium content.

Conclusions

1. Statistical analysis of an experiment designed to evaluate the effects of carbon, manganese, nickel, chromium, and molybdenum on the temper embrittlement of 5Ni-Cr-Mo-V steel showed that manganese and molybdenum contributed most to the embrittlement. The optimum

composition for a 5Ni-Cr-Mo-V steel resistant to temper embrittlement was:

C	Mn	Ni	Cr	Mo	V
0.10..........	0.25	5.75	0.75	0.35	0.07

2. A separate evaluation of the effect of vanadium on temper embrittlement in the 5Ni-Cr-Mo-V steel indicated that vanadium did not contribute to temper embrittlement.

3. An investigation of the effects of phosphorus, nitrogen, aluminum, and oxygen showed that only phosphorus contributed to temper embrittlement and that embrittlement occurred when the phosphorus content was increased above about 0.006 per cent. High-oxygen content lowered the toughness of the steel but did not contribute to temper embrittlement.

4. Comparison of plates from production heats of a low-manganese and a standard-manganese 5Ni-Cr-Mo-V steel showed that the low-manganese steel exhibited about half as much temper embrittlement as did the standard-manganese composition. Embrittlement occurred after holding for 25 h at 1000 F and on slow cooling from the elevated temperature. No embrittlement occurred during holding at 1050 F for times up to 25 h. Prestraining the steel 1 per cent in tension did not change the temper-embrittling characteristics of the two steels.

Acknowledgment

The work described in this paper was conducted under Naval Ship Systems Command Contract No. NObs-94535(FBM). The support, encouragement, and advice of the various Navy activities associated with the project are gratefully acknowledged. This paper is published for information only and does not necessarily represent the recommendations or conclusions of the Naval Ship Systems Command.

The authors also wish to acknowledge the assistance of T. L. Boblenz in providing information on the mechanical properties of the undeformed and cold-deformed production steels.

References

[*1*] Box, G. E. P. and Behnken, D. W., "Some New Three Level Designs for the Study of Quantitative Variables," *Technometrics*, Vol. 2, No. 4, Nov. 1960, pp. 455–475.

[*2*] Woodfine, B. C., "Temper-Brittleness: A Critical Review of the Literature," *Journal of the Iron and Steel Institute*, Vol. 173, March 1953, pp. 229–239.

[*3*] Low, J. R., Jr., "Temper Brittleness—A Review of Recent Work," *Fracture of Engineering Materials*, American Society for Metals, 1964, pp. 127–141.

[*4*] Military Standard, "Welding and Allied Process for Machinery for Ships of the United States Navy," MIL-STD-278(SHIPS), 19 Sept. 1956.

[*5*] Connor, L. P., Rathbone, A. M., and Gross, J. H., "Effects of Composition on the Heat-Affected-Zone Toughness of Constructional Alloy Steels," *Research Supplement of the Welding Journal*, Vol. 46, No. 5, May 1967, pp. 2175–2345.

A. H. Rosenstein[1] *and W. H. Asche*[2]

Stress-Relief Embrittlement of High-Strength Quenched and Tempered Alloy Steels*

REFERENCE: Rosenstein, A. H. and Asche, W. H., **"Stress-Relief Embrittlement of High-Strength Quenched and Tempered Alloy Steels,"** *Temper Embrittlement in Steel, ASTM STP 407*, American Society for Testing and Materials, 1968, pp. 46–58.

ABSTRACT: An investigation was undertaken of the time-temperature-embrittlement relationships of two high-strength quenched and tempered steels. Optimum stress-relief treatments were developed which incorporate the maximum reduction in residual stress accompanied by the minimum increase in transition temperature. It was determined that stress-relief embrittlement in Steel A (5Ni-Cr-Mo-V, 140 ksi yield strength) is most severe in the 900 to 1000 F temperature range, and that Steel B (3Ni-Cr-Mo, 100 ksi yield strength) is not significantly embrittled by stress relief. The optimum stress-relief treatments for Steels A and B are obtained by heat treatment at as high a stress-relieving temperature as possible. The maximum stress-relieving temperature is limited to that which will not result in loss of yield strength.

KEY WORDS: stress-relieving, temper embrittlement, high-strength steels, alloy steels, toughness, residual stress, heat treatment, tempering, evaluation

A study of embrittlement during thermal stress-relief of two high-strength quenched and tempered alloy steels was made. Investigation of the effects of tempering on tensile and Charpy impact properties showed these materials to have high toughness when water quenched from the tempering temperature. Embrittlement is avoided during tempering by the relatively short duration of exposure at the tempering temperature and by water quenching. Thermal stress-relief treatments of structures, on the other hand, generally involve slow heating and cooling rates, as well as extended soaking periods, to maintain uniform temperature

---

* The opinions for assertions made in this paper are those of the authors and are not to be construed as official or reflecting the views of the Department of the Navy or the naval service at large.

[1] Senior project engineer, high strength steels, Annapolis Div., Naval Ship Research and Development Center, Annapolis, Md. Personal member ASTM.

[2] Metallurgist, Annapolis Div., Naval Ship Research and Development Center, Annapolis, Md. Personal member ASTM.

conditions. Preliminary studies showed that one alloy, Steel A, was susceptible to embrittlement when held at temperature for prolonged periods and then air or furnace cooled.

It was postulated that a combination of time and temperature could be specified which would provide substantial relief of elastic strains with only minimal embrittlement of the steels. Accordingly, this investigation was undertaken: (*a*) to determine the effects of various stress-relieving temperatures and times on transition temperature, (*b*) to obtain a measure of the effectiveness of these stress-relieving treatments for lowering the residual stress, and (*c*) to compare the reduction of residual stress for a given treatment with the change in transition temperature due to that treatment. Embrittlement was measured by an increase in 50 per cent shear fracture appearance transition temperature and a decrease in Charpy V-notch shelf energy.

TABLE 1—*Chemical composition and tensile properties.*

	Steel A	Steel B
Composition, weight %:		
Carbon	0.11	0.18
Manganese	0.78	0.30
Phosphorus	0.008	0.009
Sulfur	0.006	0.028
Silicon	0.29	0.22
Nickel	5.03	2.91
Chromium	0.56	1.65
Molybdenum	0.42	0.42
Vanadium	0.05	...
Aluminum	0.015	...
Nitrogen	0.011	...
Properties of longitudinal specimens:		
Tensile strength, ksi	154	120
Yield strength (0.2% offset), ksi	143	105
Elongation in 2 in., %	18	24
Reduction in area, %	62	71

Materials and Procedure

The material for this investigation was removed from 2-in.-thick plates. Steel A is a 5Ni-Cr-Mo-V composition of 140 ksi nominal yield strength; Steel B is a 3Ni-Cr-Mo composition of 100 ksi nominal yield strength. Chemical compositions and tensile properties of the materials are shown in Table 1.

Stress-Relief Embrittlement

Stress-relief embrittlement is characterized by a rise in the temperature of transition from brittle to ductile fracture with no change in hardness or strength. The Charpy V-notch (CVN) impact test is a convenient method of measuring susceptibility to embrittlement.

Charpy V-notch impact properties were determined over the temperature range −300 to +200 F, with longitudinal specimens cut from the quarter and midthickness levels of the 2-in.-thick plates. For Steel A, ten specimens each were stress relieved at 900, 950, 1000, and 1050 F for 1, 10, 24, and 100 h. For Steel B, ten specimens each were stress relieved at 950, 1000, 1050, and 1100 F for 1, 10, 24, and 100 h. All specimens were air cooled. The fracture appearance transition temperatures (FATT) were determined by the 50 per cent shear criterion. For comparison the transition temperatures were also determined from lateral expansion measurements by taking the temperature on the curve corresponding to half the value between minimum and maximum lateral expansion.

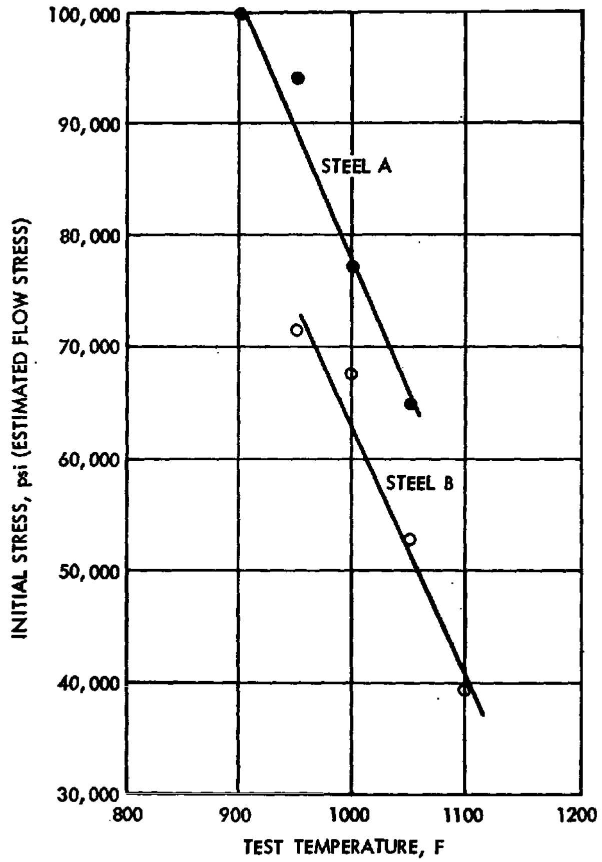

FIG. 1—*Initial stresses in relaxation tests.*

TABLE 2—*Charpy V-notch properties of Steel A after stress-relief treatments.*

Stress-Relieving Temperature and Time	+80 F			−60 F			−120 F			−200 F			Transition Temperature, deg F	
	Energy, ft·lb	Lateral Expansion, mils	Shear, %	Energy, ft·lb	Lateral Expansion, mils	Shear, %	Energy, ft·lb	Lateral Expansion, mils	Shear, %	Energy, ft·lb	Lateral Expansion, mils	Shear, %		
As-received	95	43	100	80	33	75	35	16	30	30	12	5	−100[a]	−80[b]
900 F, 1 h, AC[c]	90	44	100	54	23	60	34	15	30	16	7	2	−80	−65
900 F, 10 h, AC	76	36	100	35	17	35	20	10	8	6	2	0	−30	−50
900 F, 24 h, AC	85	36	98	34	13	30	14	5	5	2	0	0	−30	−40
900 F, 100 h, AC	32	20	30	12	4	5	4	0	0	0	0	0	+160	+60
950 F, 1 h, AC	80	35	100	64	25	50	32	12	20	16	6	2	−60	−70
950 F, 10 h, AC	86	35	96	40	15	30	18	5	5	4	0	0	−30	−40
950 F, 24 h, AC	72	30	86	40	12	14	20	6	0	6	3	0	+10	−10
950 F, 100 h, AC	30	12	30	8	2	0	2	0	0	0	0	0	+130	+80
1000 F, 1 h, AC	95	38	100	50	17	55	32	10	20	16	3	2	−70	−50
1000 F, 10 h, AC	90	40	100	50	20	50	30	10	15	12	1	0	−60	−60
1000 F, 24 h, AC	83	30	95	40	15	30	10	3	5	10	0	0	−20	−60
1000 F, 100 h, AC	60	32	75	30	10	5	14	4	2	2	0	0	+40	+40
1050 F, 1 h, AC	90	40	100	60	20	55	40	10	20	10	0	0	−70	−70
1050 F, 10 h, AC	90	40	100	60	22	50	35	10	15	6	0	0	−60	−70
1050 F, 24 h, AC	95	42	100	55	20	40	30	7	10	16	3	0	−50	−50
1050 F, 100 h, AC	116	45	100	76	35	60	44	20	25	20	8	2	−80	−80

[a] Transition temperature by fracture appearance.

[b] Transition temperature by lateral expansion.

[c] AC = air cooled.

TABLE 3—*Charpy V-notch properties of Steel B after stress-relief treatments.*

Stress-Relieving Temperature and Time	+80 F			−120 F			−200 F			−300 F			Transition Temperature, deg F	
	Energy, ft·lb	Lateral Expansion, mils	Shear, %	Energy, ft·lb	Lateral Expansion, mils	Shear, %	Energy, ft·lb	Lateral Expansion, mils	Shear, %	Energy, ft·lb	Lateral Expansion, mils	Shear, %		
As-received	92	50	100	84	43	90	58	30	50	22	8	0	−200[a]	−200[b]
950 F, 1 h, AC[c]	90	45	100	76	35	100	44	18	50	16	5	0	−200	−170
950 F, 10 h, AC	92	40	100	70	32	95	32	15	20	10	2	0	−180	−180
950 F, 24 h, AC	84	50	100	64	30	80	24	12	10	10	4	0	−150	−130
950 F, 100 h, AC	90	45	100	52	27	65	24	10	0	6	2	0	−130	−140
1000 F, 1 h, AC	95	50	100	78	36	100	55	25	50	20	5	0	−200	−190
1000 F, 10 h, AC	85	45	100	64	35	80	36	15	5	12	5	0	−140	−150
1000 F, 24 h, AC	90	48	100	70	35	80	30	15	5	14	4	0	−140	−160
1000 F, 100 h, AC	92	50	100	58	30	55	25	10	2	8	2	0	−130	−130
1050 F, 1 h, AC	90	50	100	76	37	100	42	20	50	22	6	0	−200	−170
1050 F, 10 h, AC	90	47	100	74	36	100	40	20	30	16	6	0	−190	−180
1050 F, 24 h, AC	110	58	100	75	36	100	50	22	30	10	5	0	−190	−190
1050 F, 100 h, AC	88	46	100	50	27	70	20	12	2	6	2	0	−140	−140
1100 F, 1 h, AC	95	50	100	84	40	100	60	30	50	25	7	0	−200	−200
1100 F, 10 h, AC	90	47	100	75	37	100	42	23	50	20	7	0	−200	−180
1100 F, 24, AC	95	52	100	74	36	95	40	20	10	10	3	0	−170	−160
1100 F, 100 h, AC	106	58	100	80	45	85	42	20	5	10	5	0	−130	−170

[a] Transition temperature by fracture appearance.
[b] Transition temperature by lateral expansion.
[c] AC = air cooled.

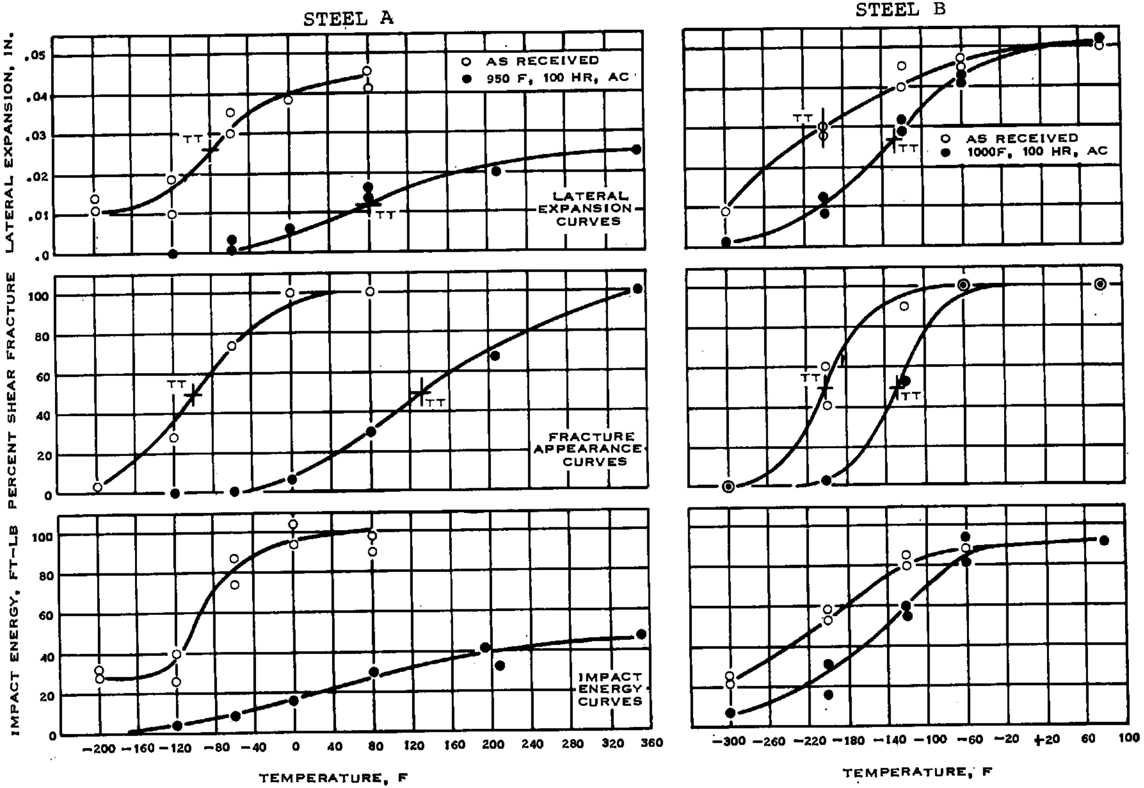

FIG. 2—*Representative Charpy V-notch impact results.*

Stress Relaxation

Relaxation is the reduction of stress in an elastically strained member as the initial elastic strain is replaced by plastic creep strain. Relaxation data can be utilized to develop and evaluate stress-relief treatments.[3]

Relaxation specimens (0.252 in. diameter) of as-received material were tested in a 4000-lb automatic creep relaxation testing machine. The initial stress was set at the approximate yield strength of the material at the testing temperature (see Fig. 1). The plastic strain due to creep was continuously monitored and automatically balanced by small decrements in load, thereby decreasing the elastic strain to maintain a constant total strain (that is, constant specimen length). Load versus time charts were automatically recorded over a 24-h period, permitting calculation of the stress remaining at any given time.

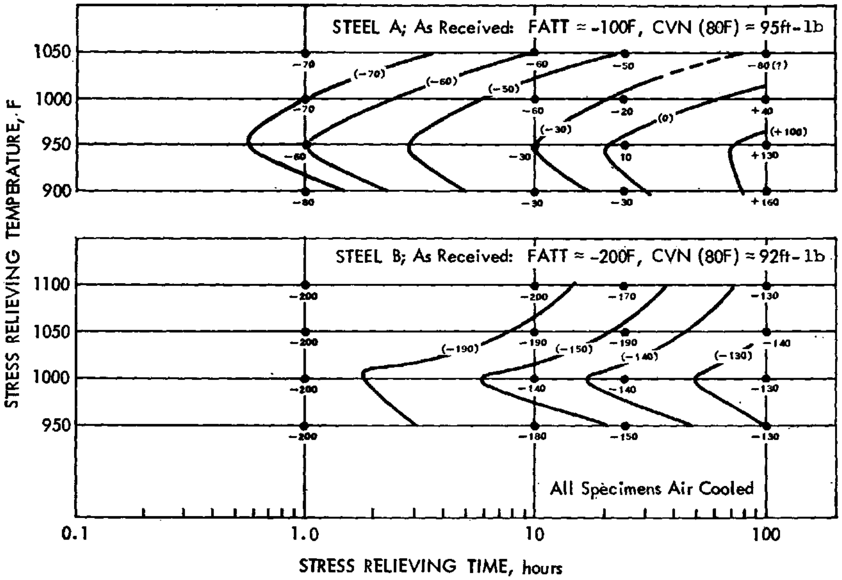

FIG. 3—*Effect of stress-relieving temperature and time on fracture appearance transition temperature.*

Since the test was run under fixed-length conditions, the resultant residual stress levels at a given time and temperature are minimum values that can be obtained by stress relief (maximum amount of stress relief).[3]

---

[3] Freeman, J. W. and Voorhees, H. R., *Relaxation Properties of Steels and Super-Strength Alloys at Elevated Temperatures, ASTM STP 187,* American Society for Testing and Materials, 1956.

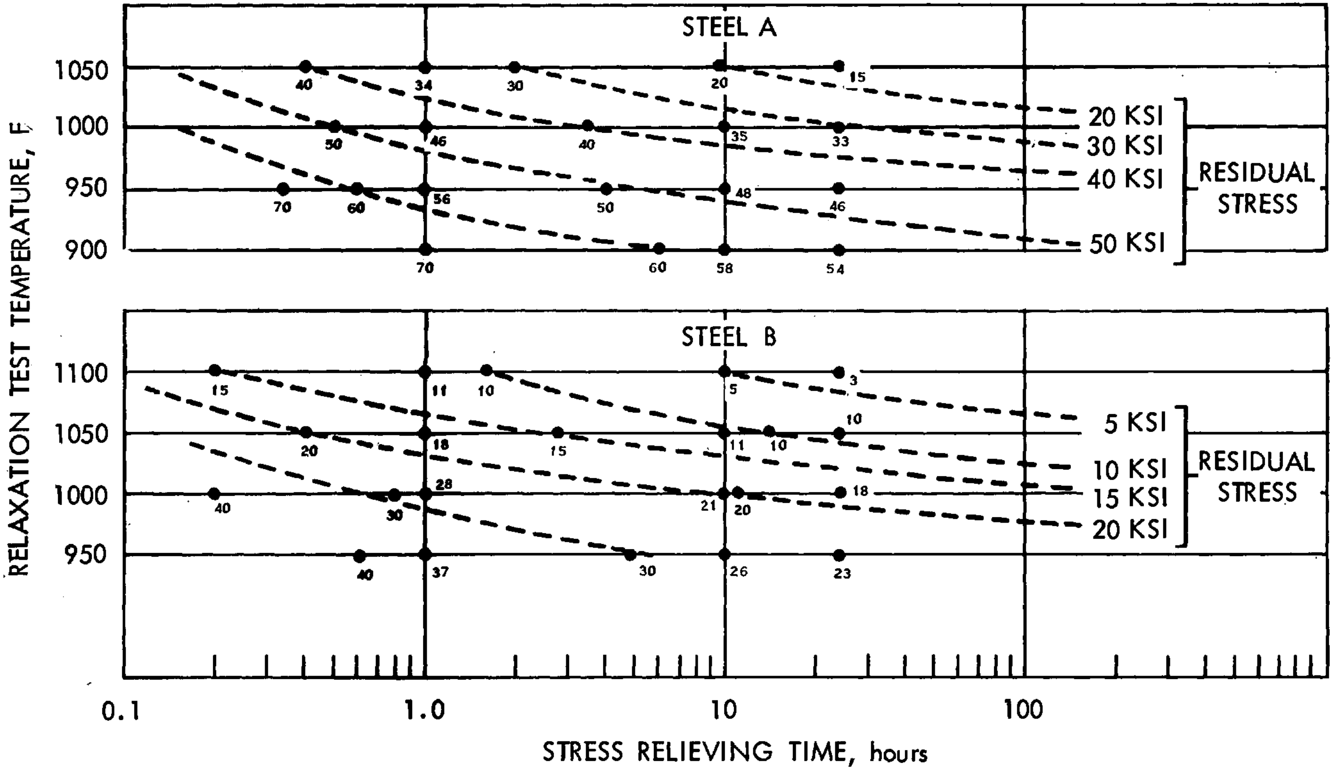

FIG. 4—*Effect of relaxation test temperature and time on residual stress.*

Results and Discussion

Impact Properties

The results of the CVN impact tests of the materials in the as-received condition and after stress relieving are summarized in Tables 2 and 3. Representative CVN impact data are plotted in Fig. 2. The transition temperatures determined by fracture appearance were in good agreement with those determined by lateral expansion.

The data in Tables 2 and 3, and Fig. 2 show that a main effect of the stress-relief treatments is to raise the transition temperature. A considerable increase is seen for Steel A in the temperature range of 900 to 1000 F as stress-relieving time increased from 1 to 100 h. In contrast to a 230 F increase in FATT for Steel A when stress relieved for 100 h at 950 F (compared to the as-received material), Steel B under the same conditions exhibited only a 70 F increase in FATT.

For Steel A, stress relieving for increasing times also caused a drop in shelf energy, indicating an increased propensity for low-energy shear. However, an increase in temperature to 1050 F had little effect on the transition temperature, which remained fairly constant at approximately −70 F with increasing stress-relieving time. The shelf energy, at this stress-relieving temperature, showed an increase with longer holding time.

Steel B was found to be more resistant to an increase in transition temperature than Steel A, and no appreciable drop in shelf energy was observed for the treatments investigated.

Figure 3 shows the effect of stress-relieving temperature and time on the 50 per cent shear FATT for Steels A and B. The data are plotted according to a concept presented by Jaffe.[4] Each dot is accompanied by a number which represents the transition temperature of material stress relieved at the temperature and time specified by the dot. Solid lines were then drawn to indicate the combinations of temperatures and times which produced a given transition temperature. Thus, the solid lines are lines of constant transition temperature. The large increase in the FATT of Steel A after prolonged holding between 900 and 1000 F is apparent.

Relaxation Properties

The results of the stress relaxation tests of the materials in the as-received condition are summarized in Fig. 4. These results are indicative of the effectiveness of heat treatments in reducing residual stresses. Maximum temperatures of 1050 F for Steel A and 1100 F

[4] Jaffe, L. D., "Temper Brittleness of Pressure Vessel Steels," *Welding Journal Research Supplement,* Vol. 30, March 1955, pp. 141s–148s.

for Steel B were used. Higher temperatures, although beneficial from a stress-relieving point of view, are higher than recommended tempering temperatures, and would lead to an unacceptable decrease in yield strength. Expected decreases in residual stress levels were obtained for increases in stress-relieving temperatures and times. Stress-relief treatments consisting of 2 h at maximum temperature produced residual stress levels of 30 ksi (approximately 20 per cent of room temperature yield strength) in Steel A and 10 ksi (10 per cent of yield) in Steel B.

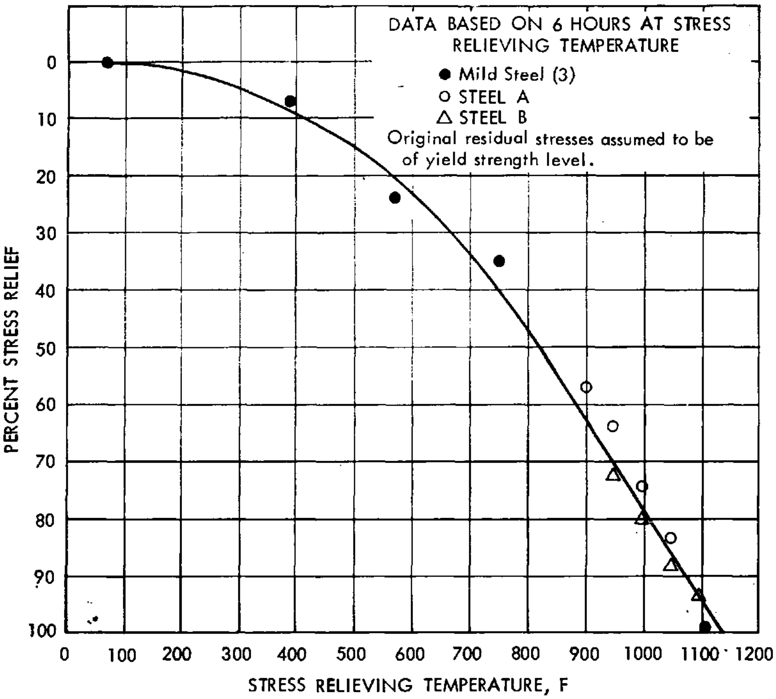

FIG. 5—*Comparsion of stress-relief data.*

A comparison is made in Fig. 5 between residual stresses determined from the stress relaxation tests on Steels A and B, and the residual stresses measured by a dissection technique after annealing butt-welded ¼-in. mild steel plates.[5] The comparison is made on the basis of per cent stress-relief after 6 h at temperature. The agreement of the data is interesting because of the variety of materials being investigated and the different methods used to measure residual stress.

---

[5] Benson, L. E. and Watson, S. J., "Low Temperature Stress Relieving of Mild Steel Welded Structures," *Transactions of the Institute of Welding,* Aug. 1953, pp. 90–95.

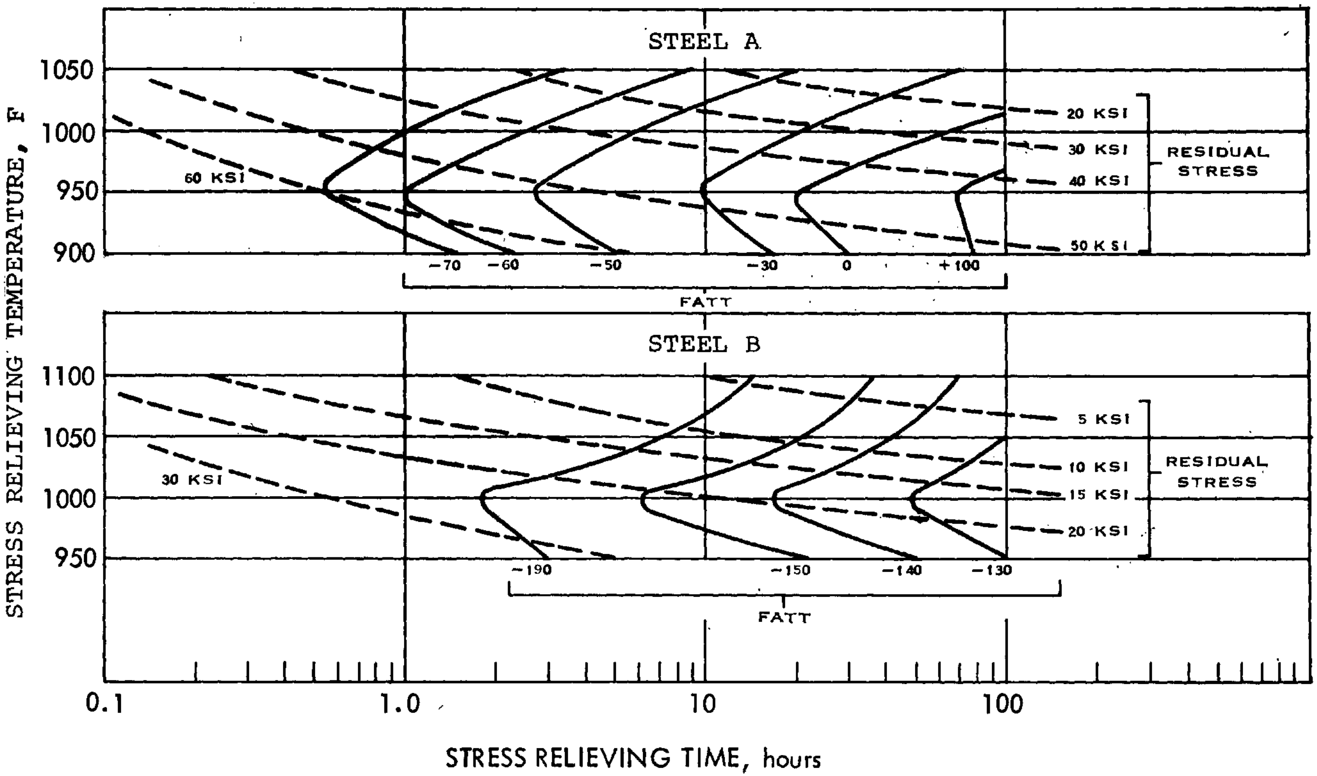

FIG. 6—*Effect of stress-relieving temperature and time on fracture appearance transition temperature and residual stress.*

Optimum Stress-Relief Treatments

The effect of stress-relieving temperature and time on the FATT and residual stress is shown in Fig. 6. The solid lines, reproduced from Fig. 3, represent combinations of temperatures and times which produce a given FATT; the dashed lines, as produced from Fig. 4, represent minimum levels of residual stress obtained for time-temperature combinations.

The interpretation of this diagram may be illustrated by taking one time-temperature combination. For example, consider Steel A specimens stress relieved at 950 F for 10 h. The resulting transition temperature would be −30 F, as compared to an as-received transition temperature of −100 F, and the resultant residual stress, if it were of yield intensity initially, would be approximately 50 ksi. It is to be emphasized that the data are indicative of trends in behavior only, and the values of transition temperature and residual stress shown may not be the values in a structure having the same history as the data point. A "value" of "transition temperature" merely serves as a convenient means of showing the relative susceptibility of a material to brittle fracture.

An optimum stress-relief treatment would maximize the reduction of residual stress, while minimizing the increase in transition temperature due to the treatment. This condition is most closely approached for stress-relief treatments at high temperatures, with the upper limit of the tempering temperature being that beyond which loss of yield strength would result. Temperatures of 950 F for Steel A and 1000 F for Steel B are particularly embrittling, and cause an increase in transition temperature depending upon time at temperature.

Summary

The optimum stress-relief treatment for these steels (that is, the maximum reduction in residual stress accompanied by the minimum increase in transition temperature) is obtained by heat treatment at as high a stress-relieving temperature as possible. The maximum stress-relieving temperature is limited to that which will not result in loss of yield strength.

Short times at high temperatures, and long times at lower temperatures, are not equivalent because of the phenomenon of embrittlement at the lower temperatures.

Acknowledgement

The authors acknowledge the helpful comments of M. R. Gross and R. B. Niederberger. The work presented was performed in the Marine Engineering Laboratory at the Annapolis Division of the Naval Ship Research and Development Center, Annapolis, Md.

APPENDIX

Table of conversion factors.

To Convert From	To	Multiply By
Fahrenheit (temperature)	celsius	$t_c = (t_f - 32)/1.8$
Inch	meter	0.02540
Ksi	newton/meter^2	6.895×10^6
lbf-foot	newton meter	1.256

G. C. Gould[1]

Temper Embrittlement in High Purity 3.5Ni, 1.75Cr, 0.20C Steel

---

REFERENCE: Gould, G. C., **"Temper Embrittlement in High Purity 3.5Ni, 1.75Cr, 0.20C Steel,"** *Temper Embrittlement in Steel, ASTM STP 407,* American Society for Testing and Materials, 1968, pp. 59–73.

ASTRACT: A number of trace elements and some intentional steelmaking additions are known to contribute to the temper embrittlement of susceptible steels. Most of the work done to date has been on individual elements in tempered martensitic steels. This work is concerned with steels in a tempered bainitic condition whose heat treatment and final structure simulate closely that of a large forging, and is designed to study some solute element interactions that were thought to exist. The effects of manganese and molybdenum on embrittlement by phosphorus are investigated as well as that of manganese in combination with silicon. A series of 18 heats of 3.5 nickel, 1.75 chromium, 0.20 carbon steel were made by vacuum-induction melting using high purity components. The levels of phosphorus, manganese, silicon, and molybdenum were varied to measure their influence on temper embrittlement. Embrittlement was measured as a shift in the transition temperature determined from the conventional V-notch Charpy impact tests. Both a step-cooling heat treatment and isothermal exposures at 750, 850, and 950 F were used as embrittling treatments. Isothermal exposures were run to 3500 h with embrittlement measured at 100, 1000, and 3500-h exposure.

It was found that manganese contributes to temper embrittlement and magnifies or interacts with the effect of phosphorus. Molybdenum varying between 0.2 and 0.84 per cent is demonstrated to curtail embrittlement by phosphorus and not contribute to temper embrittlement itself. Silicon alone or with manganese is shown to contribute to temper embrittlement both during isothermal exposures and slow cooling through the critical temperature range. Limits on solutes may be placed so that a Ni-Cr-Mo-V steel will show no significant temper embrittlement during slow cooling or subsequent isothermal exposure.

KEY WORDS: temper embrittlement, transition temperature, brittle fracture, intergranular, isothermal, long exposure, evaluation

Temper embrittlement of low-alloy steels has been a perplexing problem for a long time. Woodfine [*1*][2] and, more recently, Low [*2*] have presented excellent reviews of the work done in the field.

---

[1] Metallurgist, Materials and Processes Laboratory, Power Generation Div., General Electric Co., Schenectady, N. Y.

[2] The italic numbers in brackets refer to the list of references appended to this paper.

TABLE 1—*Chemical analyses of steels, weight per cent.*

Steel No.	C[a]	P[a]	S[a]	Ni	Cr	V	Mo	Mn	Si	Sb[b]	As[b]	Al	Ti	N_2	Sn[b]	O_2[b]
1..	0.20	0.003	0.005	3.71	1.77	0.09	0.057	<0.02	0.02	(<5)	(<10)	<0.005	<0.005	0.059	(8)	12
2..	0.19	0.003	0.004	3.80	1.73	0.09	0.60	<0.02	0.02	(<5)	(<10)	<0.005	<0.005	0.009	(8)	10
3..	0.21	0.003	0.004	3.76	1.70	0.09	0.73	<0.02	0.02	(<5)	(<10)	<0.005	<0.005	0.009	(8)	11
4..	0.18	0.004	0.005	3.65	1.67	0.09	0.84	0.72	0.02	(<5)	(<10)	<0.005	<0.005	0.021	(8)	23
5..	0.19	0.005	0.004	3.75	1.71	0.10	0.75	<0.02	0.03	(<5)	(<10)	<0.005	<0.005	0.010	(8)	41
6..	0.17	0.006	0.004	3.73	1.72	0.10	0.62	<0.02	0.02	(<5)	(<10)	<0.005	<0.005	0.016	(8)	12
7..	0.20	0.007	0.005	3.71	1.71	0.10	0.024	<0.02	0.02	(<5)	(<10)	<0.005	<0.005	0.011	(8)	15
8..	0.17	0.004	0.005	3.72	1.68	0.09	0.62	<0.02	0.12	(<5)	(<10)	<0.005	<0.005	0.005	(8)	31
9..	0.18	0.003	0.005	3.73	1.71	0.09	0.61	<0.02	0.25	6	<10	<0.005	<0.005	0.009	10	13
10..	0.18	0.004	0.004	3.67	1.69	0.09	0.60	0.31	0.24	<5	(<10)	<0.005	<0.005	0.002	9	10
11..	0.21	0.004	0.004	3.65	1.69	0.09	0.60	0.31	0.10	<5	(<10)	<0.005	<0.005	0.001	9	10
12..	0.21	0.003	0.004	3.70	1.70	0.09	0.60	0.31	0.10	11	(<10)	<0.005	<0.005	0.001	8	8
13..	0.18	0.003	0.004	3.68	1.69	0.09	0.60	0.32	0.10	20	(<10)	<0.005	<0.005	0.002	6	45
15..	(0.19)	0.014	(0.004)	(3.71)	(1.70)	(0.09)	0.58	(<0.02)	(0.02)	(<5)	(<10)	(<0.005)	(<0.005)	0.001	(8)	12
169..	0.19	0.017	0.013	3.70	1.59	0.09	0.54	0.20	0.27	4	10	...	...	...	30	..
170..	0.22	0.017	0.013	3.73	1.67	0.09	0.54	0.66	0.27	4	10	...	...	...	10	..
172..	0.22	<0.001	0.006	3.68	1.58	0.11	0.43	1.66	0.26	4	(<10)	...	...	...	(8)	..
173..	0.21	<0.001	0.005	3.74	1.62	0.12	0.54	0.71	0.25	6	(<10)	...	...	...	(8)	..

[a] These determinations were made with wet analytical techniques.

[b] These values are parts per million, ppm.

( ) Although no analyses for these elements were made, it is assumed that these values would be very similar to those in which analyses were made, since the same procedures were used in making these steels. These values are estimates.

Temper embrittlement normally occurs in low-alloy steels when they are held in or cooled through the temperature range 700 to 1050 F. The prime manifestation of temper embrittlement is an increase in the impact transition temperature, and a concomitant feature is a change in mode of brittle fracture from cleavage to intergranular along prior austenite boundaries in the embrittled condition.

The significance of trace elements in contributing to temper embrittlement has been shown clearly by Balajiva et al [*3*] when they demonstrated that a "pure" steel was not susceptible to temper embrittlement. Subsequently, Stevens and Balajiva [*4*] carried out experiments to determine the role of individual solutes on a tempered martensitic 3 nickel, 0.75 chromium, 0.30 carbon steel with and without additions of molybdenum. They determined that phosphorus, antimony, arsenic, tin, manganese, and silicon could each induce temper embrittlement during exposures of 1000 h at 850 F in tempered martensitic structures.

The present work was undertaken using a 3.5 nickel, 1.75 chromium, 0.20 carbon steel heat treated to a bainitic structure.

The purpose of the investigation was to determine:

1. Susceptibility of well-tempered bainitic structures to temper embrittlement during slow cooling and long-time isothermal exposure.
2. Importance, if any, of interactions if two or more embrittling elements are present in the steel.
3. Effect of molybdenum additions on temper embrittlement susceptibility of low-alloy steels in the bainitic condition.

Procedure

Eighteen heats of steel were made for the study of temper embrittlement. The identity and chemical analyses of these steels appear in Table 1. All of the steels fall in the following base composition range:

P	C	Si	Ni	Cr	V	Mn	Mo
0.003 to 0.014	0.17 to 0.22	0.02 to 0.25	3.65 to 3.80	1.69 to 1.77	0.09 to 0.10	0.02 to 1.66	0.02 to 0.84

For these specially melted high purity steels, the iron used was Plast-Iron[3] melting stock, Grade A104. This material is typically 99.99 per cent iron. Alloying elements used were of comparable purity. A typical heat was made by induction melting the chromium, nickel, molybdenum, and iron together in a magnesium oxide (MgO) crucible, bubbling hydrogen (H_2) for 10 min to deoxidize the melt, evacuating the furnace and

---

[3] Trademark, The Glidden Co., Johnstown, Pa.

cycling between liquid and solid until gas evolution ceased, and finally adding the remaining components.

Carefully controlled additions of the elements manganese, molybdenum, phosphorus, silicon, and antimony were made to various melts, and 25-lb ingots were cast under one atmosphere of argon. The ingots were hot forged to bar stock with a 2000 F max forging temperature. Charpy specimen blanks were cut with the long dimension of the specimen parallel to the long dimension of the bar stock. In addition, four other steels of similar base chemistry were carried through the study. They are labeled 169, 170, 172, 173, and their composition also appears in Table 1.

Heat treatment of the specimen blanks was done in batches of 180 blanks, or all of the blanks of three heats of material. The treatment used simulated the thermal cycle and cooling rates of a large forging. A complete description of the heat treatment appears in Appendix I. The final machining and notching was carried out after all heat treating was completed.

Extensive chemical analyses were performed on 17 of the 18 heats. Carbon, phosphorus, and sulfur determinations were made using wet analytical techniques. The oxygen analyses were made by vacuum fusion and the nitrogen by micro-kjeldahl technique. All other determinations were made by means of X-ray spectrography.

Rockwell A hardness measurements were made on ground and lapped specimens of each heat after the double tempering treatment.

Five Charpy specimens were broken at suitable test temperatures to determine the fracture appearance transition temperature (FATT) of each condition tested. Both impact energy and per cent fibrosity were recorded for each test. The temperature at which the area of brittle fracture was 50 per cent of the original area under the notch was designated as the FATT. Embrittlement was measured as an increase in the FATT.

The FATT of each material was determined for each of the following conditions:

1. As-heat treated (unembrittled condition).
2. After a step-cooling embrittling treatment which is fully described in Appendix I.
3. After isothermal exposures at 750, 850, and 950 F for 100, 1000, and 3500 h.

The broken Charpy bar from the lowest test temperature of the as-heat treated condition of Steels 1 to 15 was subjected to metallographic examination. The same procedure was applied to the bar broken at the lowest test temperature from a set of specimens that showed a pronounced rise in FATT. In the event no shift in FATT was found, the specimen from the set exposed 3500 h at 850 F condition was used.

TABLE 2—*FATT from each condition of exposure for all steels, deg F.*

Steel No.	As-Heat Treated	Step-Cooled	750 F			850 F			950 F		
			100 h	1000 h	3500 h	100 h	1000 h	3500 h	100 h	1000 h	3500 h
1	+75	+70	+85	+85	+90	+75	+90	+90	+75	+100	+75
2	−37	−37	−30	−29	−30	−40	−39	−45	−20	−30	−52
3	−132	−132	−135	−135	−130	−134	−140	−145	−135	−130	−135
4	−40	−15	−35	+10	−5	−25	−30	+40	−10	−5	−45
5	−50	−50	−45	−45	−35	−40	−50	−35	−50	−35	−50
6	−80	−55	−75	−65	−50	−80	−65	−55	−40	−50	−65
7	−85	−10	−65	−55	−15	−35	−10	+30	−20	−25	−25
8	+15	+50	+55	+55	+15	+35	+40	+15	+50	+15	+20
9	+50	+50	+60	+50	+45	+40	+50	+65	+50	+35	+30
10	−50	−10	−10	−16	+35	−5	+5	+40	−20	−5	+10
11	−20	−10	−15	−35	−15	−25	−30	−20	−10	−30	−20
12	−25	−15	−15	+5	+5	−5	0	+25	0	0	0
13	+70	+70	+105	+75	+65	+55	+95	+75	+60	+60	+60
15	+45	+45	+45	+40	+40	+50	+55	+50	+45	+40	+45
169	−50	80	−45	−25	35	−5	95	170	10	70	...
170	−70	215	−55	40	110	70	190	215	100	150	...
172	−105	155	...	40	65	80	165	...	30	...	...
173	−100	−5	...	−40	−30	−50	15	...	−40	...	...

TABLE 3—*ASTM grain size and fracture mode of brittle specimens.*

Steel No.	Hardness, R_A	ASTM Grain Size No. (austenitic)	Material Condition	Brittle Fracture Mode	Reaction to Saturated Aqueous Picric Acid Etch
1	63.0	7.0	as-heat treated	cleavage	general
1		7.0	3500 h at 950 F	cleavage	general
2	63.0	7.5	as-heat treated	cleavage	general
2		7.5	100 h at 750 F	cleavage	general
3	64.5	7.5	as-heat treated	cleavage	general
3		7.5	3500 h at 950 F	cleavage	general
4	63.5	6.0	as-heat treated	cleavage	slight grain boundary
4		6.0	3500 h at 850 F	grain boundary	grain boundary
5	65.5	8.0	as-heat treated	cleavage	general
5		8.0	1000 h at 950 F	cleavage	general
6	63.0	7.5	as-heat treated	cleavage	general
6		7.5	3500 h at 750 F	cleavage	slight grain boundary
7	62.0	7.5	as-heat treated	cleavage	general
7		7.5	3500 h at 850 F	grain boundary	slight grain boundary
8	67.0	6.5	as-heat treated	cleavage	general
8		6.5	100 h at 750 F	cleavage	general
9	66.0	5.5	as-heat treated	cleavage	general
9		5.5	3500 h at 850 F	cleavage	slight grain boundary
10	63.5	7.5	as-heat treated	cleavage	slight grain boundary
10		7.5	3500 h at 850 F	grain boundary	grain boundary
11	67.0	6.75	as-heat treated	cleavage	general
11		6.75	3500 h at 950 F	grain boundary	general
12	66.5	6.5	as-heat treated	cleavage	general
12		6.5	3500 h at 850 F	cleavage	general
13	66.0	5.75	as-heat treated	cleavage	some grain boundary
13		5.75	100 h at 750 F	cleavage	some grain boundary
15	64.0	6.75	as-heat treated	cleavage	general
15		6.75	3500 h at 850 F	cleavage	general
169	63.0	6.9	as-heat treated	cleavage	...
169		6.9	step-cooled	grain boundary	grain boundary
170	63.0	6.9	as-heat treated	cleavage	general
172	64.5	6.8	as-heat treated	cleavage	general
173	63.5	6.0	as-heat treated	cleavage	general

TABLE 4—*Embrittlement after step-cooling and isothermal exposure.*

Steel No.	Composition Variation							Step-Cooled Embrittlement, deg F	Max Isothermal Embrittlement, deg F	Max Isothermal Embrittlement Minus Step-Cooled Embrittlement, deg F	Isothermal Exposure Leading to Max Embrittlement
	Mn	P	Si	Mo	As[a]	Sb[a]	Sn[a]				
170	0.66	0.017	0.27	0.54	...	4	...	285	285	0	3500 h at 850 F
172	1.66	<0.001	0.26	0.43	...	4	...	260	270	10	1000 h at 850 F
169	0.20	0.017	0.27	0.54	...	4	...	130	220	90	3500 h at 850 F
173	0.71	<0.001	0.25	0.54	...	6	...	95	115	20	1000 h at 850 F
7	<0.02	0.007	0.02	0.024	<10	<5	<10	75	115	40	3500 h at 850 F
10	0.31	0.004	0.24	0.60	<10	<5	<10	40	90	50	3500 h at 850 F
8	<0.02	0.004	0.12	0.62	<10	<5	<10	35	40	5	100 h at 750 F
6	<0.02	0.006	0.02	0.62	<10	<5	<10	25	30	5	3500 h at 750 F
4	0.72	0.004	0.02	0.84	<10	<5	<10	25	80	55	3500 h at 850 F
11	0.31	0.004	0.10	0.60	<10	<5	9	10	10	0	100 h at 750 F
12	0.31	0.003	0.10	0.60	<10	11	8	10	50	40	3500 h at 850 F
1	<0.02	0.003	0.02	0.057	<10	<5	<10	−5	30	35	1000 h at 950 F
9	<0.02	0.003	0.25	0.61	<10	6	10	0	15	15	3500 h at 850 F
13	0.32	0.003	0.10	0.60	<10	20	6	0	25	25	1000 h at 850 F
2	<0.02	0.003	0.02	0.60	<10	<5	<10	0	17	17	100 h at 750 F
3	<0.02	0.003	0.02	0.73	<10	<5	<10	0	0	0	...
5	<0.02	0.005	0.03	0.75	<10	<5	<10	0	15	15	3500 h at 850 F
15	...	0.014	...	0.58	...	...	...	0	10	10	1000 h at 850 F

[a] These values are parts per million, ppm.

The specimens were etched with saturated aqueous picric acid and the fracture examined to determine the mode of brittle fracture.

The austenite grain size was determined from these same specimens, and further, any pronounced susceptibility to grain boundary attack by picric acid was also noted when it occurred.

Results

Charpy V-Notch Impact Tests

The FATT values as determined for the various exposure conditions appear in Table 2.

Hardness

The hardness values were determined after the full heat treatment and after 3500-h exposure at 950 F. Steels 8, 11, and 12 softened 1.5 points Rockwell A scale while all others remained constant within experimental error; ±½ point. The values are listed in Table 3.

Grain Size

The ASTM grain size number of the prior austenite grains, as determined metallographically, appears in Table 3.

Fracture Mode

Table 3 lists the fracture mode as determined metallographically, and also noted is any pronounced grain boundary etching of specimens subjected to saturated aqueous picric acid etching.

Discussion

For the purpose of analysis of the data only FATT shifts greater than 15 F were considered significant.

Step-Cooling Embrittlement

Only nine of the eighteen steels tested showed any embrittlement. The steels and the amount of step-cooled embrittlement are shown in Table 4.

The shift in transition temperature, determined by comparison of the as-heat treated and step-cooled FATT's, should provide a liberal indication of the amount of embrittlement that a large rotor forging might undergo during its normal production heat treatment cycle.

FATT after Isothermal Exposure

All the steels that exhibited embrittlement after the step-cooling heat treatment embrittled during the isothermal exposure as well. In addition, Steels 1, 12, and 13 also show embrittlement after various isothermal exposures, although no embrittlement was observed after step-cooling. The shift in FATT due to step-cooling, the maximum shift due to isothermal exposure, and the exposure condition for maximum embrittlement for these steels are listed in Table 4.

In 11 of the 18 cases, maximum isothermal embrittlement was observed at 850 F, and in eight of these cases the 3500-h value was the highest indicating that maximum isothermal (850 F) embrittlement may not have been reached. It may be noted also that the step-cooling embrittling exposure yielded the same order of embrittlement as the 850 F isothermal exposure. The relationship between these values can be reasonably expressed by the equation:

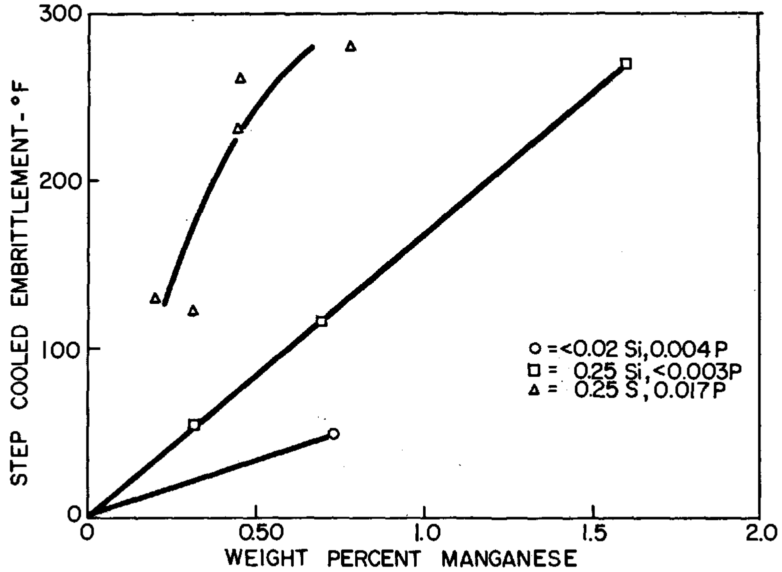

FIG. 1—*Embrittlement by manganese alone, with 0.25 silicon and with 0.25 silicon and 0.017 phosphorus present in Ni-Cr-Mo-V steels.*

$$I = 1.4\,(S_c) + 10$$

where:

I = isothermal embrittlement at 850 F for 3500 h (deg F), and
S_c = embrittlement after step-cooling treatment (deg F).

Insofar as these data go, the step-cooling embrittlement exposure is able to rank the steels showing pronounced embrittlement, but it did not show up those with minor susceptibility; namely, Steels 1, 12, and 13.

Among all the steels that demonstrate isothermal and step-cooled embrittlement, the embrittlement can be attributed to one or more of the elements phosphorus, manganese, silicon, and antimony. The steels in this program that showed no embrittlement can be examined for tolerable levels of impurities. No embrittlement is observed when <0.02 per cent silicon, <0.02 per cent manganese, <0.005 per cent phosphorus, and <6-ppm antimony are present. If only one element is present, considerably greater amounts are required to cause significant embrittlement, but is becomes apparent that interactions between embrittling solutes are important. By examining the levels of silicon and manganese in Steels 8 to 11, it becomes apparent that an interaction between these elements exist. Steel 8 containing 0.12 per cent silicon as the only embrittling solute shows rapid, but definite embrittlement during low-temperature exposure. Steel 9 contains 0.25 per cent silicon and shows a high FATT even after quenching from 1100 F. Steel 10 containing 0.31 per cent manganese and 0.24 per cent silicon shows substantial embrittlement but at a very much lower rate than either Steel 8 or Steel 9. When the level of manganese is high and silicon is low as in Steel 11 containing 0.31 per cent manganese and 0.10 per cent silicon, the embrittlement

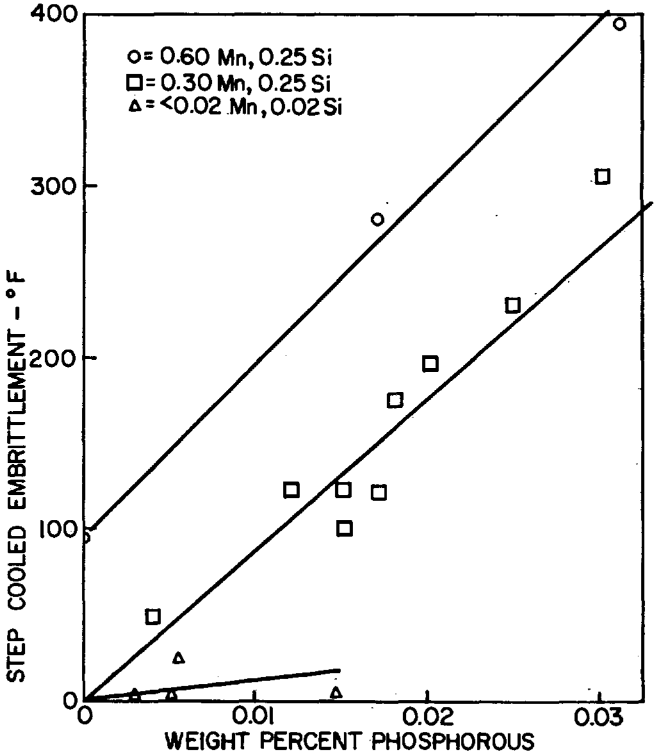

FIG. 2—*Embrittlement by phosphorus alone, with 0.30 manganese and 0.25 silicon and 0.60 manganese and 0.25 silicon present in Ni-Cr-Mo-V steel.*

TABLE 5—*Chemical analyses and amount of embrittlement by step-cooling heat treatment*[a] *of steels from ASTM* [5] *temper brittleness program.*

Steel	Weight %										Water Quenched From 1100 F FATT, deg F	Step-Cooled FATT, deg F	Step-Cooled Embrittlement, deg F
	C	Mn	P	S	Si	Ni	Cr	Mo	V	N			
B	0.20	0.31	0.017	0.013	0.28	3.75	1.56	0.56	0.09	0.006	−50	70	120
C	0.20	0.45	0.017	0.013	0.25	3.77	1.66	0.55	0.09	0.006	−70	160	230
E	0.22	0.31	0.012	0.019	0.27	3.70	1.69	0.54	0.08	0.006	−50	70	120
F	0.21	0.30	0.020	0.015	0.24	3.76	1.68	0.55	0.09	0.007	−80	110	190
G	0.20	0.30	0.025	0.019	0.23	3.80	1.70	0.55	0.09	0.007	−90	140	230
J	0.20	0.25	0.030	0.018	0.27	3.75	1.67	0.58	0.09	0.006	−80	230	310
J-2	0.18	0.34	0.043	0.020	0.25	3.71	1.69	0.55	0.08	0.006	−40	275	315
K	0.21	0.30	0.018	0.016	0.23	3.77	1.65	0.33	0.09	0.006	−90	0	90
L	0.20	0.31	0.018	0.022	0.21	3.75	1.64	0.44	0.08	0.006	−100	35	135
M	0.20	0.31	0.018	0.021	0.25	3.75	1.68	0.67	0.09	0.006	−80	90	170
P	0.21	0.31	0.015	0.024	0.22	3.71	1.68	0.70	0.08	0.007	−40	80	120
T	0.21	0.62	0.031	0.017	0.25	3.75	1.68	0.74	0.08	0.007	−50	340	390
W	0.19	0.46	0.018	0.014	0.27	3.77	1.69	0.54	0.09	0.004	−90	170	260

[a] Preliminary heat treatment is as described in Appendix I except tempering was at 1150 F to a given hardness of 230 to 260 BHN followed by brine quench. The embrittling by step-cooling is according to the program in Appendix I.

appears to be nonexistent. It appears that silicon contributes to a rapid embrittlement of Ni-Cr-Mo-V steel in the temperature range 750 to 900 F and that 0.10 to 0.30 per cent manganese can alter this embrittlement.

Steels 1 and 7 contain 0.003 and 0.007 per cent phosphorus and 0.057 and 0.024 per cent molybdenum, respectively, and both show susceptibility for isothermal temper embrittlement; however, steels with similar chemistry, excepting higher molybdenum content, such as Steels 2, 3, and 15, show no embrittlement with up to 0.014 per cent phosphorus. Molybdenum prevents temper embrittlement by phosphorus, and molybdenum up to 0.75 per cent does not itself contribute to temper embrittlement susceptibility.

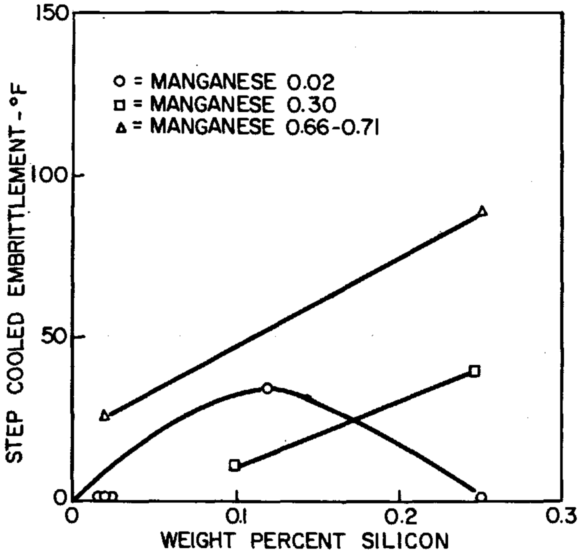

FIG. 3—*Embrittlement by silicon with and without manganese in Ni-Cr-Mo-V steel.*

Further interactions between phosphorus, manganese, and silicon are shown in Fig. 1. Data from Steels 4, 10, 169, 170, 172, and 173 are plotted with embrittlement versus per cent manganese. The tendency for manganese to cause embrittlement with phosphorus <0.003 and silicon <0.02 is small. With 0.25 silicon present, the embrittlement caused by manganese increases, and finally with 0.017 phosphorus and 0.25 silicon present the embrittlement by manganese is large.

The embrittlement caused by phosphorus is summarized in Fig. 2. In addition to the data already discussed in this work, data from the ASTM Task Force on brittle fracture [5] are presented. A tabulation of the composition and transition temperatures of these steels appears in Table 5. The embrittling treatment (step-cooling) and preliminary heat treatment for these alloys are similar to those in this work and shown in Appendix I.

It can be seen that phosphorus embrittles a Ni-Cr-Mo-V steel most when 0.7 manganese and 0.25 silicon are present, substantially when 0.3 manganese and 0.25 silicon are present but practically not at all when manganese and silicon are low, that is, <0.02. It has already been shown, however, that with molybdenum <0.05 phosphorus does indeed cause embrittlement with low silicon and manganese. This would suggest that in some way molybdenum inhibits the effect of phosphorus, but manganese and silicon in sufficient amounts overcome the inhibiting effect of molybdenum.

Figure 3 demonstrates the effect of silicon level and also the effect of manganese level on the silicon effect. In this figure only alloys with <0.005 phosphorus were included.

Steel 15 of this study contains 0.014 phosphorus with low (<0.02) manganese and shows no susceptibility to temper embrittlement whereas Alloys 169 and 170 contain similar phosphorus levels (0.017 phosphorus) and 0.20 and 0.66 manganese, respectively. With these manganese levels present the 850 F isothermal embrittlement rises to a 220 and 285 F shift in FATT for the respective manganese levels.

It appears that manganese in large amounts embrittles Ni-Cr-Mo-V steel (No. 4), that it modifies the effect of silicon, and that it magnifies the effect of phosphorus. Further, it appears that molybdenum can be used to curtail the embrittlement by phosphorus or manganese alone in small amounts.

Conclusions

It becomes apparent from this study that embrittling elements are both reinforcing and negating in their interactions and that a Ni-Cr-Mo-V steel with very small or no susceptibility to isothermal or step-cooled temper embrittlement is possible. It may also be stated that:

1. A 3.5 nickel, 1.7 chromium, 0.50 molybdenum, 0.1 vanadium steel containing <0.02 per cent silicon, <0.02 per cent manganese, <0.004 per cent phosphorus and <6–ppm antimony and <6–ppm tin in a well-tempered bainitic structure will show no susceptibility to temper embrittlement during exposures at 950 F for up to 3500 h.

2. In general, the amount of embrittlement brought about by isothermal exposure appears less for comparable solutes in these bainitic steels than that found by Stevens and Balajiva [*4*] in tempered martensitic steels of similar chemistry. This may be due to the structure *per se* or the higher molybdenum levels in the bainitic steels.

3. Manganese present in the concentration of 0.30 per cent, or higher,

magnifies the embrittlement susceptibility of steels containing phosphorus or silicon or both.

4. Molybdenum additions between 0.60 to 0.75 per cent decrease the amount of temper embrittlement induced by embrittling elements, such as phosphorus in bainitic Ni-Cr-Mo-V steels.
5. Molybdenum in amounts up to 0.75 per cent makes no contribution itself to temper embrittlement susceptibility of Ni-Cr-Mo-V steels.
6. The step-cooling embrittling exposure treatment can rank steels according to their susceptibility in the same order as much longer isothermal exposure.

Acknowledgment

The valuable assistance of H. G. Holtz in both discussion and correlating data is acknowledged.

APPENDIX I

Heat Treatment Cycles

Heat Treatment Used to Establish the Tempered Bainitic Structure

1. Specimen blanks were charged into a furnace at 1000 F and held at this temperature for 14 h.
2. The temperature was raised to 1500 F at the rate of 225 F per h. The temperature was held constant at 1500 F for 24 h.
3. The furnace was then cooled to 300 F at the rate of 100 F per h. A double temper was used, and the first step was 2 h at 1100 F plus an air cool to room temperature. This treatment was followed by 24 h at 1150 F. The specimen blanks were then water quenched from 1150 F to room temperature to insure no embrittlement was encountered while cooling through the 1000 to 700 F temperature range.

Step-Cool Embrittling Treatment

1. Charge into hot furnace and hold 1 h at 1100 F.
2. Furnace cool to 1000 F and hold 15 h.
3. Furnace cool to 975 F and hold 24 h.
4. Furnace cool to 925 F and hold 48 h.
5. Furnace cool to 875 F and hold 72 h.
6. Furnace cool to 600 F.

This treatment has been used as a measure of the susceptibility of various steels to the slow cooling experienced by large rotor forgings during heat treatment.

References

[*1*] Woodfine, B. C., "Temper Brittleness: A Critical Review of the Literature," *Journal of the Iron and Steel Institute,* Vol. 173, 1953, pp. 229.

[2] Low, J. R., "Temper Brittleness—A Review of Recent Work," *Fracture of Engineering Materials,* American Society for Metals, 1964.
[3] Balajiva, K., Cook, R. N., and Worn, D. K., "Effects of Trace Elements on Embrittlement of Steels," *Nature,* Vol. 178, 1956, p. 433.
[4] Stevens, W. and Balajiva, K., "Influence of Minor Elements on the Isothermal Embrittlement of Steels," *Journal of the Iron and Steel Institute,* Vol. 193, 1959, pp. 141–147.
[5] "Report on the Second Program of the Research Group of the ASTM Task Force on Brittle Fractures," unpublished, New York, May 1960.

J. Comon,[1] *P. F. Martin, and P. G. Bastien*

Statistical Study of Factors Influencing Impact Strength of Turbine Generator Rotors—Influence of Temper Embrittlement

REFERENCE: Comon, J., Martin, P. F., and Bastien, P. G., "**Statistical Study of Factors Influencing Impact Strength of Turbine Generator Rotors—Influence of Temper Embrittlement,**" *Temper Embrittlement in Steel, ASTM STP 407,* American Society for Testing and Materials, 1968, pp. 74–89.

ABSTRACT: The authors present a statistical analysis of the results of Charpy V-notch transition temperature obtained on 115 Ni-Cr-Mo-V, Cr-Mo, and Cr-Mo-V rotors. Because heat treatment of these forgings includes a slow cooling after tempering, a particular study or reversible temper embrittlement is made separately. The lowest transition temperature in the regenerated state (without embrittlement) is achieved by lowering the phosphorus and carbon contents, raising alloying element percentages, and accelerating the quench rate. The embrittlement is reduced by keeping phosphorus and arsenic contents to a minimum, and tempering temperature to a maximum, and replacing chromium, nickel, molybdenum, and especially manganese by carbon and vanadium. The tin and antimony contents do not vary sufficiently to enable the authors to determine their effect.

KEY WORDS: temper embrittlement, mechanical properties, statistical analysis correlation, brittle fracture, rotating generators, appearance, transition temperature, evaluation

During 1953 to 1956 five rotor bursts [*1, 2*][2] occurred in the United States. This brought out the fact that these heavy parts, rotating at high speed, could fail catastrophically. Of the five rotors which failed, four were operating near room temperature (turbine exhaust or generator), and had internal defects, but the mechanical properties were within specifications. Following these accidents, a lot of investigations were conducted in the United States and in Europe.

[1] Research engineer, head, and scientific manager, respectively, Société des Forges et Ateliers du Creusot, France. Mr. Bastien is a personal member ASTM.

[2] The italic numbers in brackets refer to the list of references appended to this paper.

One objective of these investigations was to obtain defect-free rotors. Decisive progress resulted from vacuum casting which eliminated flakes and segregation cracks. Another objective was to determine the bursting conditions for large notched disks, with a view to correlate these conditions to the toughness of the pieces. The investigations have shown that a crack starts more easily, that is, at a smaller stress/yield strength ratio [*3,4*] in rotors with a high Charpy V transition temperature. The lowering of the ductile-to-brittle transition temperature is hence one of the means of increasing the factor of safety. It is just as important as improving ultrasonic quality. The present work is a statistical analysis of test results obtained on commercial rotors produced at Le Creusot between 1958 and 1965. It is assumed from the beginning that the Charpy V-notch fracture appearance transition temperature (FATT) is a valid criterion, and we will consider as good any modification tending to lower it.

TABLE 1—*Typical compositions of the principal alloys and number of specimens in each grade.*

Type	Typical Compositions, %							No. of Specimens
	C	Si	Mn	Ni	Cr	Mo	V	
25 NCDV 15	0.25	0.25	0.4	3.5	1.8	0.4	0.10	15
30 NCDV 11	0.30	0.3	0.6	2.7	1.2	0.45	0.11	88
30 CD 12	0.30	0.3	0.6	0.4	3.2	0.6	...	65
26 CDV 4	0.26	0.3	0.65	0.45	1.0	1.1	0.28	41
Various compositions								39
Total								248

TABLE 2—*Limits and average of values of the characteristics of the studied family of rotors.*

	Min	Avg	Max
C	0.21	0.30	0.38
Si	0.11	0.25	0.45
S	0.006	0.011	0.024
P	0.008	0.013	0.028
Mn	0.39	0.61	0.99
Ni	0.12	1.64	3.80
Cr	0.05	1.59	3.37
Mo	0.24	0.57	1.23
V	0.02	0.10	0.33
Sn	0.008	0.015	0.029
As	0.009	0.034	0.052
log VI	1.9	2.65	3.25
θ C	600	639	700
Rkg/mm^2	62.5	79	95
TTR C	−120	−6	150
ΔT C	0	44	250
TTi C	−85	38	150

In the first part of this presentation, the essential rotor characteristics, namely chemical compositions, dimensions, and heat treatments are summarized. In the second part, preliminary considerations and definitions of terms used subsequently are discussed. Finally the statistical calculations, the results obtained, and a method to use these results are presented.

General Considerations on Rotors and Their Manufacture

Four principal chemical compositions were studied:

3.5 per cent Ni-Cr-Mo-V	(AFNOR 25 NCDV 15)	low-pressure turbines and generator rotors
2.7 per cent Ni-Cr-Mo-V	(AFNOR 30 NCDV 11)	
3 per cent Cr-Mo	(AFNOR 30 CD 12)	
Cr-Mo-V	(AFNOR 26 CDV 4)	—IP and HP turbines rotors (analysis selected for creep properties

Other compositions were represented in a more restrictive way (30 NCD 12, 30 NCD 7, 30 NCD 4, 30 NV 4, 30 NDV 14, 22 ND 8). These latter compositions are used only for generator and low pressure turbine rotors. The typical analyses of these materials are given in Table 1 and the range of variations in Table 2.

All rotors are forged from basic electric vacuum poured ingots (Bochumer Verein process) weighing from 20 to 190 metric tons. After forging a preliminary treatment is given (normalizing and tempering). The forgings are then rough machined in the shape of a smooth barrel with two shaft extensions of smaller diameter (generator) or of a barrel with deep grooves (turbines). At this stage the weight varies from 10 to 80 tons, the diameter from 800 to 1600 mm.

Heat treatment is done in a vertical electric furnace, and consists of the following steps:

1. Austenitizing at a temperature 25 to 75 C higher than the critical range for a time sufficient to equalize the temperature throughout the rotor.
2. Quenching, with a mixture of air and water spray. The cooling rate thus obtained is substantially equal to that obtained by oil quenching.
3. Tempering for a time and at a temperature so adjusted as to satisfy the mechanical properties and ensure complete stress relief.
4. A slow cooling in the furnace after tempering (3 to 10 C/h). This cooling rate is at the present time considered necessary to ensure freedom from residual stresses and to maintain dimensional stability.

Mechanical tests are performed after heat treatment to check tensile properties and Charpy V-notch transition temperature. These tests are made on specimens taken from the rotor as indicated in Fig. 1. For each rotor we have tests run in one, two, or three locations. The 248 test results are compiled from 115 rotors.

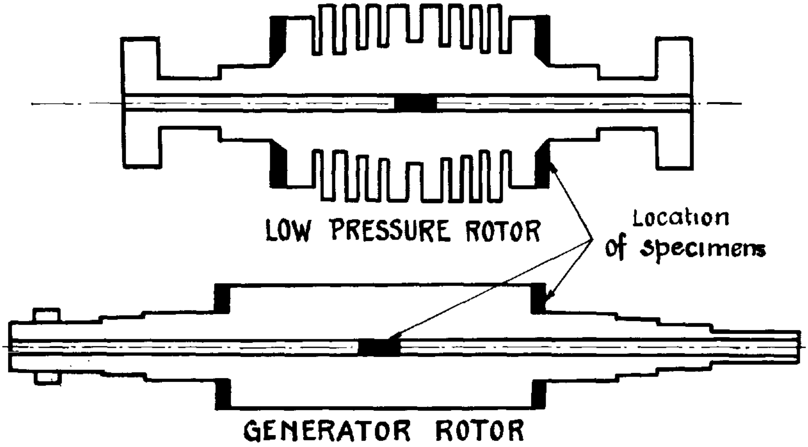

FIG. 1—*Location of specimens in the rotors.*

Preliminary Considerations (for terms and symbols used later in the paper)

Principle of the Calculations

All the statistical calculations consist in establishing correlations between a value G and factors f_1, $f_2 \cdots f_n$ on which it depends.

An equation of the following type is obtained:

$$G = a_0 + a_1f_1 + a_2f_2 + \cdots + a_nf_n$$

The coefficients $a_1a_2 \cdots a_n$ are determined in such a way that there is the minimum deviation between the calculated and measured values of G. This involves applying the method of least squares at n dimensions. The calculations were made on the SFAC'S CAB 500 computer.

Chemical Analyses

In view of the large dimensions of the ingot used, the variation of composition throughout a rotor cannot be neglected. The chemical analyses considered are those made on each test specimen, and not that of the ladle. Components determined are carbon, sulfur, phosphorus, manganese, nickel, chromium, molybdenum, vanadium, copper, tin, and arsenic. But hydrogen, nitrogen, and oxygen contents are very low and uniform due to vacuum casting, so they might be considered as constant (hydrogen (H_2) about 1 ppm, nitrogen (N_2) about 80 ppm, oxygen (O_2) about 20 ppm) and without effect on studied characteristics.

Quenching Rate (VT)

Quenching rate is the average cooling rate from 800 to 600 C in the tested region. This cooling rate is determined by the size of the rotor (diameter and thickness of disks) and the temperature measurements made on rotors of various diameters.

Critical Cooling Rate (VC)

It is the minimum cooling rate required to avoid the formation of proeutectoid ferrite. It is a function of the composition. Throughout the paper we will use the following equation:

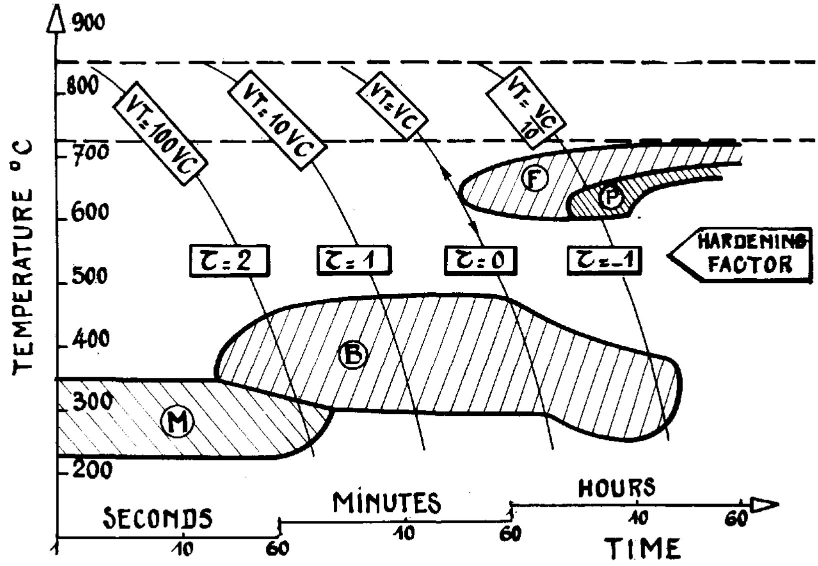

FIG. 2—*Definition of τ, hardening factor.*

$$\log \text{VC (deg C/h)} = 3.7 + \frac{0.955}{0.16 + \text{C}\ \%} - 0.965\ \text{Mn}\ \%$$
$$- 0.751\ \text{Ni}\ \% - 0.54\ \text{Cr}\ \% - 1.96\ \text{Mo}\ \% \ldots\ldots (1)$$

This formula results from a multiple correlation made from 58 continous-cooling-transformation diagrams [*5*].

Hardening Factor (τ)

We call "hardening factor" the function:

$$\tau = \log \frac{\text{VT}}{\text{VC}} = \log \text{VT} - \log \text{VC} \ldots\ldots\ldots\ldots\ldots (2)$$

This factor characterizes the margin between the actual cooling rate and that which would result in a partial transformation in ferrite. It is positive for bainitic structures, nil if the cooling curve is tangent to the nose of the higher range, and negative if the structure contains proeutectoïd ferrite (see Fig. 2). The structure observed with a microscope is, nine times out of ten, in accordance with that predicted by the sign of τ. In the tenth case, the value of τ is sufficiently close to zero to consider the error as negligible. This confirms the adequacy of the evaluation of VT and VC. It should be noted that the rare cases (11 out of 248), where the structure contains some ferrite, result from the fact that the type of alloy is usually chosen in such a way that the structure will be completely bainitic in order to obtain uniform tensile properties.

Equivalent Tempering Temperature (θ)

The duration of the effective tempering varies from 20 to 50 h, between 600 and 700 C. Admitting the existence of a relation between time and temperature, for the sake of simplification, we have kept a single parameter for tempering: it is the "equivalent temperature θ" defined as that of a tempering for 48 h whose effect is the same as the actual tempering treatment [*6*, *7*].

Ultimate Strength (R)

Before starting the study of impact strength we have calculated the relative influence of various factors on the ultimate strength of specimens (entirely bainitic).

The equation is:

$$R_{\text{kg/mm}^2} = 233.8 + 48.6 \text{ C } \% + 4.11 \text{ Mn } \% + 3.43 \text{ Ni } \% + 2.96 \text{ Cr } \% + 14.16 \text{ Mo } \% + 50.5 \text{ V } \% - 0.304\ \theta \text{ C} \quad \ldots (3)$$

It should be noted that the quenching rate does not appear in Eq 3. When the structure is entirely bainitic, the ultimate strength depends only on the chemistry and tempering.

Reference Ultimate Strength (ρ)

It is the ultimate strength of a structure having been tempered at 650 C for 48 h.

$$\rho = R + 0.304\ (\theta - 650) \quad \ldots\ldots\ldots\ldots\ldots (4)$$

According to Eq 3, ρ may be calculated from the chemistry:

$$\rho = 36.1 + 48.6 \text{ C } \% + 4.11 \text{ Mn } \% + 3.43 \text{ Ni } \% + 2.96 \text{ Cr } \% + 14.16 \text{ Mo } \% + 50.5 \text{ V } \% \quad \ldots\ldots\ldots\ldots\ldots (5)$$

However, when we will use the factor ρ in our calculations, it will be the measured value of ρ (according to Eq 4) and not the approximate value calculated from the chemistry.

Transition Temperature in the Regenerated State (TTR)

The impact strength of rotors slowly cooled after tempering is frequently affected by temper embrittlement. We call transition temperature in the regenerated state, that of the metal having received a treatment to eliminate the reversible part of embrittlement. This transition temperature is determined in the Laboratory, by giving the specimen a second tempering of 30 min at the tempering temperature of the forging, followed by water cooling [*8*]; this treatment does not affect the strength of the material.

Initial Transition Temperature (TTi)

It is the transition temperature determined directly from specimens taken from the finished rotor.

Embrittlement (ΔT)

ΔT is the difference between TTi and TTR and constitutes the value of the reversible embrittlement:

$$\Delta T = \text{TTi} - \text{TTR}$$

In the rotors studied, ΔT varies from 0 to 250 C with an average of 44 C.

Study of the Transition Temperature in the Regenerated State

After some trials consisting mainly of graphical studies and of calculations involving various combinations of factors, we found that the best relation giving TTR is:

$$\text{TTR} = -393 - 101\tau + 3.85\rho + 480\ \text{C}\ \% + 1640\ \text{P}\ \% \ldots. (6)$$

The phosphorus content was found to be 98 per cent significant; the other factors had a significance higher than 99.5 per cent.

This equation shows that a lower value of the transition temperature in the regenerated state is obtained when:

1. Hardening factor is high (strong hardenability and drastic quench).
2. Reference ultimate strength is low (low percentage of elements increasing the strength).
3. Carbon content is low.
4. Phosphorus content is low.

It does not appear that softening the material by higher tempering temperature would increase the impact strength in the regenerated state.

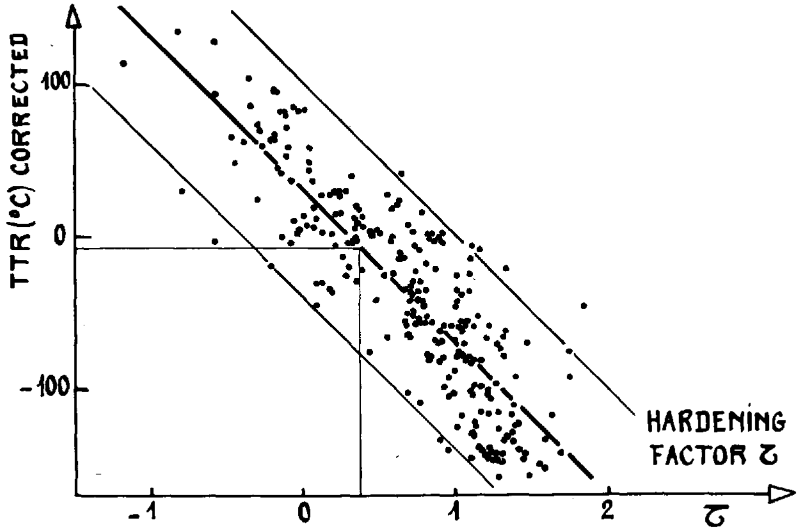

FIG. 3—*Relationship between hardening factor* (τ) *and transition temperature in the degenerated state* (*TTR*).

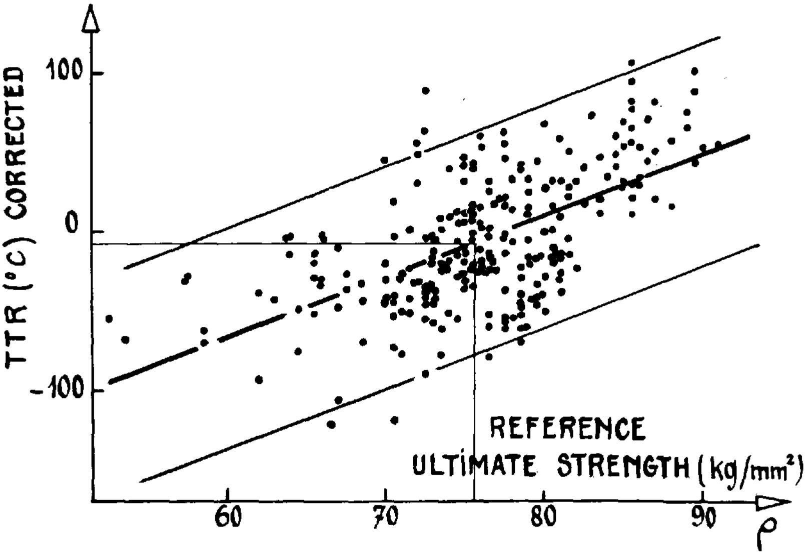

FIG. 4—*Relationship between reference ultimate strength and transition temperature in the regenerated state* (*TTR*).

On Fig. 3 the influence of τ on corrected TTR is shown. The purpose of this correction is to eliminate the variations of other factors. TTR corrected is then the value of transition temperature in the regenerated condition, obtained if all the specimens had a carbon and phosphorus content and a Reference Ultimate Strength equal to the average value of these factors in the rotors studied. Figure 4 shows the influence of the reference ultimate strength on the value of TTR (corrected).

Here, the complexity of the effect of the alloying elements becomes apparent. Some are advantageous when increase the hardenability, and disadvantageous when they increase the ultimate strength. However, most elements have both effects. The carbon, in addition to these two effects has a definite direct influence represented by the coefficient 480.

The effect of each alloying element can be obtained by replacing τ and ρ by the Eqs 1, 2, and 5, resulting in the following equation giving TTR as a function of composition and quenching rate:

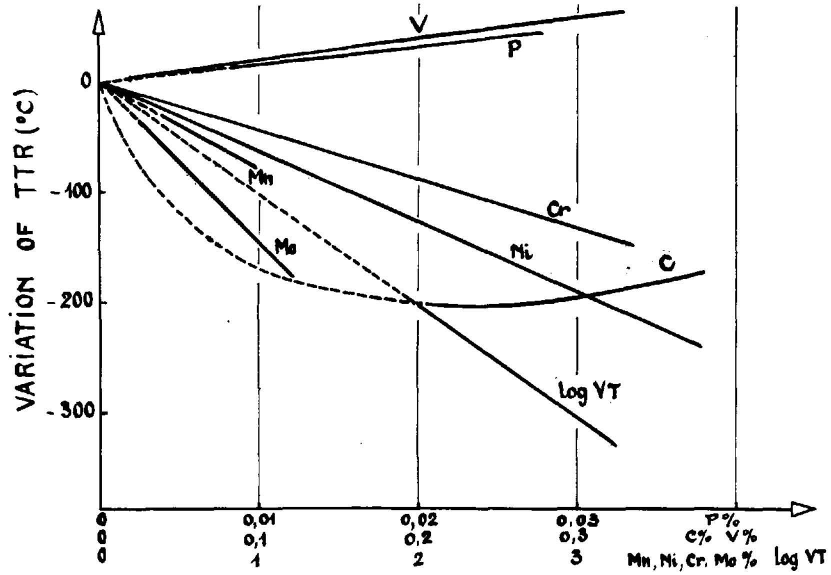

FIG. 5—*Variation of TTR resulting from the variation of each factor.*

$$\begin{aligned}\text{TTR} = {} & +121 + 668\ \text{C}\ \% + \frac{96.5}{0.16 + \text{C}\ \%} + 1640\ \text{P}\ \% \\ & - 81.7\ \text{Mn}\ \% - 62.7\ \text{Ni}\ \% - 43.7\ \text{Cr}\ \% \\ & - 143.5\ \text{Mo}\ \% + 195\ \text{V}\ \% - 101 \log \text{VT} \quad \text{........(7)}\end{aligned}$$

The favorable effect of manganese, nickel, chromium, molybdemum, and quenching rate becomes apparent, as well as the unfavorable effect of vanadium and phosphorus. The influence of carbon is unfavorable above 0.27 per cent but negligible for lower values. This is shown on Fig. 5 which makes it possible to evaluate the variation of TTR resulting from the variation of each element considered separately.

This is for the regenerated condition. We will see that these preliminary conclusions are considerably affected by temper embrittlement.

Study of Temper Embrittlement ΔT

It is not difficult to see that the external specimens are more embrittled than the bore specimens. The most hardenable alloys are also more subject to embrittlement. This statement leads naturally to consider the hardening factor τ as one of the most important to influence ΔT. Taking into account the published data concerning trace elements (impurities) and alloy elements, it was natural to retain as likely factors, phosphorus, arsenic, and silicon. Tempering temperature, carbon, and manganese were retained after graphical studies.

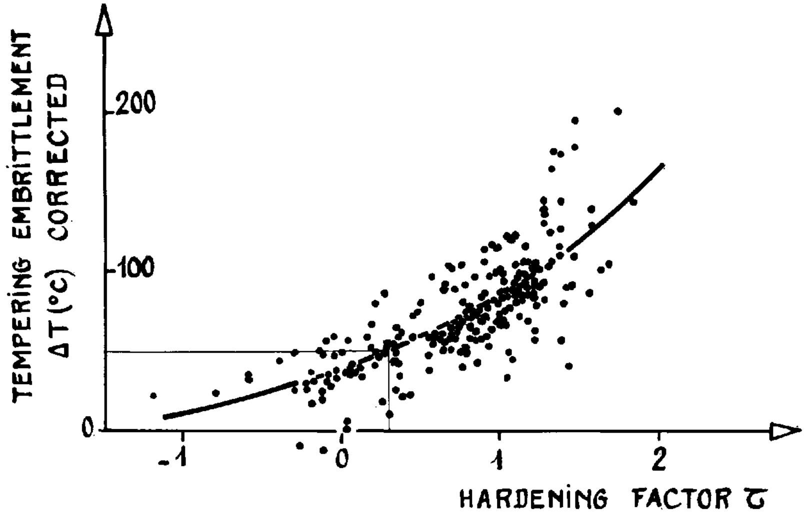

FIG. 6—*Relationship between hardening factor* (τ) *on temper embrittlement* (ΔT).

These factors being chosen, there remained to define the shape of the equation. An equation of the type:

$$\Delta T = a_0 + a_1\tau + a_2\mathrm{P} + a_3\mathrm{C} + \cdots$$

is not satisfactory for two reasons:

1. Because it implies that each factor particularly has a linear effect on ΔT, while the graphical plots indicate an influence increasing gradually.
2. Because it implies that the various influences are additive. But we could observe (it should have been expected) that phosphorus had a severe embrittling effect on alloys with high hardenability, while it had practically no effect on the low ΔT of alloys with low hardenability.

Rather than using cross-products such as P %, × τ, As % × P %, we preferred replacing ΔT by a logarithmic function of ΔT, while keeping the remaining part of the equation in its simple form. Without discussing the complex considerations which enabled us to determine it, the final equation is:

$$\log (\Delta T + 27) = 5.00 - 1.62\ \mathrm{C}\ \% + 10.7\ \mathrm{P}\ \% + 5.18\ \mathrm{As}\ \% + 0.387\ \mathrm{Mn}\ \% - 0.00665\ \theta\ \mathrm{C} + 0.233\ \tau \qquad (8)$$

All the factors are significant to 99.9 per cent except manganese (98 per cent). Silicon, being insignificant, is neglected. As an example, on Fig. 6, we give the effect of τ on ΔT corrected. It must be noted that this equation was established only from specimens that did have an embrittlement factor ($\Delta t \neq 0$). Later application of Eq 8 on specimens for which the embrittlement was nil, confirmed this assumption. For these specimens the equation gives an average embrittlement of 7 C, that we consider as a good approximation.

The qualitative interpretation of this equation is easy: increasing carbon content and tempering temperature tends to decrease temper embrittlement, while phosphorus, arsenic, and manganese have a detrimental effect. It is, however, difficult to draw definite conclusions concerning the means of reducing ΔT, because some of the factors are not independent: it is usually not possible to increase the tempering temperature, without compensating for it by changing the alloy, the required strength being usually well defined. Therefore it is interesting to rewrite Eq 8, replacing τ by its developed form from Eqs 1 and 2 and expressing θ, the equivalent tempering temperature to be made, as a function of the expected strength and composition, Eq 3. We then obtain:

$$\begin{aligned}\log (\Delta \mathrm{T} + 27) = {} & -0.13 - 2.66\ \mathrm{C}\ \% - \frac{0.222}{0.16 + \mathrm{C}\ \%} + 10.7\ \mathrm{P}\ \% \\ & + 5.18\ \mathrm{Ag}\ \% + 0.603\ \mathrm{Mn}\ \% + 0.100\ \mathrm{Ni}\ \% \\ & + 0.061\ \mathrm{Cr}\ \% + 0.47\ \mathrm{Mo}\ \% - 1.105\ \mathrm{V}\ \% \\ & + 0.233 \log \mathrm{VT} + 0.0219\ \mathrm{R} \qquad (9)\end{aligned}$$

The tempering temperature being obviously given by:

$$\begin{aligned}0.304\ \theta = {} & 233.8 + 48.6\ \mathrm{C}\ \% + 4.11\ \mathrm{Mn}\ \% + 3.43\ \mathrm{Ni}\ \% + 2.96\ \mathrm{Cr}\ \% \\ & + 14.6\ \mathrm{Mo}\ \% + 50.5\ \mathrm{V}\ \% - \mathrm{R}\end{aligned}$$

It thus appears that for a given strength, the embrittlement may be reduced by replacing manganese, chromium, nickel, and molybdenum by carbon and vanadium. Of course, the impurities phosphorus and arsenic must be kept to a minimum.

It may be surprising molybdenum is an embrittlement enhancing factor, while it is known to inhibit it. We then must make the following comments:

1. The influence of molybdenum is indirect: according to our findings, molybdenum increases embrittlement because it gives a more hardened structure. In the case of a martensitic structure the properties of which are independent of the quenching cooling rate (VT), we do not believe that we should suspect molybdenum to have a harmful effect.

2. It is generally recognized that a small addition of molybdenum (0.3 per cent) is beneficial. However the range of variation of molybdenum that we have studied is 0.24 to 1.23 per cent where its effect is more complex [*10*]. Therefore we believe that molybdenum is beneficial below 0.3 per cent and detrimental above 0.3 per cent.

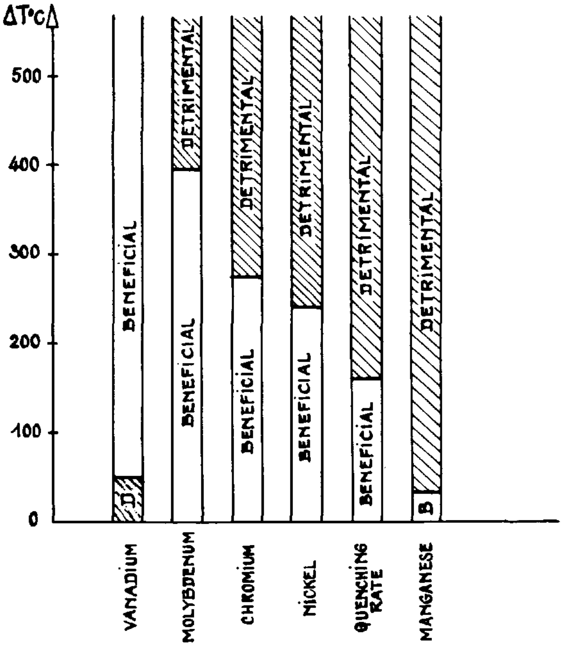

FIG. 7—*Influence of an increase of some factors on the value of TTi versus the value of* ΔT.

3. A late American study on the 25 NCDV 15 [*9*] alloy supports this conclusion (embrittlement increases as molybdenum is increased from 0.3 to 0.7 per cent).

Improvement of Transition Temperature (TTR) of Rotor in Final Condition

The transition temperature in the final condition is:

$$\text{TTi} = \text{TTR} + \Delta T$$

We have found that TTR and ΔT rise as phosphorus is increased.

Furthermore, strength and arsenic are influencial upon ΔT without affecting TTR. Phosphorus, arsenic, and strength should therefore be kept to a minimum to improve TTi.

All other factors (manganese, nickel, chromium, molybdenum, carbon, and quenching rate) have an adverse effect on TTR and ΔT. Thus the direction in which these factors should be varied is not clearly apparent and requires a more involved study. We will give only our conclusions with the warning that they are strict interpretations of the equations and that the results must be carefully considered. The beneficial or detrimental effect of these seven factors depends on the value of ΔT which is considered.

Given an alloy and heat treatment, it is possible, according to the equation established, to calculate the value of ΔT. An increase of manganese content, for instance, will be beneficial if the value of ΔT is less than 32 C. If ΔT is more than 32 C, it will be advantageous to reduce the manganese content in order to meet a better value of TTi. For the other six terms, the mechanism is the same with other critical values of ΔT. Details are given in Fig. 7. But carbon has a still more complex effect, because the critical value of ΔT is a function of the carbon content (see Fig. 8). With high carbon contents and low embrittlement values its effect is detrimental. It is beneficial for the opposite conditions. The border between the two regions is shown on Fig. 8.

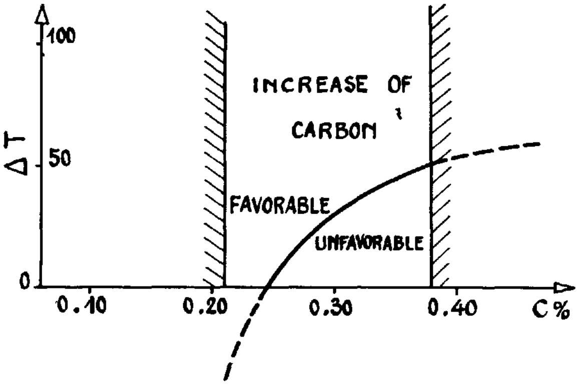

FIG. 8—*Influence of an increase of the carbon content on transition temperature in the final condition versus the value of* ΔT.

As an application of the results of the investigation we determined the influence of the various factors studied in 16 specific instances.

1. Four reference compositions were selected; these are the typical analyses of the four alloy steels: 25 NCDV 15, 30 NCDV 11, 30 CD 12, and 26 CDV 4, (see analyses in Table 1). For each alloy, an expected ultimate strength was selected corresponding to current practice.
2. Two levels of impurities, were considered: one (impure) with 0.015

per cent phosphorus, 0.04 per cent arsenic; the other (pure) with 0.008 per cent phosphorus, 0.01 per cent arsenic.

3. Two quenching cooling rates: the first one (1000 C/h) corresponding to the skin of an average size rotor. The second one (160 C/h) corresponding to the center of the same rotor.

TABLE 3—*Effect of an increase of carbon, manganese, and vanadium contents and of the quenching rate on the transition temperature in some cases.*

	TTR	ΔT	TTi	C	Mn	V	VT
25 NCDV 15:							
impure							
skin	−121	175	54	B	D	B	d
center	−40	105	65	B	D	B	B
pure							
skin	−133	95	−38	B	D	B	B
center	−52	51	−1	B	D	b	B
30 NCDV 11							
impure							
skin	−60	86	26	B	D	B	B
center	21	47	68	B	d	o	B
pure							
skin	−72	40	−32	b	d	d	B
center	9	16	25	d	B	D	B
30 CD 12							
impure							
skin	−41	76	35	B	D	B	B
center	40	40	80	b	d	d	B
pure							
skin	−53	34	−19	o	o	D	B
center	28	13	41	D	B	D	B
26 CDV 4							
impure							
skin	20	13	33	o	B	D	B
center	101	0	101	d	B	D	B
pure							
skin	8	0	8	d	B	D	B
center	89	0	89	d	B	D	B

NOTE—B = beneficial increase.
b = increase slightly beneficial.
o = optimum condition.
d = increase slightly detrimental.
D = detrimental increase.

Table 3 summarizes the results for the 16 combinations thus obtained; the calculated values of TTR ΔT, TTi (which are in good agreement with results obtained commercially), and the direction in which its is desirable to change the four factors: carbon, manganese, vanadium, and quenching rate. We have not mentioned the factors which have an unvariable effect: nickel, chromium, molybdenum—beneficial; phosphorus, arsenic, ultimate strength—detrimental.

It appears in particular that:

1. Carbon and vanadium could advantageously replace manganese

in rotors made of 25 NCDV 15 alloy, while the opposite would be desirable in case of 26 CDV 4 alloy steel rotors.

2. The means of improving 30 NCDV 11, 30 CD 12 alloys depends to a certain extent on the final contents of impurities actually achieved.

3. Minimizing the impurities is beneficial particularly with high alloyed steels 25 NCDV 15, but less with 30 NCDV 11 and 30 CD 12 alloys and has practically no effect with 26 CDV 4 alloy steel.

4. It should be noted that fast quenching rates are always beneficial, except in one case (periphery of rotor 25 NCDV 15 impure), where ΔT is the highest.

It must be stated that these conclusions are derived with the assumption that strength is held constant: when it is concluded, for example, that increasing the vanadium has a beneficial influence, it must be implied that this increase is accompanied with an increase in tempering temperature. The benefit actually results from the latter, and not directly from the former.

A similar study was made in the United States by Boyle et al [*9*]. This study dealt only with the 25 NCDV 15 alloy, and the type of equations was different. However, the conclusions drawn by the authors are similar to our own. The effect of impurities, as shown by our equations corresponds to the observations that we were able to make, when in 1962 we began to replace 30 NCDV 11 by a 25 NCDV 15 alloy: a reduction in impurities appeared as quite necessary to obtain all the advantages of the new alloy.

It must be also stated that such other elements as tin and antimony are known to affect temper embrittlement. The fact that they do not appear in our equations is only because we were unable to determine their effects. The antimony content was measured only on a few rotors. The tin content in the investigated rotors does not vary sufficiently to enable us to determine its action (90 per cent of the specimens had a tin content between 0.010 and 0.020 per cent). But we do not deny the importance of such elements.

Conclusions

We think the essential information has been derived from tests made on *commercial* orders. It might appear, however, that part of the conclusion is missing: we did not mention the search for the optimum composition, that is, making it possible to obtain the lowest transition temperature while remaining in the *n* dimensions region as defined by the composition range of the family of forgings considered. It appears that the optimum to which our calculations should lead would not have been realistic. It would be necessary, in fact, to introduce many limitations to the permissible variation of the composition: for instance, tempering temperature must not be too high, but only below critical range temperature. Other conditions, about such properties as creep, ultrasonic permeability, magnetic properties, and price, should have to be set forth. We have not carried out our study this far. It appears, however, that the use of 25 NCDV 15 alloy with a minimum of impurities, with fast quenching rates throughout the mass, together with the highest possible tempering temperature, will result in a transition temperature near the optimum. Therefore, during the next ten years, we would not expect to report an advance equivalent to that achieved during the last decade. To solve the problems resulting from increasing sizes and improved mechanical properties, new processes, with new types of alloy steels might be necessary.

The present study covers "embrittlement" resulting from slow cooling after tempering. Outside the effects of metallurgical factors, embrittlement may be reduced by the use of faster cooling rates after tempering. A critical study of the dimensional stability, during machining or in service, should permit a gradual increase of the cooling rates after tempering.

Lastly, although such results were obtained on heavy components such as commercial rotors, we believe that the results can be applied to a wider field of application, for example, in high strength weldable steels. It is likely that the 25 NCDV 15 alloy with a lower carbon content will be successful as indicated by tests in the United States.

References

[*1*] Thum, E. E., "Recent Accidents With Large Forgings," *Metal Progress,* Vol. 69, No. 2, Feb. 1956, pp. 49–57.

[*2*] De Forest, D. R. et al, "Investigation of the Generator Rotor Burst at the Pittsburg Station," ASME Paper 57-PWR-12, American Society of Mechanical Engineers Power Division Conference, Allentown, Pa. 21–23 Oct. 1957.

[*3*] Winne, D. H. and Wundt, B. M., "Application of the Griffith-Irwin Theory of Crack Propagation to the Bursting Behavior of Disks, *Transactions,* American Society of Mechanical Engineers, Vol. 80, 1958, pp. 1643–1658.

[*4*] Brothers, A. J., Newhouse, D. L., and Wundt, B. M., "Results of Bursting Tests of Alloy Steel Disks and Their Application to Design Against Brittle Fracture," ASTM Annual Meeting, Lafayette, Ind., 13–18 June 1965.

[*5*] Maynier Ph. and Toitot M., "Vitesse critique des aciers faiblement alliés," Feb. 1964, SFAC paper, not published.

[*6*] Maynier Ph. et al, "Etablissement d'une équivalence entre le temps et la température d'austénitisation. Communication presented at the journées d'Automne 1965," *Memoires Scientifiques de la Revue de Metallurgie,* Vol. 43, No. 12, 1966, p. 997.

[*7*] Hollomon J. H. and Jaffe L. D., "Time-Temperature Relations in Tempering Steels," *Transactions,* American Society of Mechanical Engineers, Technical Publication No. 103, 1965.

[*8*] Jaffe L. D. and Buffum, D. C., "Réversibilité de la fragilité de revenu," *Revue de Métallurgie,* Vol. 48, 1951, pp. 609–612.

[*9*] Boyle, C. J. et al, "Further Progress in the Development of Large Steam Turbine and Generator Rotors," ASTM Annual Meeting, Lafayette, Ind., 13–18 June 1965.

[*10*] Powers, A. E., "A Study of Temper Embrittleness in Cr-Mn Steel Containing Large Amounts of Molybdenum, Tungsten, and Vanadium," *Journal of the Iron and Steel Institute,* Vol. 186, No. 3, 1957, p. 323.

G. C. Gould[1]

Long Time Isothermal Embrittlement in 3.5Ni, 1.75Cr, 0.50Mo, 0.20C Steel

REFERENCE: Gould, G. C., **"Long Time Isothermal Embrittlement in 3.5Ni, 1.75Cr, 0.50Mo, 0.20C Steel,"** *Temper Embrittlement in Steel, ASTM STP 407,* American Society for Testing and Materials, 1968, pp. 90–105.

ABSTRACT: Eighteen commercial heats of Ni-Cr-Mo-V steel have been subjected to both step-cooling embrittling heat treatments and isothermal exposures at 750, 850, 950, and 1050 F for times up to 40,000 h. Embrittlement was measured in the as-heat treated condition on both rotor forgings and bucket wheel forgings, as well as in a de-embrittled condition after water quenching from 1100 F. The steels were heat treated to a bainitic structure and tempered for a minimum of 24 h at 1100 F. The composition, including antimony, arsenic, and tin, along with the mechanical properties of each steel in the specimen, are included in the data. The temper embrittlement was measured as a shift in transition temperature as determined by the conventional V-notch Charpy test. The materials studied include both silicon and vacuum-carbon deoxidized steels, and a difference in rate of isothermal embrittlement is noted. The silicon deoxidized steels show a greater rate of embrittlement, and total embrittlement, at 850 F than at 750 F; vacuum-carbon deoxidized heats do not show this difference. The maximum amount of embrittlement during isothermal exposure is shown to decrease with increasing exposure temperature, with embrittlement very small at 1050 F exposures.

The reversibility of the embrittling reaction is demonstrated using material that had been isothermally embrittled for 4800 h at 850 F. Removal of most of the embrittlement was accomplished by 20-h exposure at 1050 F, and embrittlement was measured again after isothermal exposure for 100, 1000, and 2800 h at 850 F. The reaction is shown to be fully reversible, but little insight into the mechanism is gained. In addition, it is demonstrated that exposures of both embrittlement and nonembrittled steels at higher temperatures in the embrittling temperature range (1000 to 1100 F) cause the transition temperature to shift to a common value; the nonembrittled steel demonstrating rapid embrittlement, while the embrittled steel de-embrittles to the same transition temperature which is apparently characteristic of the final exposure temperature. It can be shown that temper embrittlement, measured as an increase in transition temperature by the conventional V-notch Charpy test, can be suppressed by avoiding long exposure in

---

[1] Metallurgist, Materials and Process Laboratory, Power Generation Div., General Electric Co., Schenectady, N.Y.

the temperature range 750 to 1000 F during heat treatment. However, if long exposures in the 750 to 1000 F temperature range do occur either during heat treatment, fabrication, or subsequent service, it appears that temper embrittlement of present commercial Ni-Cr-Mo-V steels is unavoidable.

KEY WORDS: temper embrittlement, fracture, transition temperature, brittle, intergranular, isothermal, long exposure

Temper embrittlement has been a long-standing metallurgical problem with the heat treatment of low-alloy steels. Embrittlement is observed after exposure of a susceptible steel to the temperature range 700 to 1050 F. The exposure may be isothermal or not, with embrittlement observed in either case. The prime manifestation of temper embrittlement is an increase in the notched bar impact transition temperatures, with the mode of brittle fracture changing from cleavage in the unembrittled condition to intergranular along prior austenite grain boundaries in temper embrittled steels. The impact energy of an embrittled steel is not impaired unless it is measured below the transition temperature of the steel. Although the mechanism of temper embrittlement is not known, the role of impurity and trace elements has been explored by Balajiva et al [*1*],[2] Stevens and Balajiva [*2*], and others. A thorough critical review of the work done on temper embrittlement was written by Woodfine [*3*] and more recently updated by Low [*4*].

The increased size of some turbine-generator rotors has caused strength and toughness requirements to reach values necessitating a material change from Ni-Mo-V (3.5 nickel, 0.50 molybdenum, 0.20 carbon, 0.10 vanadium) to a Ni-Cr-Mo-V (3.5 nickel, 1.75 chromium, 0.50 molybdenum, 0.20 carbon, 0.10 vanadium) steel in some cases. These developments have been discussed in detail by Boyle et al [*5,6*]. Early in the experience with Ni-Cr-Mo-V steel, the susceptibility of these steels to temper embrittlement became apparent.

A surveillance program of all Ni-Cr-Mo-V steels was instituted some years ago by the Large Steam Turbine Division of the General Electric Co. In this program specimens of these steels were placed in isothermal exposure conditions at temperatures at, and above, their intended service temperatures to determine both their stability at present operating temperatures and their potential for application at higher temperatures.

Procedure

Both turbine rotors and bucket wheels are melted to the same chemical specification. The nominal composition is 3.5 nickel, 1.75 chromium, 0.50 molybdenum, 0.20 carbon, 0.10 vanadium. The forgings range in

---

[2] The italic numbers in brackets refer to the list of references appended to this paper.

TABLE 1—*Chemical composition and mechanical properties of steels subjected to isothermal exposure.*

Steel	Composition, weight %									ppm			Mechanical Properties			
	C	Mn	P	S	Si	Ni	Cr	Mo	V	As	Sb	Sn	Tensile Strength, kpsi	0.02% Yield Strength, kpsi	Elongation, %	Reduction of Area, %
FAH	0.24	0.66	0.019	0.022	0.18	2.68	1.35	0.48	0.08	100	27	100	105	81	24	58
FAJ	0.27	0.31	0.012	0.010	0.26	2.55	1.46	0.61	0.02	95	19	73	97	69	23	57
FAN	0.30	0.44	0.008	0.016	0.26	2.76	1.36	0.59	0.10	57	9	22	115	94	22	60
FAP	0.29	0.37	0.013	0.011	0.24	2.72	1.46	0.59	0.13	81	19	85	113	96	24	63
FAY	0.29	0.34	0.008	0.008	0.28	3.35	1.69	0.46	0.14	110	15	210	128	106	21	61
FAZ[a]	0.21	0.28	0.007	0.014	0.02	3.53	1.59	0.49	0.11	104	28	93	122	101	21	64
FBB[b]	0.24	0.30	0.008	0.012	0.27	3.45	1.74	0.50	0.11	55	10	63	151	124	20	61
FBC[a]	0.25	0.31	0.008	0.009	0.02	3.57	1.80	0.39	0.10	120	16	200	120	102	23	65
FBD[a]	0.23	0.31	0.007	0.010	0.03	3.58	1.79	0.49	0.14	92	27	190	119	96	20	66
FBE[a]	0.23	0.29	0.007	0.010	0.04	3.52	1.70	0.48	0.12	61	24	210	132	109	21	64
FBG[a]	0.26	0.34	0.010	0.011	0.05	3.66	1.79	0.36	0.13	70	19	160	112	89	23	71
FBH[a]	0.27	0.26	0.012	0.014	0.01	3.52	1.81	0.42	0.12	80	20	120	130	108	20	64
FBJ[a]	0.20	0.29	0.010	0.013	0.03	3.54	1.56	0.37	0.09	50	25	91	114	95	19	52
FBK	0.27	0.24	0.012	0.010	0.30	3.44	1.72	0.54	0.09	85	12	108	126	101	20	62
FBL[a]	0.25	0.26	0.010	0.023	0.02	3.57	1.77	0.50	0.07	90	11	40	117	95	20	56
FBM[a]	0.25	0.39	0.010	0.019	0.03	3.55	1.83	0.38	0.10	90	10	70	125	102	20	62
FBN[a,b]	0.23	0.32	0.007	0.013	0.03	3.49	1.71	0.53	0.09	40	8	42	133	112	20	67
FBP[a]	0.27	0.36	0.010	0.014	0.01	3.48	1.77	0.41	0.09	44	8	58	114	93	21	55

[a] These steels were deoxidized by means of carbon-vacuum technique, while the remainder were silicon killed and vacuum degassed.

[b] Bucket wheel forging, others are rotor forgings.

size up to 150,000 lb with diameters ranging up to 60 in. The size of the pieces necessitate long, slow, heat treatments ending in slow cooling from 1100 F tempering. This slow cooling gives rise to some embrittlement as the forgings are received. Portions of each forging from the center core trepan were placed in furnaces held at 650, 750, and 850 F. The temperatures were regulated within ±5 F by means of a controller on each furnace, and readings were taken daily to ensure that thermostats were functioning. The code number, chemical composition, and mechanical properties of each steel are listed in Table 1.

The transition temperature of each material was determined after the rotor heat treatment but before it was placed in the exposure program. Material was removed from the various exposure furnaces after exposures of 3000, 8800, 18,000, 20,000, 30,000 and 40,000 h, and the transition temperature was determined for each case. Additional exposures of 10, 100, and 1000 h were made at 850, 950, and 1050 F on materials FAN, FAZ, and FBM, and the transition temperatures were also determined for each of these cases.

The transition temperature determination was made using five conventional V-notch Charpy bars and a 120 ft·lb Tinius Olsen impact tester. The transition temperature was measured by reading the percent fibrous fracture in each broken Charpy specimen and designating the transition temperature as the temperature at which the area of brittle fracture, cleavage, or intergranular, equaled 50 percent of the original area under the notch (80 mm^2). This transition temperature is conventionally called the fracture appearance transition temperature (FATT).

As subsequent tests were made on a material in the program, the number of Charpy test specimens was reduced to four. In some cases, after the material was heat treated as a rotor, specimens were removed and subjected to a heat treatment consisting of 1100 F for 1 h followed by a water quench. This treatment is known [*4*] to remove all temper embrittlement incurred during rotor heat treatment and gives the unembrittled FATT for a given composition and microstructure. The FATT was measured after a step-cooling heat treatment in many cases. This heat treatment consisted of the following steps:

1. Charge material into a hot furnace at 1100 F.
2. Furnace cool to 1000 F and hold 15 h.
3. Furnace cool to 975 F and hold 24 h.
4. Furnace cool to 925 F and hold 48 h.
5. Furnace cool to 875 F and hold 72 h.
6. Furnace cool to 600 F and finally cooled to room temperature.

This treatment has been devised to give a greater amount of temper embrittlement than that incurred during a rotor heat treatment with its slow cooling rate from tempering temperatures. It also is known to

TABLE 2—*Fracture appearance transition temperatures and embrittlement of all steels after various exposure conditions.*

Steel	Water Quenched FATT, deg F^a	Step-Cooled FATT, deg F^b	Step-Cooled Embrittlement, deg F^c	Exposure Time, h	650 F Isothermal Exposure			750 F Isothermal Exposure			850 F Isothermal Exposure		
					FATT, deg F	Isothermal Embrittlement, deg F^d	Total Embrittlement, deg F^e	FATT, deg F	Isothermal Embrittlement, deg F	Total Embrittlement, deg F	FATT, deg F	Isothermal Embrittlement, deg F	Total Embrittlement, deg F
FAH......	−80	...	...	as-received	35	...	115	35	...	115	35	...	115
				100	...	...	...	60	25	140	150	115	230
				1 000	...	...	...	120	85	200	340	305	420
				10 000	...	...	...	315	280	395	350	315	430
				20 000	...	...	...	315	280	395	400	365	480
				32 300	...	...	...	310	275	390	400	365	480
FAJ......	50	...	...	as-received	75	...	25	75	...	25	75	...	25
				100	...	...	...	100	25	50	105	30	55
				1 000	...	...	...	100	25	50	175	100	125
				10 000	...	...	...	170	95	120	250	175	200
				20 000	...	...	...	235	160	185	305	230	255
				32 300	...	...	...	260	185	210	325	250	275
FAN.....	45	...	...	as-received	75	...	30	75	...	30	75	...	30
				3 000	85	10	40	140	65	95	205	130	160
				8 800	90	15	45	190	115	145	300	225	255
				18 000	115	40	70	210	135	165	285	210	240
				30 000	110	35	65	235	160	190	265	190	220
FAP......	20	...	...	as-received	65	...	45	65	...	45	65	...	45
				3 000	60	−5	40	120	55	100	170	105	150
				8 800	70	5	50	170	105	150	295	230	275
				18 000	85	20	65	185	120	165	290	225	270
				30 000	95	30	75	200	135	180	300	235	280

FAY......	−40	100	140	as-received	25	...	65	25	...	65	25	...	65
				8 800	45	20	85	165	140	205	285	260	325
				20 000	55	30	95	185	160	225	320	295	360
				40 000	...	...	...	175	150	215	...	...	...
FAZ......	−50	65	115	as-received	0	...	50	0	...	50	0	...	50
				8 800	15	15	65	130	130	180	145	145	195
				20 000	35	35	85	205	205	255	140	140	190
				40 000	...	...	...	190	190	240	...	...	...
				de-embrittled 20 h at 1050 F	−25	...	0	−25	...	0	−25	...	0
				de-embrittled plus 100 h	...	...	...	...	...	...	25	50	50
				de-embrittled plus 1000 h	...	...	...	...	...	...	110	135	135
				de-embrittled plus 2800 h	...	...	...	...	...	...	155	180	180
FBB......	...	...	...	as-received	−50	...	...	−50	...	...	−50	...	...
				8 800	−30	20	...	65	115	...	285	335	...
				20 000	−5	45	...	115	165	...	465	515	...
FBC......	−105	...	...	as-received	−20	...	85	−20	...	85	−20	...	85
				8 800	−35	−15	70	65	85	170	60	80	165
				20 000	−10	10	95	105	125	210	85	105	190
FBD......	−25	85	110	as-received	−5	...	20	−5	...	20	−5	...	20
				8 800	0	5	25	145	150	170	145	150	170
				20 000	20	25	45	200	205	225	170	175	195
FBE......	−30	85	115	as-received	−5	...	25	−5	...	25	−5	...	25
				8 800	5	10	35	165	170	195	130	135	160
				20 000	45	50	75	185	190	215	165	170	195

TABLE 2—*Continued*

Steel	Water Quenched FATT, deg F[a]	Step-Cooled FATT, deg F[b]	Step-Cooled Embrittlement, deg F[c]	Exposure Time, h	650 F Isothermal Exposure			750 F Isothermal Exposure			850 F Isothremal Exposure		
					FATT, deg F	Isothermal Embrittlement, deg F	Total Embrittlement, deg F[e]	FATT, deg F	Isothermal Embrittlement, deg F	Total Embrittlement, deg F	FATT, deg F	Isothermal Embrittlement, deg F	Total Embrittlement, deg F
FBG......	−130	−10	120	as-received	−85	...	45	−85	...	45	−85	...	45
				8 800	−80	5	50	25	110	155	20	105	150
				20 000	−65	20	65	70	155	200	65	150	195
FBH......	−60	65	125	as-received	55	...	115	55	...	115	55	...	115
				8 800	75	20	135	130	75	190	160	105	220
				20 000	70	15	130	180	125	240	155	100	215
FBJ......	−20	80	100	as-received	−20	...	0	−20	...	0	−20	...	0
				8 800	−65	−45	−45	90	110	110	65	85	85
				20 000	−30	−10	−10	75	95	95	105	125	125
FBK......	40	160	120	as-received	55	...	15	55	...	16	55	...	15
				8 800	90	35	50	100	45	60	125	70	85
				20 000	85	30	45	120	65	80	145	90	105
FBL......	−65	30	85	as-received	−25	...	40	−25	...	40	−25	...	40
				8 800	0	25	65	135	160	200	130	155	195
				20 000	−5	20	60	130	155	195	165	190	230
FBM.....	−90	5	95	as-received	−5	...	85	−5	...	85	−5	...	85
				8 800	−10	−5	80	135	140	225	95	100	185
				20 000	−5	0	85	155	160	245	105	110	195
FBN......	−130	−65	65	as-received	−95	...	35	−95	...	35	−95	...	35
				8 800	−70	25	60	45	140	175	5	100	135
				20 000	−70	25	60	135	230	265	90	185	220

FBP......	−65	−55	10	as-received	−65	...	0	−65	...	0	−65	...	0
				3 000	−82	−17	−17	−60	5	5	−35	30	30
				8 800	−80	−15	−15	−35	30	30	−5	60	60
				20 000	−70	−5	−5	15	80	80	20	85	85

[a] FATT measured after 1 h 1100 F exposure followed by water quench to remove all temper embrittlement.

[b] FATT after step-cooling cycle was applied to as-received steel.

[c] Step-cooled embrittlement equals step-cooled FATT minus water quenched FATT.

[d] Isothermal embrittlement equals isothermal FATT minus as-received FATT.

[e] Total embrittlement equals isothermal or as-received FATT minus water quenched FATT.

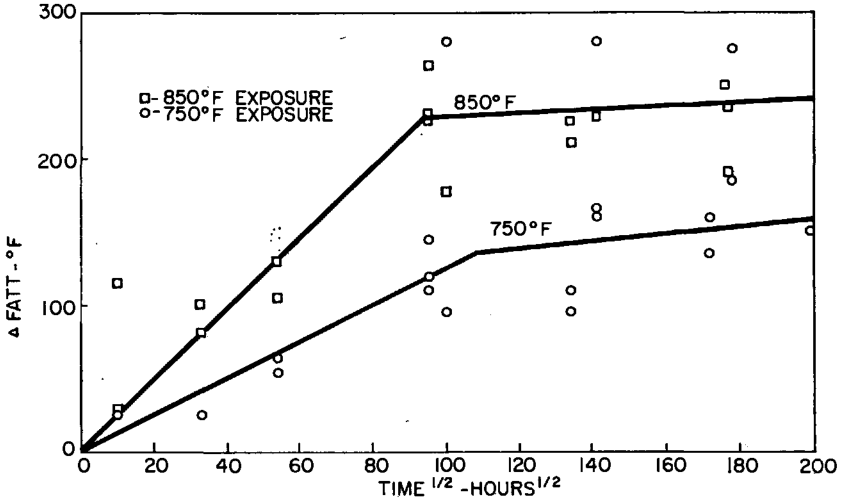

FIG. 1—*Embrittlement due to 750 and 850 F exposure of all silicon-killed heats.*

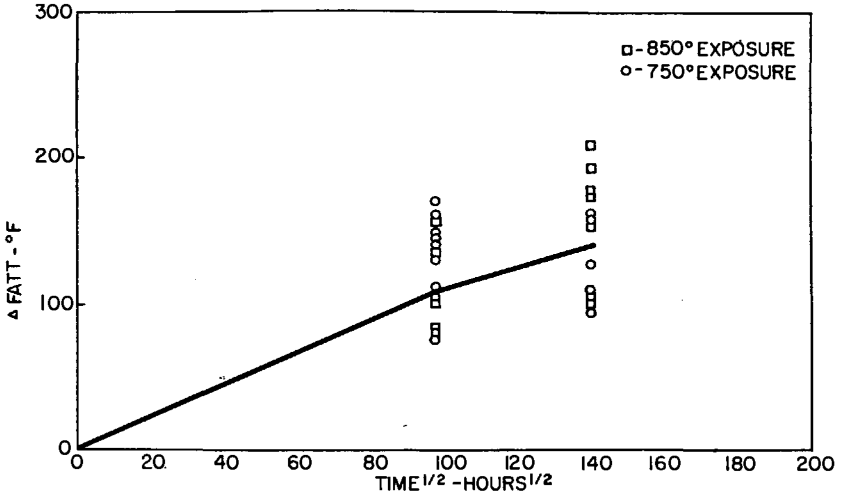

FIG. 2—*Embrittlement due to 750 and 850 F exposure of all vacuum-carbon deoxidized heats.*

induce a greater amount of embrittlement than any isothermal exposure of equivalent time. It should be noted also that since this treatment begins at 1100 F, all prior temper embrittlement is removed and the resulting embrittlement arises from the step-cooling treatment alone.

The Charpy bar from the lowest Charpy test temperature of most exposure conditions was subjected to a fractographic examination by means of low magnification microscopy to determine whether the frac-

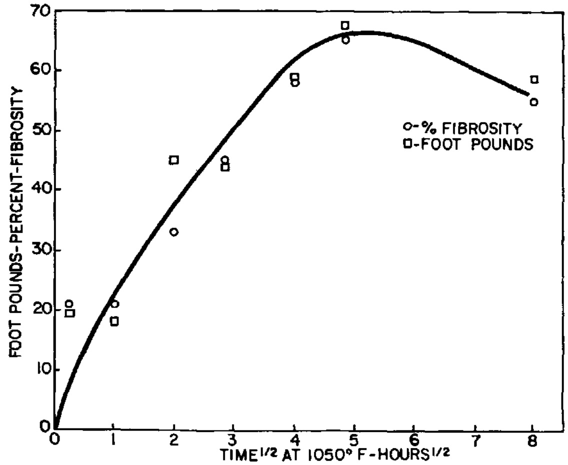

FIG. 3—*Charpy impact values measured at —25 F test temperature after 1050 F exposure.*

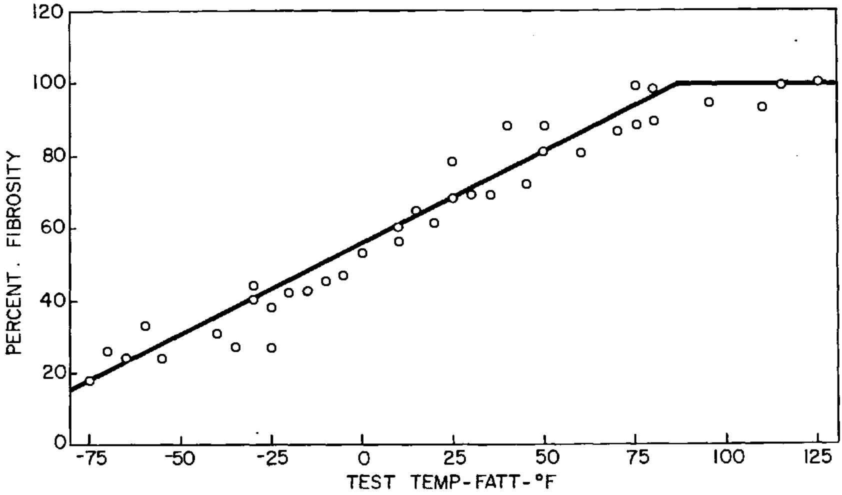

FIG. 4—*Normalized fracture transition curve for Steel FAZ.*

ture was cleavage, intergranular along prior austenite gran boundaries, or a mixture of the two.

Reversibility of Temper Embrittlement

A second facet of this investigation was devoted to determining the reversibility of the embrittling reaction. For this part of the study, specimens of Steel FAZ were removed from the 850 F embrittling exposure after 4800 h and subjected to a de-embrittling treatment by exposure at 1050 F. Single Charpy specimens were broken after

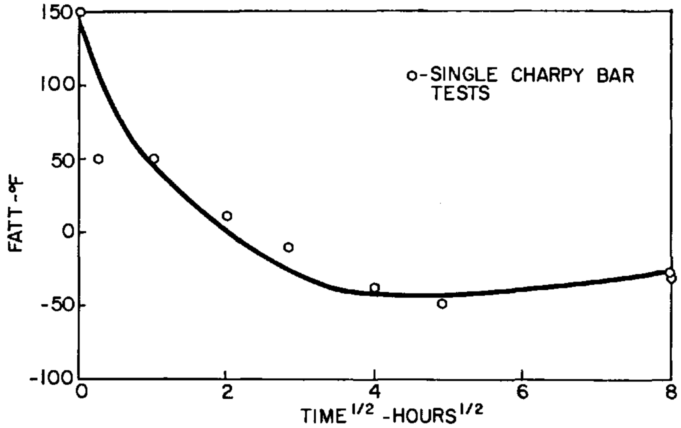

FIG. 5—*FATT after various times at 1050 F.*

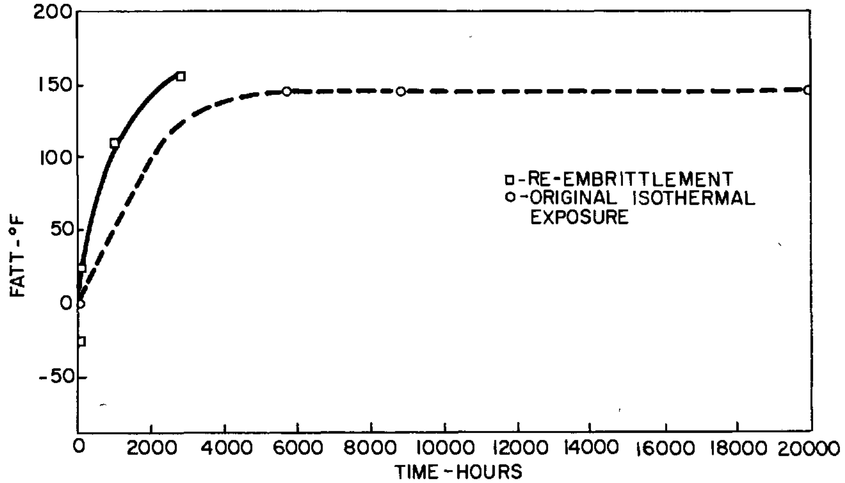

FIG. 6—*FATT after isothermal exposure at 850 F.*

exposures of ½, 1, 4, 8, 16, 24, and 64 h at 1050 F. The FATT in this case can be determined from these single bars as noted below. Once the time necessary for minimizing embrittlement at this temperature was established, material sufficient for several sets of Charpy specimens was de-embrittled. This treatment consisted of a 20-h exposure at 1050 F, plus a water quench. The transition temperature of this material was determined in the de-embrittled condition and again after subsequent re-exposure for 100, 1000, and 2800 h in the 850 F exposure furnace.

Results

The FATT values determined for each steel in the rotor heat treated, step-cooled, de-embrittled, and various exposure conditions are listed in Table 2, and the isothermal exposure data are plotted in Figs. 1 and 2. The measured FATT is listed; included in parenthesis in Table 2 is the increase over the initial rotor heat-treated condition which is, in fact, the amount of temper embrittlement brought about by the exposure.

The data from the de-embrittling of Steel FAZ work at 1050 F are presented in Fig. 3 where the percent fibrosity and energy at a test temperature of −25 F is plotted versus the square root of exposure time at 1050 F. A normalized FATT curve was made using all the Charpy test data from the rotor as heat treated, step-cooled, de-embrittled and as well the 8800 and 20,000-h data after exposure at 650, 750, and 850 F. The data were normalized by plotting percent fibrosity versus the quantity test temperature minus FATT. This plot is shown in Fig. 4. The normalized data can then be used to convert the single specimen test data shown in Fig. 3 to FATT values. These single specimen FATT's are plotted versus the square root of time at 1050 F in Fig. 5 showing the rate of de-embrittlement.

The amount of embrittlement incurred by this steel on subsequent reexposure at 850 F is shown in Fig. 6 along with the original isothermal embrittlement. Within experimental error the FATT on re-embrittlement duplicates the original FATT during isothermal exposure.

A low magnification (×5) inspection of the brittle fractures of the Charpy bars showed that the brittle fracture in the de-embrittled condition was always cleavage. In the brittle fractures of the steels embrittled, either by step-cooling or isothermal exposure, the fracture showed both cleavage and intergranular paths. In all cases an increase in FATT, that is, embrittlement, was accompanied by a change in mode of brittle fracture to include at least some intergranular fracture along prior austenite boundaries.

Discussion

The steels used in this study can be classified with respect to their deoxidation practice, that is, either silicon killed or vacuum-carbon deoxidized. This designation also categorizes the steels with respect to time of manufacture, that is, the vacuum-carbon deoxidized steels have been made more recently. Plotting amount of embrittlement versus square root of time shown in Figs. 1 and 2, demonstrates several interesting features of the embrittlement data. The silicon killed steels show a pronounced difference in rate of temper embrittlement when isothermal 750 and 850 F exposure data are compared; however, a decrease in rate of embrittlement occurs at about 10,000-h exposure in either exposure. It appears that the steels approach a maximum or saturation value of temper embrittlement at this time. The data do not indicate clearly whether or not additional exposure causes a decrease in amount of embrittlement with longer exposure. Although the data scatter, the silicon deoxidized steels clearly show a greater rate of embrittlement and a higher saturation value during 850 F exposure than they show during 750 F exposure. The vacuum-carbon deoxidized steels, containing < 0.06 silicon, show no difference in rate of embrittlement between exposures at 750 and 850 F. The data most nearly approximate the rates found during 750 F exposure of silicon deoxidized steels. It must be pointed out that the average concentrations of known [*1,2*] embrittling solutes (from Table 1) are, except for silicon, very similar:

	Average						
	Weight %				ppm		
	Mn	P	S	Si	As	Sb	Sn
Silicon deoxidized...........	0.39	0.011	0.013	0.25	83	16	94
Vacuum-carbon deoxidized...	0.29	0.008	0.012	0.03	76	18	116

No rationalization of the amount or rate of embrittlement by amounts of embrittling solutes can be made here; however, it appears that silicon makes a major contribution to temper embrittlement at 850 F in steels of this type, more so than that reported for silicon alone in high-purity steels [*7*].

Boyle et al [*5*] have used a computerized regression analysis to show that the amount of temper embrittlement incurred can be attributed to the known embrittling solutes. This analysis was performed on specimens whose embrittlement was induced by the step-cooling treatment outlined previously, and the relationship of the resultant equation to isothermally induced embrittlement remains unclear; however, it seems quite probable that a similar correlation could be established with isothermally induced temper embrittlement, and, in fact, this work is under way as data are accumulated.

The fact that temper embrittlement is reversible is clearly demonstrated with the data from Steel FAZ, wherein the steel has been embrittled almost 200 F by isothermal exposure for 4800 h at 850 F, then the embrittlement removed by a 20-h exposure at 1050 F, and finally the embrittlement re-established by a subsequent 850 F exposure of 2500 h.

Further work demonstrating the reversibility of temper embrittlement was carried out on Steels FAY and FBD. In this study, Steel FAY was re-austenitized and transformed and consequently has different values of the FATT than appear in Table 2. Specimens of each steel were de-embrittled by quenching from 1100 F and embrittled by the aforementioned step-cooling treatment. Specimens in each condition, embrittled and not embrittled, were then heated at about 40 F/h to 1100,

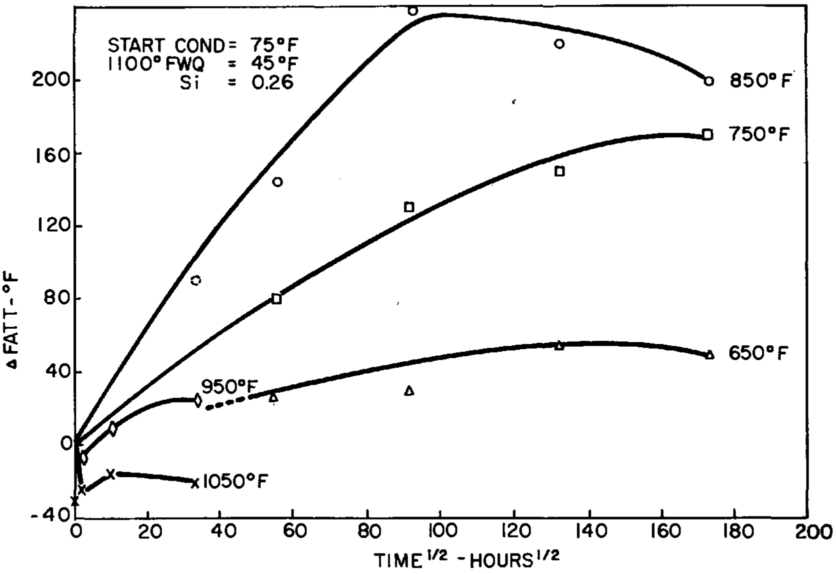

FIG. 7—*Shift in FATT with isothermal exposures at 650, 750, 850, 950, 1050 F of Steel FAN.*

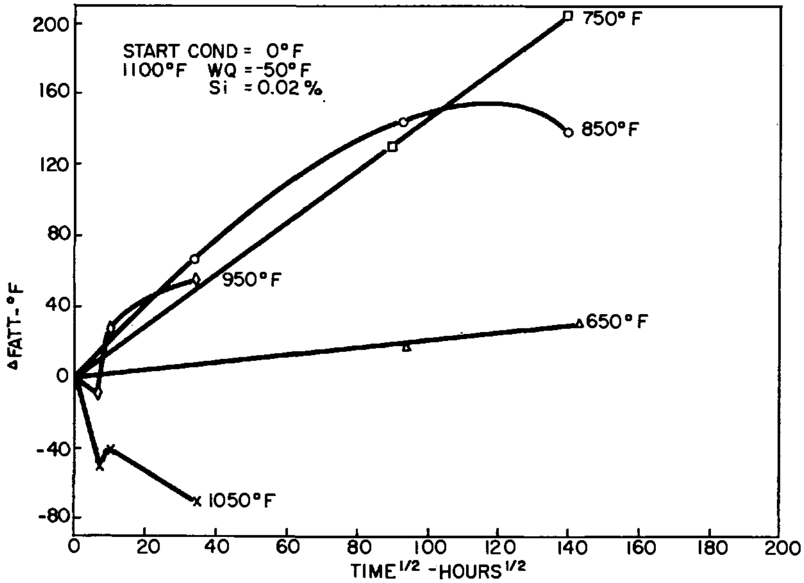

FIG. 8—*Shift in FATT time$^{1/2}$ for Steel FAZ.*

1060, and 1000 F, held for 6 h and then cooled at approximately 35 F/h to 400 F. The results are shown below:

	FATT, approximate deg F			
	FAY		FBD	
	Unembrittled	Embrittled	Unembrittled	Embrittled
No further exposure..........	0	155	−15	95
After heating to 1100 F.......	55	50	0	0
After heating to 1060 F.......	65	75	...	...
After heating to 1000 F.......	85	90	5	30

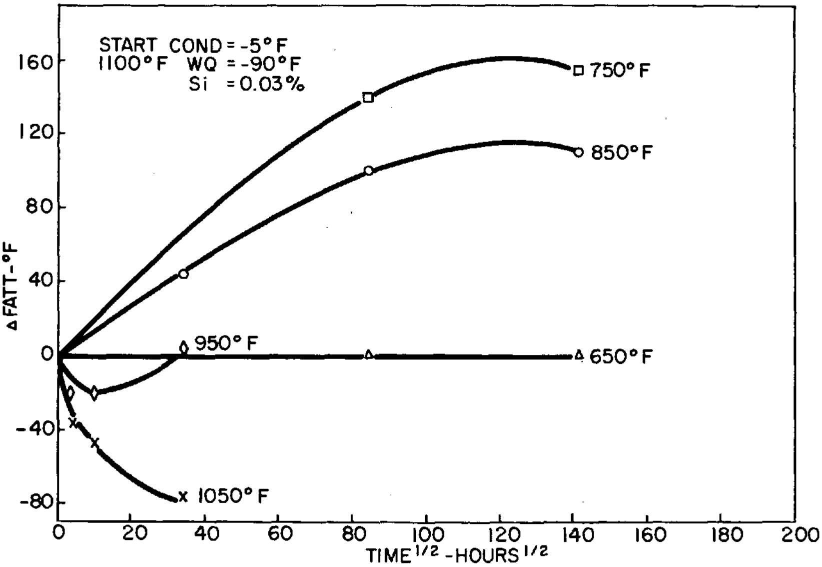

FIG. 9—*Shift in FATT versus time$^{1/2}$ for Steel FBM.*

It has already been noted that heating to 1100 F, followed by quenching, removes all embrittlement, so it can be concluded here that the final FATT after slow cooling is due to the slow cooling rate from 1100 F. In the cases of 1060 and 1000 F reheat, the final FATT is made up of the isothermal embrittlement at these temperatures plus the embrittlement produced by the slow cooling from these temperatures. In all cases prior embrittlement (by step-cooling) is at least partially eradicated by the subsequent, less severe, exposure treatment.

Other investigations [7][3] have shown a relationship between the embrittlement induced by step-cooling and that observed after some isothermal treatment. No such relationship can be seen in these data.

Steels FAN and FAP were exposed at higher temperatures and shorter times to better define the kinetics of the embrittling reaction.

---

[3] See p. 59.

All embrittlement data for these steels appear in Figs. 7 to 9. Although C curves can be plotted from the data for each steel, each curve is different from the next and no generalization can be made. This might be expected when one considers the number of solute elements that are known to contribute to the reaction. One interesting facet of this extended exposure was the apparent retrogression in the early stages of the 950 and 1050 F exposures. The steels used were embrittled to some degree during heat treatment as a rotor. Upon exposure at the 950 or 1050 F temperature, the first reaction is de-embrittlement and then, in most cases, re-embrittlement. This behavior most nearly approximates retrogression in an age-hardening alloy.

Although the role of silicon in temper embrittlement seems more clearly defined and the kinetics of the reaction can be likened, at times, to precipitation hardening, no further insight into the precise mechanism of the embrittling reaction can be set forth.

APPENDIX I

Metric or International System of Units (SI) and Conversions for U.S. Customary Units

Temperature in degrees Celsius (centigrade) = 5/9 (temperature in degrees Fahrenheit −32)
Change in temperature in degrees Celsius, ΔT = change in temperature in degrees Fahrenheit × 5/9
Length, in meters = inches × 0.0254
Stress in kg/mm^2 = psi × 7.0307 × 10^{-4}
Energy (kgf-m/cm^2) = (0.173) (ft·lb)

References

[1] Balajiva, K., Cook, R. N., and Worn, D. K., "Effects of Trace Elements on Embrittlement of Steels," *Nature,* Vol. 178, 1956, p. 433.
[2] Stevens, W. and Balajiva, K., "Influence of Minor Elements on the Isothermal Embrittlement of Steels," *Journal of the Iron and Steel Institute,* Vol. 193, 1959, pp. 141–147.
[3] Woodfine, B. C., "Temper Brittleness: A Critical Review of the Literature," *Journal of the Iron and Steel Institute,* Vol. 171, 1953, p. 229.
[4] Low, J. R., "Temper Brittleness—A Review of Recent Work," *Fracture of Engineering Materials,* American Society for Metals, 1964.
[5] Boyle, C. J. et al, "Significant Progress in the Development of Large Steam Turbine and Generator Rotors," *Proceedings,* American Society for Testing and Materials, Vol. 62, 1962, p. 1156.
[6] Boyle, C. J. et al, "Further Progress in the Development of Large Steam Turbine and Generator Rotors," presented at the 68th Annual Meeting of American Society for Testing and Materials, Purdue University, Lafayette, Ind., June 1965.
[7] Powers, A. E., "The Influence of Molybdenum and Tungsten on Temper Embrittlement," *Transactions,* American Society for Metals, Vol. 48, 1956, p. 149.

D. L. Newhouse[1] *and H. G. Holtz*[1]

Temper Embrittlement of Rotor Steels

REFERENCE: Newhouse, D. L. and Holtz, H. G., "**Temper Embrittlement of Rotor Steels,**" *Temper Embrittlement in Steel, ASTM STP 407,* American Society for Testing and Materials, 1968, pp. 106–126.

ABSTRACT: The susceptiblity to temper embrittlement during heat treatment of several large steam turbine generator rotor steels was investigated. Tests were performed on laboratory heats and on material from test prolongations and center core trepans from a number of rotor forgings. Chemical compositions, tensile, and Charpy impact properties were determined and are included for a number of Ni-Mo-V, Cr-Mo-V, and Ni-Cr-Mo-V steels. The latter included some which were silicon deoxidized (silicon 0.15 to 0.35 percent) and others which were vacuum-carbon deoxidized (silicon 0.10 percent max) by vacuum degassing without addition of metallic deoxidizers. Charpy fracture appearance transition temperatures are given for the as-received condition, after deembrittlement by water quenching from 1100 F (594 C), and after embrittlement by slow step cooling from 1100 F (TTSC).

The results of computer analyses of the relationship between properties, temper embrittlement, and chemical composition are presented and discussed. It was found that embrittlement susceptibility varies greatly with composition. These differences in susceptibility are associated with the presence of the known embrittling elements, phosphorus, silicon, arsenic, antimony, and tin. The balance of major elements such as nickel, manganese, molybdenum, and chromium also affects the degree of embrittlement. The presence of both nickel and chromium sharply increases the embrittling effect of phosphorus and perhaps of other elements as compared with compositions which contain only one or the other. Restrictions on manganese and molybdenum also appear beneficial. From as-received fracture appearance transition temperature and as-received embrittlement data it is apparent that temper embrittlement produced during heat treatment limits the fracture toughness attainable in massive sections of these steels and makes the control of temper embrittlement susceptibility of great value in components which must be heated within, or cooled slowly through, the range of embrittlement. Improved control of the residual elements to attain the low levels which appear desirable will require further advances in melting practice and selection of raw materials, in analytical procedures, testing, and specification of materials.

KEY WORDS: temper embrittlement, rotor forging, steam turbines, turbogenerators, steel, composition, transition temperature, impact tests, evaluation

---

[1] Manager, Forgings Development and metallurgical engineer, respectively, Materials and Processes Laboratory, Power Generation Div., General Electric Co., Schenectady, N.Y. Mr. Holtz is a personal member ASTM.

A great deal has been accomplished in delineation of the many aspects of temper embrittlement and in establishing methods of measurement, as a result of many investigations in the past two or three decades, but understanding the mechanisms involved and reliable methods of control have remained elusive. Woodfine [*1*][2] in 1952 reviewed the work which had been done prior to that time, and Low [*2*] in 1959 reviewed subsequent developments.

The term temper embrittlement, as defined by Low [*2*] and as used in this investigation, refers to a shift upward in the brittle-to-ductile transition temperature produced in many heat treatable steels by heating within or cooling slowly through the temperature range 662 to 1067 F (350 to 575 C). It is reversible, may be removed in a few minutes time at 1100 F (594 C) or higher.

Trends toward increased size and higher operating stresses in such components as large turbine-generator rotors and pressure vessels, require consideration and application of higher hardenability steels which can provide the increased strength and fracture toughness needed in these massive components. However, higher hardenability steels, especially those containing both nickel and chromium, are usually much more susceptible to temper embrittlement than simple carbon and low-alloy steels. Control of this phenomenon, therefore, assumes major importance in the design, selection, manufacture, and fabrication of heavy section components which must usually be tempered and stress relieved above the temper embrittlement range and cooled through it at rates which are slow enough, because of section thickness and residual stress considerations, to produce significant embrittlement in susceptible steels. Furthermore, the usually pronounced susceptibility to isothermal embrittlement of nickel-chromium-molybdenum-vanadium (Ni-Cr-Mo-V) steels of commercial purity, as reported by Gould[3] and other investigators, makes them unsuitable for components which operate at temperatures in the temperature range of greatest embrittlement, 750 to 950 F (399 to 510 C), if they must also retain low-temperature fracture toughness.

It is important to note at this point that, for components which operate below the temperature range which produces embrittlement, susceptibility to embrittlement during heat treatment is not important if a satisfactory level of fracture toughness can be consistently achieved in the presence of such embrittlement as is produced during heat treatment. Conversely, freedom from temper embrittlement itself is not meaningful for such parts unless the as-received transition temperature is satisfactorily low.

---

[2] The italic numbers in brackets refer to the list of references appended to this paper.

[3] See p. 90.

Boyle et al [*3,4*] presented a brief analysis of the accumulating results of an investigation of temper embrittlement susceptibility in large low-temperature turbine rotor forgings. This program is now complete, and the data and a series of statistical analyses of them are presented in this paper. The purposes of the analyses were to determine the variability of embrittlement susceptibility in such rotors, how such variability may be related to variations in composition and certain other factors, and how susceptibility to embrittlement during heat treatment, as well as transition temperature, may be improved by modifications of composition and manufacturing practice. Susceptibility to embrittlement during isothermal exposure in the embrittlement temperature range was not included in this study but has been investigated by Gould.[3, 4]

Procedure and Test Results

Test material was obtained from surface radial and center core trepans or from test prolongations of a number of production rotor forgings of three alloy types; generator and low-temperature turbine rotors of the Ni-Mo-V and Ni-Cr-Mo-V alloys described by Boyle et al [*3,4*], a number of 1Cr-1Mo-¼V high-temperature rotors and several developmental rotor steels of the series described by DeForest et al [*5*].

The fracture appearance transition temperature (FATT) and maximum Charpy fibrous energy (Em) were determined as-received (TTAR and EmAR), after heating specimens 1 h at 1100 F (594 C) and water quenching to remove reversible temper embrittlement (TTWQ and EmWQ) and after holding 1 h at 1100 F (594 C) and step cooling through the range of temper embrittlement (TTSC and EmSC), as described in definitions in Appendix I.

The amount of temper embrittlement present in the material as-received and the amount produced by step cooling was determined by subtracting TTWQ from TTAR and TTSC, respectively.

The chemical composition, grain size, tensile and yield strength, Charpy impact transition temperature, and temper embrittlement data are given in Table 1[5] for center core samples from 23 Cr-Mo-V rotor forgings (material category 1),[6] together with a summation of mean, minimum, maximum, and standard deviation for each column. Means and standard deviations are also summarized in Table 7. Similar data are given in Table 2 for 105 specimens of Ni-Mo-V rotor material

---

[4] See p. 59.

[5] Tables 1 to 5 have not been included in this publication but are available from University Microfilm, Inc., 300 N. Zeeb Road, Ann Arbor, Mich. 48106, at a cost of $3.00 per set.

[6] The data considered in this investigation were divided into a number of categories because they represent several populations which differ distinctly in chemical composition or in processing. The effects of these differences must be carefully considered in evaluating the results of regression analyses of combinations of categories.

(Category 2). As indicated by the description code, Columns A, B, and C, some of these tests were performed on laboratory heats or heat treatments (indicated by a "1" in Column A) and some represent a rotor surface radial position (indicated by a "0" in Column C).

Table 3 represents a group of 66 samples from silicon deoxidized Ni-Cr-Mo-V rotors (Category 3), some water quenched and others air cooled from austenitized and from bore and surface positions, as indicated in description code, Columns B and C. Results of analyses for arsenic, antimony, and tin are also shown in parts per million (ppm), with some information about heat treatment and rotor diameter. Charpy impact maximum fibrous energy values were obtained and listed for these rotors.

Table 4 presents similar results for 130 tests of vacuum-carbon deoxidized rotors (Category 4) differing from the silicon deoxidized rotors of Table 3 primarily in their lower silicon and higher nickel content and in all having been water quenched from the final austenitizing temperature.

In Tables 1 to 4, the last digit of the sequence number indicates the number of the test within a given rotor or heat. The preceding two digits in Table 1 and three digits in Tables 2 to 4 identify a particular rotor or heat.

In addition, the results of several test programs on laboratory induction heats or laboratory heat treatment of rotor samples of Ni-Cr-Mo-V steel were included for analysis with the results of tests performed on material from production rotors.

Some of the results obtained by Gould[4] on high-purity heats are included in Table 5 as sequence numbers 9001 to 9031 (Category 5).

The results of the ASTM study of temper embrittlement [8][7] in which molybdenum, phosphorus, and manganese levels were varied systematically in 20 heats of commercial purity are included in Table 5 as numbers 9501 to 9520 (Category 6). Item 9502 represents the reference composition; variations from it are underlined in the other compositions. Two series of tests in which austenitizing temperature and composition were varied are included as numbers 9611 to 9632 and 9651 to 9714 in Table 5 (Category 7).

The chemical compositions shown for rotors in Tables 1 to 4 are usually the vendor heat analyses for surface tests and check analyses of the center core trepan for the bore position. Only the bore location was analyzed for arsenic, antimony, and tin. In cases where both surface and bore tests are listed, the values determined in the center core for arsenic, antimony, and tin were listed also for the surface tests. Only three of the ASTM series, 9501 to 9520, were analyzed for arsenic, antimony, and

---

[7] Report on the Second Program of the Research Group of the ASTM Task Force on Brittle Fractures," unpublished, New York, May 1960.

tin. It was assumed that the others contained similar amounts because of the close control exercised in the melting of these heats.

The analyses for antimony were performed by a methyl violet photometric method, for arsenic an ammonium molybdate distillation photometric method was used, and tin was determined by an X-ray spectrographic method.

Analysis of Results

Variation of FATT and Embrittlement Susceptibility

It is of interest first to examine the variation of FATT and temper embrittlement susceptibility in the rotor forgings of Categories 1 to 4, to determine their characteristics and the opportunities for improvement. Table 6 compares the minimum and maximum values for as-received FATT (TTAR) and temper embrittlement (TBAR) and for step-cooled temper embrittlement (TBSC) in center core tests.

TABLE 6—*Range of variation of TTAR, TTWQ, and TBSC in center core tests of rotors.*

Category	Material Type	TTAR			TBAR			TBSC		
		Range		Percent <0 F	Range		Percent >20 F	Range		Percent <30 F
		Max	Min		Max	Min		Max	Min	
1.....	Cr-Mo-V	305	155	0	40	0	9	60	0	74
2.....	Ni-Mo-V	280	50	0	65	0	28	140	0	82
3.....	Ni-Cr-Mo-V (Si deoxidized)	225	−10	27	215	10	87	285	10	4
4.....	Ni-Cr-Mo-V (low Si)	105	−160	74	80	0	39	240	5	8

In addition, percentages are shown for each category for TTAR less than 0 F (−18 C), TBAR greater than 20 F (11 C), and TBSC less than 30 F (16.5 C). The steels of the Cr-Mo-V Category 1 are heat treated for high-temperature strength and exhibit a high as-received FATT, but as-received and step-cooled embrittlement are low. The range of as-received FATT of Ni-Mo-V, Category 2, is lower, but again temper embrittlement is generally not an important factor. In both of these alloys, increased susceptibility to temper embrittlement is usually associated with high phosphorus levels in acid open hearth steel.

The Ni-Cr-Mo-V steels of Category 3 show a wide range of as-received and step-cooled embrittlement, and as-received embrittlement appears to have a major effect on as-received FATT, being greater than 20 F (11 C) in 87 per cent of the observations. Temper embrittlement is a major factor affecting the as-received fracture toughness of this type of

TABLE 7—*Means and standard deviations for important variables in the seven categories studied.*

Category No.	1	2	3	4
Table No.	1	2	3	4
Sequence No's.	101 to 331	1101 to 1893	2101 to 3334	5001 to 8141
n	23	105	66	130
Material	Cr-Mo-V	Ni-Mo-V	Ni-Cr-Mo-V	Ni-Cr-Mo-V
Deoxidation	Si	Si	Si	vacuum-carbon
Composition, %:				
C	0.30 ± 0.05	0.25 ± 0.04	0.28 ± 0.04	0.25 ± 0.03
Mn	0.84 ± 0.10	0.61 ± 0.10	0.35 ± 0.09	0.32 ± 0.04
P	0.014 ± 0.008	0.016 ± 0.009	0.012 ± 0.004	0.008 ± 0.002
S	0.013 ± 0.005	0.017 ± 0.007	0.014 ± 0.004	0.014 ± 0.003
Si	0.28 ± 0.05	0.21 ± 0.05	0.25 ± 0.04	0.04 ± 0.02
Ni	0.20 ± 0.10	2.92 ± 0.50	2.88 ± 0.39	3.45 ± 0.13
Cr	1.05 ± 0.11	0.20 ± 0.10	1.54 ± 0.21	1.73 ± 0.09
Mo	1.16 ± 0.08	0.40 ± 0.10	0.55 ± 0.08	0.40 ± 0.04
V	0.24 ± 0.02	0.08 ± 0.02	0.10 ± 0.04	0.10 ± 0.03
As, ppm	...	...	...	69 ± 18
Sb, ppm	...	...	16 ± 4	14 ± 5
Sn, ppm	...	...	...	97 ± 48
Properties:				
TS, ksi	117 ± 4	105 ± 9	117 ± 14	120 ± 9
TTAR, deg F	228 ± 37	126 ± 50	98 ± 49	−30 ± 42
TTWQ, deg F	219 ± 38	116 ± 42	55 ± 50	−44 ± 38
TTSC, deg F	236 ± 41	131 ± 63	162 ± 68	43 ± 56
EmAR, ft·lb	...	...	63 ± 14	99 ± 20
EmWQ, ft·lb	...	...	65 ± 15	72 ± 12
EmSC, ft·lb	...	...	62 ± 14	70 ± 12
TBAR, deg F	9 ± 11	10 ± 21	42 ± 32	13 ± 30
TBSC, deg F	17 ± 22	15 ± 34	107 ± 74	87 ± 49

Category No.	5	6	7	5 to 7
Table No.	5	5	5	5
Sequence No.'s	9001 to 9031	9501 to 9520	9611 to 9714	9001 to 9714
n	16	20	34	70
Material	Ni-Cr-Mo-V	Ni-Cr-Mo-V	Ni-Cr-Mo-V	Ni-Cr-Mo-V
Melting	vacuum induction	induction	induction	...
Composition, %:				
C	0.19 ± 0.016	0.20 ± 0.01	0.20 ± 0.03	0.20 ± 0.02
Mn	0.28 ± 0.44	0.35 ± 0.13	0.33 ± 0.17	0.32 ± 0.25
P	0.004 ± 0.003	0.022 ± 0.008	0.014 ± 0.010	0.014 ± 0.011
S	0.004 ± 0.001	0.018 ± 0.004	0.016 ± 0.006	0.014 ± 0.007
Si	0.10 ± 0.10	0.25 ± 0.02	0.17 ± 0.08	0.18 ± 0.09
Ni	3.71 ± 0.04	3.75 ± 0.03	3.55 ± 0.41	3.64 ± 0.30
Cr	1.69 ± 0.04	1.66 ± 0.04	1.63 ± 0.16	1.65 ± 0.11
Mo	0.55 ± 0.22	0.54 ± 0.11	0.51 ± 0.06	0.53 ± 0.13
V	0.10 ± 0.01	0.08 ± 0.016	0.11 ± 0.05	0.10 ± 0.04
As, ppm	5	10	92 ± 17	67 ± 67
Sb, ppm	5 ± 5	5 ± 0.3	16 ± 7	10 ± 8
Sn, ppm	8 ± 1	20 ± 3	135 ± 35	55 ± 44

TABLE 7—*Continued*

Category No.	5	6	7	5 to 7
Table No	5	5	5	5
Sequence No.'s	9001 to 9031	9501 to 9520	9611 to 9714	9001 to 9714
n	16	20	34	70
Material	Ni-Cr-Mo-V	Ni-Cr-Mo-V	Ni-Cr-Mo-V	Ni-Cr-Mo-V
Melting	vacuum induction	induction	induction	...
Properties:				
TS, ksi	130 ± 11	116 ± 5	127 ± 13	124 ± 12
TTAR, deg F	...	...	...	...
TTWQ, deg F	−29 ± 65	−68 ± 20	26 ± 61	−13 ± 67
TTSC, deg F	6 ± 66	134 ± 97	170 ± 139	122 ± 131
EmAR, deg F	...	...	...	...
EmWQ, deg F	122 ± 26	83 ± 9	72 ± 21	87 ± 28
EmSC, deg F	...	...	...	83 ± 28
TBAR, deg F	...	...	...	...
TBSC, deg F	36 ± 66	203 ± 92	143 ± 114	135 ± 114

steel. In many of these steels, the as-received and step-cooled FATT were lower than the water quenched FATT producing an indication of negative embrittlement which has no apparent reason or meaning. Their magnitude seems too large to be entirely attributable to testing error.

The Ni-Cr-Mo-V steels of Category 4, vacuum-carbon deoxidized, water quenched from austenitize and with high nickel and chromium content show markedly lower FATT, as-received embrittlement, and step-cooled embrittlement. The best of these show virtually no susceptibility to step-cooled embrittlement and 8 per cent showed less than a 30 F (16.5 C) shift on step cooling. Nevertheless, the variability of FATT and embrittlement susceptibility are very substantial; in 40 per cent of the samples the embrittlement present as-received was greater than 20 F (11 C), and so there appears to be both opportunity and need for further reductions of embrittlement susceptibility in this class of steel.

Similar effects are shown in the means and standard deviations shown for Categories 1 to 7 in Table 7. In addition, the much higher average TBSC of Category 6 compared with that of the high-purity heats of Category 5 is noteworthy. Categories 5 and 6 have similar levels of arsenic, antimony, and tin, but Category 6 has much higher phosphorus, manganese, and silicon.

The Charpy maximum fibrous energy (EmSC) is only slightly lower on the average than that for the unembrittled condition (EmWQ). The higher value for EmAR, Category 4, is due to the longitudinal orientation of test specimens used. The Charpy impact tests for the embrittled and de-embrittled conditions were performed on transverse specimens.

The rotors included in Categories 1 to 4 were made over a period of about 15 years with Categories 1 and 2 representing earlier practice, Category 3 an intermediate period, and category 4 a more recent prac-

TABLE 8—*Linear equations for step-cooled temper embrittlement (TBSC + 10).*

Equation No.	1	2	3	4	5	6	7	8
Category	1	2	6	6	5 to 7	4	4	3 + 4
Material	Cr-Mo-V	Ni-Mo-V	Ni-Cr-Mo-V	Ni-Cr-Mo-V	Ni-Cr-Mo-V	Ni-Cr-Mo-V	Ni-Cr-Mo-V	Ni-Cr-Mo-V
n	23	105	20	20	70	130	130	196
Equation:								
Constant	8	−55	−206	−251	−354	−517	27	279
Coefficients[a] for:								
1. C	...	...	...	...	...	...	...	...
2. Mn	...	...	375	339	123	277	...	175
3. P	1406[b]	1556	7236	8057	4661	5861	...	5618
4. S	X	X	X	X	X	X	X	X
5. Si	...	...	X	582[b]	565	367	...	328
6. Ni	...	23	...	...	...	68	...	...
7. Cr	...	63	X	X	148[b]	...	...	88
8. Mo	...	69[b]	220[b]	290	...	431	246	209
9. V	...	...	...	...	...	−377	...	−617
10. As	Xi	Xi	XC	XC	...	0.53	0.57	X
11. Sb	Xi	Xi	XC	XC	3.93	1.68[b]	2.33	4.40
12. Sn	Xi	Xi	XC	XC	...	0.21	...	X
13. T_a	Xi	Xi	XC	XC	...	X	...	.30
14. T_t	Xi	Xi	XC	XC	...	X	−2.18	...
15. Par	Xi	Xi	X	X	...	X	70.4[b]	−29.9
16. Lab	XC	XC	XC	XC	XC	XC	XC	XC
17. WQ	XC	XC	XC	XC	XC	XC	XC	...
18. Bore	XC	XC	XC	XC	XC	XC	XC	...
19. GS	...	−7.7	...	...	...	Xi	Xi	Xi
20. Dia	Xi	Xi	X	X	X	X	...	0.96[b]
21. TS	...	...	...	...	...	X	...	...
23. TTWQ + 200	...	...	X	−1.09	...	X	−0.44	−0.40
54. WQ × Bore	...	...	XC	XC	XC	XC	XC	41
Variation removed (R^2)	0.24	0.40	0.89	0.94	0.75	0.57	0.66	0.74
Standard error	19	27	33	26	59	34	30	31
Lowest level of significance[b]	0.98	0.98	0.99	0.92	0.97	>0.95	0.99	0.97

[a] Some variables omitted because of choice (X), data were missing or incomplete (Xi), invariant (XC), or did not meet the significance test for inclusion (...).

[b] Indicates the variable with lowest significance, underlining the variable with highest significance.

tice. Improvements in melting practice over this period are reflected in reductions in average phosphorus and sulfur from Categories 1 to 4.

Factors Affecting Temper Embrittlement, TBSC

Boyle et al [4] investigated a sample of 102 determinations of temper embrittlement on rotors plus 78 on laboratory heats, using multiple regression analysis and both linear and nonlinear models. Linear, second order, and interaction effects were observed for various chemical elements.

In this work, preliminary manual plots were made for selected categories, and a series of multiple regression analyses were performed, first using linear models for relatively homogeneous samples, and then nonlinear models for less homogeneous samples. Even though it is clear that the true effects of variables are likely to be nonlinear over a considerable range of variation, a linear model may be adequate over small variations in a homogeneous sample, and a comparison of linear equations on several different types of steel can provide evidence of interactions which should be considered in higher order models of combined samples.

As in any analysis of process data, it was necessary to consider carefully the problems which are presented by interrelationships between independent variables and other defects of the sample, both in choice of models and in interpretation of results. For example, arsenic, antimony, and tin are highly related to each other in most of the samples, and so their effects cannot be separated. If antimony is included in an equation, the effect indicated for it by its coefficient may include contributions from arsenic and tin. There is also the likelihood of unknown correlations between the variables investigated and processing variables, so that effects attributed to known variables may reflect such influences.

Little effort was made to develop predicting equations; only those terms were included which were highly significant as to the effect expressed by their coefficients. Nor were variables standardized by subtracting the mean of each variable from each individual value as was done by Boyle et al [*4*]. In particular the regression equations must be considered as applicable only for the types of steel from which they were developed and within the range of variation of the categories used in each case.

Linear equations for step-cooled temper embrittlement are listed in Table 8. All values of TBSC were increased by 10 to avoid negative values in the dependent variable in some of the Ni-Cr-Mo-V samples, which might otherwise cause numerical problems. The coefficients listed show the effects of TBSC+10 of a 1 per cent increase in a particular element except for arsenic, antimony, and tin where the coefficient indicates the effect of an increase of one part per million. As noted in the table, some variables were deleted by choice, some because data were missing, and some were excluded by the multiple regression program because they did not meet a significance test for inclusion. The coefficient of determination (R^2) indicates the fraction of the initial variation of the dependent variable accounted for by the equation. It is the fraction of the initial sum of squared deviations from the mean removed by regression and has a minimum value of zero and a maximum of one. The

TABLE 9—*Nonlinear equations for step-cooled temper embrittlement* (*TBSC* + *10*).

Equation No.	9	10	11	12	13	14
Category	4	3 + 4	3–7	1–7	5–7	4
Material	Ni-Cr-Mo-V	Ni-Cr-Mo-V	Ni-Cr-Mo-V	all	Ni-Cr-Mo-V	Ni-Cr-Mo-V
n	130	196	266	394	38	130
Equation:						
Constant	134	135	258	−31	−137	470
Coefficients variables:						
1. C	...	...	...	...	...	...
4. Mn	...	...	...	...	...	369
3. P	...	...	...	...	...	...
4. S	X	X	X	X	X	X
5. Si	...	...	...	...	...	...
6. Ni	...	...	...	...	...	...
7. Cr	...	...	97	...	...	...
8. Mo	...	...	...	...	207	...
9. V	...	−610	−400	...	...	−444
10. As	0.60	X	X	Xi	...	.48
11. Sb	...	...	...	Xi	...	...
12. Sn	...	X	X	Xi	...	...
13. T_a	...	0.43^a	0.23	Xi	...	...
14. T_t	−1.99	−0.66	−0.60	Xi	...	−0.545
15. Par	62.5^a	...	...	Xi	...	...
16. Lab	XC	XC	...	...	XC	XC
17. WQ	XC	...	...	...	XC	XC
18. Bore	XC	...	...	...	XC	XC
19..GS	Xi	Xi	Xi	Xi	...	Xi
20. Dia	...	...	Xi	Xi	X	X
21. Ts	...	...	...	...	...	...
23. TTWQ + 200	−0.41	−0.38	−0.40	...	...	X
30. Mn·P	...	18223	5647^a	3350	5368^a	...
31. Mn·Si	...	...	613	...	666	−5583^a
34. Mn·Mo	...	...	...	...	...	...
33. Mn·Sb	...	...	...	Xi	...	...
34. P·Si	...	...	...	...	21163	...
35. P·Mo	...	...	12743	...	...	...
36. P·Sb	264	...	−360	Xi	...	359
38. Si·Mo	...	...	...	...	...	5412
39. Si·Sb	...	...	11	Xi	17.2	...
41. Ni-Cr	...	...	...	...	X	...
42. $(Mn)^2$	...	...	...	...	...	...
43. $(P)^2$	...	...	...	...	...	...
44. $(Si)^2$	...	...	...	...	...	...
45. $(Mo)^2$	304	...	...	...	...	...
46. $(Sb)^2$	...	...	0.216	Xi	...	...
48. $(TS)^2$	...	...	...	...	...	...

TABLE 9—*Continued*

Equation No Category Material n	4 9 Ni-Cr-Mo-V 130	10 3 + 4 Ni-Cr-Mo-V 196	11 3−7 Ni-Cr-Mo-V 266	12 1−7 all 394	13 5−7 Ni-Cr-Mo-V 38	14 4 Ni-Cr-Mo-v 130
49. Ni·Cr·Mn	...	...	...	22	X	...
50. Ni·Cr·P	...	...	...	525	X	...
51. Ni·Cr·Si	...	58	...	66	X	...
52. Ni·Cr·Mo	...	17	...	...	X	31.8
53. Ni·Cr·Sb	...	0.70	...	Xi	X	...
54. WQ × bore	...	...	28	33[a]	XC	XC
Variation removed (R^2)	0.66	0.74	0.80	0.66	0.94	0.64
Standard error	29	31	37	47	29	31
Lowest level of significance	0.99	0.999	0.98	0.999	0.99	0.95

[a] Indicates the variable with lowest significance.

most significant variable in each equation is underlined, the least is indicated by an asterisk.

A comparison between Eq 1 for Cr-Mo-V, Eq 2 for Ni-Mo-V, and Eqs 3 or 6 for Ni-Cr-Mo-V reveals important differences between these materials. In Cr-Mo-V only phosphorus appears related to variations in temper embrittlement, and the proportion of variance removed is low, 0.24. In Ni-Mo-V the effect attributed to phosphorus is slightly greater, and nickel, chromium, and molybdenum all have a small adverse effect, while increasing the ASTM grain size number (reducing actual grain size) tends to reduce TBSC. However, for Ni-Cr-Mo-V the effect of phosphorus is several times greater and variations of other elements (manganese, silicon, vanadium, arsenic, antimony, and tin) become significant or have larger effects in the case of chromium and molybdenum. The fracture appearance transition temperature in the absence of embrittlement (TTWQ) was included in several models as an independent variable, though it clearly is not, because it had been observed that steels with high austenite transformation temperatures and higher TTWQ tended to be less susceptible to temper embrittlement. In several of the Ni-Cr-Mo-V equations, (Numbers 4, 7, and 8) TTWQ was included as significant, inversely related to TBSC as expected.

The variation in the coefficient for phosphorus and other elements between the several types of steel is shown below.

Category	Type	Composition			Coefficients for			
		Ni	Cr	Mo	Mn	P	Si	Mo
1	Cr-Mo-V	0.2	1.0	1.2	...	1406	...	...
2	Ni-Mo-V	2.9	0.2	0.4	...	1556	...	69
4	Ni-Cr-Mo-V	3.4	1.7	0.4	277	5861	367	431

It may be inferred from these data that nickel added to Cr-Mo-V or chromium added to Ni-Mo-V greatly increased the effect of phosphorus and other embrittling elements on temper embrittlement.

To explore these interactions and other second order effects, cross product and squared terms were added for the major alloying and potentially embrittling elements, nickel, chromium, molybdenum, phosphorus, silicon, and antimony. The results of regression analysis including these terms are shown in Table 9, Eqs 9 to 12.

With increasing diversity in the combined samples of Nos. 10, 11, and 12, various interaction and squared terms became significant. The P·Mn, P·Mo, P·Sb, Ni·Cr·Mn, Ni·Cr·P, Ni·Cr·Si, Ni·Cr·Mo and Ni·Cr·Sb were significant in one or more of these equations, but R^2 values were never very high, indicating scatter in the data, inadequate models, or lack of information about other factors which contribute to variability of embrittlement.

The effect of type of quench and test position is shown by the values for water quenched bore (WQ·bore) in Eqs 8, 11, and 12. They suggest that the TBSC is significantly higher at the center than at the surface of a water quenched rotor, or at the center or surface of an air cooled rotor, composition and other factors considered being equivalent.

The results of Eq 13 may be the most revealing of the interactions affecting embrittlement in Ni-Cr-Mo-V. The sample used in Categories 5 to 7 was edited to remove all observations with very low molybdenum (less than 0.1 per cent), high austenitizing temperature (above 1500 F, 816 C), and high tensile strength (above 130 ksi). It produced a very good fit with one linear term and four cross product terms involving manganese, phosphorus, silicon, molybdenum, and antimony, at very high levels of significance. However, when an attempt was made to use Eq 13 to predict TBSC observed for Category 4 the results were not satisfactory. Variations in embrittlement in Category 4 were much greater than predicted by Eq 13. Equation 14 was developed for Category 4 without TTWQ as an independent variable, and produced nearly as good a correlation as Eq 9 in terms of R^2 and standard error of estimate.

Examination of the steels in Table 4 shows that low embrittlement susceptibility together with desirably low FATT has been achieved in a number of forgings, and these provide some information about levels of alloying and residual elements which can be tolerated. It must be noted, however, that considerable variation in TBSC exists in determinations within the same rotor or in rotors from the same heat, only partly attributable to factors considered in this study. An analysis of variation of TBSC, where more than one test was performed on a particular rotor, or when more than one rotor was made from one heat, revealed a standard deviation from the mean of such "within groups" tests of about 19.

Other factors contributing to the rather high-standard error of estimate in these calculations are the small range of some chemical elements in relation to the precision of measurement and the fact that the fracture paths in embrittled transverse Charpy test specimens from the center of large forgings tend to follow interdendritic segregate areas where the amount of embrittling elements may be much higher than the average determined by conventional sampling procedures. The effect of such segregates is not nearly so apparent in longitudinal tests.

TABLE 10—*Equations for de-embrittled transition temperature (TTWQ + 200) in Cr-Mo-V (Category 1) Ni-Mo-V (Category 2), Ni-Cr-Mo-V (Categories 3 to 7) and all combined (Categories 1 to 7).*

Equation	Category	*n*	
21......	1	23	TTWQ + 200 = 828 − 228 (%Mn) − 146 (%Cr) − 15.8 (GS) (R^2 = 0.68, standard error of estimate = 23)
22......	2	105	TTWQ + 200 = 178 + 254 (%C) + 101 (%Mn) + 1280 (%P) + 122 (%Mo) − 8.6 (GS) (R^2 = 0.65, standard error = 25)
23......	3 + 4	196	TTWQ + 200 = 26 + 231 (%Si) − 48 (%Ni) − 119 (%Cr) + 1.1 (Sb) + 0.21 (T_a) + 1.29 (TS) (R^2 = 0.71, standard error = 35)
24......	5 to 7	70	TTWQ + 200 = −440 + 940 (%P) − 32 (%Ni) − 78 (%Mo) + 1.5 (Sb[a]) + 0.21 (T_a) + 3.39 (TS) (R^2 = 0.77, standard error = 33)
25......	3 to 7	266	TTWQ + 200 = −15 − 56 (%Mn) + 150 (%Si) − 66 (%Ni) − 109 (%Cr) + 1.0 (Sb[a]) + 0.23 (T_a) + 1.95 (TS) (R^2 = 0.65, standard error = 38)
26......	1 to 7	394	TTWQ + 200 = 689 − 31 (%Ni) − 6.35 (TS) − 27 (%Ni)(%Cr) + 31052 $(\%P)^2$ + 0.0351 $(TS)^2$ − 8.55 (%Ni)(%Cr)(%Mn) + 22.9 (%Ni)(%Cr)(%Si) (R^2 = 0.81, standard error = 40)

[a] Sb, ppm.

In summation, the results of regression analysis show that the amounts and combinations of alloying elements present, such as nickel, chromium, manganese, and molybdenum, have an effect on the embrittlement produced by the known embrittling residual elements, phosphorus, silicon, arsenic, antimony, and tin. Embrittlement susceptibility is most directly minimized by avoiding the use of nickel and chromium together. In Ni-Cr-Mo steels, the use of minimum practical levels of manganese, silicon, and molybdenum and of the residual elements phosphorus, arsenic, antimony, and tin are indicated. The values of the coefficients should permit assessment of the probable benefits to be expected from particular combinations of chemical elements except that the relative importance of arsenic, antimony, and tin cannot be assessed.

Factors Related to Deembrittled Transition Temperature, TTWQ

Results of similar analyses of factors affecting TTWQ are shown in Table 10, in the form of a series of regression equations. Equations 21 to 25 contain only linear terms but Eq 26 for all materials, Categories 1 to 7, required a number of interaction and squared terms to fit the data. All values of TTWQ were increased by 200 F to eliminate negative values and the equations reflect this.

TABLE 11—*Equations for step-cooled transition temperature (TTSC + 200) and Charpy impact energy at 100 percent fibrosity (E_mWQ); for Ni-Cr-Mo-V steels.*

Equation	Category	*n*	
31......	3 + 4	196	$\mathrm{TTSC} + 200 = 54 - 183\,(\%\mathrm{C}) - 583\,(\%\mathrm{V}) + 0.51\,(T_a) - 0.51\,(\mathrm{T_t}) + 23\,(\mathrm{Bore}) + 233\,(\%\mathrm{Mn})(\%\mathrm{Mo}) + 11638\,(\%\mathrm{P})(\%\mathrm{Mo}) - 41\,(\%\mathrm{Ni})(\%\mathrm{Cr}) - 0.214\,(\mathrm{Sb})^2 + 0.0068\,(\mathrm{TS})^2 + 76\,(\%\mathrm{Ni})(\%\mathrm{Cr})(\%\mathrm{Si}) + 2\,(\%\mathrm{Ni})(\%\mathrm{Cr})(\mathrm{Sb})$ (R^2 = 0.83, standard error = 35)
32......	3 to 7	266	$\mathrm{TTSC} + 200 = -518 - 378\,(\%\mathrm{V}) + 0.35\,(T_a) + 31\,(\mathrm{bore}) + 5142\,(\%\mathrm{Mn})(\%\mathrm{P}) + 448\,(\%\mathrm{Mn})(\%\mathrm{Si}) + 8438\,(\%\mathrm{P})(\%\mathrm{Mo}) + 900\,(\%\mathrm{Si})^2 + 0.197\,(\mathrm{Sb})^2 + 0.0098\,(\mathrm{TS})^2$ (R^2 = 0.81, standard error = 43)
41......	4	130	$\mathrm{EmWQ} = 9 + 0.89\,(\mathrm{EmSC})$ (R^2 = 0.73, standard error = 6)
42......	4	130	$\mathrm{EmWQ} = 201 - 70\,(\%\mathrm{C}) - 871\,(\%\mathrm{S}) - 0.82\,(\mathrm{TS})$ (R^2 = 0.53, standard error = 9)
43......	5 to 7	70	$\log\,(\mathrm{EmWQ}) = -3.815 - 0.026\log\,(\%\mathrm{Mn}) - 0.293\log\,(\%\mathrm{S}) - 0.736\log\,(\%\mathrm{Ni}) - 1.327\log\,(T_a) + 3.780\log\,(\mathrm{T_t}) - 0.835\log\,(\mathrm{TS})$ (R^2 = 0.86, standard error = 0.055)

In Eq 21 for Cr-Mo-V rotors, manganese, chromium, and grain size number were all inversely related to TTWQ, that is, increasing each of them should tend to reduce TTWQ. Equation 22 for Ni-Mo-V rotors shows a similar effect for grain size number, but, for this steel, manganese is directly related to TTWQ as are also carbon, phosphorus, and molybdenum. Increasing any of the latter should tend to increase TTWQ and so reduce fracture toughness at ambient temperatures. These results are consistent with experience and with laboratory experiment as discussed by Boyle et al [*4*]. The structure of Cr-Mo-V steel is usually largely a high-temperature bainite, and increasing manganese and chromium tends to lower the transformation temperature and reduce the transition temperature. The structure of Ni-Mo-V is usually a mixture of ferrite and bainite, and the effect of increasing alloy content is to increase the proportion of high-temperature bainite with a concurrent increase in FATT. These contradictory effects warn of the difficulty to be expected in trying to find a mathematical model which can adequately reflect both effects. The lower temperature bainite produced by the high nickel and chromium content of the Ni-Cr-Mo-V steel accounts for its very good fracture toughness potential.

In Eqs 23 to 25 for Ni-Cr-Mo-V steels, silicon, antimony, austenitizing temperature and tensile strength all are directly related to TTWQ (increases tend to be harmful), and nickel, chromium, and molybdenum tend to be inversely related. Equation 26 suggests nonlinear effects for tensile strength and phosphorus and complex interactions between nickel, chromium, manganese, and silicon, the nature of which can be revealed by calculation and plotting for particular compositions.

The R^2 values vary from 0.65 to 0.81 for these correlations, indicating a substantial reduction in variance by regression. However, the residual error is substantial. The initial variability was so high that, although there was a big reduction by regression, a great deal of this variability was not attributed to the factors included in the correlations.

Factors Related to Step-Cooled Transition Temperature, TTSC

The results of correlations using TTSC + 200 F as the dependent variable are given in Table 11. Since TTSC = TTWQ + TBSC, it might be expected that equations for TTSC would reflect some of the effects observed for the other two. The step-cooled transition temperature is of particular interest because it reflects the transition temperature with the greatest amount of embrittlement likely to be produced during heat treatment. A comparison of as-received with step-cooled temper embrittlement in Tables 1 to 4 shows that the former is usually less than the latter.

For Ni-Cr-Mo-V rotors, Eq 31 suggests that increases in carbon, vanadium, nickel, chromium, and tempering temperature are beneficial to TTSC, while increased austenitizing temperature, tensile strength level, phosphorus, silicon, and antimony are detrimental. The beneficial effect of nickel and chromium depend upon a low level of silicon and antimony, and the detrimental effects of the latter are linked to the nickel and chromium present, as shown by the interaction terms.

Equation 32 for Categories 3 to 7 shows significance for simple interactions between manganese and phosphorus, manganese and silicon, and phosphorus and molybdenum.

Factors Related to Fibrous Charpy Impact Energy (EmWQ)

Three equations relating fibrous Charpy impact energy to other factors are also shown in Table 11. Equation 41 shows that EmWQ is very closely related to EmSC and that for the normal range of values in Category 4, the difference is usually less than 10 percent.

Equation 42 shows that EmWQ is inversely related to carbon, sulfur, and tensile strength. The effects shown for sulfur and tensile strength are consistent with those described by Hodge et al [*6*] for sulfur and hardness on the notch toughness of Ni-Cr-Mo plate. The coefficients suggest that an increase in carbon and sulfur of 0.1 and 0.01 percent, respectively, and an increase in tensile strength of 10 ksi should each reduce EmWQ in the order of 8 ft·lb, other factors assumed to remain unchanged. The R^2 value was low, but a substantial fraction of the residual variance may be due to scatter of the data, each point having been determined by a transition temperature determination utilizing as few as six or eight specimens.

A surprisingly good correlation was obtained using a logarithmic model, Eq 43, which showed the log of manganese, sulfur, nickel, austenitizing temperature, and tensile strength all to be inversely related to log (EmWQ) and the log of tempering temperature to be directly related to it.

Discussion

The test results and analyses of them show that step-cooled temper embrittlement is observed but is of minor consequence in Cr-Mo-V and Ni-Mo-V rotor steels. When both nickel and chromium are present as in Ni-Cr-Mo-V steels, step-cooled embrittlement can be as high as 310 F (172 C). The potential for embrittlement during heat treatment is in some cases realized to a considerable degree, the temper embrittlement observed as-received being as high as 215 F (120 C) in a silicon-deoxidized Ni-Cr-Mo-V steel and 80 F (44 C) in a vacuum-carbon-deoxidized steel. On the other hand, some steels of both types are not susceptible to step-cooled embrittlement and have little or none as-received. This variation in susceptibility to temper embrittlement imposes a serious burden on the effective application of the Ni-Cr-Mo-V steel which finds its primary use in applications where low-temperature fracture toughness is desired at high yield strength levels in heavy section components. It also suggests that temper embrittlement during heat treatment of rotor forgings and other heavy components can be avoided or minimized by control of composition and processing variables, though it may be difficult to achieve consistently the low levels of residual elements which may be required.

Of the properties investigated, the fracture-appearance-transition-temperature and the maximum Charpy fibrous energy have the most direct physical significance, since both were shown by Brothers et al [7] to be correlated with notched-disk bursting strength and fracture toughness, both below and above the temperature range of transition from brittle to ductile fracture mode. The TTWQ is of interest if embrittlement can be avoided and the TTSC provides information about the combination of TTWQ and the maximum embrittlement likely to be produced during heat treatment or processing and therefore combines the information included in TTWQ and TBSC.

To show the effect of each active variable on the properties of vacuum-carbon deoxidized Ni-Cr-Mo-V rotors, Eq 14 for TBSC, Eq 23 for TTWQ, and Eq 32 for TTSC were applied to a composition approximately the average for Category 4, and then each active variable was varied an appropriate amount above and below the average and within its range in Category 4. The results are shown in Table 12.

TABLE 12—*Effect of variations of single variables on the calculated values of TBSC, TTWQ, and TTSC using Eqs 14, 23, and 32, respectively.*

Variable	Assumed Mean, %[a]	Variation	TBSC		TTWQ		TTSC	
			(−)	(+)	(−)	(+)	(−)	(+)
C......	0.25	±0.05	106	106	−39	−39	56	56
Mn.....	0.32	±0.10	103	110	−39	−39	49	64
P......	0.010	±0.005	79	133	−39	−39	31	82
S.......	0.015	±0.005	106	106	−39	−39	56	56
Si......	0.06	±0.05	87	125	−50	−27	46	71
Ni.....	3.50	±0.25	101	112	−27	−51	56	56
Cr.....	1.70	±0.25	95	118	−9	−69	56	56
Mo.....	0.40	±0.10	55	158	−39	−39	48	65
V......	0.10	±0.05	129	84	−39	−39	75	38
As.....	70 ppm	±40	87	126	−39	−39	56	56
Sb.....	15 ppm	±10	70	142	−50	−28	17	135
Sn.....	100 ppm	±80	106	106	−39	−39	56	56
T_a.....	1525 F	±25	106	106	−44	−34	48	65
T_t......	1125 F	±50	134	79	−39	−39	56	56
TS.....	120 ksi	±10	106	106	−52	−26	34	81

[a] Units are per cent unless noted otherwise.

For the ranges of variation explored, increases in molybdenum, antimony, phosphorus, arsenic, and silicon had the largest adverse effects on TBSC. For TTWQ, increases in tensile strength, silicon, antimony, and austenitizing temperature were unfavorable and for TTSC, antimony appears most unfavorable, followed by phosphorus, tensile strength, silicon, molybdenum, austenitizing temperature, and manganese.

These equations were also used to estimate the effect on TBSC, TTWQ, and TTSC of combined adjustments of active variables, first assuming low levels for arsenic, antimony, and tin and then assuming average levels for these elements, as follows:

Mn	P	Si	Ni	Cr	Mo	V	As	Sb	Sn	T_a	T_t	TS	TB SC	TT WQ	TT SC
0.22	0.005	0.01	3.75	1.8	0.3	0.1	30	5	40	1500	1100	125	−11	−84	−22
0.22	0.005	0.01	3.75	1.8	0.3	0.1	70	15	100	1500	1100	125	26	−73	17

These calculations suggest that susceptibility to embrittlement during heat treatment in this steel may be virtually eliminated by control of major embrittling elements and adjustments in alloying elements and substantially reduced even if arsenic, antimony, and tin are held to average values for the steels in this study. Of the changes examined, those of alloying elements and austenitizing temperature are most readily applied, those involving phosphorus and silicon somewhat more difficult, while the control of arsenic, antimony, and tin involves difficult problems in analysis and selection of raw materials, especially melting scrap.

The adverse effect shown for molybdenum in these and other investigations is something of an anomaly because it is well known that molybdenum additions reduce temper embrittlement susceptibility in nickel-chromium steels. However, it seems clear that increases in molybdenum in the range of 0.3 to 0.6 percent tend to increase susceptibility to temper embrittlement.

Arsenic, antimony, and tin tended to vary together in the steels investigated, and the effects shown for them in the equations are important. While the effects shown are consistent with work by earlier investigators, the effects shown in this study for them may also reflect differences in melting and processing, and so should not be interpreted too literally.

Because of the apparent importance and the very real difficulty of control of these residual elements, further work would be desirable to better define their relative importance and the limits which can be tolerated. The Research Subgroup on Temper Embrittlement of the ASTM Special Task Force on Large Turbine and Generator Rotor Forgings has undertaken such a study.

Summary and Conclusions

The data presented in this study show that susceptibility to temper embrittlement in heat treatment varies greatly within the several types of rotor steels, Ni-Mo-V, Cr-Mo-V, and Ni-Cr-Mo-V and that as-received embrittlement is an important factor affecting the variability of as-received transition temperature and fracture toughness of the latter steel.

The results of data analyses suggest that the embrittling effect of phosphorus and perhaps of other embrittling elements is much greater in Ni-Cr-Mo-V than in Ni-Mo-V or Cr-Mo-V, that nickel and chromium interact to increase the effect of these elements on embrittlement. They also suggest that the use of minimum effective amounts of manganese and molybdenum, and close control of phosphorus, silicon, arsenic, antimony, and tin should be effective in achieving very low levels of susceptibility to embrittlement in heat treatment.

Factors affecting Charpy fracture appearance transition temperature, both embrittled and with temper embrittlement removed, were also investigated, and it appears that these too may be improved by further refinement of composition and practice.

Temper embrittlement does not affect appreciably the notch toughness of this class of steel above the brittle-to-ductile transition temperature range as measured by the Charpy impact energy for completely fibrous fracture. However increasing carbon and sulfur content and tensile strength level does reduce ductile fracture toughness.

The results of this investigation are relevant indirectly to the problem of long time isothermal embrittlement in that any steel, to be resistant to long time isothermal embrittlement, must also be virtually immune to short time or step-cooled embrittlement, that is, a low value of step-cooled embrittlement (TBSC) is necessary.

APPENDIX I

Definitions

X	Independent variable in equation $Y = a_0 + a_1X_1 + a_2X_2 + a_3X_3 + \cdots a_nX_n$
Y	Dependent variable
n	Number of observations
$\bar{X}$	$\Sigma x/N$ = average for sample
T_a	Austenitizing temperature, F
T_t	Tempering temperature, F
Par	Tempering parameter = $(T_t + 459)$ (20 + log (tempering time, h)) $\times 10^{-3}$
Lab	A value of "1" for Lab indicates a laboratory heat or rotor sample given a laboratory heat treatment. A value of "0" indicates a test specimen from a rotor as-received
WQ	A value of "1" indicates a rotor water quench "0" indicates a rotor air cool or simulated air cool, the latter if Lab = 1
Bore	"1" indicates a specimen machined from a center core trepan from a rotor forging, "O" indicates a surface specimen from a rotor
Dia	Maximum rotor diameter, in.
FATT	V-notch Charpy fracture appearance transition temperature (temperature at which area of cleavage or intergranular fracture is 50 percent of the original area under the notch), F
TTWQ	FATT after heating specimens to 1100 F, holding 1 h, and water quenching to remove reversible temper embrittlement, F

TTSC	FATT deg F after the following step-cooling treatment; heat to 1100 F (594 C), hold 1 h, furnace cool to 1000 F (538 C), hold 15 h, furnace cool to 975 F (524 C), hold 24 h, furnace cool to 925 F (496 C), hold 48 h, furnace cool to 875 F (468 C), hold 72 h, furnace cool to 600 F (613 C) or lower, air cool to room temperature
TTAR	FATT as-received, F
TBSC	step-cooled embrittlement susceptibility, deg F
TBSC	TTSC-TTWQ
TBAR	As-received embrittlement, deg F
Em	Charpy impact maximum fibrous energy, ft·lb
EmAR	Em as-received, ft·lb
EmWQ	Em as water quenched from 1100 F (594 C), ft·lb
EmSC	Em as step cooled from 1100 F (594 C), ft·lb

APPENDIX II

SI Equivalents and Conversions for U.S. Customary Units

T_F	Temperature, degrees Fahrenheit
T_C	Temperature, degrees Celsius
T_K	Temperature, degrees Kelvin

		Applicable to
Temperature	$T_C = (5/9)\ (T_F - 32)$ $T_K = (5/9)\ (T_F + 459.67)$	TTAR, TTWQ, TTSC
Change in temperature	$\Delta T_C = \Delta T_K = (5/9)(\Delta T_F)$	TBAR, TBSC
Length	Meters = (0.0254), inches	Diameter
Stress	Newton/meter^2 = (6.894757E + 6), ksi	TS, YS
Energy	N-m = (1.355818), ft·lb	EmAR, EmWQ, EmSC
Charpy Impact Energy	(Kgf-m)/cm^2 = (0.17281), ft·lb	EmAR, EmWQ, EmSC

References

[1] Woodfine, B. C., "Temper Brittleness: A Critical Review of the Literature," *Journal of the Iron and Steel Institute,* Vol. 173, 1953, p. 229.

[2] Low, J. R., "Temper Brittleness—A Review of Recent Work," *Fracture of Engineering Materials,* American Socitey for Metals, 1964, pp. 127–142.

[3] Boyle, C. J., Curran, R. M. et al, "Significant Progress in the Development of Large Turbine and Generator Rotors," *Proceedings,* American Society for Testing and Materials, 1962, pp. 1156–1175.

[4] Boyle, C. J., Curran, R. M. et al, "Further Progress in the Development of Large Steam Turbine and Generators Rotors," paper presented at Annual Meeting of ASTM at Purdue University, W. Lafayette, Ind., June 1965.

[5] DeForest, D. R., Newhouse, D. L., and Seguin, B. R., "Progress in the Development of Steam Turbine Generator Rotor Materials," ASME Paper 57-A-280, American Society of Mechanical Engineers, Annual Meeting, New York City, Dec. 1957.

[6] Hodge, J. M., Frazier, R. H., and Boulger, F. W., "The Effect of Sulphur on

the Notch Toughness of Heat Treated Steel," *Transactions,* Metallurgical Society of American Institute of Mining, Metallurgical, and Petroleum Engineers, Vol. 215, No. 5, Oct. 1959, pp. 745–753.

[7] Brothers, A. J., Newhouse, D. L., and Wundt, B. M., "Results of Bursting Tests of Alloy Steel Disks and Their Application to Design Against Brittle Fracture," paper presented at Annual Meeting of ASTM at Purdue University, W. Lafayette, Ind., June 1965.

C. J. McMahon, Jr.[1]

Temper Brittleness—An Interpretive Review

REFERENCE: McMahon, C. J., Jr., "**Temper Brittleness—An Interpretive Review,**" *Temper Embrittlement in Steel, ASTM STP 407*, American Society for Testing and Materials, 1968, pp. 127–167.

ABSTRACTS: The history of the problem of temper brittleness is surveyed; the reviews of Hollomon, Woodfine, and Low are reexamined in the light of recent developments, and the work carried out since 1959 is reviewed. Included in the latter is a model which has been proposed to explain the phenomenon. The problem of "500 F embrittlement" and its connection with temper brittleness are discussed, and a rudimentary model is proposed. Suggested directions for future research are indicated.

KEY WORDS: temper embrittlement, mechanical properties, steel, metallography, evaluation, history

The problem of temper brittleness of alloy steels has been with us for more than seven decades, and the study of it now appears to be entering the most sophisticated and, hopefully, final stage. It is therefore appropriate to examine the history of the problem, as well as its later development, so that the early work can be interpreted in the light of more recent knowledge. To this end an attempt is made to review all of the major advances that have been made in the study of temper brittleness. The task is made easier by the general reviews of Hollomon [*1*][2] in 1946 and Woodfine [*2*] in 1953, and the recent review by Low [*3*] in 1959.

Early History of The Problem

Temper brittleness, one of the classical problems of physical metallurgy, refers to the decrease in notch toughness[3] which often occurs in alloy steels when heated in, or cooled slowly through, the temperature range about 375 to 575 C. The term was coined by Dickenson [*4*] in 1917, but the phenomenon was recognized at least several decades

---

[1] School of Metallurgy and Materials Science and Laboratory for Research on the Structure of Matter, University of Pennsylvania, Philadelphia, Pa.

[2] The italic numbers in brackets refer to the list of references appended to this paper.

[3] Actually, the upward-shift of the ductile-brittle transition temperature.

before that.[4] The problem became critical in the period around World War I with the widespread use of alloy steels in thick sections for armor and ordnance.[5]

Significant progress in understanding and combating the problem was made in the period 1917 to 1925, particularly in England. Brearley [*7*] had recognized by 1917 that the decreases in toughness resulting both from slowly cooling through, and tempering (or retempering) in, the critical temperature range were related phenomena. In 1919 Greaves [*8*] reported several now-well-known characteristics:

1. Steels of apparently similar compositions could exhibit wide variations of susceptibility under the same conditions of heat treatment.

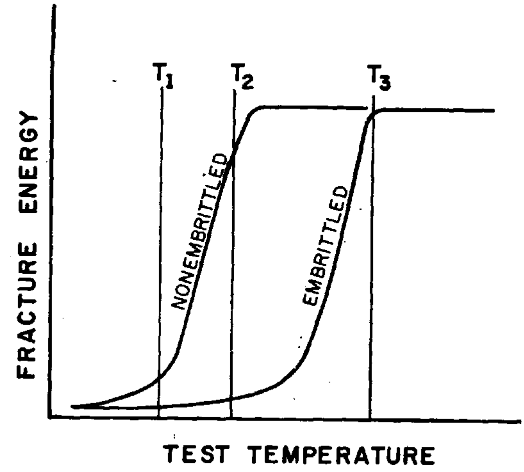

FIG. 1—*Schematic impact curves showing shift due to temper brittleness and dependence of susceptibility ratio, SR, on test temperature. If test temperature were* T_1 *or* T_3*, SR would be small, indicating nonsuspectibility; if test temperature were* T_2*, SR would be large.*

2. Notch toughness decreased as austenitizing temperature increased.
3. Reheating in the temperature region around 500 C always resulted in embrittlement, regardless of the subsequent cooling rate.
4. An initially tough steel could be embrittled by reheating in, or slowly cooling through, the critical range, while an embrittled steel could be made tough by reheating above 600 C and rapidly cooling, that is, embrittlement was reversible.

---

[4] Howe [*5*] noted in 1919 that blacksmiths realized as early as 1883 that it was often necessary to water quench after tempering above 600 C to avoid the brittleness that resulted from slow cooling. They called the treatment "water annealing."

[5] Krupp armor steels became notorious for brittle failures under impact, so much so that the early name for temper brittleness was "Krupp krankheit." Krupp patents issued in 1900 prescribe a water quench after tempering of nickel-chromium steels as a remedy for this "sickness" [*6*]. This, of course, was not practicable for thick sections.

Later work by Greaves and Jones [*9*] revealed in 1920 that the degree of embrittlement increased with time in the critical region, and in 1925 they reported that, while manganese and chromium increased the embrittlement susceptibility in the presence of phosphorus in a nickel steel, the problem could be reduced and often eliminated by additions of molybdenum [*10*]. This latter discovery was viewed as a practical remedy for the problem, and intensity of research slackened for some time.

The standard test to determine a steel's susceptibility to temper brittleness was to compare the fracture energies of two specimens in a notched-bar impact test *at room temperature.* Both specimens were oil-hardened from 900 C and tempered for 2 h at 650 C; one specimen was then water quenched, while the other was slowly cooled (0.3 C/min between 600 and 400 C). The fracture energy of the quenched specimen divided by that of the slowly cooled specimen was called the *susceptibility ratio.*

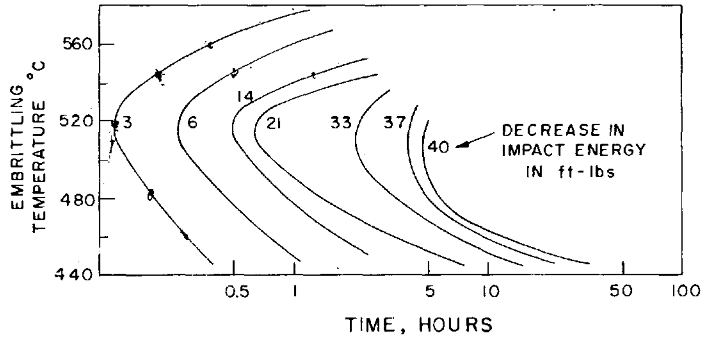

FIG. 2—*Plot by Holloman* [1] *of results of Greaves and Jones* [9] *for a 0.26 per cent carbon, 0.66 per cent manganese, 3.53 per cent nickel, 0.84 per cent chromium, 0.026 per cent phosphorus steel showing C-curve behavior.*

Virtually all work prior to 1944 utilized this susceptibility ratio test. This was unfortunate, because the test is actually of little value as a quantitative measure of embrittlement susceptibility, and its use probably contributed significantly to the lack of progress in understanding the mechanisms of the phenomenon. Jolivet and Vidal [*11*] showed in 1944 that the fundamental characteristic of temper brittleness was the shift of the ductile-brittle transition curve to higher temperatures, and that the use of the susceptibility ratio could be quite misleading, as illustrated in Fig. 1. Hence, it was necessary to establish the fracture transition curves by tests over a *range* of temperatures before a meaningful measure of embrittlement could be obtained. This same conclusion was reached independently by Hollomon [*1*].

Status of the Problem in 1946—Hollomon's Review

Hollomon recognized that the earlier work based on measurements of susceptibility ratio had to be interpreted with caution; however, some fairly well-founded conclusions had been drawn. In addition to those of Greaves and Jones, already mentioned above, it appeared that plain carbon steel with less than 0.6 to 0.7 per cent manganese was *not* susceptible. Whether molybdenum actually eliminated all or part of the embrittlement susceptibility, or whether it merely delayed the attainment of full embrittlement, was still unclear. There was unanimous agreement by that time that fracture of embrittled steel occurred mainly along prior austenitic grain boundaries. This had been accepted by many since the turn of the century; however, debate continued on this point as late as 1920 [*9*].

Hollomon [*1*] replotted the data of Greaves and Jones [*9*] to show the apparent C-curve nature of the embrittlement behavior (Fig. 2). In view of the similarity between this and many phase transformations, he concluded that temper brittleness is caused by a precipitation from alpha iron, which occurs preferentially at prior austenitic grain boundaries.[6] The precipitate was assumed to be soluble above about 600 C, and the rate of (diffusion controlled) precipitation was a maximum at about 500 C. The nature of the precipitate was a mystery; oxides, phosphides, carbides, and nitrides had been suggested [*1*]. Hollomon tentatively favored nitrides and suggested that alloying elements acted by changing the nitrogen solubility in ferrite.

Status of the Problem in 1953—Woodfine's Review

An important benchmark in the history of this problem is the astute critical review published by Woodfine in 1953 [*2*]. It is still essential reading for anyone with serious interest in temper brittleness. Without hoping to do it justice, its main conclusions are summarized here.

Testing Methods

After reviewing many attempts at detecting the presence of temper brittleness by the measurement of other mechanical and physical properties, Woodfine concluded that the notched-bar impact test was still the only reliable method. The importance of using the shift in transition temperature as the criterion was re-emphasized. It was noted that in some extreme cases temper embrittlement could be detected in tension tests by a drop-off in reduction of area values and deviations from cup-and-cone fracture, but these indications were usually not very dramatic.

Metallographic Tests

It had been discovered by Cohen et al [*12*] that grain boundaries in an embrittled steel could be revealed by etching with an ethereal picric

---

[6] It will be shown later that the temper brittleness C-curve is due to a set of phenomena different from those of a nucleation-and-growth type of phase transformation. The term "C-curve" is used here in conformity with past references, but is not meant to imply its more common meaning.

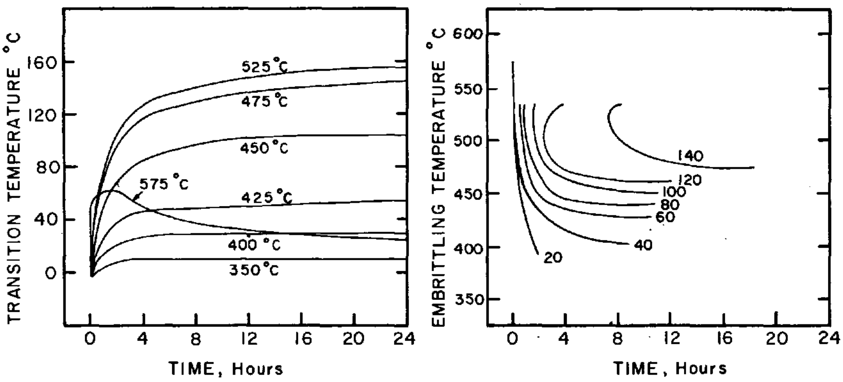

FIG. 3—(left) *Results of Vidal* [16] *for a chromium steel (0.25 per cent carbon, 0.030 per cent manganese, 1.38 per cent chromium, 0.044 per cent phosphorus) originally quenched and tempered at 650 C. Transition temperature, determined by arbitrary fracture energy, versus time of embrittlement at various temperatures.*

(right) *Same replotted to show rough C-curve behavior; rise in transition temperature indicated on each curve in deg C.*

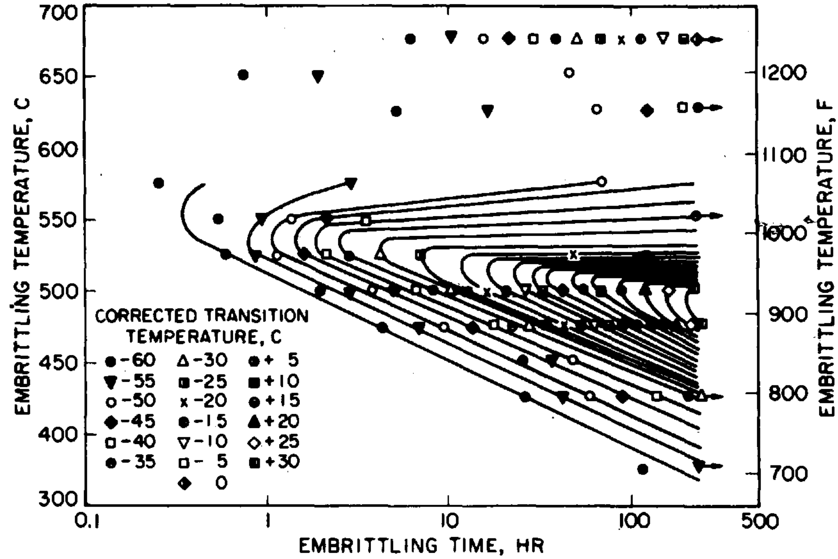

FIG. 4—*Isoembrittlement curves of Jaffe and Buffum* [17] *plotted as a time-temperature diagram, for a Ni-Cr steel (0.39 per cent carbon, 0.79 per cent manganese, 0.77 per cent chromium, 1.26 per cent nickel, 0.015 per cent phosphorus), incorporating later correction* [18].

acid solution containing Zephiran chloride.[7] Later McLean and Northcott [*13*] showed that other solutions based on picric acid gave similar results; in particular, aqueous picric acid seemed to work almost as well

---

[7] A common germicide, one of several surface-active agents which enhances the action of picric acid etches.

as any, and it was the easiest to prepare. These etchants were found to differentiate between the embrittled and tough conditions of steels containing phosphorus.[8] The main attack appeared to occur along prior austenite grain boundaries, although ferrite boundaries within the prior austenite grains were sometimes revealed. Woodfine showed in a succeeding paper [*14*] that etching produced grooves along austenitic and ferritic boundaries, as if due to segregated impurities, but no precipitate was revealed.

Woodfine noted that temper brittleness, *per se*, was often confused with other forms of loss of toughness after quenching, and that this only helped to obscure the real nature of temper brittleness. He suggested that the term be applied only to the phenomenon originally observed in nickel-chromium steels and that such effects as "500 F embrittlement" and the rise in transition temperature due to simple structural coarsening at high temperatures be excluded.

Effects of Time and Temperature

The 'C-curve' nature of temper embrittlement had been confirmed by the work of Vidal [*16*] (Fig. 3) and Jaffe and Buffum [*17*] (Fig. 4). Both the rate of embrittlement and the maximum temperature at which embrittlement can occur are expected to vary somewhat with the composition of the steel. For example, Jaffe and Buffum's results for their nickel-chromium steel (Fig. 4) show that initial embrittlement is most rapid at about 550 C, whereas at a later stage the rate is greatest at about 500 C. Vidal's results for a 1.4 per cent chromium steel, although less extensive, show that the rate is greatest initially at 575 C and later at 525 C (Fig. 3).

Data on the maximum temperature at which temper embrittlement can occur are less clear, since in most of the steels studied, tempering at high temperatures led to coarsening of the ferrite grain size and agglomeration of carbides, with a concomitant rise in transition temperature. This "embrittlement" was often confused with temper embrittlement, and the practice of checking the fracture appearance to see whether intergranular fracture was actually present was not yet universally adopted. Hence, the conclusion by Jaffe and Buffum [*17*] that embrittlement could occur in their nickel-chromium steel up to the A_1 line can be questioned; however, they do seem to make a case for some embrittlement occurring up to 650 C. Cohen et al [*12*] showed that the Zephiran chloride etch produced slight grain boundary attack in a steel tempered at 630 C, which might have indicated embrittlement; however, they did not present any transition temperature evidence to support this.

[8] They do not work on susceptible steels which do not contain phosphorus (J. R. Low, Jr., private communication).

Several workers have observed "overaging effects" in which the amount of embrittlement passes through a maximum at higher temperatures (see Fig. 3). These observations are summarized in Table 1. (Some of these data appeared just subsequent to Woodfine's review but are included for completeness.) It still does not seem possible to reach any conclusions about the influences of various alloying elements; however, Preece and Carter [*19*] did conclude that in their phosphorus-containing high-purity steels the overaging effect was enhanced by the presence of chromium.

TABLE 1—*Summary of "overaging" observations.*

Composition of Steel						Temperature at Which Overaging Observed, deg C	Tempering Time at Maximum, h	Reference
C	Mn	Ni	Cr	P	S			
0.25	0.30	...	1.38	0.044	...	575	1	Vidal [*16*]
0.39	0.79	1.26	0.77	0.015	0.30	550	~48	Jaffe and Buffum [*17*]
0.33	0.59	2.92	0.87	0.037	0.27	550	8	Woodfine [*14*]
						575	½	
0.21	<0.01	0.01	2.40	0.044	0.01	525	~48	Preece and Carter [*19*]
						575	<48	
						600	<10	
0.19	1.36	<0.01	0.01	0.048	0.1	600	10	Preece and Carter [*19*]
0.19	0.99	0.1	2.31	0.053	0.1	600	<10	Preece and Carter [*19*]
0.19	0.12	3.2	2.13	0.058	0.05	500	168	Preece and Carter [*19*]
						525	48	
						550	<48	
						575	<48	
						600	10	
0.20	0.01	0.01	1.98	0.094	0.01	500	48	Preece and Carter [*19*]
						525	<48	
						575	<48	
						600	10	

Effect of Composition

At the time of Woodfine's review, knowledge of the effects of various elements on the susceptibility to temper brittleness was still quite incomplete; the work of Steven and Balajiva [*20*], which finally identified the impurities responsible for the problem, was not to appear until 1959. In fact, the effects of the various *alloying* elements are still being unravelled at the present time. Nevertheless, certain aspects had become clear by that time, and these will be summarized at this point.

Plain Carbon Steels

A consensus had been reached, based mainly on the work of Greaves and Jones [*10*] and Hollomon [*1*], that plain carbon steels containing less than 0.5 per cent manganese are not susceptible. This view was challenged by Jaffe and Buffum [*21*] and by Libsch et al [*15*], who took the position that embrittlement occurs so rapidly in plain carbon steels that it cannot be prevented by quenching. The "plain carbon steel" used by Jaffe and Buffum actually contained 0.8 per cent manganese, and it is now fairly clear that this is enough (with the 0.013 per cent phosphorus also present) to produce the slight embritlement observed (see Fig. 6). Entwisle and Smith [*22*] later showed that a 0.4 per cent carbon, 0.65 per cent manganese steel of unspecified purity treated at 480 C for 24 h showed only about 5 per cent intergranular fracture, and thus was not susceptible to temper brittleness in the usual sense of the term. Woodfine carefully reviewed the paper by Libsch et al [*15*] and was able to show that their "embrittlement" was due to structural coarsening and could be correlated with the decrease in hardness during tempering. Since the embrittlement kinetics did not match those of temper embrittlement, and no evidence could be found of their grain boundary attack by the Zephiran chloride etch or intergranular fracture, it was concluded that their results had nothing to do with temper brittleness. Thus, the original conclusion about plain carbon steels remained intact.

Carbon

Jolivet and Vidal [*11*] showed that a reduction of carbon content from 0.22 to 0.73 per cent in a chromium steel led to a reduction in embrittlement. Buffum et al [*23*] later reported that a high-purity alloy containing 0.003 per cent carbon, 0.0004 per cent nitrogen, 0.8 per cent manganese, 1.5 per cent nickel, and 0.6 per cent chromium was not susceptible to temper embrittlement, and they concluded that carbon or nitrogen, or both are necessary for temper brittleness.[9]

Nickel, Chromium, and Manganese

There was wide agreement that increasing amounts of any of these elements led to increased embrittlement; however, there was conflicting evidence as to whether plain nickel steels were susceptible [*10,13,24*].

Molybdenum

It was accepted that additions of up to 0.5 per cent either decreased or eliminated embrittlement [*10,11*], whereas larger amounts permitted embrittlement to occur [*16*].

---

[9] In the light of more recent developments which will be discussed later, this conclusion is no longer acceptable. What Buffum et al probably succeeded in doing was to make a steel which was pure enough that it did not contain sufficient levels of the specific impurities that lead to embrittlement.

Vanadium and Tungsten

The addition of 0.23 per cent vanadium to a chromium steel was reported to enhance embrittlement [*11*] and a 3.8 per cent tungsten steel with no chromium and low manganese was found to be susceptible [*16*].

Phosphorus

It was generally recognized that temper brittleness increased with phosphorus content, but it was also known that it could be observed at phosphorus levels as low as 0.008 per cent [*11*]. Virtually every published study of temper brittleness listed the phosphorus content in the composition tables.

Antimony and Arsenic

Although Jolivet and Vidal [*11*] showed that antimony produced severe embrittlement in a chromium steel, Woodfine, for some unknown reason, was unwilling to regard this as genuine temper embrittlement [*2*]. However, just after his review Austen et al [*25*] showed that both antimony and arsenic produced embrittlement in a nickel-chromium (Ni-Cr) steel, and that the effect of antimony was so strong that it could be detected in a low-temperature tension test.[10]

The information available about other elements, such as oxygen, sulfur, silicon, nitrogen, aluminum, boron, titanium, and zirconium was sketchy; they did not appear to be strongly involved in temper embrittlement.

It should be reemphasized that the work reviewed up to this point had been carried out before the identity of the embrittling agents was documented. Hence, it is often not possible to know which elements were acting in each case, or whether differences in embrittling tendency attributed to various alloying elements were not sometimes due to different, but unmeasured, levels of the embrittling elements. Therefore, many of the conclusions up to this point about various alloying elements are open to question.

Effect of Microstructure

It was well known that an increase in the austenite grain size led to increasing severity of embrittlement. This is not surprising, since fracture of temper brittle steels occurs mainly along prior austenitic grain boundaries. There was ample evidence that pearlitic and bainitic steels could be embrittled in the same manner as tempered martensitic structures. The degree of embrittlement was thought to be less severe in these former cases, although quantitative evidence was lacking. Woodfine [*14*]

---

[10] Unfortunately, their steels also contained 200 to 300-ppm phosphorus, and this effect must have been superimposed upon those of arsenic and antimony.

later compared the temper brittleness developed in all three microstructures in a 0.33 per cent carbon, 0.6 per cent manganese, 2.9 per cent nickel, 0.9 per cent chromium, 0.04 per cent phosphorus steel. The results are shown in Table 2; they indicate that embrittlement is most severe in tempered martensite and least severe in pearlite, when measured by the shift in transition temperature. (Note, however, that the embrittled-state transition temperatures are roughly equal for all three structures.)

TABLE 2—*Development of temper brittleness in different microstructures in a Ni-Cr steel (after Woodfine* [14]).

Microstructure	Treatment	Transition Temperature, deg C	Embrittlement, deg C	Vickers Hardness, 50 kg
Pearlite.........	austenize 900 C, transition 620 C temper at 650 C, ½ h	+70		214
	same plus embrittlement at 500 C, 32 h	+121	51	210
Bainite.........	austenize 900 C, transition 350 C temper at 650 C, ½ h	+53		257
	same plus embrittlement at 500 C, 32 h	+162	109	253
Martensite......	austenize 900 C, oil quench, temper at 650 C, 1 h	−59		280
	same plus embrittlement at 500 C, 32 h	+137	196	278
Martensite......	austenize 900 C, oil quench temper at 650 C, 50 h	−52		223
	same plus embrittlement at 500 C, 32 h	+56	108	220

Effects of Prolonged Tempering Above Embrittling Range and of Double Tempering

A significant result of two separate investigations was that prolonged tempering at high temperatures reduces the amount of embrittlement which subsequently occurs during tempering in the embrittling range. Woodfine [*14*] showed that an increase in tempering time at 650 C from 1 to 50 h decreased the embrittlement obtained at 500 C by almost one half. This is shown in Table 2. He also found that a double temper of 128 h at 575 C, then 2 h at 500 C, gave *less* embrittlement than observed after only 2 h at 500 C. This same type of effect was shown to occur in arsenical steels by Austen et al [*25*], and more recently by Keh[11] in a phosphorus-containing 5140 steel. Woodfine [*14*] also showed that double tempering treatments of 8 h at 500 C, then 8 h at 550 C and

---

[11] A. S. Keh, presented at ASTM Symposium on Temper Embrittlement of Steel.

vice versa, gave degrees of embrittlement characteristic of the last treatment. (Both these sets of observations can be rationalized in terms of an equilibrium segregation of impurities to grain boundaries, which is reversible and which is inversely proportional to temperature. This will be discussed more fully later.)

Status of the Problem in 1959—Low's Review

The next review of the problem of temper brittleness was that of Low [*3*] in 1959; it concentrated mainly on the work reported since Woodfine's review. That work will be summarized in this section, with some differences in interpretation in the light of more recent work.

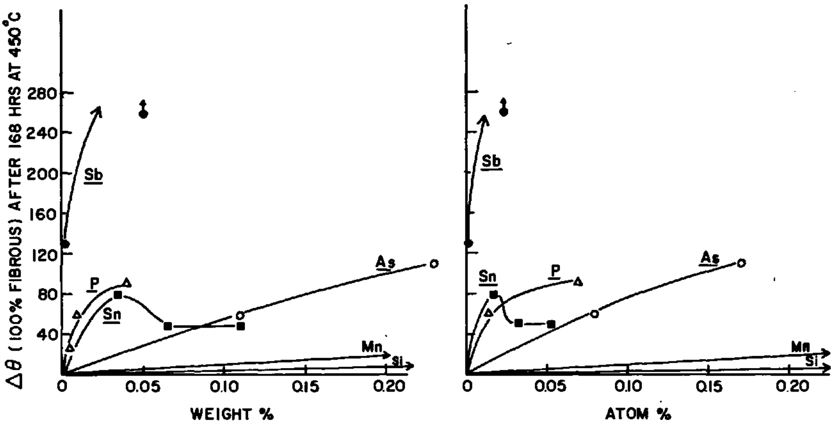

FIG. 5—*Data of Steven and Balajiva* [20] *plotted in manner of Low* [3] *to show amount of embrittlement produced by various elements for an arbitrary embrittling treatment of 168 h at 450 C. Base steel was 0.2 to 0.3 per cent carbon, 3 per cent nickel, 0.8 per cent chromium.*

Composition

Perhaps the most important single advance toward the understanding of temper brittleness came from the Mond Nickel Co. laboratories between 1956 and 1958. First, Balajiva et al [*26*] demonstrated that it was possible to make a steel consisting of 0.3 per cent carbon, 3.0 per cent nickel, and 0.75 per cent chromium under high-purity conditions that was *not* susceptible to temper brittleness, whereas a commercial steel of the same carbon, nickel, and chromium contents was susceptible. Later, Steven and Balajiva [*20*] determined the effects of specific elements added to the same high-purity alloy, one at a time. They found that the elements primarily responsible for temper brittleness are antimony, phosphorus, tin, and arsenic, and that manganese and silicon were also effective, but to a lesser degree. These results are summarized in

TABLE 3—*Influence of minor elements on temper embrittlement according to Steven and Balajiva* [20].

Elements Which Can Cause Embrittlement		Elements Which Do Not Cause Embrittlement When Present Singly	
Element	Maximum Amount Added in Study, weight %	Element	Maximum Amount Added in Study, weight %
Sb	0.05	Bi	0.002
P	0.04	Co	0.05
Sn	0.11	Cu	0.22
As	0.23	Ge	0.01
Si	0.74	Ga	0.01
Mn	1.5	Zn	0.05
		N	0.019

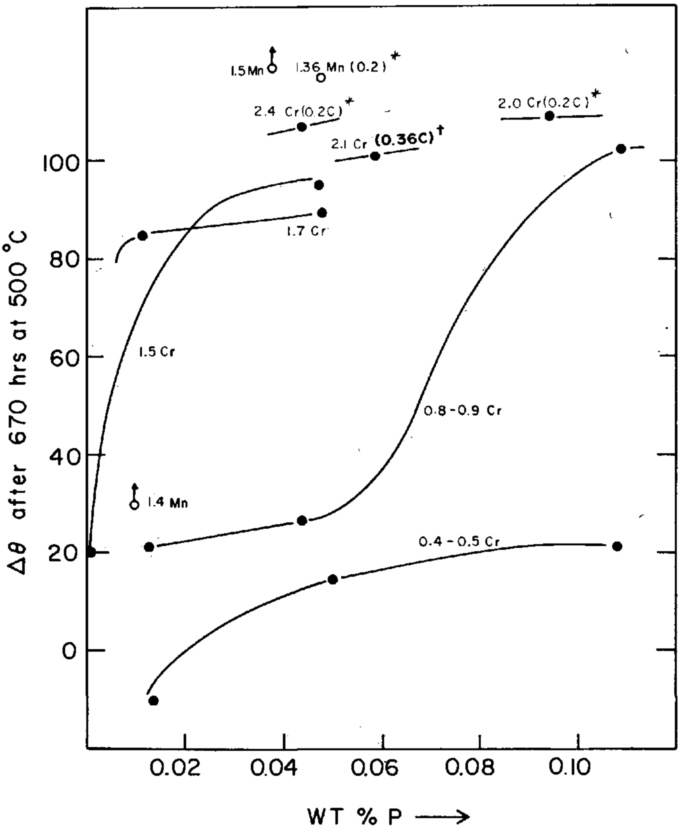

FIG. 6—*Embrittlement data for Cr-C-P steels (solid points) and Mn-C-P steels (open points) showing enhancement of phosphorus effect by chromium and manganese from Preece and Carter* [19] *and Low et al* [27]. *All points for 0.1 per cent carbon except as indicated, and embrittlement for 670 h at 500 C except for those marked by * (670 h at 450 C) and † (step cooled).*

Table 3. The relative effects of the embrittling elements are plotted in Fig. 5. It can be seen that the effects of manganese and silicon are of much lower magnitude than the other four elements. Indeed, it will be suggested later that these two should be discussed separately and that they might act in a different manner from the others.

With regard to the four main embrittling elements, it should be noted that the intensity of their effects might be significantly modified in steels of different compositions. In fact, recent work by Low et al [*27*] has shown that this is so. Also, much of the data of Fig. 5 is for very low concentrations where analytical techniques are perhaps susceptible to further improvement; thus, the exact shape of the curves shown should not be taken as the final word on the subject. In particular, the curve for tin seems a bit strange, and the intensity of the effect of antimony seems incredibly large.

Aside from the work of Steven and Balajiva [*20*], one of the few studies of temper brittleness carried out on high-purity steels (and thus amenable to unambiguous interpretation) was the work of Preece and Carter [*19*] which appeared in 1953. Their data enable one to get some understanding of the effects of alloying elements on the intensity of embrittlement by phosphorus. For example, Fig. 6 shows the effect of chromium; it can be seen that at low chromium contents (<0.6 per cent) even large amounts of phosphorus (about 0.1 per cent) are not too potent, whereas at higher chromium contents (>1.5 per cent) even small amounts of phosphorus (about 0.01 per cent) give large effects. What the effect of chromium is on the other three embrittling elements is not so clear; however, Preece and Carter did show that a 2.3 per cent chromium, 0.2 per cent carbon, 0.06 per cent arsenic steel had a $\Delta\theta$ of 64 C (where $\Delta\theta = \theta_E - \theta_{UE}$; θ_E is the transition temperature after embrittlement and θ_{UE} is that before). This would mean that, on a weight per cent basis, arsenic has about two thirds the embrittling strength of phosphorus, which agrees qualitatively with the findings of Steven and Balajiva [*20*] for a 3 per cent nickel, 0.8 per cent chromium steel. Finally, it is worth noting that Preece and Carter found that the Zephiran chloride etch indicated the presence of embrittlement only in steels which contained chromium.

Also shown on the plot in Fig. 6 are three points for plain manganese steels; they demonstrate that manganese is roughly twice as strong as chromium as an enhancer of the phosphorus effect. Some idea of the power of manganese can be seen from the fact that in a 2 per cent manganese, 0.2 per cent carbon steel with impurity contents of *less than* 0.001 per cent phosphorus, 0.02 per cent tin, 0.005 per cent antimony and 0.002 per cent arsenic, an embrittling treatment of 670 h at 500 C still produced a $\Delta\theta$ of 45 C. This can be compared with the 2.3 per cent chromium, 0.2 per cent carbon steel with less than 0.001 per cent phosphorus, 0.005 per cent antimony, and 0.002 per cent arsenic which showed a $\Delta\theta$ of only 20 C after the same treatment.

As noted earlier, there had been some controversy over whether a plain nickel steel will embrittle. The data in Table 4 show that it will, if both the phosphorus and nickel contents are high enough. It is obviously much less effective than chromium or manganese. It has been shown recently that plain nickel steels containing antimony, arsenic, and tin in the range 0.046 to 0.080 per cent are also susceptible [*27*].

Preece and Carter [*19*] also obtained some information on the effects of combinations of alloying elements. This is given in Table 5, which shows that the combination of 1 per cent manganese and 2 per cent chromium is much worse than 1 per cent manganese plus 3 per cent nickel, which in turn is somewhat worse than 3 per cent nickel plus 2 per cent chromium. This is in line with the previous conclusion that the embrittlement-enhancing power decreases in the order: manganese, chromium, nickel.

TABLE 4—*Effect of nickel on embrittlement due to phosphorus.*

Composition, weight %			$\Delta\theta$	Embrittlement Treatment	Reference
Ni	C	P			
4	0.20	<0.001	0	670 h, 500 C	Preece and Carter [*19*]
1.7	0.17	0.048	0	144 h, 500 C	Preece and Carter [*19*]
3.8	0.19	0.119[a]	51	670 h, 500 C	Preece and Carter [*19*]
2.94	0.27	0.134	84	24 h, 500 C	Woodfine [*14*]
3.6	0.35	0.054	41	step-cooled	Low et al [*27*]

[a] Also contained 0.1 per cent chromium—probably not significant.

TABLE 5—*Some effects of nickel, chromium, manganese combinations in a 0.2 per cent carbon, 0.05 per cent phosphorus steel.*

Composition			$\Delta\theta$[a]
Ni	Cr	Mn	
0.1	2.3	1.0	228
3.0	...	1.6	166
3.2	2.1	0.1	132

[a] After 670 h at 450 C.

With regard to the importance of carbon, Preece and Carter showed that lowering the carbon content to 0.014 per cent in a 1.4 per cent chromium, 0.04 per cent phosphorous steel decreased, but did not remove, the susceptibility to temper brittleness; the $\Delta\theta$ was still in excess of 35 C.[12] They also decarburized some of their alloys to carbon levels of about 0.003 per cent. In all cases the "unembrittled" transition tem-

---

[12] After 48 h at 500 C.

peratures were raised by about 100 C, probably due to the oxygen embrittlement which is common in low-carbon ferrite. The results of the "embrittling" treatments were erratic; in some cases the transition temperature increased as if embrittlement had occurred, and in other cases the transition temperature decreased, as if the aging treatment at 500 C were enough to permit carbon to return to grain boundary sites to counteract the oxygen [*28,29*]. In any case, their conclusion that temper embrittlement could not occur without carbon was questionable; it has since been shown to be incorrect by Low et al [*27*]. Preece and Carter did confirm, however, the fact that plain carbon phosphorus-bearing (0.13 per cent carbon, 0.03 per cent phosphorus) steels are not susceptible to temper brittleness.

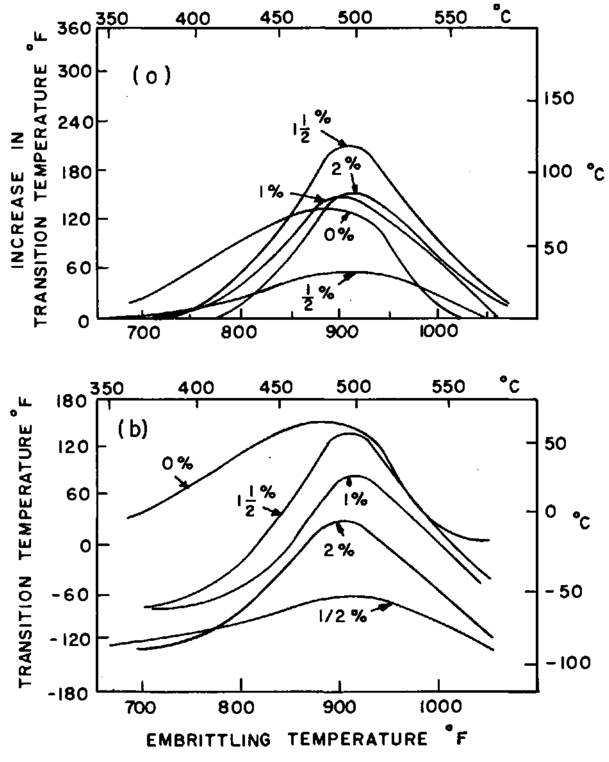

FIG. 7—(a) *Powers' plot showing effect of molybdenum on development of temper brittleness in 0.24 per cent carbon, 0.95 per cent chromium, 0.98 per cent manganese steel* [30]. (b) *Same plot modified to show actual transition temperatures.*

The work of Powers [*30,31*] in the mid-1950's affords the most extensive information on the effects of the strong carbide formers: molybdenum, tungsten, and vanadium. These results must be interpreted with great caution, however, since they contain no information on the levels of the embrittling elements: phosphorus, antimony, tin, and arsenic. Thus, some of the differences in $\Delta\theta$ attributed to variations in the alloy content may have arisen from differences in embrittling element content.

Powers [*30*] found that small amounts of both molybdenum and tungsten retard embrittlement produced by step cooling (see below), and that large amounts enhance it. Vanadium appears to enhance it in all amounts [*31*]. Molybdenum and tungsten seem to have roughly the same effectiveness on an atomic per cent basis, and the optimum addition appears to be three-fourths weight per cent molybdenum. There seems to be some benefit in adding combinations of molybdenum and tungsten or vanadium; however, these conclusions should be rechecked with high-purity steels.

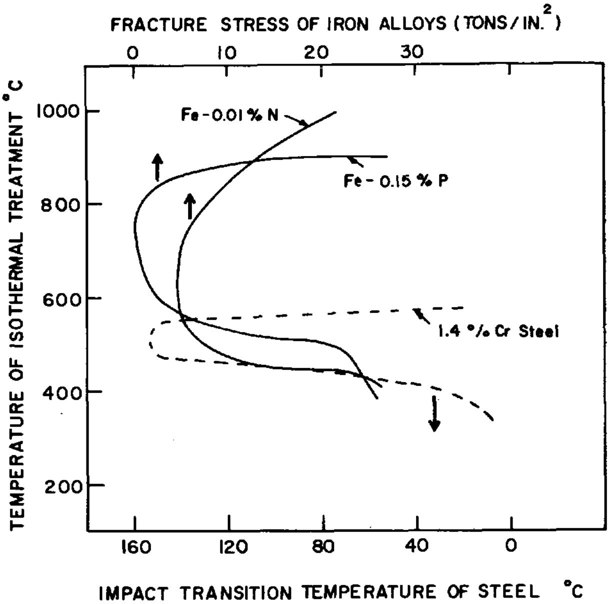

FIG. 8—*Result of Hopkins and Tipler* [32,33] *showing fracture stress at 77 K of two low-carbon iron alloys water quenched from various temperatures* (*solid lines*). *Superimposed on these plots are data of Vidal* [16] *showing degree of embrittlement in a chromium steel in 24 h at different tempering temperatures.*

In this regard one other point is worth mentioning. It is not settled whether such results should be evaluated as plotted in Fig. 7*a*, after Powers, or according to the slightly modified plot of Fig. 7*b*. That is, should one be most concerned with amount of embrittlement, that is, with $\Delta\theta$, or with the magnitude of the embrittled-state transition temperature? The point is that the lowering of *unembrittled* transition temperatures can more than compensate for an increase in $\Delta\theta$. The probable reason for this is that some embrittlement by impurity segregation can occur during the standard tempering treatment in the 625 to 675 C range (that is, before the embrittlement treatment is carried out). This has been indicated by intergranular fractures and response to the Zephiran chloride etch for some steels in the unembrittled condition. Additions of molybdenum may decrease this effect, thus lowering the curves in Fig. 7 and producing the apparent paradox of high susceptibility and low (embrittled) transition temperature. It is probable that the data shown in Figs. 7*a* and *b* could be better understood if one could know the impurity contents of each heat.

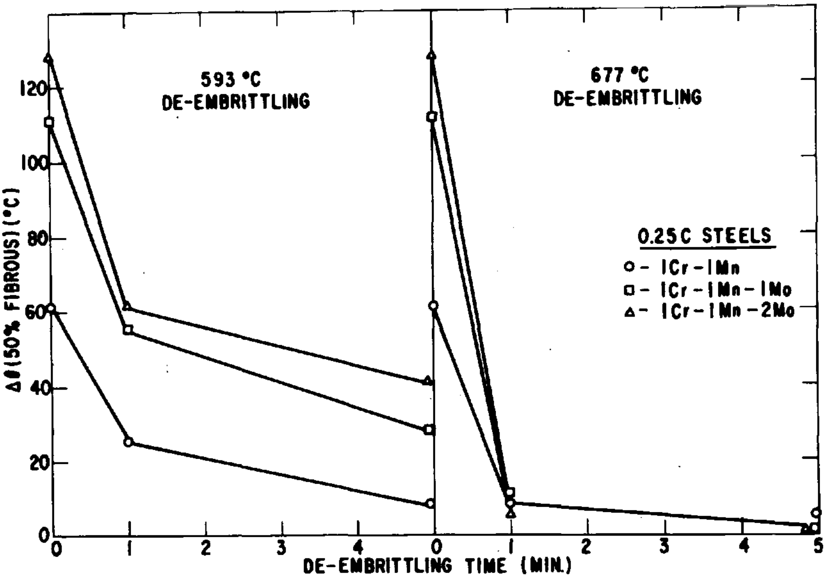

FIG. 9—*Results of Powers* [31] *plotted according to Low* [3] *showing reversal of temper embrittlement by short time heating above the embrittling range for two different temperatures.*

While on the subject of composition it would be well to clarify an ambiguity which has arisen in the literature. Hopkins [*32*] has suggested that the embrittlement phenomena observed by Hopkins and Tipler in low-carbon iron-nitrogen [*33*] and iron-phosphorus alloys [*34*] is an extreme manifestation of temper brittleness. There are several reasons to suspect that these observations have little to do with temper brittleness. First, the two types of embrittlement occur in two widely separated temperature regions, as shown by the superposition of curves in Fig. 8. Secondly, it is now well recognized that temper embrittlement does not occur in plain carbon steels, let alone high-purity irons. Thirdly, the results of Hopkins and Tipler, which were attributed to the grain boundary segregation of nitrogen and phosphorus, can equally well be explained by the embrittling effect of trace amounts of oxygen in low-carbon irons, and by changes in the carbon-oxygen ratio at the grain boundaries brought about by the quenching treatments employed. In fact, their results are strikingly similar to those obtained with the same kinds of heat treatments on high-purity, low-carbon iron containing *no* appreciable amounts of nitrogen or phosphorus [*29*]. These latter observations were explained in terms of the grain boundary strengthening effects of segregated carbon.

Effect of Time and Temperature

The 'C-curve' nature of embrittlement behavior, best characterized by Jaffe and Buffum and co-workers (Fig. 4), and the "overaging" effects (Table 1) have already been discussed, as have the observations of retardation of embrittlement by long-time tempering at high temperatures.

Two important additional contributions by Powers should be noted. The first is his quantitative determination of the reversion of embrittlement when embrittled specimens are heated to temperatures above the embrittling range [*31*]. This is shown best by Fig. 9, taken from the report of Low [*3*]. Note that these steels had been embrittled by a step cooling treatment of about *two weeks;* the molybdenum-free steel could be almost completely de-embrittled by a *5-min* treatment at 593 C, and that all of the steels could be reverted in *1* min at 677 C!

The second significant contribution [*30*] was the discovery that step cooling from around 590 C could produce as much embrittlement as much longer isothermal treatments at the maximum embrittling temperature.[13] Powers rationalized this behavior on the basis of Fig. 4, which shows that initial embrittlement is most rapid at about 540 C, whereas *maximum* embrittlement can be achieved only at lower temperatures. The step-cooling treatment thus attempts to optimize the effects of the whole embrittling range.

Effects of Plastic Deformation

Low [*3*] reviewed a series of Russian papers which dealt with beneficial effects of plastic deformation both on steels in the austenitic condition (prior to quenching) and on steels which had been embrittled (prior to impact testing). In the former case it could not be determined whether the benefits were derived from the deformation, *per se,* or from simple austenitic grain refinement. Low pointed out that some of the results observed could be explained from the latter effects alone. Very

---

[13] Low [*3*] reports that the step-cooling treatment now used to produce the same results is a shortened modification of Power's original method, as follows: hold 1 h at 593 C, furnace cool to 538 C, hold 15 h, cool to 524 C, hold 24 h, cool to 496 C, hold 48 h, cool to 468 C, hold 72 h.

definite improvement in toughness following a room temperature tensile deformation of 1.5 to 4 per cent of *embrittled* 0.10 per cent carbon, 0.97 per cent manganese, 0.96 per cent silicon, 0.36 per cent carbon, 1.10 per cent nickel steel was demonstrated by Stepanov [*36*].

Keh and Porr [*35*] studied the effects of cold work on 5140 steels of two different purities and found that if an *embrittled* steel was cold rolled and then reheated to the embrittling temperature, the degree of embrittlement was decreased. The amount of the decrease was proportional to the amount of cold work. If the steel was not reheated after cold work, the result was mainly a lowering of the impact energy in the ductile region and an obscuring of transition behavior. They attributed the effect of cold work plus annealing to a preferential segregation of impurities to dislocations, thus decreasing the concentration at grain boundaries.

Steeb and Rosenthal [*64*] found that a small strain in tension at 480 C lowered the subsequent susceptibility to embrittlement in 24 h at the same temperature. Recent work by Woodford [*37*] of the General Electric Co. on a nickel-chromium-molybdenum-vanadium (Ni-Cr-Mo-V) steel has shown that creep deformation in tension *during* the embrittling treatment succeeds only in delaying the development of embrittlement, but does not reduce the total embrittlement possible.

TABLE 6—*Etchants which reveal prior austenite grain boundaries in temper brittle steels.*

Etchant	Reference
Ethereal aqueous picric acid with Zephiran chloride	Cohen, Hurlich, and Jacobson [*12*]
Saturated aqueous picric acid	McLean and Northcott [*13*]
Ethereal aqueous picric with cetyl-trimethyl ammonium bromide (CTAB)	McLean and Northcott [*13*]
Ethereal aqueous picric with aryl ether of polyethylene glycol (aryl EPG)	McLean and Northcott [*13*]

Evidence for Structural and Chemical Change at Grain Boundaries

The key to the understanding of temper brittleness lies in the microstructure and composition of prior austenitic grain boundaries. This fact has been realized for decades, but the examinations of these boundaries by numerous analytical techniques have yielded little in the way of understanding until quite recently.

Many hundreds of specimens have been etched with reagents based on picric acid, first used by Cohen et al [*12*]. The consensus is that these etchants produce grooving of prior austenitic grain boundaries of embrittled specimens containing phosphorus, but no precipitate is ever revealed. In severe cases, ferrite boundaries are also revealed. Examples of some of the more effective etchants are given in Table 6. The response of embrittled chromium-free steels is negative-to-marginal for all except the last etchant in Table 6. The grain boundary grooving strongly suggests the segregation of impurities to grain boundaries, but of course does not prove it.

Evidence for the presence of a precipitate which would explain the embrittlement has been sought by many of the best electron microscopists without success. In 1959 it could be stated that: "In particular, no evidence has been found for any intergranular film or for any precipitation process in the grain boundary region" [*3*]. It will be shown later that this position should now be somewhat modified to take account of the carbide platelets which occur on prior austenite grain boundaries and which do play a significant role in the problem.

An important step forward was the work of Arkharov et al [*38*] which demonstrated that phosphorus segregated to prior austenite grain boundaries in embrittled Ni-Cr steels, and that this segregation was reduced by additions of molybdenum. His method consisted of etching the fracture surface of impact specimens with one drop of 1:1 nitric acid, then washing the surface with distilled water, and analyzing the resulting solution. Even with an embrittling treatment of only 3 h at 550 C, Arkharov found about 1.7 times the bulk phosphorus content on the intergranular fracture surfaces of steels containing 0.025 to 0.058 per cent phosphorus. When 0.18 to 0.80 per cent molybdenum was present, the results became somewhat erratic, but the excess averaged around 1.4 times the bulk content. Low [*3*] pointed out that Arkharov did not show that grain boundaries in unembrittled steels were free of excess phosphorus, since the fractures in these cases were fibrous.

Progress Since 1959

Most of the work done since Low's review has been concerned with the effects of composition and microstructure and the study of grain boundary segregation. Throughout this period the consensus has been, and remains, that reversible segregation of impurities to grain boundaries is at the root of the problem.

Composition

The major investigation of this period dealing with compositional effects is the recently completed study by Low et al [*27*]. In the most exhaustive study since Steven and Balajiva [*20*], they examined the roles of chromium and nickel, together and separately, in conjunction with the four main embrittling impurities: antimony, tin, phosphorus, and arsenic. Their base steel contained 3.5 per cent nickel, 1.7 per cent chromium, and 0.4 per cent carbon, and it was shown to be essentially nonsusceptible when high-purity melting practice was employed and with the impurities absent. The heat treatments involved oil, then liquid nitrogen (N_2), quenching from 870 C, tempering at 625 C for 1 h, and either quenching to give the unembrittled condition, or step cooling to give the embrittled condition. The criterion of embrittlement was the shift in transition temperature ($\Delta\theta$) as measured by a 50 per cent fibrous appearance.

Their findings on the interrelations between nickel and chromium and the embrittling elements are shown in Fig. 10. From this we can see the following:

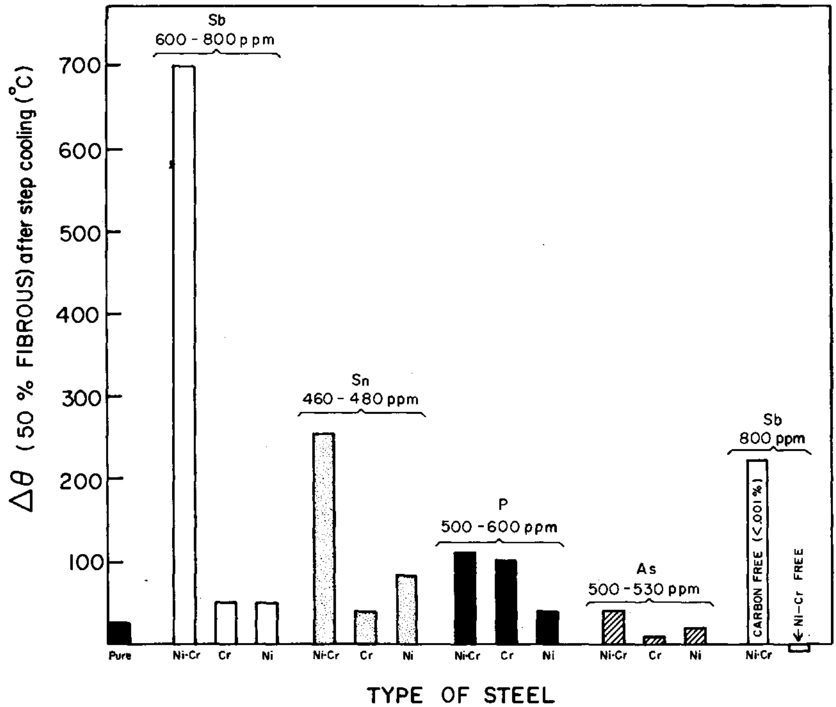

FIG. 10—*Results of Low et al* [27] *showing effects of alloying elements on temper embrittlement in steels containing 400 to 800-ppm (by weight) antimony, tin, phosphorus and arsenic.*

1. The $\Delta\theta$ for the high-purity base steel is 27 C, and is considered negligible. The fact that it is not zero is no doubt due to the 53 ppm (by weight) residual impurities.
2. Antimony has the largest effect in all cases, with tin, phosphorus, and arsenic following in that order.
3. The combination of nickel and chromium always leads to a greater $\Delta\theta$ than either separately. The relative effects of nickel and chromium, when present individually, depend on the specific embrittler present, as shown.

4. Embrittlement is possible in the absence of carbon. Indeed, it is quite pronounced in the presence of 800-ppm antimony. It can be seen that the effect of removing the carbon (or carbides) is to reduce the $\Delta\theta$ by about 480 C.

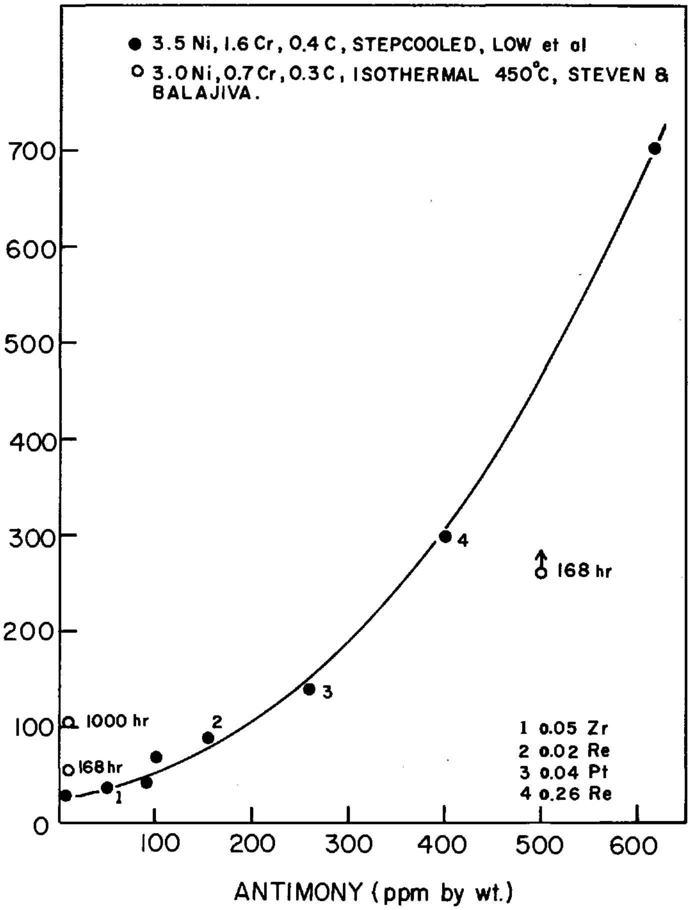

FIG. 11—*Results of Low et al* [27] *showing effect of antimony concentration on temper embrittlement of Ni-Cr steel, compared with results of Steven and Balajiva* [20]. *Small additions of other elements, as noted, had no apparent effect.*

5. Embrittlement does not occur (with 800-ppm antimony) if alloying elements are not present. Thus, a true plain carbon steel (that is, with no manganese) *is not* susceptible.

Low et al point out that the combination of nickel and chromium should be avoided in steels to be used in situations where temper brittleness can be troublesome. (It was concluded earlier in this review that the combination of chromium and manganese is even worse.) They made the important point that the results that they obtained may reflect differences in *rate* of embrittlement rather than in maximum attainable embrittlement, since the same thermal cycle was used to evaluate all cases.

Other results pertaining to compositional effects stemming from this investigation can be summarized as follows:

1. Additions of up to 0.3 per cent zirconium to an impure steel (206-ppm total embrittlers) and to a steel containing antimony, yielded no beneficial effect.
2. Additions of up to 0.26 per cent rhenium and 0.04 per cent platinum to antimony bearing steels had no effect.

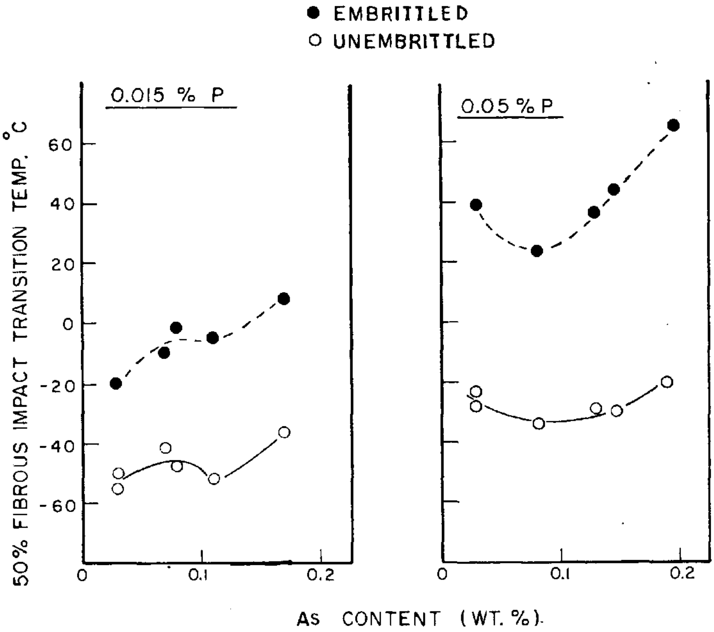

FIG. 12—*Results of Kal'ner* [39] *showing effect of arsenic concentration on transition temperature of two steels of low and high phosphorus content. Dotted curve for embrittled steel; solid curve for steel embrittled for 16 h at 520 C.*

3. The addition of 0.3 per cent lanthanum to an impure steel appears to give some reduction in embrittlement, although the results are somewhat uncertain due to variations in the manganese content.
4. Investigation of the effect of sulfur showed that it is capable of producing or enhancing embrittlement. Addition of 200-ppm sulfur to the high-purity steel raised $\Delta\theta$ from 27 to 50 C.[14]

[14] This is in contrast to the results of Capus and Mayer [*65*] who reported that the addition of 0.01 per cent sulfur to a 0.3 per cent carbon, 0.08 per cent chromium, 3 per cent nickel, 0.11 per cent manganese steel produced no susceptibility to either temper embrittlement or 500 F embrittlement. The difference in manganese contents between the two steels may have been critical, since this element appears to have enormous capability of enhancing the embrittling effects of small amounts of the embrittling elements (see Fig. 6).

5. The increase in embrittlement with antimony content was measured and compared with the results of Steven and Balajiva (Fig. 11). It would seem possible that the values for antimony content given in the latter work in the low-antimony steel could have been in error.

It is worthwhile pointing out that the impure steels mentioned above were made under the same conditions as the pure steels, except that Armco iron was substituted for electrolytic iron. A comparison of typical impurity contents and $\Delta\theta$ values is shown herewith:

	ppm				$\Delta\theta$ (deg C)
	Sb	Sn	P	As	
Pure steel	4	3	45	1	27
Impure steel	11	45	90	60	259

An interesting interaction between arsenic and phosphorus was reported by Kal'ner [39], who studied the effects of variation in arsenic content in steels containing two levels of phosphorus as follows:

	% C	% Mn	% Cr	% Ni	% Si	% S	% P
Steel A	0.42	0.65	1.03	0.08	0.31	0.010	0.015
Steel B	0.42	0.63	0.94	0.11	0.25	0.013	0.050

The effects of arsenic variation are shown in Fig. 12. It would appear that in the presence of phosphorus about 0.10 per cent arsenic can have some mitigating effect. This, of course, assumes that the levels of antimony and tin in these steels were negligible and constant. Since they appeared to be of essentially commercial quality, this may not have been true. In any event, Kal'ner attributed the effect to preferential segregation of arsenic to grain boundaries coupled with the fact that arsenic is a less severe embrittler than phosphorus. Even if real, the effect is too small to have any practical significance.

Microstructure

The investigation by Low et al [27] included an exhaustive search for a difference in appearance of prior austenite grain boundaries between embrittled and unembrittled steels. Their techniques included electron microscopic examination of both normal two-step and carbon extraction replicas of etched and unetched intergranular fractures, as well as transmission electron microscopy of grain boundary regions in thinned foils. No differences could be found, and it must be concluded that the embrittlement mechanism involves some form of atomic segregation not resolvable with current electron microscope techniques.

An investigation by Capus [*40*] produced some important information on the effect of prior austenitic grain size as well as on embrittlement at high tempering temperatures. He used the same type of high-purity steel as Steven and Balajiva [*20*]: 3 per cent nickel, 0.75 per cent chromium, 0.3 per cent carbon, and added either 0.023 per cent phosphorus or 0.074 per cent tin (that is, about 0.04 atm per cent of each). His thermal treatments involved oil hardening from 850 C, tempering at 600 C for 1 h, then either water quenching (giving the unembrittled state) or quenching and reheating for 168 h at 450 C to produce embrittlement. Austenitic grain size was varied by heating to higher temperatures before hardening, but the steels were always cooled to 850 C before quenching.

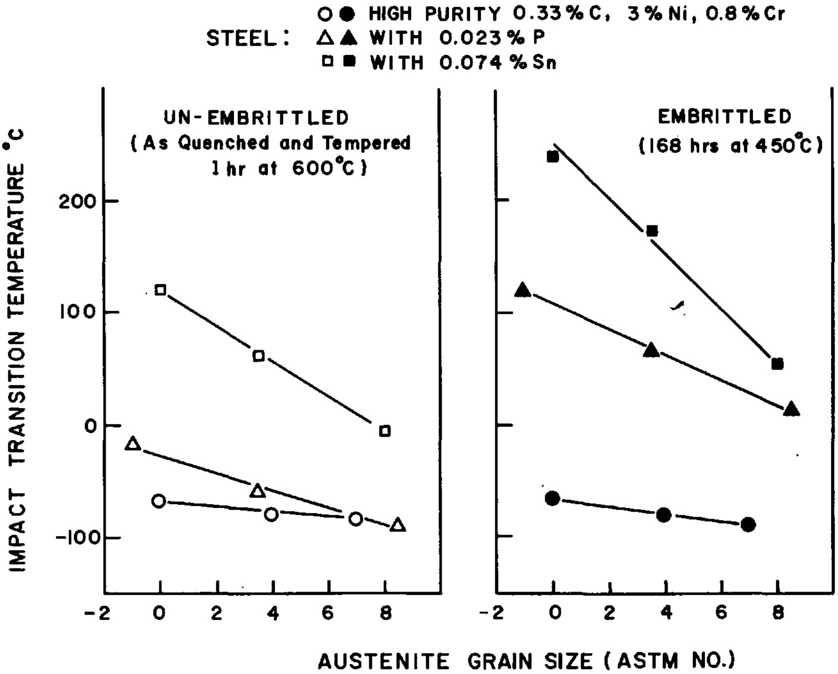

FIG. 13—*Results of Capus* [40] *showing influence of austenitic grain size on transition temperature of high-purity-base Ni-Cr steels.*

His most important results are shown in Fig. 13. First it should be noted that the $\Delta\theta$ for the pure steel is *zero,* and that a change in austenitic grain size has essentially *no effect* on transition temperature in either the tempered or embrittled conditions.[15] The other results can be summarized as follows:

---

[15] The only effect was that for the coarsest grain size (ASTM 0) the maximum impact energy was reduced from 145 to 115 ft·lb. It was not apparent whether this could be explained in terms of a coarser ferrite-carbide aggregate in the steel.

1. The grain size effect in the phosphorus and tin steels is present in the unembrittled condition and is roughly the same magnitude as for the embrittled condition. The effect of tin is particularly strong. Thus, it appears that substantial embrittlement can occur at the 600 C tempering treatment used.
2. The actual $\Delta\theta$ measured was greater for phosphorus than for tin. This seems to be a reflection of the fact that a large part of the tin segregation had already occurred at 600 C.
3. Segregation of phosphorus could be detected by the aqueous picric acid etch, even for tempering temperatures of 650 C, but segregation of tin was not detectable in this manner.
4. The relative amount of intergranular fracture increased with increasing austenitic grain size in both the as-tempered and embrittled conditions.

The austenitic grain size effect can be attributed to two sources:

(*a*) For a given total amount of segregated solute (in austenite) the amount *per unit boundary area* can be greater for larger grain sizes.

(*b*) In cases of grain boundary fracture, a larger grain size allows the crack to propagate with fewer deflections as it passes through the structure.

Two recent studies have focused attention on an important factor in temper brittleness that had been overlooked. The first was that of Hill and Martin [*41*] who carried out a fractographic examination, via an extraction replica technique, on steels of the types used by Austin et al [*25*]. They were basically: 3 per cent nickel, 0.8 per cent chromium, 0.4 per cent carbon, with about 300-ppm phosphorus and 50 to 880-ppm antimony, with and without additions of molybdenum. They used an Izod test and found very large embrittlement in the high-antimony, low-molybdenum steel, with a tempering treatment of 620 C for 2 h and embrittling treatment of 525 C for 4 h.

The primary finding was that a great number of large platelets of cementite could be extracted from the intergranular fracture surfaces of embrittled steels. It was fairly definite that the fracture had taken place *along* the cementite-ferrite interface, rather than through the cementite itself, which indicated that this usually tenacious interface [*42,43*] had been weakened, presumably by the presence of antimony. They noted that as much as 75 per cent of the surface of prior austenite grain boundaries could be covered by this cementite.

They concluded that antimony segregates in austenite during austenitization, and they attributed the embrittling effect of antimony to a lowering of the ferrite-comentite interfacial energy which: (*a*) catalyzed the the nucleation and growth of plate-like cementite in prior austenite grain boundaries, and (*b*) led to a large amount of low-fracture-energy interface. They did not report the appearance of grain boundaries in unembrittled steels.

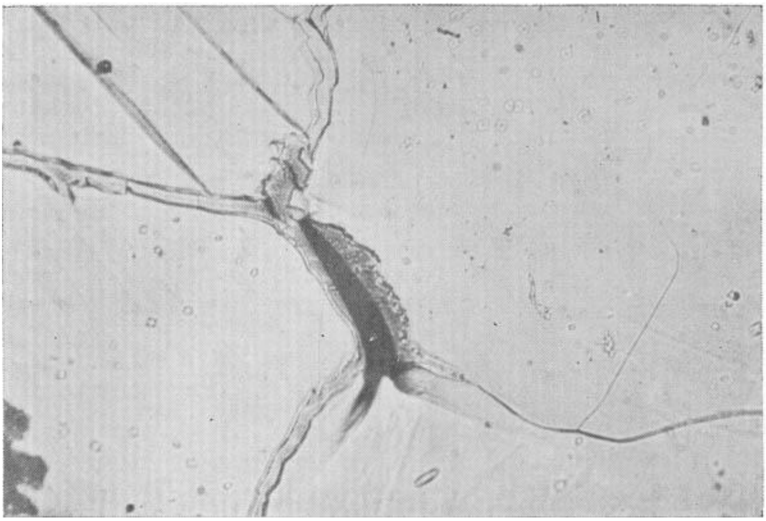

FIG. 14—*Example of longitudinal crack in grain boundary carbide in antimony free iron-0.035 per cent alloy tested in tension at 150 K; note tenacity of interface. Tensile axis horizontal* (×*500*) (*Ref.* 43).

FIG. 15—*Example of ferrite-cementite interface crack in Fe-0.02C-0.07Sb alloy embrittled for 24 h at 480 C and tested in tension at 77 K. Tensile axis horizontal* (×*500*) (*Ref* 44).

In an investigation designed to examine the implications of Hill and Martin's work, the effect of antimony on the cohesive strength of ferritic interfaces was studied by Restaino and McMahon [*44*]. A vacuum melted ferrite containing 0.02 per cent carbon and 700 to 800-ppm antimony was heat treated to give a microstructure of large ferrite grains (about 0.1

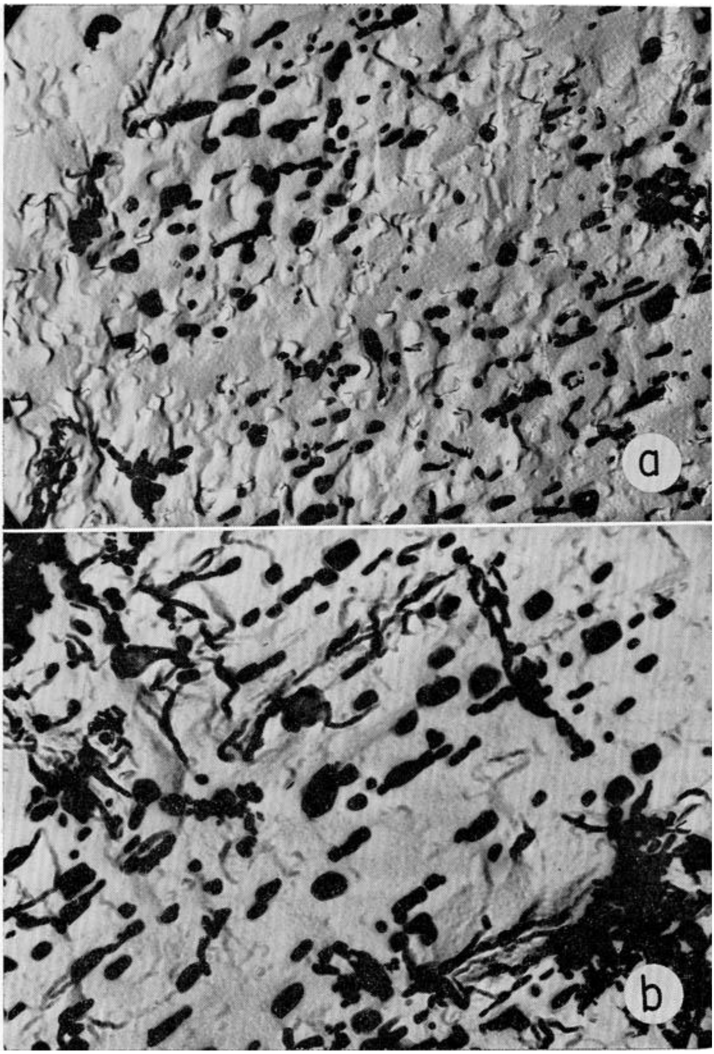

(*a*) Embrittled (×17,000). (*b*) Unembrittled (×23,000).

FIG. 16—*Carbon extraction replicas showing cementite platelets on austenitic grain boundary fracture facets of 3340 steel in the embrittled and unembrittled conditions* (*Ref* 44).

mm diameter) with coarse cementite plates in the grain boundaries. This was done so that light microscopy could be used to study interface effects in a structure which was a coarse-scale analog of a tempered steel.

When such a material *without antimony* is tested in tension at low temperatures, carbides are found to crack [*43*], usually across their thickness, but occasionally along their length, as shown in Fig. 14.

They never crack along the interface; the tenacity of this interface has been recognized for many years [*42*].

In the antimony-bearing ferrite [*44*] it was found that the interfaces could be made to split open (Fig. 15) if the specimens were embrittled at 480 C for 24 h prior to testing,[16] and they could be de-embrittled (that is, no interface splitting) if they were reheated for short times above 600 C. The de-embrittlement time-temperature curve looked much like that of Powers (Fig. 9) for reversal of temper brittleness; it is felt that they both represent the same phenomenon: the dispersion of segregated embrittling elements away from the interface, back into solution.

In order to carry these observations over to a steel, fractographic observations were carried out on a 3.5 per cent nickel, 1.6 per cent chromium, 0.4 per cent carbon heat with 620-ppm antimony (one of the steels used by Low et al [*27*]). It was found that carbide platelets could indeed be found on prior austenite grain boundaries in all three conditions: un-embrittled, embrittled, and de-embrittled (Fig. 16). (Intergranular fractures were obtained at low temperatures by using a very coarse austenitic grain size.) The appearance of these fractures was the same for all three cases; presumably the carbides formed during the initial 675 C tempering treatment. However, a striking difference was found when the antimony content on the fracture surface was determined by the one-drop etching technique of Arkharov [*38*]. Whereas the antimony content of the unembrittled and de-embrittled (650 C, ½ h) grain boundaries was below the limit of detectibility, the embrittled boundaries contained an average of 10 weight per cent antimony in the region within about 600Å of the fracture surface. (This was about 2½ times greater than the detectibility limit.) The conclusion drawn from this work was that antimony segregates in austenite during austenitization at high temperatures, but that it can segregate and de-segregate reversibly in ferrite at lower temperatures, thereby causing embrittlement and de-embrittlement.[17] The carbides provide a path of easy fracture (along the weakened interfaces) and intensify the embrittlement. Low et al [*27*] showed that by elimination of the carbides from this alloy, the embrittlement could be reduced by about two thirds (Fig. 10).

Evidence for Segregation

The direct evidence that has been obtained so far includes the demonstrations of phosphorus segregation in steel by Arkharov [*38*], of antimony segregation in steel by Restaino and McMahon [*44*], and the phos-

---

[16] Ferrite-ferrite interfaces were also embrittled, but to a much lesser degree.

[17] It has been found [*45*] that brittle fractures of the as-hardened and quenched antimony-bearing steel discussed here are largely intergranular, especially for coarse grain sizes. This would indicate that segregation occurs during the austentization.

phorus segregation in iron by Inman and Tipler [*46*]. There have been several types of indirect evidence: the grain boundary grooving by picric acid etches in the presence of chromium and phosphorus, and the observation by Plateau et al [*47*] of striations (indicating surface rearrangements due to absorption) on parts of the intergranular fracture of an embrittled steel, and the recent demonstration by Low et al [*27*] that a slight difference in microhardness exists between grain interior and embrittled grain boundaries in carbon-free steel containing antimony. This latter technique had been used by Westbrook and Aust [*48*] in previous segregation studies.

Evidence of a negative sort is the fact that grain boundary precipitates cannot be found, whereas all indications point to either a precipitate or segregation as the cause of temper brittleness. Several attempts at using autoradiography have been made [*31,49*] including the recent one by Low et al [*27*], but none with success. Stein [*50*] has discussed the limitations of this technique.

It would seem that the case for segregation is fairly well established; it now remains to work out the factors which control it.

Other Recent Work

There have been several other investigations during this period which are reported here for completeness, even though they do not materially alter the picture developed so far.

Banerjee [*51*] carried out a transmission and replication electron microscopic study of several steels tempered over a range of temperatures. He described the alteration of carbide type and morphology in detail, and concluded that both "500 F embrittlement" and temper brittleness were due to locking of dislocations by precipitates and to changes in dislocation density during tempering. These observations cannot hope to explain the classic characteristics of temper brittleness, such as reversibility, sensitivity to impurity content, and intergranular fracture mode, and therefore they will not be discussed further.

Various workers have made many other kinds of measurements in efforts to find correlated effects and to discover the nature of temper brittleness. They include magnetic coercivity and electrical resistivity [*66*], thermal emf [*67*] and internal friction [*68–71*], all without being very convincing. In particular, Kaddou and Rosenthal [*68*] compared internal friction peaks in embrittled and unembrittled 3310 steel and concluded that temper embrittlement was due to the pinning of dislocations by carbon and nitrogen, which occurred during the embrittling treatment. Keh and Swartz [*72*] later showed that such measurements could *not* differentiate between two 5140 steels with quite different embrittling susceptibilities, and Capus [*73*] detailed the arguments against the model, which will not be repeated here. Later, Wert and Rosenthal [*69*] modified the position somewhat when they found that the internal friction measurements did not always correlate with embrittlement and that decarburization of a 3310 steel did not remove the susceptibility. They concluded that the primary cause of temper brittleness was the segregation of unspecified substitutional and interstitial elements to ferrite grain boundaries. However, they ignored the work of Steven and Balajiva [*20*] and did not say why the prior austenitic grain boundaries were preferred fracture sites.

Weiss and co-workers [*74*] have demonstrated that the impact transition temperature of heat treated steel *is* raised after coarsening of the ferrite plus carbide structure by prolonged heating at 600 to 700 C, as suggested earlier by Woodfine [*2*]. They also showed that this type of treatment had no additional effect on the temper embrittlement phenomenon. More recently, they found [*75*] that temper brittleness affects the fatigue properties of a 0.65 per cent carbon, 0.92 per cent manganese, 1.86 per cent silicon, 0.03 per cent phosphorus, 0.019 per cent sulfur, 0.40 per cent chromium steel by lowering the fatigue life at stresses above the fatigue limit. In notched specimens it was found that the fatigue cracks start earlier and propagate more rapidly in the steel after a temper embrittlement treatment.

Finally, it is worth noting that the presence of temper embrittlement can be detected by a hydrogen embrittlement type of experiment, that is, by cathodic charging of specimens statically loaded in tension. Cabral et al [*76*] have shown that in a 0.3 per cent carbon, 3 per cent nickel, 0.6 per cent chromium steel containing more than 1100-ppm phosphorus, arsenic, and tin, the endurance curve (stress-to-fracture versus loading time) was markedly lowered when the steel was tested in the embrittled condition (48 h at 500 C) as opposed to the unembrittled condition (quenched from 625 C). In the former case the hydrogen-induced fracture occurred along prior austenite grain boundaries, and in the latter it was transcrystalline. These tests were done with *unnotched* specimens. Since fractures of commercial purity heat treated steels caused by hydrogen embrittlement or stress corrosion cracking are often observed to be intergranular [*59*], there seems to be some justification for suspecting that impurities can enhance these embrittlement phenomena by producing weak interfaces along which H_2 can be formed.

Theories of Temper Brittleness

The mechanisms which had been suggested to explain temper brittleness up to 1959 have been reviewed by Woodfine [*2*] and Low [*3*]. They covered a wide spectrum and were usually rather simply stated propositions which did not attempt to rationalize the very complex set of manifestations which characterize the problem. It is appropriate at this point to summarize these characteristics in Table 7; the primary characteristics must all be accounted for by any general theory, while the secondary ones might wait for the development of later details of the theory. Of

TABLE 7—*Summary of characteristics of temper brittleness.*

A. PRIMARY

1. Embrittlement can occur in alloy steels having ferrite + carbide microstructures which are heated in or cooled slowly through the range $\sim$375 to 575 C.
   A time-temperature-embrittlement diagram exhibits a set of C-curves. Embrittlement can occur to a minor degree at temperatures above the nose, but appears to be diffusion-limited below the nose [*1,17,18*].
2. Embrittlement occurs only in the presence of specific impurities and increases in severity with the concentration of these impurities.
   Antimony, phosphorus, tin and arsenic are the major embrittlers, listed in decreasing order of strength on a weight per cent basis. Manganese and silicon *appear* to be active in larger amounts, but this is less certain [*20*]. The increase in embrittlement with increasing concentration appears to saturate for As, P, and Sn.
3. Embrittlement is reversible.
   Even severely embrittled steels can be de-embrittled in a matter of a few minutes when heated above the nose of the C-curve [*31*].
4. Embrittlement consists of a decrease in cohesion along prior austenitic grain boundaries.
   The decohesion actually occurs in ferritic boundaries, but is restricted almost entirely to those which lie along surfaces of the prior austenite grains [*1–3*].
5. The degree and rate of embrittlement are profoundly affected by the alloy content.
   Plain carbon steels (with $< \sim$0.5 per cent Mn) are not susceptible [*2,27*]. Susceptibility is enhanced greatly by chromium and manganese (Fig. 6) and less strongly by nickel (Table 4). Small amounts of molybdenum and tungsten are inhibitors but larger amounts are enhancers [*31*]. Decreases in carbon content can diminish, but not prevent, embrittlement [*27*].
6. The only metallographic indication of the embrittled state is the grooving of the embrittled grain boundaries by several specific etchants in steels containing phosphorus.
   These etchants do not reveal a precipitate; neither is a precipitate to which embrittlement could be attributed observable by techniques of electron microscopy [*3,14,27*].

B. SECONDARY

1. In most cases a notched-bar impact test is required to show a significant difference in behavior between embrittled and unembrittled steels. (The shift in transition temperature is the usual criterion.)
   In more severe cases low temperature tension tests can indicate embrittlement, but in general normal plasticity must be severely restricted (by high strain rates or low temperatures) to allow the intergranular weakness to manifest itself [*3*].
2. Prolonged heating at temperatures above the nose of the C-curve (but below A_1) causes a decrease in the rate of embrittlement at lower (normal embrittling) temperatures (Table 2; Refs *25* and *77*).
3. When embrittled at temperatures somewhat above the nose of the C-curve, many steels exhibit an "overaging" type of response; that is, the degree of

TABLE 7—*Concluded.*

embrittlement goes through a maximum with increasing embrittling time (Table 1).

4. The shift in transition temperature ($\Delta\theta$) after embrittlement is greatest for steels of the tempered martensite microstructure and least for pearlitic steels, with bainitic steels falling in between (Table 2).
5. Increases in prior austenitic grain size result in proportionate increases in $\Delta\theta$, all other things being equal [*40,52*].
   This is normal behavior for an intergranular mode of fracture. The effect is even more pronounced if the steel is equilibrated at a lower temperature in the austenite region prior to quenching [*52*].
6. Plastic deformation after embrittlement, but before impact testing, appears to lower the transition temperature [*36*]. Plastic deformation during embrittlement delays the development of embrittlement [*37*].

course, any general theory must at least be able to be developed to account for the secondary characteristics.

The suggested mechanisms which appear to have any connection with reality all involve the segregation of some element to ferritic grain boundaries, with or without precipitation or ordering. That this must be the case is inescapable, considering the characteristics listed in Table 7.

Many suggestions involved segregation of carbon or nitrogen or the precipitation of carbide or nitride films. These can now be ruled out with confidence, if only on the evidence that removal of carbon and nitrogen does not prevent embrittlement [*27*]. In addition, it has been shown that segregated carbon increases cohesion of ferritic boundaries [*29*]. Furthermore, it has been demonstrated that prior austenite grain boundaries in quenched and tempered steels susceptible to temper brittleness already contain cementite platelets [*41,44*]. Thus, it is extremely unlikely that any revertible carbide or nitride film would form in this location.

A Recently Proposed Model

Temper brittleness is a very involved metallurgical phenomenon whose complexities appear to multiply the more closely one examines it. It is obvious that no simple model will explain all of its manifestations. A model has been proposed recently [*44*], however, which is believed to offer promise for the further development of a complete theory. Most importantly, it raises some specific questions which should be experimentally answerable.

Concentrating initially on the four main embrittling elements antimony, phosphorus, tin, and arsenic, we note that their equilibrium diagrams with iron are all similar in that they exhibit restricted gamma loops [*53*]. That is, these elements tend to stabilize the alpha phase. Thus, they are expected to show a stronger tendency to segregate to interfaces in the gamma than in the alpha phase [*54,44*]. This means that appreciable segregation could occur in austenite at high temperatures, but that the temperature range for strong segregation in ferrite could be much lower. The reasoning behind this proposition is that the forces which promote reduced solubility should be precisely those which promote segregation, for example, lattice strain, electron energy levels, etc. [*54*].

The proposal is that the embrittling elements segregate to austenite grain boundaries during austenitization and are retained there upon quenching. It is suggested that the tendency to segregate in ferrite is strong below about 550 C, but that the effect of entropy becomes too important above that range and the embrittlers tend to be "boiled off" the interfaces and driven back into solution (compare A-3, Table 7). When a steel is initially tempered above about 600 C, two things happen: first, the embrittlers are progressively dispersed away from the prior austenite boundaries, and, secondly, large carbide platelets form *preferentially* along these boundaries.[18] When the steel is then held for long times at temperatures below about 550 C, the embrittlers tend to segregate back to interfaces. Since they are always in the general vicinity of prior austenite grain boundaries, the ferrite-ferrite and ferrite-carbide interfaces in these regions get a large dose of them (compare A-6, Table 7). *It is postulated that these elements act to lower the cohesion of these interfaces*[19] (compare A-2, Table 7). This is especially damaging in the case of ferrite-carbide interfaces, since the lack of plasticity of the carbide tends to accentuate any tendency for interfacial weakness. The prior austenite grain boundaries are thus the preferred site for fracture for two reasons: they are in the regions richest in embrittling element content, and they contain a large density of carbide platelets which, when poisoned by an embrittling element, provide a path of easy fracture (compare A-4, Table 7).

When a susceptible steel is heated below about 375 C after having been tempered at >600 C, the diffusivities of the embrittling elements are so low that they cannot get back to the interfaces in significant amounts in reasonable times, and embrittlement is not observed. The net result is an apparent C-curve behavior (compare A-1, Table 7).

It follows that the longer the tempering time at the high temperatures, the greater will be the dispersion of embrittlers. Hence, development of embrittlement at lower temperatures will occur more slowly (compare B-2, Table 7).

It is not at all unusual for an intercrystalline weakness to require a type of test which severely limits plasticity in order for the weakness to manifest itself. A good example is oxygen embrittlement of iron, which usually shows up best at low test temperatures or high strain rates. In

---

[18] The reason for the preference for prior austenite boundaries is not known, but it appears to be rather general. Perhaps it is related to the segregation of some alloy or impurity elements. This matter should be given more attention in future research.

[19] This has already been demonstrated for the case of antimony [*44*].

general, the less severe the embrittlement, the more extreme is the test necessary to manifest it. Thus, it is not of fundamental significance that most temper brittleness is only detected unambiguously in an impact test. (A notched-bar tension test at low temperatures would probably serve almost as well.)

The only important gap in the model, as it now stands, is that it says nothing about the roles of the alloying elements in temper brittleness. It is now clear that these elements act to either enhance or retard the action of the embrittling elements, or to modify the morphology or size of grain-boundary carbides. At this stage it is only possible to list some of the more likely possibilities and to suggest in a few cases the roles that may be played by particular elements (Table 8).

TABLE 8—*Possible roles of alloying elements in temper brittleness (speculative).*

Role	
1. Enhancement of diffusivity of embrittling element thereby increasing rate of embrittlement	Mn increases diffusivity of P in Fe [*55*]
2. Reduction of diffusivity of embrittling element	. . .
3. Enhancement of segregation tendency of embrittling elements in austenite due to the segregation of the alloying element itself	(Cr?)
4. Enhancement of segregation of embrittling element in *ferrite*	. . .
5. Modification of carbide morphology	(Does Cr promote formation of carbides on prior austenite grain boundaries? Do Mo, W, and Cb inhibit this?)
6. Scavenging of embrittling elements	. . .
7. Solid solution hardening of ferrite so as to increase temperature and strain rate sensitivity of flow stress, thereby intensifying brittle tendencies	(Si?)

It will obviously require further work to answer the questions that are raised here. In particular, we must have data on the diffusitivies of the embrittling elements in iron and the effect that alloying elements have on these values. In addition, it will be necessary to determine the solubilities of the embrittling elements in iron and in the alloy steels. Virtually no information exists in this connection.

Finally, it has been shown in two cases (phosphorus in iron [*56*] and antimony in 3340 steel [*44*]) that the amounts of segregated impurity seem to be well in excess of the maximum amounts predicted by thermodynamic considerations. This raises the question of what is the state in which the segregated impurities exist. This question is completely open;

speculation would seem idle until we learn more about the solubility limits mentioned above, as well as the possible existence of metastable precipitation stages.

"500 F Embrittlement"

There exists another type of embrittlement which occurs during the tempering of low-alloy steels and which has been variously referred to as "500 F embrittlement" [*57*], "350 C embrittlement" [*58*], and "tempered martensite embrittlement [*59*]." All three terms refer to the same phenomenon: the minimum in the notched-bar impact energy as a function of tempering temperature, as shown in Fig. 17. The impact test is usually performed at room temperature, although a temperature of −78 is sometimes used to distinguish mild cases [*58*]. It is important to note that the specimens are *not* tempered at some high temperature (as in the test for temper brittleness) before the tempering treatment to be studied.

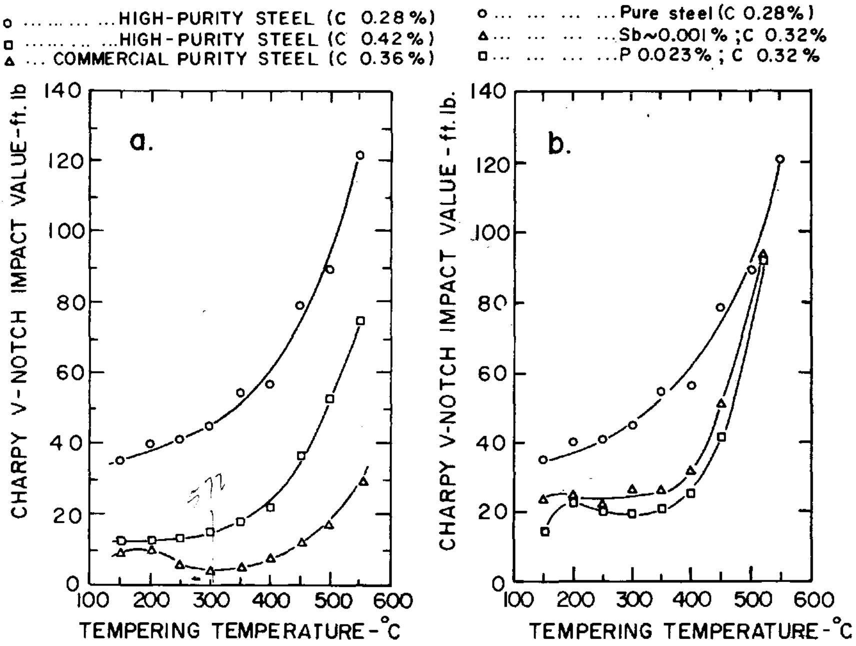

FIG. 17—*Results of Capus and Mayer* [58] *showing fracture energy versus tempering temperature for Charpy V-notch impact tests at 20 C:* (a) *high-purity steel versus commercial purity;* (b) *Influence of phosphorus and antimony.*

There are some rather striking similarities between the two types of embrittlement, enough to make one wonder whether they are not really variations of the same phenomenon [*59*]. Accordingly, the characteristics of 500 F embrittlement will be briefly summarized, and some tentative suggestions will be made regarding its mechanism. These suggestions are made to indicate the connection which seems likely to exist between the two phenomena and to provoke discussion and investigation of the problem.

The characteristics of 500 F embrittlement are as follows:

1. It appears as an anomalously low room-temperature impact energy when a quenched steel is tested after tempering in the range about 250 to 400 C (about 430 to 690 F) [*57*].
2. It is revealed only by a notched-bar impact test or by a fracture toughness test at low temperatures [*57*,*60*].
3. It does not occur in high-purity steels with sufficiently low levels of antimony, phosphorus, tin, and arsenic; higher levels of manganese are also said to lead to embrittlement [*58*].
4. The embrittlement appears to be connected with a lowering of cohesion along prior austenite grain boundaries; fractures of specimens tested between about 500 and 650 F (300 and 380 C) are largely intergranular [*61*,*62*].
5. Only martensitic steels are susceptible; bainitic steels are not [*57*].
6. The addition of silicon, which retards the third stage of tempering (low carbon martensite + epsilon carbide → ferrite + Fe_3C), displaces the impact energy minimum to higher temperatures [*63*,*58*].

Tentative Model

It is important to emphasize the difference in testing procedures used to study the two phenomena. In the case of temper brittleness one measures a shift in transition temperature, as a function of tempering time and temperature, in specimens which had been previously tempered at a higher temperature; in the other case, room temperature impact energy is measured as a function of tempering temperature. This is probably the main reason why they are often taken to be two different phenomena. It might be pointed out that a maximum in transition temperature occurs at the same tempering temperature as the impact energy minimum [*60*].

It is suggested that the explanation of 500 F embrittlement lies along the following lines: the embrittling impurities, which have segregated to austenite grain boundaries prior to quenching, remain there during tempering at temperatures below about 600 C. They act to promote intergranular decohesion in *untempered* martensite. (This is demonstrated by the large amounts of intergranular fracture in as-quenched 3340 steel containing antimony [*45*].) When the steel is tempered below about 200 C, the softening which occurs tends to offset this factor, and the impact energy rises. The decrease in impact energy and general lowering of the impact curve at higher tempering temperatures is caused by the formation of carbides on prior austenite grain boundaries, which acts to intensify the action of the still-segregated embrittling elements. As the tempering temperature is further increased, the impact values of a susceptible steel and a pure steel of the same basic composition should approach each other and should be about the same above 600 C, where dispersion of the embrittling elements has occurred. This effect can be seen in Fig. 17*b*.

If this model withstands future testing, there are still some questions which will need answering. For example, why does nitrogen [*58*] have such a strong enhancing effect in 500 F embrittlement? What role does it play in and around prior austenite grain boundaries? Also, is plain carbon steel really susceptible to 500 F embrittlement, as claimed [*58*], or is this just another case of the manganese content not being taken into account? Further research is necessary to clarify these issues.

Acknowledgments

It is a pleasure to acknowledge the contributions of P. A. Restaino and the valuable discussions with J. R. Rellick, and Drs. J. R. Low, and D. F. Stein and Miss Ann Turkalo; I am especially indebted to the latter for allowing me to see their manuscript (Ref *27*) prior to publication. Dr. Low also made many helpful comments in reviewing the manuscript.

The financial support of the Advanced Research Projects Agency of the Department of Defense is gratefully acknowledged.

References

[*1*] Hollomon, J. H., "Temper Brittleness," *Transactions*, American Society for Metals, Vol. 36, 1946, pp. 473–540.

[*2*] Woodfine, B. C., "Temper-Brittleness: A Critical Review of the Literature," *Journal of the Iron and Steel Institute*, Vol. 173, 1953, pp. 229–240.

[*3*] Low, J. R., Jr., "Temper Brittleness—A Review of Recent Work," in *Fracture of Engineering Materials*, American Society for Metals, 1964, pp. 127–142 (Proceedings of Conference held in Aug. 1959).

[*4*] Dickenson, J. H. S., *Proceedings*, Institute of Automotive Engineers, Vol. 12, 1917–18, p. 342.

[*5*] Howe, H. M., discussion to paper by W. H. Hatfield, *Proceedings*, Institute Mechanical Engineers, Jan.–May, 1919, pp. 405–407.

[*6*] See Ref *1*.

[*7*] Brearley, H., discussion to paper by R. K. Bagnall-Wild, *Proceedings*, Institute of Automotive Engineers, Vol. 11, 1916–17, p. 347.

[*8*] Greaves, R. H., "Temper Brittleness of Nickel-Chrome Steel," *Journal of the Iron and Steel Institute*, Vol. 100, 1919, pp. 329–339.

[*9*] Greaves, R. H. and Jones, J. A., "Temper Brittleness of Nickel-Chromium Steels," *Journal of the Iron and Steel Institute*, Vol. 102, 1920, p. 171.

[*10*] Greaves, R. H. and Jones, J. A., "Temper Brittleness of Steel; Susceptibility to Temper Brittleness in Relation to Chemical Composition," *Journal of the Iron and Steel Institute*, Vol. 111, 1925, pp. 231–255.

[*11*] Jolivet, H. and Vidal, G., "Valeur de l'essai de resilience pour l'etude de la fragilite de revenu," *Revue de Metallurgie*, Vol. 41, 1944, pp. 378–388.

[*12*] Cohen, J. B., Hurlich, A., and Jacobson, M., "A Metallographic Etchant to Reveal Temper Brittleness in Steel," *Transactions*, American Society for Metals, Vol. 39, 1947, pp. 109–138.

[*13*] McLean, D. and Northcott, L., "Micro-Examination and Electrode-Potential Measurements of Temper-Brittle Steels," *Journal of the Iron and Steel Institute*, Vol. 158, 1948, pp. 169–177.

[*14*] Woodfine, B. C., "Some Aspects of Temper Brittleness," *Journal of the Iron and Steel Institute,* Vol. 173, 1953, pp. 240–255.

[*15*] Libsch, J. F., Powers, A. E., and Bhat, G., "Temper Embrittlement in Plain Carbon Steels," *Transactions,* American Society for Metals, Vol. 44, 1952, pp. 1058–1068.

[*16*] Vidal, G., "Sur la fragilite de revenu des aciers au Chrome, au Molybdene, au Tungstene," *Revue de Metallurgie,* Vol. 42, 1945, pp. 149–155.

[*17*] Jaffe, L. D. and Buffum, D. C., "Isothermal Temper, Embrittlement," *Transactions,* American Society for Metals, Vol. 42, 1950, pp. 604–618.

[*18*] Carr, F. L. et al, "Isothermal Temper Embrittlement of SAE 3140 Steel," *Transactions,* American Institute of Mining, Metallurgical, and Petroleum Engineers, Vol. 197, 1953, p. 197.

[*19*] Preece, A. and Carter, R. D., "Temper-Brittleness in High-Purity Iron-Base Alloys," *Journal of the Iron and Steel Institute,* Vol. 173, 1953, pp. 387–398.

[*20*] Steven, W. and Balajiva, K., "The Influence of Minor Elements on the Isothermal Embrittlement of Steels," *Journal of the Iron and Steel Institute,* Vol. 193, 1959, pp. 141–147.

[*21*] Jaffee, L. D. and Buffum, D. C., "Temper Brittleness of Plain Carbon Steels," *Transactions,* American Institute of Mining, Metallurgical, and Petroleum Engineers, Vol. 180, 1948, pp. 513–518.

[*22*] Entwisle, A. R. and Smith, G. C., discussion to paper by J. W. Spretnak and R. Speiser, *Transactions,* American Society for Metals, Vol. 43, 1951, pp. 751–753.

[*23*] Buffum, D. C., Jaffe, L. D., and Clancy, W. P., "Effect of Carbon and Nitrogen on Temper Brittleness," *Transactions,* American Institute of Mining, Metallurgical, and Petroleum Engineers, Vol. 185, 1949, pp. 499–500.

[*24*] Jones, J. A., *Metal Treatment,* Vol. 4, 1938 (autumn), p. 97.

[*25*] Austin, G. W., Entwisle, A. R., and Smith, G. C., "Effect of Arsenic and Antimony on Temper-Brittleness," *Journal of the Iron and Steel Institute,* Vol. 173, 1953, pp. 376–386.

[*26*] Balajiva, K., Cook, R. N., and Worn, D. K., "Effect of Trace Elements on Embrittlement of Steels," *Nature,* Vol. 178, 1956, p. 433.

[*27*] Low, J. R., Jr., et al, "Alloy and Impurity Effects on Temper Brittleness of Steel," *Transactions,* Metallurgical Society, Americal Institute of Mining, Metallurgical and Petroleum Engineers, Vol. 242, 1968, p. 14.

[*28*] Low, J. R., Jr., and Feustel, R. G., "Intercrystalline Fracture and Twinning of Iron at Low Temperatures," *Acta Metallurgica,* Vol. 1, 1953, pp. 185–192.

[*29*] McMahon, C. J., Jr., "Intergranular Brittleness in Iron," *Acta Metallurgica,* Vol. 14, 1966, pp. 839–845.

[*30*] Powers, A. E., "The Influence of Molybdenum and Tungsten on Temper Embrittlement," *Transactions,* American Society for Metals, Vol. 48, 1956, pp. 149–164.

[*31*] Powers, A. E., "A Study of Temper-Brittleness in Cr-Mn Steel Containing Large Amounts of Molybdenum, Tungsten, and Vanadium," *Journal of the Iron and Steel Institute,* Vol. 186, 1957, pp. 323–328.

[*32*] Hopkins, B. E., "Intergranular Fracture in Wrought Steels," *Precipitation Processes in Steels,* Iron Steel Institute Special Report No. 64, 1959, pp. 137–156.

[*33*] Hopkins, B. E. and Tipler, H. R., "Effect of Heat-Treatment on the Brittleness of High-Purity Iron-Nitrogen Alloys, *Journal of the Iron and Steel Institute,* Vol. 137, 1954, pp. 110–117.

[*34*] Hopkins, B. E. and Tipler, H. R., "The Effect of Phosphorus on the Tensile and Notch-impact Properties of High-purity Iron and Iron-Carbon Alloys," *Journal of the Iron and Steel Institute,* Vol. 188, 1958, pp. 218–237.

[*35*] Keh, A. S. and Porr, W. C., "Effect of Cold Work on Temper Brittleness," *Transactions,* American Society for Metals, Vol. 52, 1960, pp. 81–93.

[*36*] Stepanov, F. P., *Fizika Metallov i Metallovedenie,* Vol. 6, 1958, p. 483.

[*37*] Woodford, D. A., "Effect of Creep Deformation and the Role of Grain Boundary Segregation on Temper Embrittlement," to be published.

[*38*] Arkharov, V. I. et al, *Fizika Metallov i Metallovedenie,* Vol. 2, 1956, p. 57.

[*39*] Kal'ner, D. A., "Effect of Arsenic on Properties of Alloy Structural Steel," *Steel* (USSR), No. 11, 1963, pp. 903–905.

[*40*] Capus, J. M., "Austenite Grain Size and Temper Brittleness," *Journal of the Iron and Steel Institute,* Vol. 200, 1962, pp. 922–927.

[*41*] Hill, R. G. C. and Martin, J. W., "A Fractographic Study of Some Temper Brittle Steels," *Metal Treatment and Drop Forging,* Aug. 1962, pp. 301–307.

[*42*] Hanemann, H. and Schrader, A., *Atlas Metallographica,* No. 1, 1933, plates 88–90.

[*43*] McMahon, C. J., Jr., "Micromechanisms of Cleavage Fracture in Polycrystalline Iron," Ship Structure Committee Report SSC 161, Washington, 1964.

[*44*] Restaino, P. A. and McMahon, C. J., Jr., "The Role of Antimony in Temper Brittleness," *Transactions,* American Society for Metals, Vol. 60, 1967, p. 699.

[*45*] McMahon, C. J., Jr., to be published.

[*46*] Inman, M. C. and Tipler, H. R., "Grain Boundary Segregation of Phosphorous in an Iron-Phosphorous Alloy and the Effect Upon Mechanical Properties," *Acta Metallurgica,* Vol. 6, 1958, p. 73.

[*47*] Plateau, J., Henry, G., and Crussard, C., "Influence of Physico-Chemical Conditions of Grain Boundaries on Intergranular Brittleness at Low Temperatures," *Precipitation Processes in Steels,* Iron and Steel Institute Special Report No. 64, 1959, p. 157.

[*48*] Westbrook, J. H. and Aust, K. T., "Solute Hardening at Interfaces in High Purity Lead—I. Grain and Twin Boundaries," *Acta Metallurgica,* Vol. 11, 1963, pp. 1151–1164.

[*49*] Mikus, E. B. and Siebert, C. A., "A Study of the Role of Carbon in Temper Embrittlement," *Transactions,* American Society for Metals, Vol. 50, 1958.

[*50*] Stein, D. F., *Transactions,* American Institute of Mining, Metallurgical, and Petroleum Engineers, in press.

[*51*] Banerjee, B. R., "Embrittlement of High-Strength Tempered Alloy Martensites," *Journal of the Iron and Steel Institute,* Vol. 203, 1965, pp. 166–174.

[*52*] Jaffe, L. D., Carr, F. L., and Buffum, D. C., "Effect of Grain Size Upon Temper Brittleness," *Transactions,* American Institute of Mining, Metalurgical, and Petroleum Engineers, Vol. 197, 1953, pp. 1147–1148.

[*53*] Hanson, M., *Constitution of Binary Alloys,* McGraw-Hill, New York, 1958.

[*54*] Cahn, R. W., "Grain Boundaries, Substructures, and Impurities," *Impurities and Imperfections,* American Society for Metals, Cleveland, 1955, pp. 41–83.

[*55*] Gruzin, P. L. and Minal, V. V., "Effect of Alloying Upon the Diffusion of Phosphorus in Ferrite," *Fizika Metallov i Metalovedenie,* Vol. 17, 1964, pp. 62–67.

[*56*] Cahn, J. W. and Hilliard, J. E., "On the Equilibrium Segregation at a Grain Boundary," *Acta Metallurgica,* Vol. 7, 1959, pp. 219–221.

[*57*] Klinger, L. J. et al, "The Embrittlement of Alloy Steel at High Strength Levels," *Transactions,* American Society for Metals, Vol. 46, 1954, pp. 1557–1598.

[*58*] Capus, J. M. and Mayer, G., "The Influence of Trace Elements on Embrittlement Phenomena in Low-Alloy Steels," *Metallurgia,* Vol. 62, 1960, pp. 133–138.

[*59*] Warke, W. R., "Some Observations on the Electron-Microscopic Fractography of Embrittled Steels," DMIC Memorandum 187, Battelle Memorial Institute, Columbus, 1964.

[*60*] Kula, E. B. and Anctil, A. A., "Tempered Martensite Embrittlement and Fracture Toughness in 4340 Steel," U.S. Army Materials Research Agency Technical Report No. 67-06 (AD 651066), Jan. 1967.

[*61*] Capus, J. M., "L'influence d'oligo-elements sur la resilience des aciers faiblement allies, trempes et revenus," *Revue de Metallurgie,* Vol. 56, 1959, pp. 181–189.

[*62*] Bucher, J. H., Powell, G. W., and Spretnak, J. W., *Application of Fracture Toughness Parameters to Structural Materials*, Greenberg, H. D. ed., Gordon Breach, New York, 1966, p. 323.

[*63*] Lement, B. S., Averbach, B. L., and Cohen, M., "Microstructural Changes on Tempering Iron-Carbon Alloys," *Transactions*, American Society for Metals, Vol. 46, 1954, pp. 851–877.

[*64*] Steeb, E. F. and Rosenthal, P. C., "The Effect of Strain and Temper Embrittlement on the Impact Transition Temperature of an AISI E-6150 Steel," *Transactions*, American Institute of Mining, Metallurgical, and Petroleum Engineers, Vol. 203, 1965, pp. 1254 1255.

[*65*] Capus, J. M. and Mayer ,G., "Temper Brittleness and the Residual Sulphur Content of Alloy Steels," *Journal of the Iron and Steel Institute*, Vol. 203, 1965, pp. 1254–1255.

[*66*] Tomilov, G. S., "The Magnetic and Electrical Properties of Certain Structural Steels in Relation to their Structure and Tendency to Temper Brittleness," *Physics of Metals and Metallography*, Vol. 10, No. 5, 1960, pp. 46–53.

[*67*] Shadrunova, A. P., "The Application of Thermoelectromotive Force for the Study of Temper Brittleness of Steel," (in Russain) *Izvestiya Vysshikh Uchebnykh Zavedenii, Chernaya Metallurgia,* No. 10, 1963, pp. 109–112.

[*68*] Kaddou, A. K. and Rosenthal, P. C., "Correlation between Internal Friction and Temper Brittleness in Steel," *Transactions*, American Society for Metals, Vol. 52, 1960, pp. 116–127.

[*69*] Wert, J. J. and Rosenthal, P. C., "An Internal Friction Study of an Alloy Steel Subject to Temper Brittleness," *Transactions*, American Society for Metals, Vol. 55, 1962, pp. 439–450.

[*70*] Makhykov, N. G., "Temper Brittleness and Internal Friction in Alloys of Type K40NXM," (in Russian) *Izvestiya Vysshikh Uchebnykh Zavedenii, Chernaya Metallurgia,* No. 1, 1964, pp. 142–144.

[*71*] Vishnyakov, D. Ya., Piguzov, Iu. V., and Tin-Tsiuan, Lei, "An Investigation by the Method of Internal Friction of Temper Brittleness of Manganic Construction Steel and the Influence on it of Molybdenum," (in Russian), *Izvestiya Vysshikh Uchebnykh Zavedenii, Chernaya Metallurgia,* No. 1, 1961, pp. 143–150.

[*72*] Keh, A. S. and Swartz, J. C., discussion of Ref *68, Transactions*, American Society for Metals, Vol. 52, 1960, pp. 128–130.

[*73*] Capus, J. M., discussion of Ref *68, Transactions*, American Society for Metals, Vol. 52, 1960, pp. 131–132.

[*74*] Weiss, B. Z., Freed, C., and Taub, A., "Anlassen und Anlassversprodung in Siliziumreichen Stahlen," *Haerterei-Technische Mitteilungen*, Vol. 19, 1964, pp. 141–145.

[*75*] Weiss, B. Z., Niedzwiedz, S., and Breuer, M., "Influence of Temper Brittleness on Fatigue Properties and the Initiation and Propagation of Fatigue Cracks in Silicon Steels," *Journal of the Iron and Steel Institute,* Vol. 204, 1966, pp. 152–156.

[*76*] Cabral, U. Q., Hache, A., and Constant, A., "Mise en evidence de la fragilité de revenu par des essais de corrosion sous tension en presence d'hydrogene." *Comptes Rendus,* Academic des Sciences, Paris, Vol. 260, 1965, Group 7, pp. 6887–6890.

J. J. Irani,[1] *M. J. May,*[1] *and D. Elliott*[1]

Effect of Thermal and Thermomechanical Treatments on the Temper Embrittlement of Low-Alloy Steels

REFERENCE: Irani, J. J., May, M. J., and Elliott, D., "**Effect of Thermal and Thermomechanical Treatments on the Temper Embrittlement of** Low-Alloy Steels,' *Temper Embrittlement of Steel, ASTM STP 407,* American Society for Testing and Materials, 1968, pp. 168–202.

ABSTRACT: The effects of rapid heating and ausforming on the phenomenon of temper embrittlement were examined in two alloy martensitic steels (BS 970 En 30B and En 40C), and the results contrasted with those for conventionally treated material. Standard Charpy V-notch impact tests and tensile data were supplemented by plane strain fracture toughness (K_{Ic}) measurements. A deailed structural and fractographic examination was carried out in order to correlate the microstructural changes with the mechanical properties. The results are discussed in the light of current theories. The experimental results indicate that several mechanisms can be responsible for temper embrittlement. A tentative model is proposed to explain the temper embrittlement trough observed in low-alloy steels, which is based on a combination of two mechanisms involving coarse carbide precipitation and high dislocation density resulting from dislocation pinning.

KEY WORDS: temper embrittlement, martensitic stainless steels, rapid heating, ausforming, tension impact tests, fracture toughness, sulfur carbide precipitation, dislocations, recovery, evaluation

Certain low-alloy steels suffer from an embrittling effect after they have been heated to (or slowly cooled through) a critical temperature range. This problem of temper embrittlement is particularly acute in large components, for example, heavy forgings, etc., which must necessarily, because of the masses involved, cool down very slowly from the heat treatment temperature. This type of embrittlement, which can be a serious problem in low-alloy engineering steels, is usually overcome by rapid cooling through the temperature range 600 to 400 C (1100 to 750 F) or by the addition of small amounts of molybdenum. In practice the latter technique is generally adopted.

---

[1] Senior scientific officers, BISRA—The Inter-Group Laboratories of the Metallurgy Division of British Steel Corporation, Sheffield, England.

The temper embrittlement referred to in this paper is that brought about by heating for short periods to temperatures in the range 250 to 450 C (500 to 850 F), and can be eliminated by re-tempering at temperatures above this range. The embrittlement phenomenon is that associated with tempering martensitic steels and cannot be measured by a shift in transition temperature. Therefore, this paper is not confined to embrittlement normally brought about by heating for long periods at temperatures in the range 600 to 950 F.

The aim of this paper is to show the effect of nonconventional thermal and thermomechanical treatments on this temper embrittlement phenomena, particularly with a view to clarifying the mechanisms involved. The treatments examined are rapid reaustenitizing and ausforming, and the results are compared with those obtained from conventionally heat treated material. Previous work [*1,2*][2] has shown that the rapid reaustenitizing treatment results in a marked refinement of the prior austenite grain size. In view of the suggestion [*3,4*] that temper embrittlement is due to the segregation of trace elements to austenite grain boundaries, a grain refining effect would be expected to reduce the susceptibility. Ausforming also results in a marked refinement of the structure, and, therefore, its effect on temper embrittlement is examined.

TABLE 1—*Chemical analyses of materials*

Material	Cast Number	Element, weight %								
		C	Si	Mn	Ni	Cr	Mo	V	S	P
En 30B...	JG	0.27	0.20	0.53	3.93	1.11	0.14	...	0.009	0.012
En 30B...	B 7365	0.32	0.20	0.49	4.09	1.22	0.24	...	0.040	0.027
En 40C...	E 3048	0.37	0.26	0.54	0.13	2.98	0.90	0.23	0.013	0.015
En 40C...	S 574	0.32	0.26	0.76	0.25	3.20	0.80	<0.03	0.024	0.011

Tensile, conventional Charpy V-notch and fracture toughness (K_{Ic}) data for two typical low-alloy steels subjected to various thermal and thermomechanical treatments and subsequently tempered are presented together with the results of structural and fractographic examination.

Experimental Procedure

Materials Used

The two steels selected for the study were to BS Specification 970, En 30B and En 40C. Two variants of each steel were examined, and the compositions are given in Table 1. All the steels were commerically melted except cast S 574 (En 40C) which was a 50-lb vacuum melted

---

[2] The italic numbers in brackets refer to the list of references appended to this paper.

cast. The significant difference between the two casts of En 30B (JG and B 7365) was the level of sulfur and phosphorus while the main difference between the two casts of En 40C (E 3048 and S 574) was the vanadium content.

Thermal and Thermomechanical Treatments

In the rapid reaustenitizing process bars $\frac{9}{16}$ in.^{2} by 6 in. long were resistance heated by a direct electric current from a welding transformer rated at 45 kVA. The heating current was controlled by an electronic timer and phase shift unit in the primary winding circuit. A more detailed description of the apparatus and heating technique has been given elsewhere [*1*]. Each bar was heated at a rate of 30 C/s to a temperature just above the Ac_3 temperature for the steel followed by an immediate water quench to room temperature. The time at temperature above Ac_3 was 2 to 3 s, and the complete heating cycle was of the order of 25 s.

For the ausforming operation, $\frac{9}{8}$-in.-diameter bars were austenitized at 980 C for 1 h and then quenched into a lead bath (at 500 C for En 30B and 550 C for En 40C) and subsequently ausformed by drawing in $\frac{1}{16}$-in. passes down to a final diameter of $\frac{5}{8}$-in. The total amount of deformation was approximately 70 percent and the bars were air cooled after the final pass.

For purposes of comparison some of the material was conventionally hot rolled, air cooled, and reheated for 1 h at 830 C and oil quenched.

Tempering Treatments

Specimens were examined in the untempered condition and after tempering in the range 200 to 600 C (400 to 1100 F) for 1-h periods.

Mechanical Test Technique

The conventional taper tension and Charpy V-notch impact specimens were tested in the normal way. These tests were supplemented by precracked Charpy size specimens (55 by 10 by 10 mm) tested at two strain rates. Specimens were fatigue pre-cracked using an Amsler vibrophore, and were tested in 3-point bending in slow bend at a rate of 0.020 in./min and in impact using a Manlabs 24 ft·lb impact machine, at a rate of about 11 ft/s. These results are reported in terms of the comparative energy, which is the computed fracture energy for a precracked specimen of fracture area comparable to that of a standard uncracked Charpy specimen.

Plane strain fracture toughness K_{Ic} values were determined using single edge notch bend specimens, fatigue pre-cracked in an Amsler vibrophore and tested in 3-point bending using a 35-ton Amsler tension

TABLE 2—*Fracture toughness of En 30B (Cast B 7365) conventional heat treatment 830 C oil quenched.*

Treatment	0.2% Proof Stress, ksi	Tensile Strength, ksi	Reduction of Area, %	Elongation, %	K_{Ic}, ksi $\sqrt{\text{in.}}$	G_{Ic}, in lb/in.^{2}
Untempered......	176	305	43.7	11.5	45.4	68.5
	...	...	...	...	43.05	62.5
	...	...	...	...	43.0	62.0
T 200 C...........	198	265	...	...	68.2	155
	...	...	...	...	65.6	143
	...	...	53.6	14.3	69.7	162
T 250 C...........	196	246	53.2	13.5	66.9	149.5
	...	...	...	...	67.3	151
	...	...	...	...	71.0	168
	...	...	...	...	70.9	166.5
	...	...	...	...	65.6	143
	...	...	...	...	68.2	155
T 300 C...........	195	240	...	...	62.1	128.5
	...	...	...	...	64.6	138.0
	...	...	55.0	13.1	62.5	130.0
	...	...	...	...	63.2	132.5
	...	...	...	...	63.2	132.5
	...	...	...	...	68.6	156.5
	...	...	...	...	62.7	130.0
T 350 C...........	190	228	...	...	67.0	150.0
	...	...	...	...	62.4	129.0
	...	...	54.5	12.7	63.1	133.0
	...	...	...	...	62.7	130.0
T 400 C...........	186	248	...	...	58.4	113.5
	...	...	...	...	58.5	114.0
	...	...	...	...	57.2	109.5
T 500 C...........	171	189	57.1	13.9	78.0^a	202.5
	...	...	...	...	69.8^a	162.5
	...	...	...	...	70.2^a	164.5
T 600 C...........	156	174	58.3	17.5	75.6^a	190.0
	...	...	...	...	72.3^a	1740
	...	...	...	...	80.4^a	215.0

[a] These K_{Ic} results are "invalid" according to current ASTM measurement criteria.

testing machine. Specimens of various dimensions were tested with span-to-width ratios of 8:1 and 4:1.

"Pop-in" was determined using a linear displacement gage situated across the notch, and an acoustic pickup crystal attached to the specimen. Load/displacement curves were autographically recorded, and the acoustic signal was related to the applied load. Specific details of the K_{Ic} measurement techniques have been reported previously [5].

TABLE 3—*Fracture toughness of En 30B rapidly reaustenitized.*

Treatment	0.2% Proof Stress, ksi	Tensile Strength, ksi	Reduction of Area, %	Elongation, %	K_{Ic}, ksi $\sqrt{\text{in.}}$	G_{Ic}, in lb/in.^{2}
Untempered......	196	315	20.4	...	37.6	48
	...	...	...	...	34.8	42.0
	...	...	...	...	46.6	73
	...	...	...	...	43.2	63
	...	...	...	...	37.8	48
T 200 C...........	216	270	32.0	12.7	61.1	124
	...	...	...	...	57.0	108
	...	...	...	...	57.6	111
	...	...	...	...	54.6	98.5
	...	...	...	...	57.5	110
T 250 C...........	214	243	41.0	9.5	65.4	143
	...	...	...	...	63.9	132
	...	...	...	...	60.8	123
	...	...	...	...	61.3	127
	...	...	...	...	58.2	113
	...	...	...	...	67.5	153
T 300 C...........	211	241	53.2	11.9	58.6	114
	...	...	...	...	61.7	127
	...	...	...	...	63.0	133
	...	...	...	...	61.7	127
T 350 C...........	207	230	55.2	12.7	66.0	146
	...	...	...	...	62.8	133
	...	...	...	...	66.6	148
	...	...	...	...	64.2	138
T 400 C...........	202	217	51.8	11.9	87.2	253
	...	...	...	...	87.0	253
	...	...	...	...	83.2	235
	...	...	...	...	75.3	188
	...	...	...	...	77.8	203
T 500 C...........	185	190	54.0	16.7	83.8[a]	238
	...	...	...	...	73.8[a]	182
T 600 C...........	144	159	62.4	19.0	84.0[a]	234
	...	...	...	...	71.0[a]	168
	...	...	...	...	69.0[a]	158
	...	...	...	...	70.7[a]	167

[a] Invalid according to ASTM measurement criteria.

Structural Examination

The microstructures were examined by optical microscopy, by direct carbon replication, and by transmission electron microscopy. The fracture topography was examined microscopically and by a two-stage carbon replication technique.

Nomenclature

Since the morphological features observed in martensite have been defined in different terms in the literature, it is necessary to clarify the terminology used in the present work. Transmission electron microscopy has shown that each plate seen under the optical microscope is actually a "bundle" of very fine lamellae [*6*]. These fine lamellae are referred to as martensite "units," and the misorientation at unit boundaries is usually very small, of the order of 2 to 3 deg, while that between neighboring bundles is greater than 15 deg [*7*].

TABLE 4—*Fracture toughness of En 30B (B 7365) ausformed.*

Treatment	0.2% Proof Stress, ksi	Tensile Strength, ksi	Reduction of Area, %	Elongation, %	K_{Ic}, ksi $\sqrt{\text{in.}}$	G_{Ic}, in lb/in.^{2}
Untempered......	206	334	25.4	11.9	72.2	174.5
	...	...	...	...	69.7	161
	...	...	...	...	69.6	160.9
T 200 C...........	248	322	37.2	11.9	78.8	205.5
	...	...	...	...	74.5	185.0
	...	...	...	...	66.8	144.5
	...	...	...	...	79.5	211
	...	...	...	...	73.8	183
T 300 C...........	255	293	36.9	9.1	65.1	141
	...	...	...	...	61.8	126
	...	...	...	...	61.7	125.9
	...	...	...	...	64.4	137.5
T 400 C...........	232	252	37.8	9.5	66.4	147.5
	...	...	...	...	63.8	135
	...	...	...	...	69.6	162
	...	...	...	...	74.3	183
T 500 C...........	202	210	48.8	12.3	77.6[a]	200.5
	...	...	...	...	81.3[a]	220
	...	...	...	...	66.0[a]	145
	...	...	...	...	75.5[a]	190
	...	...	...	...	81.1[a]	218.5
T 600 C...........	167	175	56.2	16.7	73.4[a]	174.5
	...	...	...	...	75.8[a]	171
	...	...	...	...	81.4[a]	219.5
	...	...	...	...	80.1[a]	213.5

[a] Invalid according to ASTM measurement criteria.

Experimental Results for En 30B

Steel B 7365 (High Sulfur and Phosphorus)

Mechanical Properties—The mechanical properties of this steel in the conventionally treated, rapidly heated, and ausformed conditions

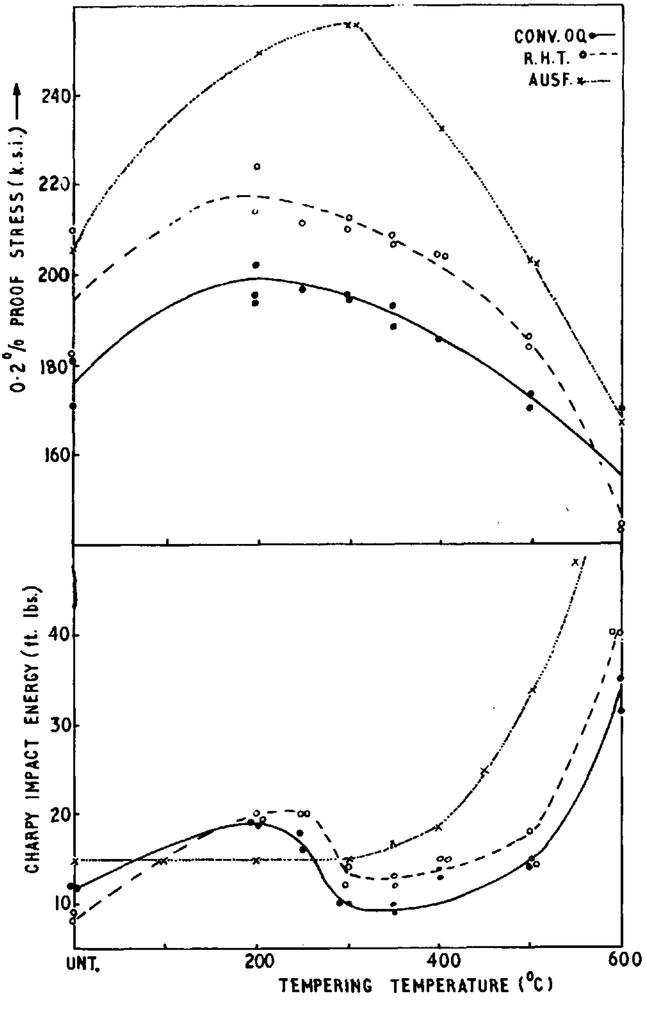

FIG. 1—*En 30B (B 7365) Effect of tempering on the 0.2 percent proof stress and Charpy impact energy.*

are presented in Tables 2, 3, and 4 respectively. The effect of tempering temperature (*T*) on the proof strength and Charpy V-notch impact energy is shown in Fig. 1. These results show the characteristic temper embrittlement trough for the conventionally treated and rapidly heated specimens, but not in the ausformed material. It can be seen that after tempering at temperatures above 500 C (930 F) there is a rapid increase in impact energy for all three conditions.

A more meaningful measure of the crack propagation resistance can be obtained from specimens containing an actual crack rather than a machined notch. Consequently, Charpy V-notch specimens (10 by 10

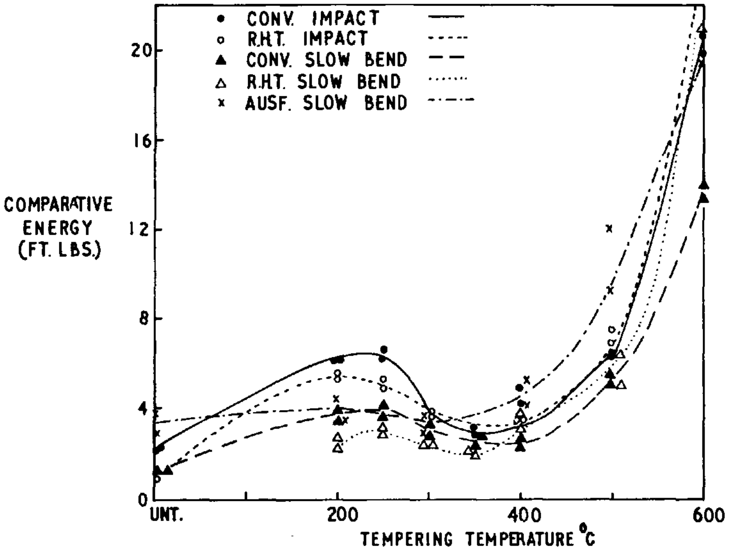

FIG. 2—*En 30B (B 7365) Effect of tempering temperature and strain rate on comparative energy (10-mm specifications).*

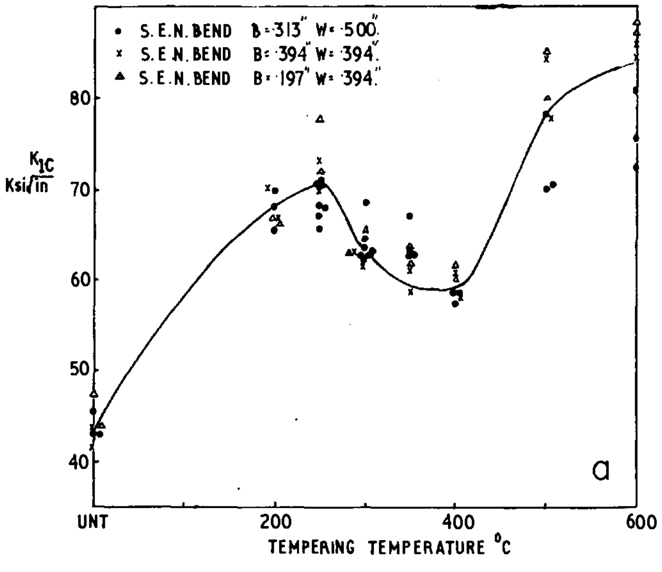

FIG. 3—*En 30B (B 7635) Effect of tempering on the fracture toughness of* (a) *conventionally oil quenched,* (b) *rapidly heated,* (c) *ausformed material, and* (d) *comparison of mean curves from a, b, and c.*

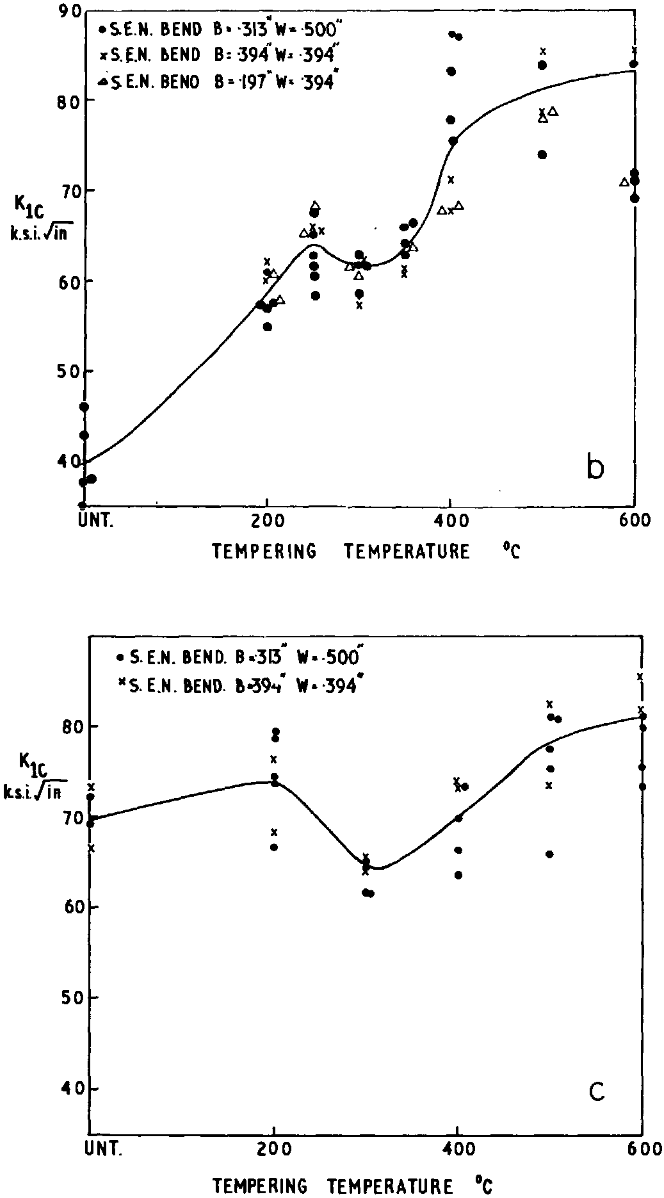

FIG. 3—*Continued.*

mm) from material in the three conditions were pre-cracked prior to testing both in impact and slow bend. The results, in terms of comparative energies, are shown in Fig. 2, and indicate for both rates of loading the same general trends as was observed from Charpy V-notch impact tests (Fig. 1). From Fig. 2 it can also be seen that the martensitic matrix

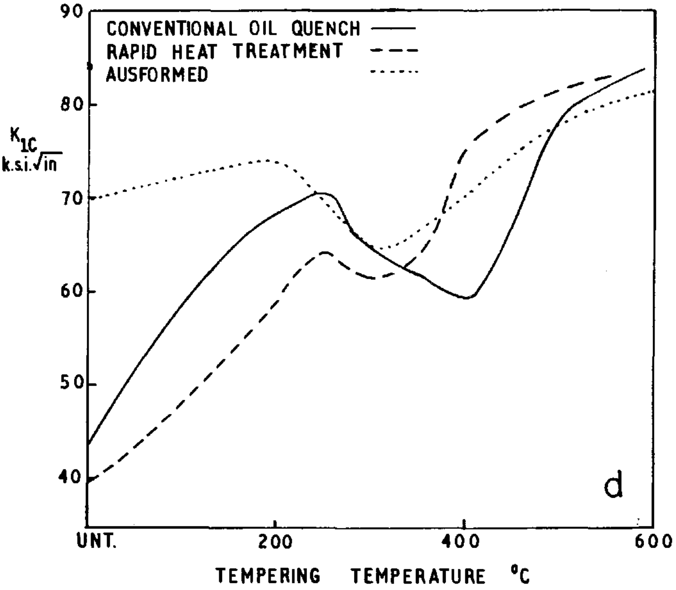

FIG. 3—*Continued.*

shows a greater resistance to crack propagation at the higher rate of loading, as has been reported previously for other carbon martensitic steels [*8,9*].

Plane strain fracture toughness (K_{Ic}) values for the steel in the conventionally treated, rapidly heated, and ausformed conditions are given in Tables 2, 3, and 4, respectively, together with the corresponding tensile data. It should be noted that the fracture toughness results for specimens tempered at the higher end of the tempering range are invalid according to current ASTM K_{Ic} measurement criteria. However, such results (indicated with an asterisk in the tables) are a good indication of the level of fracture toughness at these tempering temperatures. The K_{Ic} results obtained from various specimen dimensions are shown in Figs. 3*a–c*, and the mean curves are compared in Fig. 3*d*. It can be seen that there is a minimum K_{Ic} in the temper embrittlement range for each of the three treatments and that this effect is most pronounced in the conventionally treated material. The ausformed material offered the best fracture toughness at tempering temperatures up to approximately 400 C (750 F), while the rapidly heated material was slightly superior at the higher tempering temperatures. It should be noted that the K_{Ic} values of the ausformed material may be influenced by the grossly oblique nature of the crack propagation path (as can be seen in Fig. 4). This type of fracture is to be expected from the elongated grains produced by the ausforming process.

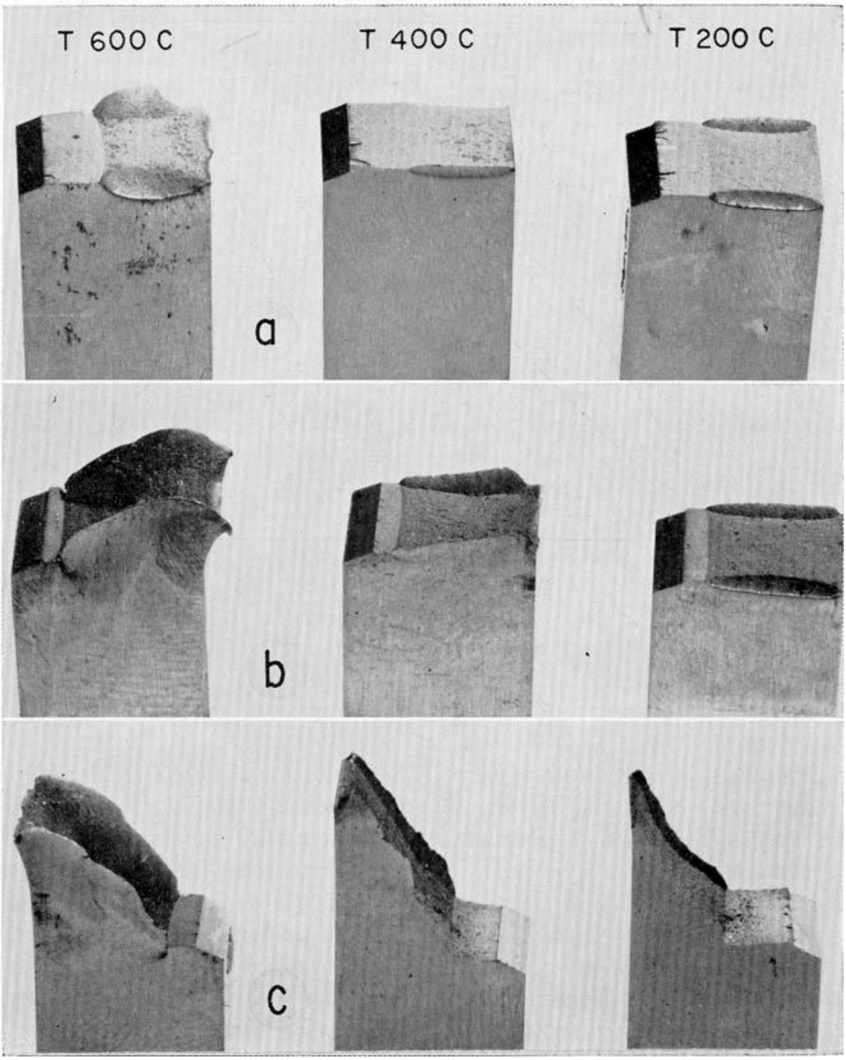

(*a*) Conventional oil quench.
(*b*) Rapid heat treatment.
(*c*) Ausformed.

FIG. 4—*Fracture appearance of En 30B (Cast B 7365) subjected to different treatments.*

Structural Examination—The optical structures observed after the three treatments are shown in Fig. 5, which indicates a marked refinement of the martensitic structure after rapid heating compared with the other two. The quantitative results of the effect of rapid heating on austenitic grain size have been reported elsewhere [*10*]. It is sufficient to mention that the conventionally treated specimens showed a prior

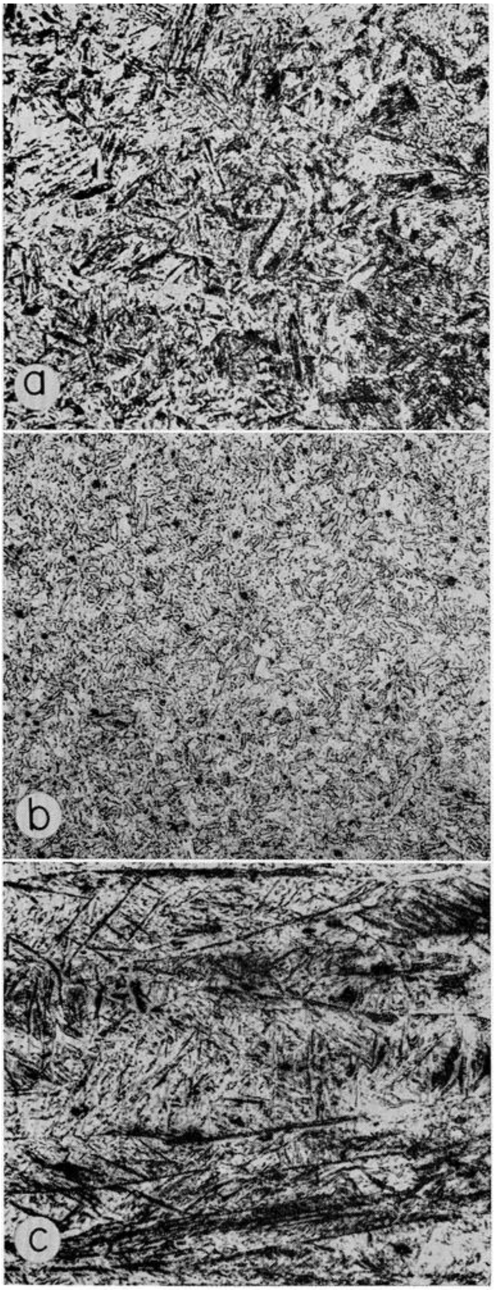

(*a*) Conventionally oil quenched, 830 C, 1 h, oil quenched.
(*b*) Rapidly heated, 30 C/s heating rate, water quenched.
(*c*) Ausformed, 980 C, 1 h, 70 per cent deformation at 500 C.

FIG. 5—*En 30B (Cast B 7365) optical microstructures, tempered 200 C.* (×*540*).

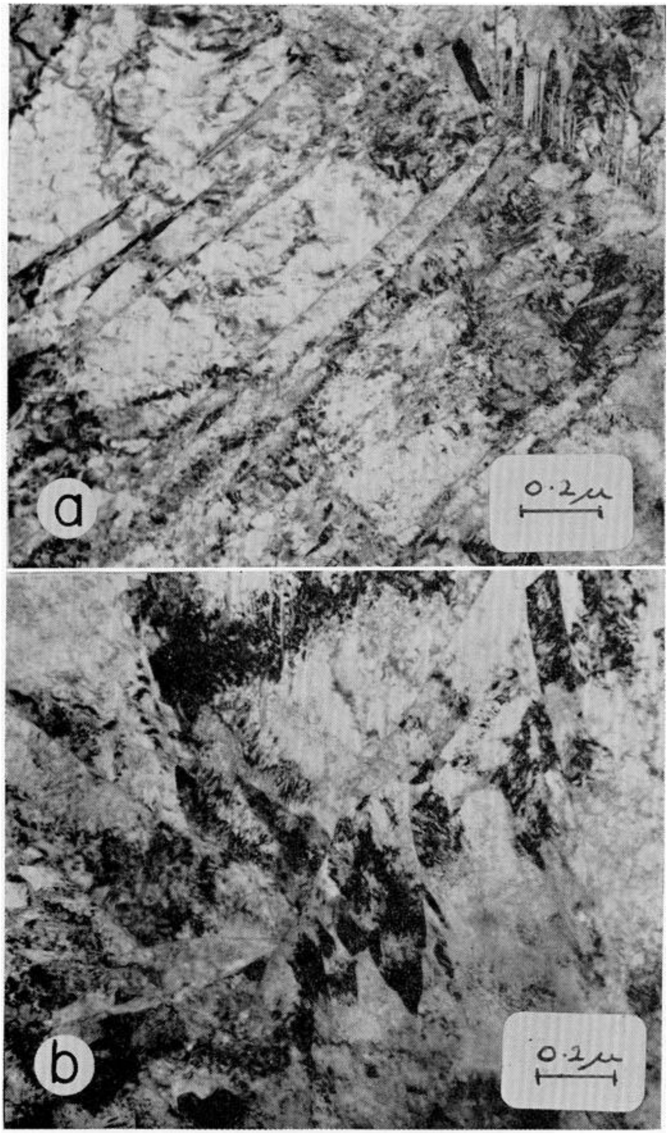

(*a*) Conventionally water quenched (×50,000). Carbide precipitation through auto-tempering.

(*b*) Rapidly heated and rapidly cooled (×50,000). No carbide precipitation.

FIG. 6—*En 30B* (*Cast B 7365*). *Transmission electron micrographs.*

austenite grain size of approximately 35 μm which was refined to approximately 7 μm after the rapid heat treatment cycle.

Transmission electron microscopy showed that in the rapid heated specimens the martensite unit size was refined (Fig. 6*b*) [*10*], though

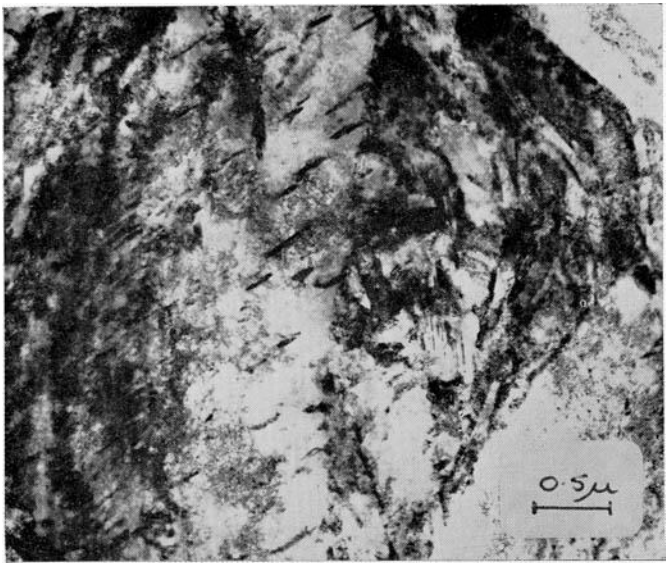

FIG. 7—*En 30B (Cast B 7365). Ausformed and tempered at 400 C (750 F). Thin foil (×20,000). Coarse cementite precipitation.*

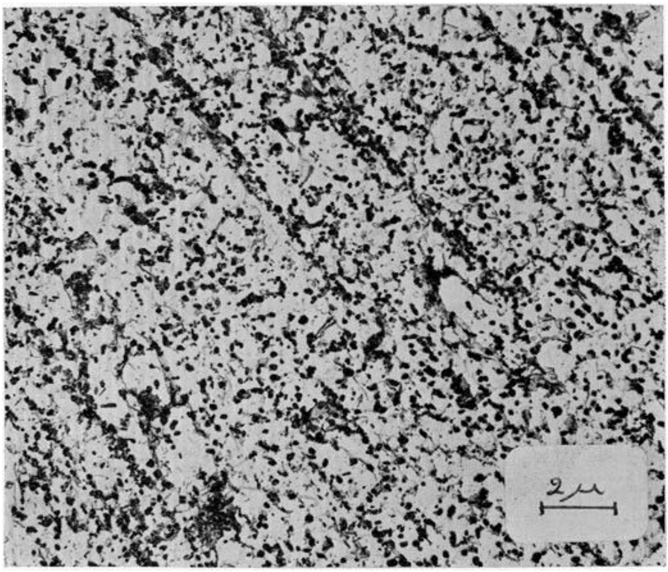

FIG. 8—*En 30B (Cast B 7365). Ausformed and tempered at 600 C (1100 F). Carbon extraction replica (×5000). Globular alloy carbide with no enhanced precipitation at martensite boundaries.*

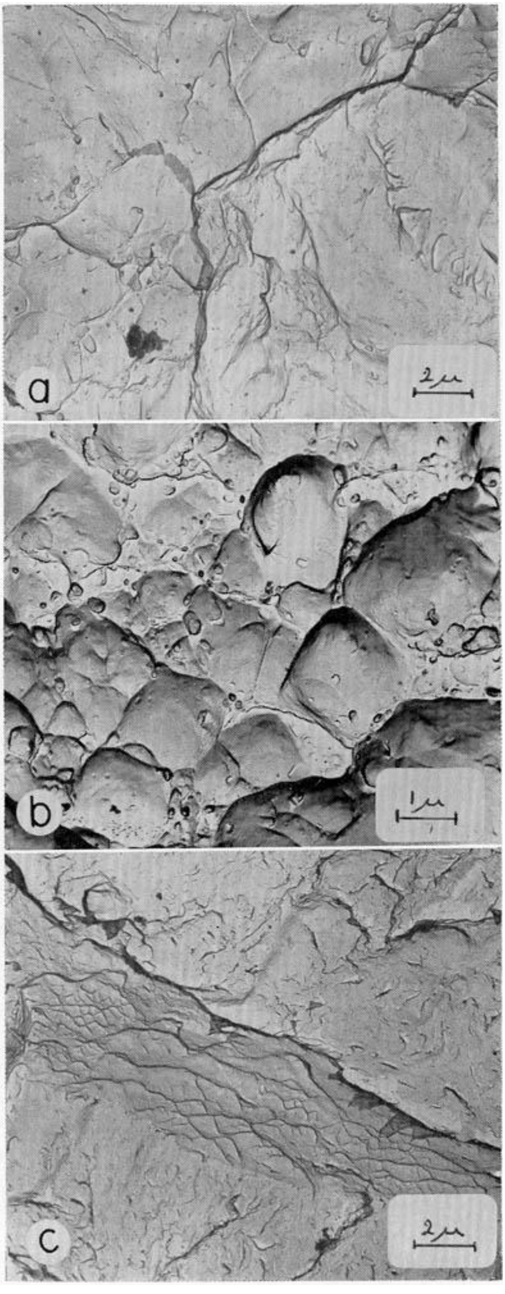

(*a*) Conventionally oil quenched (×5000). Brittle fracture.
(*b*) Rapidly heated (×10,000). Ductile dimples.
(*c*) Ausformed (×5000). Quasi-cleavage fracture on two planes.

FIG. 9—*En 30B (Cast B 7365). Electron fractographs.*

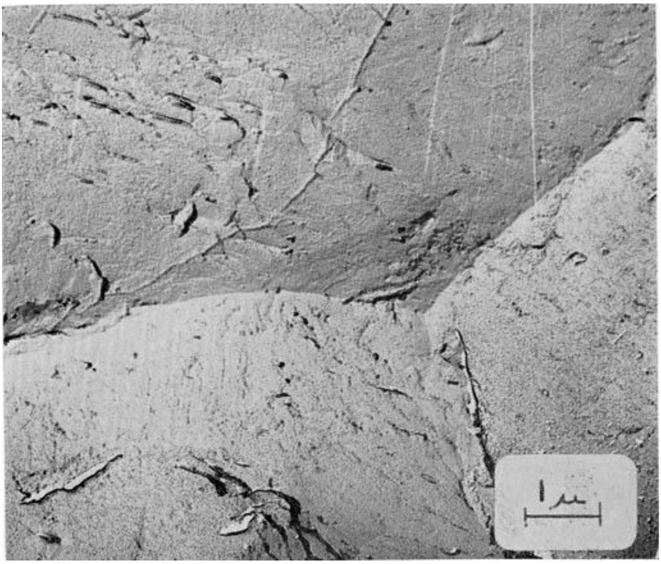

FIG. 10—*En 30B (Cast B 7365). Air cooled and tempered at 400 C (750 F) electron fractograph (×10,000). Intergranular fracture.*

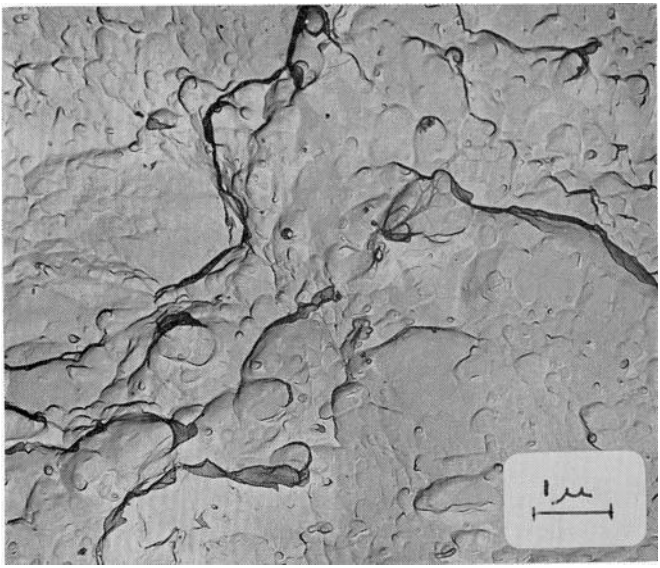

FIG. 11—*En 30B (Cast B 7365). Ausformed and tempered at 600 C (1100 F) electron fractograph (×10,000). Ductile fracture.*

not to the same extent as the prior austenite grain size. Further, autotempering effects observed in the water quenched specimens (Fig. 6*a*) were not observed in the rapidly heated specimens, (Fig. 6*b*) (autotempering during oil quenching was more pronounced than that during water quenching). The as-quenched ausformed specimens showed a fine precipitate of alloy carbide of the type observed by several investigators [*11–13*]. The ausformed material retained its distinctive features on tempering, the precipitate phase remaining spherical and finely dispersed. Figure 7 shows the structure of the ausformed material after tempering to 400 C (750 F). The coarse laths of cementite observed in the conventionally treated and rapidly heated materials were not observed. The suppression of the growth of cementite plates in ausformed material has also been observed by Castagne and co-workers [*14*]. After tempering at 600 C (1100 F) the ausformed specimens continued to show

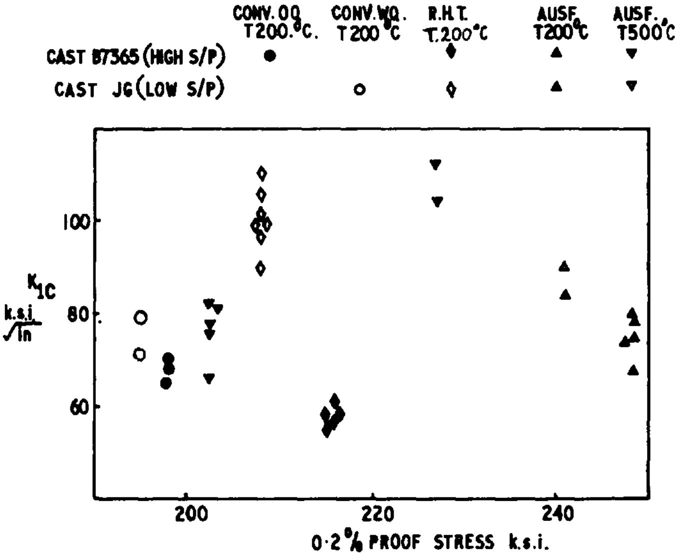

FIG. 12—*En 30B (Casts JG and B 7365). The effect of sulfur and phosphorus on the mechanical properties.*

a spheroidal precipitate with hardly any perferential precipitation at the martensite unit boundaries (Fig. 8).

Fractography—The fracture appearance of the fracture toughness specimens tempered at 600 C (1100 F), 400 C (750 F), and 200 C (400 F) is shown in Fig. 4. The conventionally treated material at 400 C (750 F) showed a flat fracture, and the size of the shear lips was at a minimum emphasizing the embrittlement at this temperature. The raipidly heated material also showed a predominantly flat fracture, but the shear lips were considerably larger than those in the corresponding conventionally treated specimens. The ausformed specimens showed oblique fractures typical of these materials.

The electron fractographs of the untempered material from the three treatments are shown in Fig. 9. The conventionally treated specimens showed a completely brittle fracture (Fig. 9*a*) while ductile cusps characterized the rapidly heated material (Fig. 9*b*). The angular nature of the fracture of the ausformed specimen can be recognized in Fig. 9*c* where brittle facets were separated by areas of ductility (where the fracture travelled from one plane to the next).

The temper embrittlement trough observed in the conventionally treated material was characterized by intergranular failure as shown in Fig. 10. There was no evidence of intergranular failure in the ausformed material, and after tempering at 600 C (1100 F) the fracture topography indicated an extremely ductile mode of failure (Fig. 11).

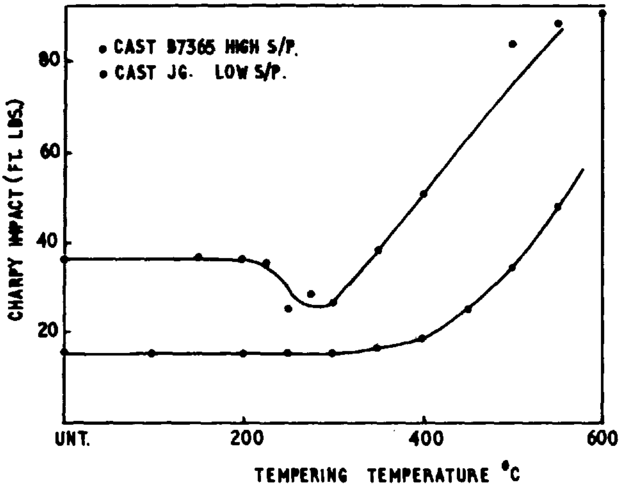

FIG. 13—*En 30B (Casts JG and B 7365). Effect of sulfur and phosphorus on the Charpy V-notch impact energy of ausformed material.*

Steel JG (Low Sulfur and Phosphorus)

Previous work [*15–17*] has indicated the significance of sulfur and phosphorus contents on the fracture toughnes of low-alloy carbon martensitic steels. Consequently, the fracture toughness results for cast B 7365 has been compared with a limited number of results obtained on a low sulfur and phosphorus En 30B steel. A summary of the fracture toughness and proof stress results for the two steels (B 7365 and JG) is given in Fig. 12 which shows the benefiical effect of low sulfur and phosphorus levels for the various treatments. This is particularly apparent in the ausformed material tempered at 200 C (400 F) and 500 C (930 F), where the drop in proof strength with increasing tempering temperature is much greater in the high sulfur and phosphorus cast than in the other cast. Further, this drop in proof strength is accompanied by an increase in fracture toughness in the case of the low sulfur and phosphorus material only.

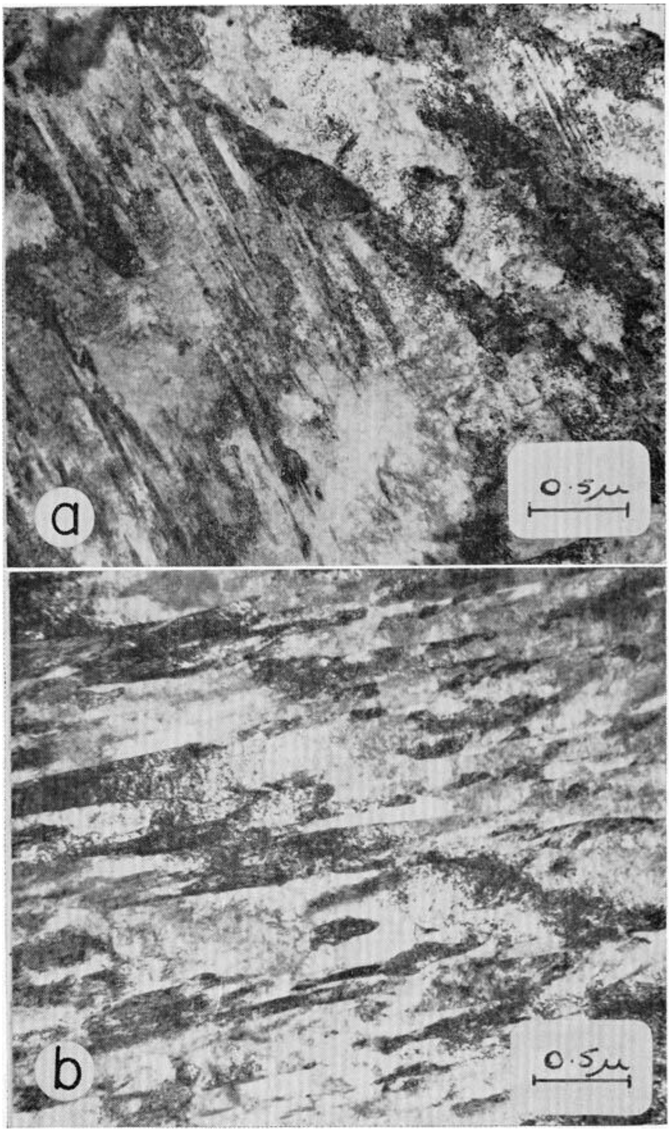

FIG. 14—*En 30B (Cast JG)* (a) *and* (b) *ausformed and tempered at 350 C (650 F). Thin foils* (×*25,000*).

Figure 13 shows the effect of tempering temperature on the Charpy V-notch impact energy for ausformed material taken from the two casts and again emphasizes the effect of sulfur and phosphorus on the overall level of the fracture energy. Although no temper embrittlement trough was observed for ausformed B 7365 materials, a pronounced dip in the impact energy curve was evident for the ausformed low sulfur and phosphorus material.

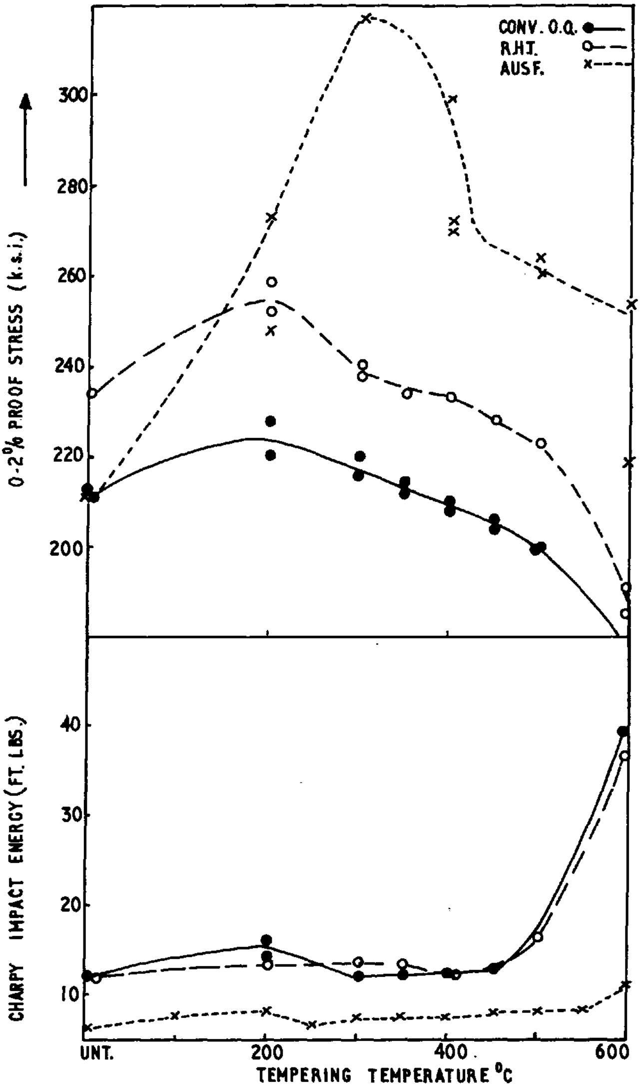

FIG. 15—*En 40C (Cast E 3048). Effect of tempering on the 0.2 percent proof stress and Charpy impact energy.*

Figure 14 illustrates the structure of the ausformed JG material subsequently tempered for 1 h at 350 C (650 F). Evidence for precipitation along internal twins in the martensite is shown in Fig. 14*a*, which with Fig. 14*b*, confirms that there is no precipitation along the martensite unit boundaries in ausformed material. In normally treated martensite, a considerable amount of precipitation can be observed at these sites.

TABLE 5—*Fracture toughness of En 40C (E 3048) conventional 900 C oil quenched*

Treatment	0.2% Proof Stress, ksi	Tensile Strength, ksi	Reduction of Area, %	Elongation, %	K_{Ic}, ksi $\sqrt{\text{in.}}$	G_{Ic}, in lb/in.^{2}
Untempered......	211	328	12.9	6.4	32.95	36.6
	...	...	...	...	28.45	27.6
	...	...	...	...	21.9	15.5
T 200 C...........	224	295	43.7	11.9	50.2	87.4
	...	...	...	...	45.6	69.5
T 300 C...........	218	266	47.4	11.9	69.5	161
	...	...	...	...	60.2	121
T 350 C...........	212	253	47.4	11.5	69.8	162
	...	...	...	...	66.9	148
	...	...	...	...	59.8	118
T 400 C...........	208	250	47.9	12.3	68.5	157
	.	...	...	...	64.3	137
	...	...	...	...	64.4	137.5
T 450 C...........	205	240	48.6	12.7	76.4	59.4
	...	...	...	...	79.1	208
	...	...	...	...	75.5	190
T 500 C...........	199	236	50.5	14.3	80.2	215
	...	...	...	...	80.3	215.5
	...	...	...	...	71.3	169
T 600 C...........	173	201	61.3	17.5	78.02[a]	203

[a] Invalid according to ASTM measurement criteria.

TABLE 6—*Fracture toughness of En 40C (E 3048) rapidly heated.*

Treatment	0.2% Proof Stress, ksi	Tensile Strength, ksi	Reduction of Area, %	Elongation, %	K_{Ic}, ksi $\sqrt{\text{in.}}$	G_{Ic}, in lb/in.^{2}
T 200 C.....	255	305	40.7	11.9	33.9	39
	...	...	...	...	36.9	45
T 300 C.....	239	274	47.2	11.5	58.4	113
	...	...	...	...	59.4	117
T 350 C.....	234	264	46.5	11.9	57.4	110
	...	...	...	...	64.2	143
T 400 C.....	233	256	48.6	11.5	53.6	96
	...	...	...	...	55.6	103
T 450 C.....	228	222	50.4	12.7	67.0	150

TABLE 7—*Fracture toughness of En 40C (E 3048) ausformed.*

Treatment	0.2% Proof Stress, ksi	Tensile Strength, ksi	Reduction of Area, %	Elongation, %	K_{Ic}, ksi $\sqrt{\text{in.}}$	G_{Ic}, in lb/in.^{2}
Untempered......	212	367	20.4	9.5	33.35	37
	...	...	...	...	35.65	43
T 200 C...........	260	359	26.6	11.9	54.75	100
T 300 C...........	317	356	34.6	11.1	44.4	63
T 400 C...........	285	347	30.1	12.7	42.55	60
	...	...	...	...	36.75	55
T 600 C...........	236	265	44.7	16.7	51.9	89
	...	...	...	...	50.1	84.5

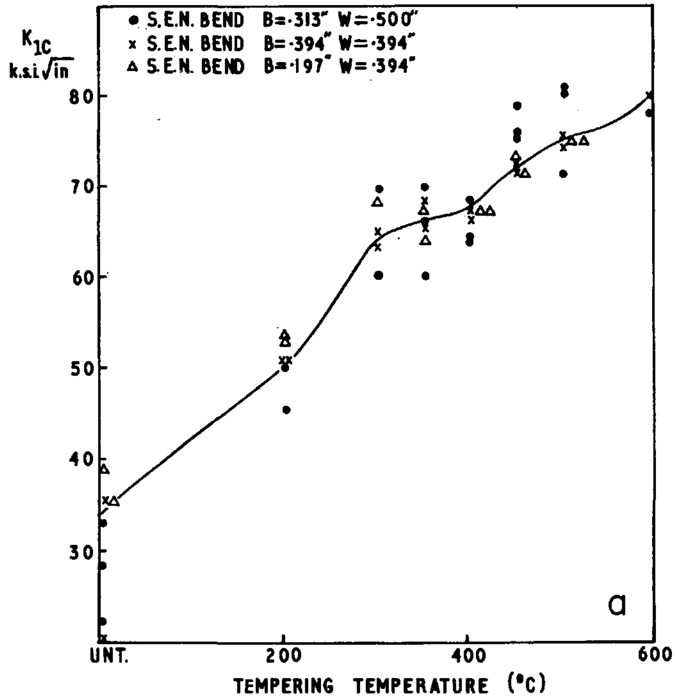

FIG. 16—*En 40C (Cast E 3048). Effect of tempering on the fracture toughness of* (a) *conventionally oil quenched,* (b) *rapidly heated,* (c) *ausformed material, and* (d) *comparison of mean curves from* a, b, *and* c.

Experimental Results for En 40C Steel

Two variations of this steel were examined, one contained 0.23 weight percent vanadium and the other a trace (less than 0.03 weight percent) of the same element. The detailed analyses of the two casts are given in Table 1.

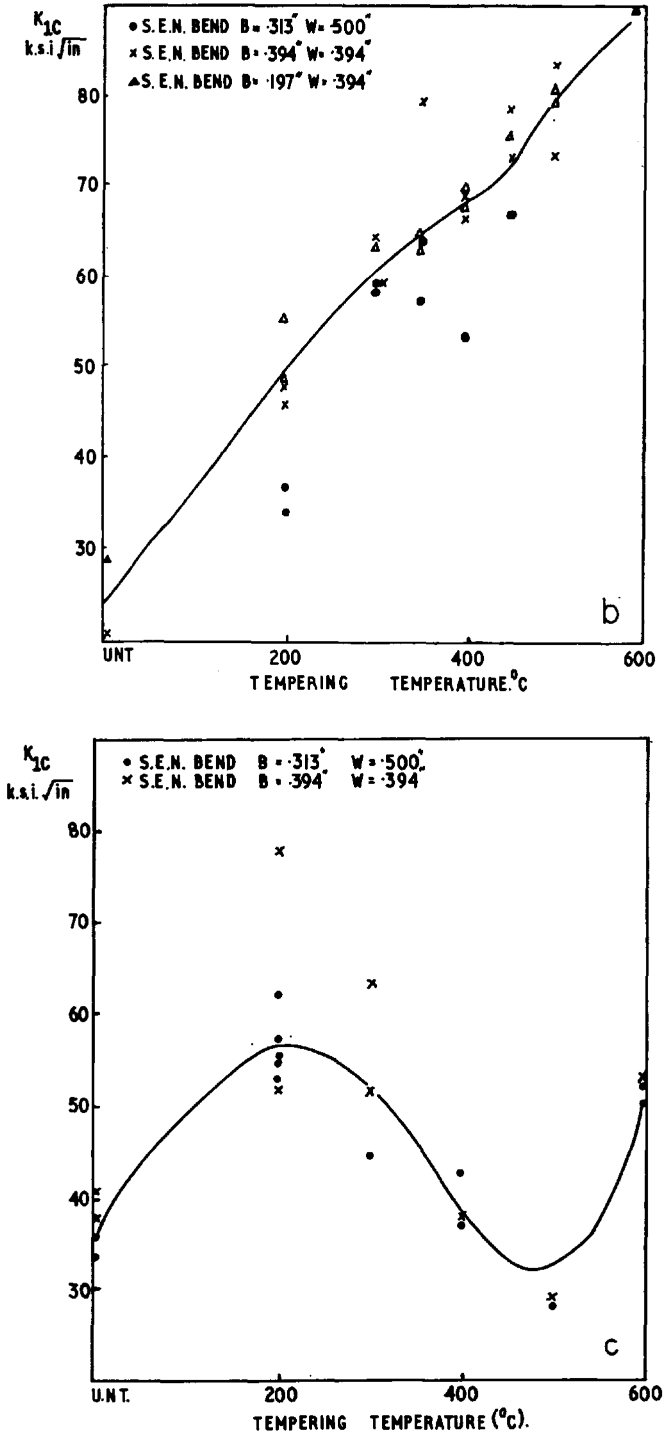

FIG. 16—*Continued.*

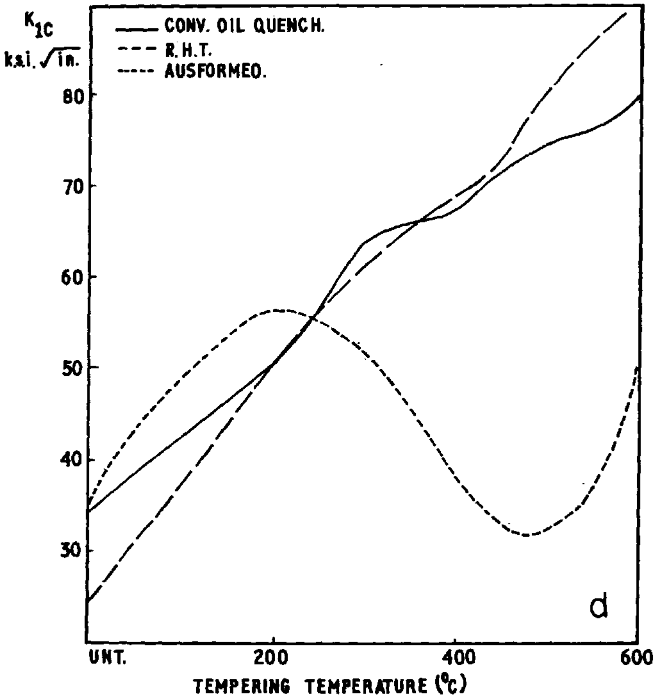

FIG. 16—*Continued.*

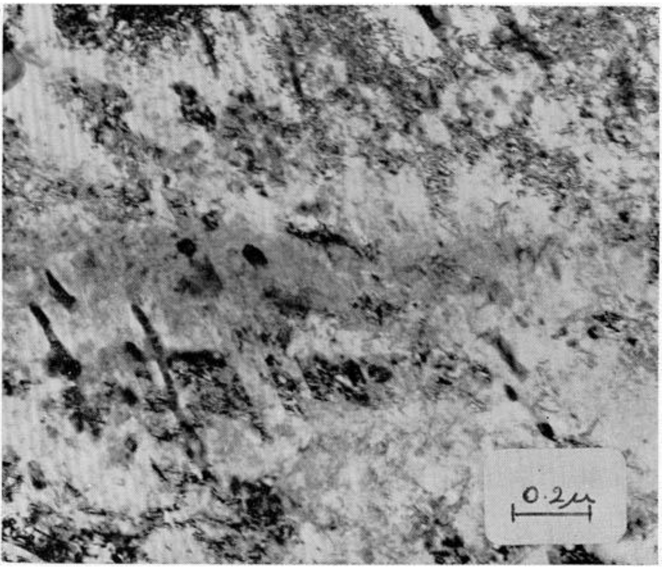

FIG. 17—*En 40C (Cast E 3048). Ausformed and tempered at 600 C (1100 F). Thin foil (×50,000). High dislocation density, no signs of recovery.*

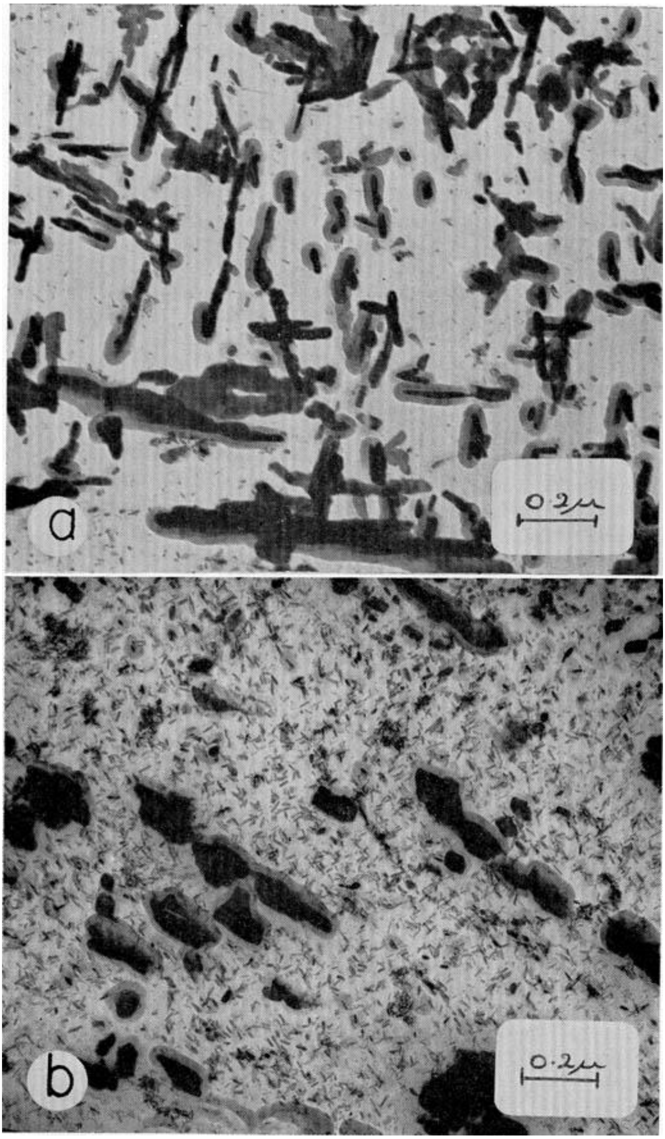

(*a*) Conventionally oil quenched and tempered at 600 C (1100 F) (×50,000). Coarse chromium carbide plates.

(*b*) Ausformed and tempered at 600 C (1100 F) (×50,000). Fine alloy carbide precipitate interspersed with chromium carbide.

FIG. 18—*En 40C (Cast E 3048). Carbon extraction replicas.*

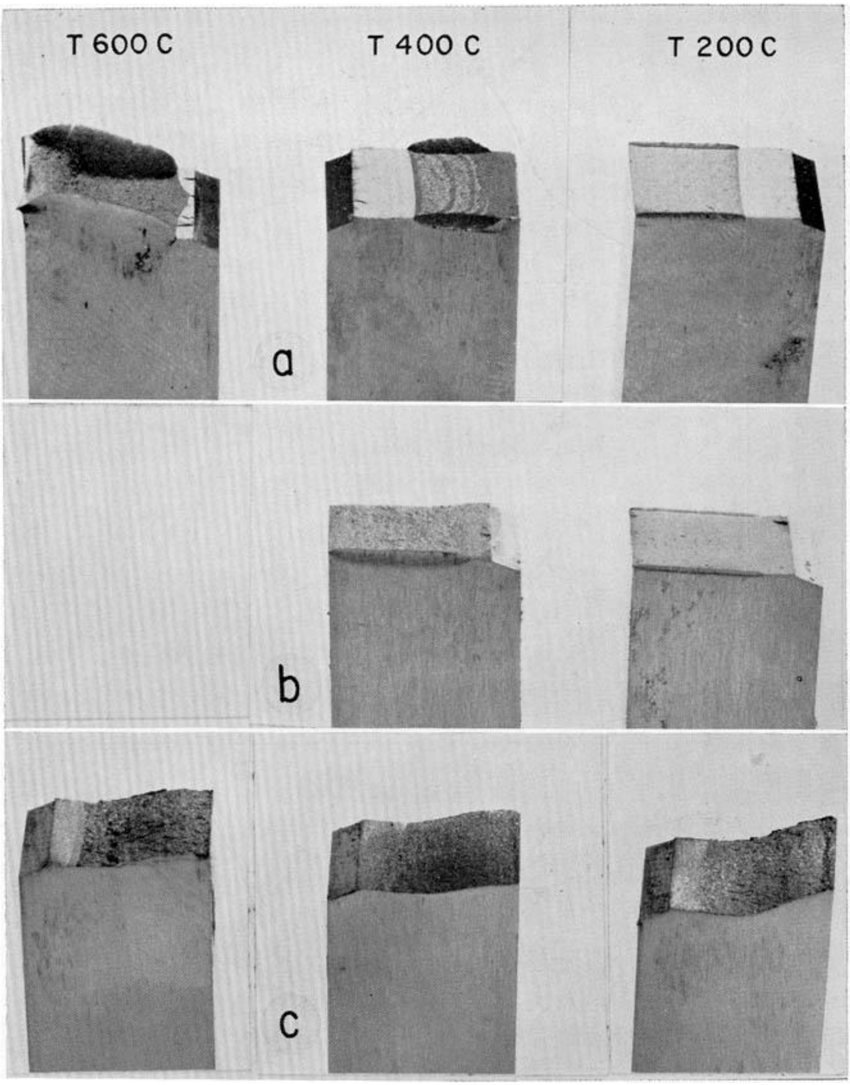

(*a*) Conventional oil quench.
(*b*) Rapid heat treatment.
(*c*) Ausformed.

FIG. 19—*Fracture appearance of En 40C (Cast E 3048) subjected to different treatments.*

Steel E 3048 (High Vanadium)

Mechanical Properties—The effect of tempering temperature on the tensile properties and Charpy V-notch impact energy for the conventionally treated, rapidly heated, and ausformed material are shown in Fig. 15.

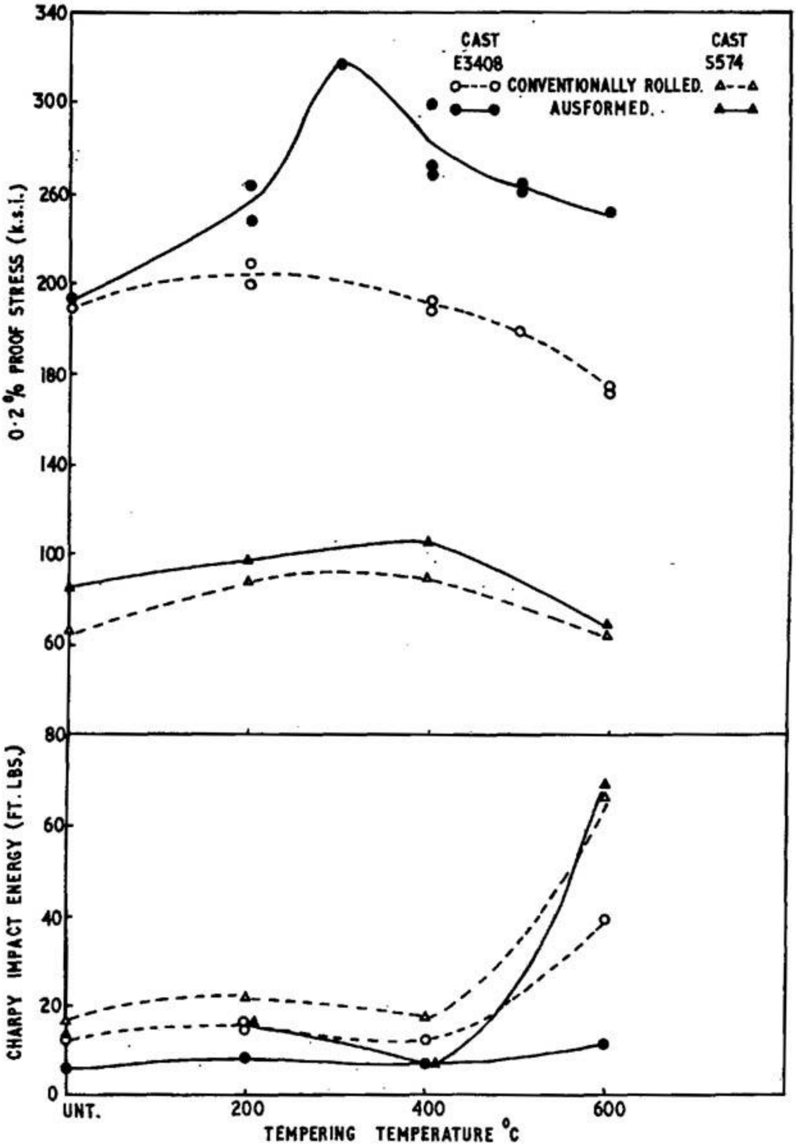

FIG. 20—*En 40C (Casts S 574 and E 3048). Effect of vanadium content on proof strength and Charpy impact energy.*

It can be seen that compared to the En 30B steels the susceptibility to temper embrittlement is reduced, but the overall level of impact energy is also lowered. Even after tempering at 600 C, the ausformed material shows an impact energy of only 11 ft·lb (as against 35 to 40 ft·lb for the equivalent conventionally treated and rapidly heated specimens).

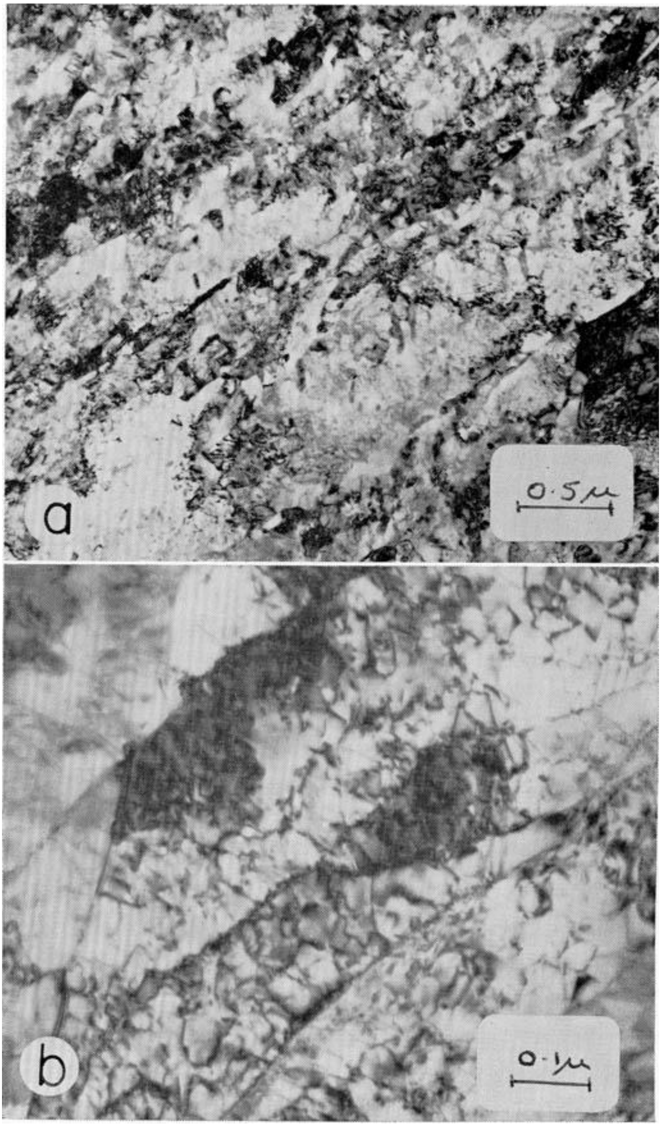

(*a*) (×25,000).
(*b*) (×100,000).

FIG. 21—*En 40C (Cast S 574). Ausformed and tempered at 600 C. Thin foils. Structure showing signs of recovery.*

Plane strain fracture toughness (K_{Ic}) values for the steel in the conventionally treated, rapidly heated, and ausformed conditions is given in Tables 5, 6, and 7, respectively, together with the corresponding tensile data. The results are also given in Fig. 16*a*–*c* and the mean curves compared in Fig. 16*d*. From the latter figure it can be seen that the conventionally treated and rapidly heated material did not show a temper embrittlement trough, but the ausformed material showed a very distinct drop in toughness afer tempering in the range 400 C (750 F) to 500 C (930 F).

Structural Examination—The high strength and low toughness of the ausformed material even after tempering at 600 C (1100 F) is reflected in the microstructure as can be seen from Fig. 17 where the martensite shows no signs of the recovery processess which are usually evident after tempering to this temperature. The differences in precipitate morphology and distribution between the conventionally treated and ausformed specimens tempered to 600 C (1100 F) are shown in Fig. 18. A fairly dense distribution of coarse chromium carbide plates is seen in the conventionally quenched and tempered specimen (Fig. 18*a*), whereas on the other hand the ausformed and tempered microstructure shows a dense dispersion of very fine platelets (probably of vanadium carbide) with a sparse distribution of the much coarser chromium carbide plates (Fig. 18*b*).

Fractography—The fracture of specimens in the three conditions and tempered over the range 200 C (400 F) to 600 C (1100 F), are shown in Fig. 19. The fractures observed in the conventionally treated specimens were very similar to those observed in corresponding specimens of En 30B, and the comments made in the earlier section apply in this case. The rapidly heated material showed a very flat fracture with some signs of ductility after tempering at 400 C (750 F). However, even in this case the shear lips were still very small.

The ausformed material *did not* show the oblique fracture which is usually associated with ausformed steels. Even after tempering at 600 C (1100 F) extremely small shear lips were observed on the specimens, confirming the brittle nature of the material in this condition.

Steel S 574 (Low Vanadium)

This steel showed significant differences from the vanadium containing variety. The effect of tempering temperature on the proof strength and Charpy V-notch impact energy data for the two steels in the ausformed condition is shown in Fig. 20. In none of the conditions was the temper embrittlement trough very marked; however, it was most pronounced in the ausformed low vanadium steel. On the other hand the lower vanadium steel showed a much higher Charpy impact energy after tempering at 600 C (1100 F). The difference in properties between the two casts could be explained by comparison of the microstructures. The 574 material showed considerable signs of recovery (Fig. 21*a*), the characteristic dislocation structures being more clearly distinguishable at higher magnification (Fig. 21*b*). A comparison of Fig. 21*b* with Fig. 17 explains the lower strength and the higher impact energy of the S 574 specimen relative to the corresponding specimen of E 3048.

General Discussion

Correlation Between the Different Mechanical Tests

The results of the program on En 30B and En 40C steels have shown that the temper embrittlement trough can be detected in fracture toughness tests as well as in the more conventional Charpy V-notch impact tests. In the En 30B steels correlation with tempering temperature of the Charpy impact and K_{Ic} results showed good agreement, even though the bases for the two types of tests are quite different. In the En 40C material, the Charpy V-notch impact curves failed to detect a clear cut embrittlement trough, whereas the K_{Ic} results showed a distinct embrittling effect between 300 and 500 C (575 and 930 F) in the ausformed material, suggesting that the latter test may be more sensitive in detecting certain types of embrittling effects. The results support the views of Banerjee [*18*] who has argued that the fracture toughness of low-alloy steels does not remain constant upon tempering to temperatures in the range 300 to 500 C (approximately 600 to 900 F).

Correlation of Microstructure to Mechanical Properties

It is possible to correlate the changes in mechanical properties with the microstructural changes by considering the effect the latter have on the former.

In En 30B steels the ausformed specimens showed superior strength and toughness compared to the corresponding conventionally quenched and rapidly heated specimens, and the temper embrittlement effect was at a minimum after the former treatment. The mechanical superiority of the ausformed and tempered specimens can be correlated with the finer and closely dispersed alloy carbide precipitates observed. The absence of precipitates at the martensite grain boundaries and coarse carbide plates within the grains (both of which were observed in conventionally tempered and in rapidly heated and tempered specimens) could account for the superior toughness of the ausformed material.

Similarly, the superior strength of the ausformed high-vanadium En 40C (Cast E 3048) over that of the cast without vanadium (S 574) can be explained in terms of the very fine plates of vanadium carbide observed in the former (as can be seen in Fig. 18*b*). These fine alloy carbides were formed during the ausforming operation and explain the resistance to tempering shown by the ausformed E 3048 material. The latter specimens did not indicate any signs of dislocation recovery even after tempering at 600 C (1100 F), and this could account for the low level of fracture toughness at this temperature (both Charpy V-notch and K_{Ic} results). On the other hand, the cast without vanadium (S 574) showed a distinct recovery in the dislocation structure after tempering at 600 C (1100 F) with an accompanying improvement in the Charpy

V-notch impact energy and a marked drop in the proof stress and tensile strength.

Current Theories of Temper Embrittlement

Several theories have been proposed to explain the phenomenon of temper embrittlement. These can be broadly divided into three groups-theories based on: (1) austenite grain boundary precipitation, (2) segregation to austenite grain boundaries, and (3) dislocation locking by precipitates or atmospheres of solute atoms. These theories will now be briefly discussed in the light of the results from the present investigation:

1. The extensive structural investigation did not indicate preferential precipitation at prior austenite grain boundaries. In all the steels examined in the various heat treated conditions there was no difference between the precipitation at the martensite bundle boundaries and that at the prior austenite grain boundaries.

2. There was no direct evidence for the theory of Capus [*3*] and others [*4*] which attribute temper embrittlement to segregation of impurities to the prior austenite grain boundaries. Nevertheless, the results on rapidly heated En 30B steel (Cast B 7365) with the high sulfur and phosphorus content suggest that segregation to grain boundaries could be relevant in this case. The rapidly heated and tempered material showed an improvement in toughness over the conventionally quenched and tempered specimens, and such behavior can be attributed to refinement of the prior austenite grain size. *If* the embrittling effect of the higher sulfur and phosphorus contents is due to their segregation to the prior austenite grain boundaries, then a rapid heating treatment would be expected to improve the toughness on two counts:

(*a*) The finer austenite grain size would result in a "dilution" of the amount of segregate per unit grain boundary area.

(*b*) The rapid heating cycle invloves a very rapid recrystallization of the austenite, and it is unlikely therefore that all the solute segregate will be present along the new austenite boundaries.

The experimental results on En 40C steels give no support for this theory.

3. Banerjee [*19*] has proposed an embrittlement mechanism involving precipitation locking of dislocation intersections and jogs along with high dislocation densities during carbide resolution and reprecipitation. A similar theory of dislocation pinning by solute atmospheres has been put forward by Kaddou and Rosenthal [*20*] based on the results of their internal friction work.

The present studies give no evidence for resolution and reprecipitation during tempering; however, the idea of precipitation on dislocations leading to dislocation locking is well supported by the microstructural observations on ausformed En 40C (Cast E 3048—with the high-vanadium content) and the mechanical properties. The fine platelets of vanadium carbide have a marked strengthening effect and delay dislocation recovery processes. The pinning of dislocations in this manner may be partly responsible for the temper embrittlement trough (K_{Ic} results) observed in the ausformed E 3048 steel.

The work of Kaddou suggests that only certain solutes could lead to the pinning of dislocations and that temper embrittlement is not necessarily a grain boundary phenomenon.

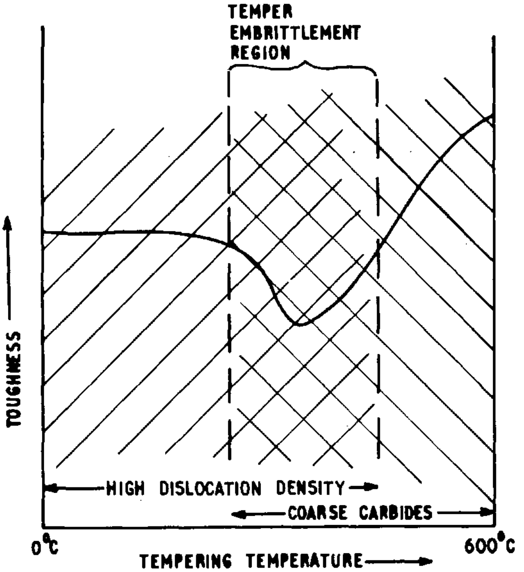

FIG. 22—*Schematic representation of a model of temper embrittlement.*

A Model for a Mechanism of Temper Embrittlement

Previous work reported in the literature and the results of the present investigation strongly suggest that several independent mechanisms can give rise to temper brittleness and that more than on mechanism may be operative in a particular steel.

The current work has examined the effect on temper embrittlement of different carbide morphologies and distributions brought about by different treatments. The beneficial effect of ausforming on toughness brought about by the elimination of coarse alloy carbide plates (and martensite grain boundary precipitates), and in addition, in En 40C, the effect of dislocation locking by fine precipitates of vanadium carbide suggest a modified model for temper embrittlement in the two steels studied:

A schematic representation of this model is given in Fig. 22. It is suggested that for the treatments considered the "embrittlement trough" can be explained in terms of two embrittling mechanisms: precipitation of coarse carbides (intragranular and intergranular) and pinning of dislocations resulting in high dislocation densities. The tempering temperature range can be different for the two embrittling mechanisms, and the "trough" occurs over that temperature range where there is an overlap. In this range the temperature is both high enough for coarse carbide formation (intra- and intergranular) and yet too low for dislocation recovery. In cases where coarse carbides are present in the untempered structure as a result of autotempering, the level of toughness approaches that of the minimum of the embrittlement trough at all tempering temperatures until recovery processes occur.

Ausforming results in the suppression of coarse carbides (due to the formation of alloy carbide "nucleii" during the thermomechanical treatment [*11–13*]), and this reduces (or eliminates) the temper brittleness trough. Coarse plates of carbides are known to have an embrittling effect, and McMahon and Cohen [*21*] have shown how, by cracking, such carbides can initiate a crack which can readily propagate through the microstructure.

In the ausformed En 40C steel (Cast E 3048) of the vanadium carbide pins the dislocation structure delaying the onset of recovery, and hence a constant level of embrittlement is obtained at tempering temperatures as high as 600 C (1100 F).

The mechanism proposed favors transgranular fracture, and, indeed, this has been observed in most of the specimens examined. From this it can be concluded that temper brittleness is not synonymous with intergranular failure, though the latter can occur under certain conditions of embrittlement. A similar conclusion is implicit from Banerjee's work and model for embrittlement [*19*].

Other Factors

It is apparent that in certain cases embrittling mechanisms other than those associated with coarse intergranular/intragranular carbides and high dislocation densities are involved. One of these which is particularly relevant to this study, is the effect of sulfur and phosphorus which primarily influences the overall level of toughness. At a certain concentration of sulfur and phosphorus, which is dependent on other factors (namely, composition and heat treatment) their segregation to grain boundaries can result in embrittlement due to intergranular failure. This mechanism involves segregation of the impurity elements to austenite grain boundaries and would favor failure along these microstructural features—as suggested by Fig. 10.

In summary it should be emphasized that several embrittling mechanisms can result in the temper embrittlement of low-alloy steels. In general, steels are embrittled as a result of the interaction of two or more of these mechanisms. The relative predominance of one mechanism over the others depends on the composition and the prior heat treatment of the steel.

Conclusions

1. Several mechanisms are involved in the temper embrittlement phenomenon, and those which operate in any particular case vary according to the composition of the steel and the thermal and mechanical history of the material.
2. A model for the temper embrittlement trough is proposed based on the combination of two mechanisms involving coarse carbide precipitation and high dislocation density resulting from dislocation pinning. Both these mechanisms can be influenced by composition and heat treatment.
3. Temper embrittlement can result in transgranular fracture, and therefore, intergranular fracture along prior austenite grain boundaries (often considered the criterion for temper embrittlement) is not synonymous with this phenomenon.
4. Segregation of sulfur and phosphorus to austenite grain boundaries in sufficient concentrations can lead to embrittlement resulting in intergranular fracture.
5. Precipitation of fine dispersions of certain carbides (for example vanadium carbide produced during ausforming) causes embrittlement by stabilization of the dislocation structure preventing recovery to temperatures as high as 600 C (1100 F).

Acknowledgments

The authors are grateful for the assistance of the technical staff of the Metallurgy Division of the British Iron and Steel Research Association. They also acknowledge the cooperation and help which they received from their colleagues during the course of the investigation.

References

[*1*] Fussell, K. J., May, M. J., and Elliott, D., "Rapid Heat Treatments," Final Report to U.S. Navy, BISRA Report MG/E/199/66, 1966.

[*2*] Grange, R. A., "Strengthening Steel by Austensite Grain Refinement," *Quarterly*, American Society for Metals, Vol. 59, 1966, p. 26.

[*3*] Capus, J. M., "Austensite Grain Size and Temper Brittleness," *Journal of the Iron and Steel Institute*, Vol. 200, 1962, p. 922.

[*4*] Austin, G. W., Entwistle, A. R., and Smith, G. C., "Effect of Arsenic and Antimony on Temper-Brittleness," *Journal of Iron and Steel Institute*, Vol. 173, 1953, p. 376.

[*5*] May, M. J. and Walker, E. F., "Fracture Toughness Testing of High Strength Steels Using Single Edge Notch Tension and Bond Specimens," BISRA Report MG/E/63/66, 1966.

[*6*] Irani, J. J., "Fracture of Martensite with Particular Reference to Ausformed Martensite," The Iron and Steel Institute Special Report 93, 1965, p. 193.

[7] Fussell, K. J. and May, M. J., "Rapid Heat Treatments," Interior Report, BISRA Report, MG/E/60/65, 1965.
[8] Priest, A. H. and May, M. J., "Fracture Toughness of Steels Using Pre-cracked Charpy Specimens," BISRA Report MG/E/62/66, 1966.
[9] Elliott, D. and May, M. J., "The Fracture Toughness of Two Low Alloy Martensitic Steels," BISRA Report, to be published.
[10] Duckworth, W. E., May, M. J., and Irani, J. J., "The Fracture of Martensite," Proceedings of the First International Conference on Fracture, Sendai, 1965, p. 919.
[11] McEvily, A. J. et al, "On the Formation of Alloy Carbides During Ausforming," *Transactions*, American Society for Metals, Vol. 56, 1963, p. 753.
[12] Johari, O. and Thomas, G., "Structures and Strength of Austened Steels," *Transactions*, American Society for Metals, Vol. 58, 1965, p. 563.
[13] Irani, J. J. and Taylor, P. R., Paper presented at Conference on Hot Deformation of Metals, Sheffield, 1966.
[14] Castagne, J. L. et al, "Ausforming-Etude de l'ecrouissage de l'austenite metastable Les Memoires Scientifiques de la Revue de Metallurgie," Vol. 64, 1967, p. 319.
[15] Cottrell, C. L. M., Langstone, P. F., and Rentall, J. H., "Improved Properties of Extra High-Porosity Steel at Tensile Strengths Up to 150 Tons/in^2," *Journal of the Iron and Steel Institute*, Vol. 201, 1963, p. 1032.
[16] Priest, A. H. and May, M. J., "The Effect of Silicon Sulfer and Phosphorus on the Fracture Toughness and Stress Corrosion Cracking Resistance of a High Strength Martensite Steel," BISRA Report MG/E/311/67, 1967.
[17] Baker, A. J., Lauta, F. J., and Wei, R. P., "Relationships Between Microstrucstructure and Toughness in Quenched and Tempered Ultrahigh-Strength Steels," *Structures and Properties of Ultrahigh-Strength Steels, ASTM STP 370*, American Society for Testing and Materials, 1965, p. 3.
[18] Banerjee, B. R., discussion of above paper, *ASTM STP 370*, 1965, p. 23.
[19] Banerjee, B. R., "Embrittlement of High-Strength Tempered Alloy Martensites," *Journal of the Iron and Steel Institute*, Vol. 203, 1965, p. 166.
[20] Kadden, A. F. K. and Rosenthal, P. C., "Correlation between Internal Friction and Temper Brittleness in Steel," *Transactions*, American Society for Metals, Vol. 52, 1960, p. 116.
[21] McMahon, C. J. and Cohen, M., "Initiation of Cleavage in Polycrystalline Iron," *Acta Metallurgica*, Vol. 13, 1965, p. 591.

F. L. Carr,[1] *J. Nunes,*[2] *and F. R. Larson*[3]

Mechanical Properties and Fracture Surface Topography of a Thermally Embrittled Steel

---

REFERENCE: Carr, F. L., Nunes, J., and Larson, F. R., "**Mechanical Properties and Fracture Surface Topography of a Thermally Embrittled Steel,**" *Temper Embrittlement in Steel, ASTM STP 407,* American Society for Testing and Materials, 1968, pp. 203–236.

ABSTRACT: Tensile flow and fracture properties of both medium and coarse grain 3140 steel in both the embrittled and unembrittled condition are presented and discussed. The fracture stress ratios of embrittled to unembrittled specimens indicate the relative decrease in toughness due to this embrittlement over the range of temperature studied. Quantitative fracture surface topography resulted in fracture transition curves for the three types of specimens utilized. Transition temperatures based on several criteria indicated differences due to grain size and temper brittleness. The well-known difference in fracture mode behavior at low-testing temperature between embrittled and unembrittled specimens was found to be due to the peculiar fracture behavior of the unembrittled material. Fractographic examination revealed that the intergranular fracture of the coarse grain material had varying degrees of deformation indicating significant differences in both ductility and energy required for separation.

KEY WORDS: temper embrittlement, stress analysis, strains, flow properties, impact specimen, tension hardness, strain hardening, fracturing, mechanical properties, impact tests, trace elements, toughness, transition temperature, tensile properties, intergranular fracture, cracking (facturing), plastic defomation, high energy rate, texture, evaluation

Differences in the fracture surface appearance of tension specimens of several low-alloy steels have been attributed to temper brittleness [*1–3*].[4] Early studies of this phenomenon concluded that tensile properties were not affected [*4,5*]. Many investigations, which followed,

---

[1] Materials engineer, Army Materials and Mechanics Research Center, Watertown, Mass. Personal member ASTM.

[2] Materials engineer, formerly U.S. Army Materials Research Agency, currently associated with Brunswick Corp., Needham, Mass. Personal member ASTM.

[3] Chief, Metals Laboratory, Army Materials and Mechanics Research Center, Watertown, Mass. Personal member ASTM.

[4] The italic numbers in brackets refer to the list of references appended to this paper.

utilized the impact test and usually neglected any systematic study of tensile properties. Fracture studies have been limited to gross comparison [*1–3*] or to differentiation between predominantly transcrystalline and intercrystalline modes at low temperatures [*6,7*]. The apparent reduction in toughness, accompanying this form of thermal embrittlement, has been attributed, in general, to intergranular fracture [*8*].

Recent studies of AISI 4340 steel provided an understanding of the plastic flow and fracture of this material, produced the tensile fracture-transition curve, and, aided by the fracture mechanics concept, explained fracture surface topography [*9–12*].

It was the purpose of this investigation to study some of the effects of thermal embrittlement on tensile flow properties and fracture surface topography of another low-alloy constructional steel, AISI 3140, which has been shown to be particularly sensitive to temper brittleness.

Procedures

The material chosen for this investigation was hot rolled ⅝-in.-diameter AISI 3140 steel having the following compositions in weight percent:

C	Mn	Ni	Cr	Mo	Al	P
0.39 to 0.40	0.78 to 0.79	1.25	0.83	0.02	0.02	0.013 to 0.014

S	As	Sb	Sn
0.022 to 0.023	0.011	0.0008	0.0012.

The material was cut to suitable lengths and heat treated as ⅝-in.-diameter barstock. Two different treatments were utilized to produce two appreciably different grain sizes. Specimen blanks were subjected to one of the following treatments.

Treatment M

1650 ± 10 F (900 C) for 1 h air cooled.
1650 ± 10 F (900 C) for 1 h oil quenched.
1157 ± 5 F (625 C) for 1 h water quenched.

Treatment C

2300 ± 20 F (1200 C) for 4 h oil quenched.
1157 ± 5 F (625 C) for 1 h water quenched.

About half of the specimen blanks from each treatment received an embrittlement treatment of 932 ± 5 F (500 C) for 48 h, followed by water quenching.

Due to the homogenization which would be incurred by Treatment C, it was deemed unnecessary to normalize prior to this treatment. Previous kinetic studies [*13*] on the same type of steel indicated 1157 F (625 C) to be a suitable tempering temperature for times of 2 h or less. These

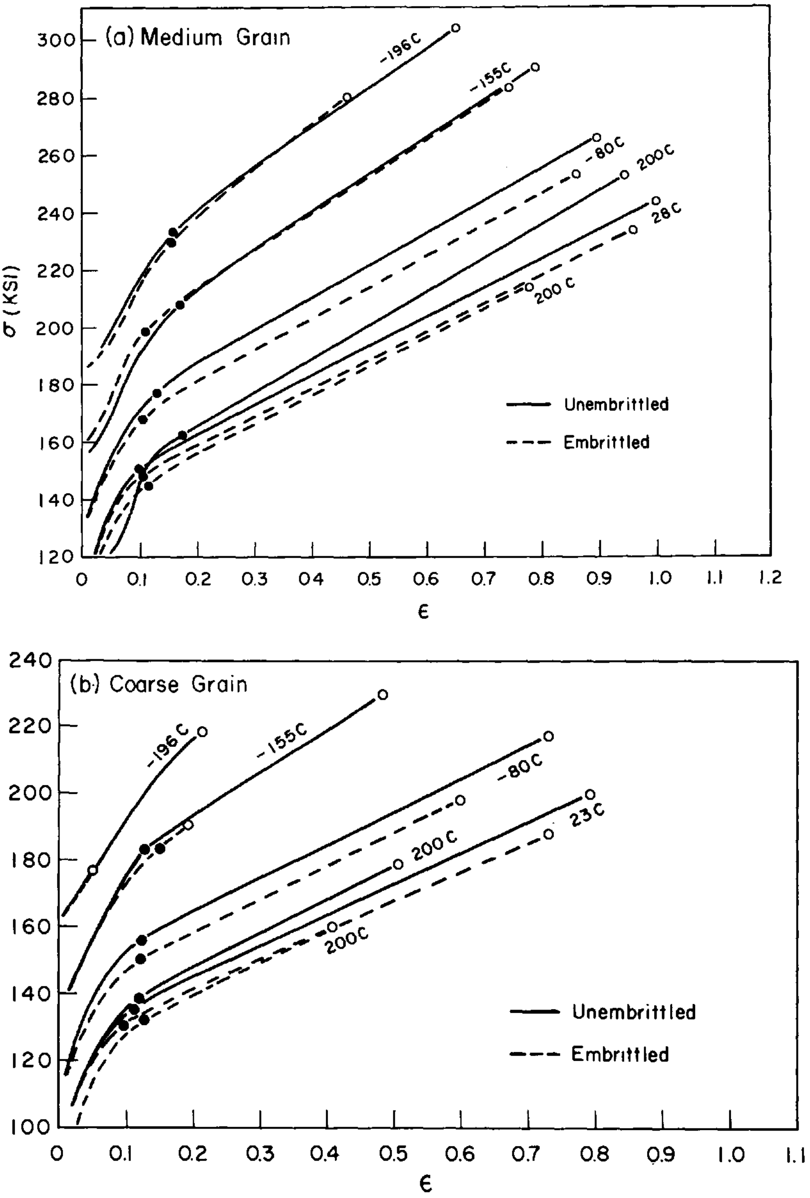

(*a*) Medium grain.
(*b*) Coarse grain.

FIG. 1—*Tensile flow curves of 3140 steel.*

same studies also indicated that for a constant time, maximum embrittlement could be obtained at 932 F (500 C).

The heat treated materials were machined into standard 0.252-in.-diameter untapered tension specimens, 0.394-in.^{2} Charpy V-notch im-

TABLE 1—*Flow and tensile data for 3140 steel*

Testing Temperature, deg C	$\sigma_{0.04}$, ksi	$\sigma_{0.19}$, ksi	σ_{ml}, ksi	σ_f, ksi	ϵ_{ml}	ϵ_f	n	Yield Strength, 0.2%, ksi	Ultimate Tensile Strength, ksi	Reduction of Area, %	Elongation, %
MEDIUM GRAIN											
Unembrittled:											
200......	119.5	164.6	162.3	253.0	0.174	0.946	0.159	97.0	136.0	61.4	23
100......	128.6	155.8	146.3	231.0	0.106	0.921	0.128	102.5	131.2	60.4	20
80......	129.0	153.9	142.5	232.0	0.090	1.024	0.104	...	130.0	64.2	20
60......	127.3	157.3	148.1	244.0	0.110	1.051	0.118	108.0	132.4	65.1	22
27......	131.1	162.1	150.4	243.5	0.098	0.998	0.120	113.0	136.0	63.2	20
0......	137.4	165.8	153.0	242.0	0.090	0.946	0.098	...	139.6	61.1	20.5
−80......	150.7	185.9	177.0	265.0	0.131	0.896	0.118	128.5	154.8	59.4	25.0
−155......	165.3	210.7	207.6	289.0	0.169	0.787	0.140	151.0	174.8	54.8	25.0
−196......	195.4	238.3	232.8	303.0	0.161	0.651	0.131	182.5	197.6	48.0	24.0
Embrittled:											
200......	126.9	154.9	144.5	214.0	0.114	0.776	0.138	97.0	129.2	54.1	17.0
160......	125.3	149.5	139.0	215.0	0.103	0.884	0.115	...	125.2	58.8	20.0
140......	128.0	148.8	140.7	211.5	0.102	0.896	0.095	...	126.8	59.4	19.5
120......	121.1	152.2	142.8	225.0	0.110	0.934	0.118	...	127.6	60.8	18.0
100......	126.5	152.4	142.7	225.0	0.106	0.934	0.120	106.0	128.0	60.8	16.0
60......	128.2	153.9	144.1	233.5	0.106	0.972	0.110	109.0	129.2	62.4	19.0
28......	131.1	158.1	148.1	233.0	0.106	0.959	0.115	112.5	132.8	61.8	20.0
0......	135.7	159.2	147.6	234.0	0.089	0.946	0.109	...	134.6	61.1	21.5
−80......	148.6	179.6	167.7	252.5	0.106	0.857	0.116	125.0	150.4	57.8	24.0
−155......	170.8	212.6	197.8	283.5	0.111	0.741	0.123	154.5	176.8	52.6	25.0
−196......	193.3	230.9	229.4	280.0	0.153	0.462	0.130	183.0	196.4	37.2	20.0

COARSE GRAIN											
Unembrittled:											
200......	117.1	146.0	137.8	178.5	0.123	0.503	0.145	97.5	121.6	39.8	15.0
100......	120.7	142.7	131.9	129.0	0.085	0.575	0.104	101.0	120.8	44.0	14.0
60......	116.7	140.5	128.9	184.0	0.081	0.684	0.110	101.0	118.6	49.8	14.0
23......	118.5	144.0	135.5	199.5	0.113	0.787	0.108	104.5	123.6	55.6	20.0
−80......	134.0	163.6	155.6	216.5	0.122	0.729	0.106	113.5	137.2	52.0	20.0
−155......	151.4	192.2	182.7	229.5	0.127	0.482	0.125	137.5	160.4	38.6	20.0
−196......	172.2	214.6	202.3	218.0	0.127	0.209	0.120	163.0	177.6	19.2	8.0
Embrittled:											
200......	109.8	138.6	132.0	160.0	0.127	0.403	0.142	96.0	115.0	33.4	13.5
100......	115.9	136.9	128.5	179.5	0.097	0.684	0.105	97.0	115.8	49.8	15.0
60......	116.9	139.1	128.9	180.0	0.089	0.662	0.105	102.0	117.6	48.6	14.0
23......	118.6	140.5	130.6	187.5	0.093	0.729	0.108	103.0	118.0	52.0	14.5
−80......	130.9	157.8	149.9	197.5	0.118	0.597	0.116	110.5	132.8	45.2	18.0
−155......	151.1	189.3	182.7	190.5	0.148	0.191	0.132	137.0	157.0	17.7	11.5
−196......	173.5	...	...	175.5	...	0.048	...	160.0	167.0	5.0	6.0

pact specimens, and notch tension specimens. These latter specimens had a cylindrical diameter of 0.357 in. with a 60-deg V-notch which had a root radius of 0.001 in. The diameter at the notch was 0.252 in. Tension tests were performed on a 60,000-lb capacity hydraulic machine at a head speed of 0.01 in./min. Continuous diameter measurements, until fracture occurred, were obtained utilizing a special diameter gage, [*14*]. Notch tension specimens were tested at a head speed of about 0.005-in./min. A few conventional tests of smooth specimens were made in order to obtain notch strength ratios at specific testing temperatures. Charpy impact specimens were tested on a pendulum type machine having a capacity of 215 ft·lb and a striking velocity of 16.8 ft/s. The percent fibrosity of the fractures was estimated by visual observation at a low magnification. Measurements of the fracture surface zones on all types of specimens were obtained by use of a special stereoscopic microscope which projected the cross hairs and which had a toolmakers stage. On tension fractures, measurements were made along two diameters approximately 90 deg apart, and these measurements were averaged to obtain the zone size in terms of the radius. On impact fractures, the lengths of both the fibrous and radial zones were obtained along a line in the center of the fracture and in a direction normal to the notch. The maximum width of the two shear lips were measured in a direction parallel to the notch, and these were averaged to obtain the size of the shear lip zone. Due to the mixed modes of fracture on the coarse grain specimens, it was deemed advisable to obtain two additional measurements of the fibrous and radial zones on impact fractures. These were also made normal to the notch at about half the distance between the original measurement and the extremities of the specimen.

Results and Discussion

Both heat treatments resulted in grains of mixed sizes. Treatment M produced prior austenitic grains of ASTM Nos. 4 to 7 with predominantly No. 5 grains, while Treatment C produced predominantly No. 0 grains. The former will be referred to as medium, and the latter as coarse.

These treatments resulted in the following average Rockwell C hardness:

	Medium Grain	Coarse Grain
Unembrittled	30.8	25.8
Embrittled	30.1	25.8

Tensile Plastic Flow and Fracture Properties

It has been generally accepted that temper embrittlement has little or no effect on the conventionally measured tensile properties of steels.

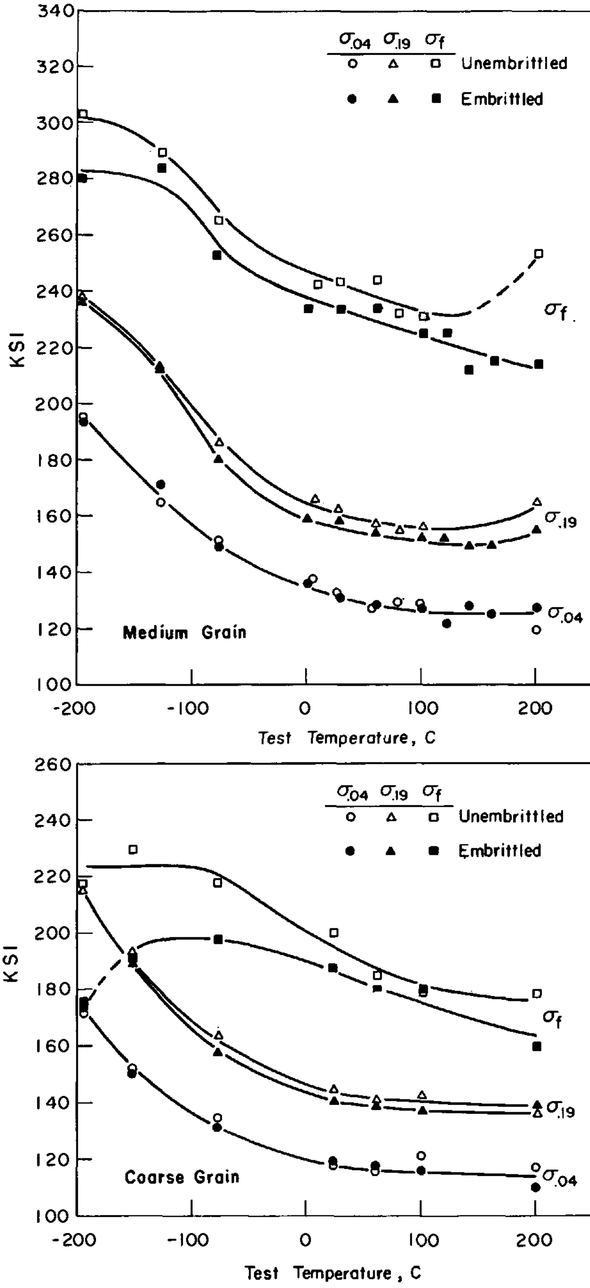

FIG. 2—*Tensile flow properties of 3140 steel.*

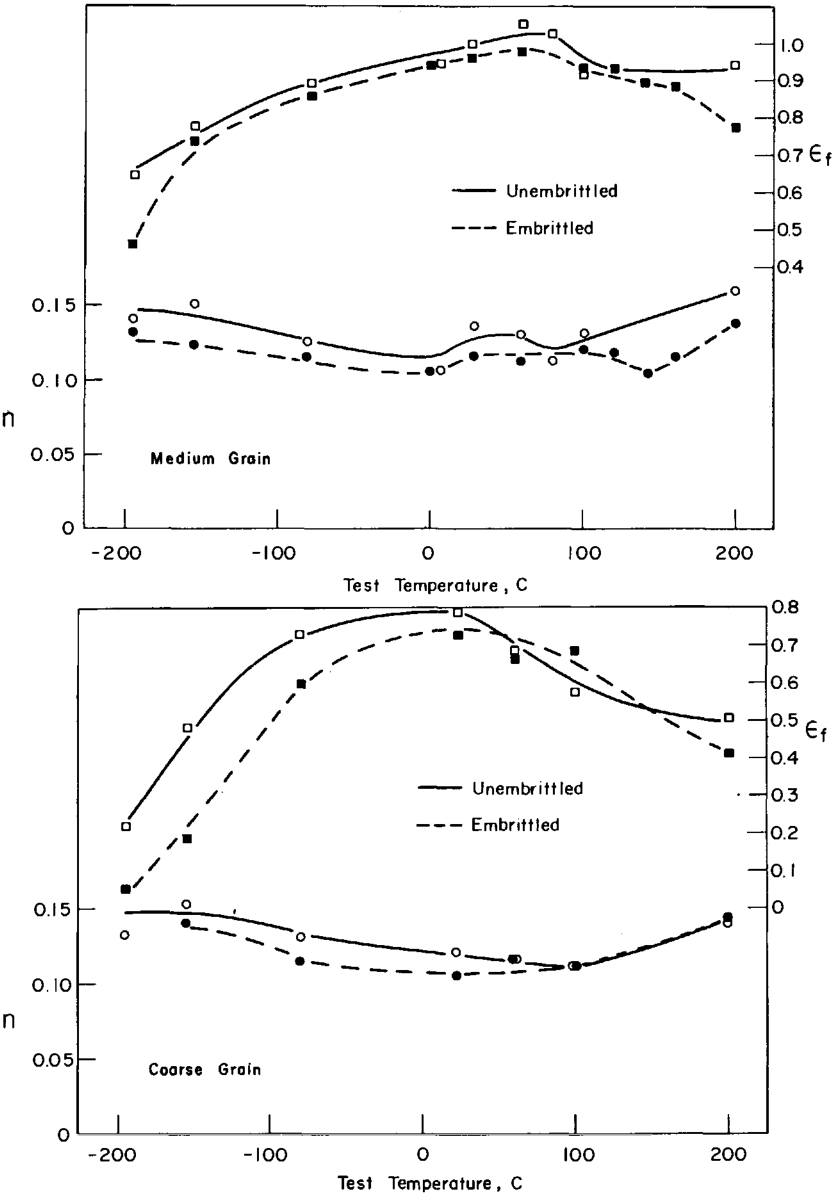

FIG. 3—*Strain hardening exponent and strain at fracture for 3140 steel.*

When flow curves are obtained for both the unembrittled and embrittled condition of these materials, measurable differences in behavior are apparent. Selected flow curves of this steel are presented in Fig. 1 for both the medium and coarse grain size specimens. Examination of these curves reveals that, at any selected testing temperature, the energy expended for total deformation of the embrittled specimen, represented by the area under the curve, is lower than that of the unembrittled specimen. This decrease in energy, for the embrittled condition, is in agreement with energy values obtained by Charpy V-notch impact tests above the 100 percent fibrous transition temperature [*15*]. At any strain beyond yielding, the stress for the embrittled specimen is generally lower, except for the medium grain size material at the two lowest testing temperatures studied (Fig. 1). This general tendency for the flow stress to be somewhat lower is not unusual by itself, as a small amount of softening may have occurred due to the long holding time (48 h) at the embrittling temperature. In contrast, both the stress and strain at fracture of the embrittled specimens are lower than the unembrittled specimens at all testing temperatures.

In order to obtain a quantitative picture of the influence of this type of embrittlement on the flow stress curve, the following parameters have been utilized: flow stress at a constant strain, strain hardening exponent, flow stress at maximum load, and the stress and strain at fracture. These data and the conventional engineering properties are listed in Table 1. Figure 2 depicts the effect of this embrittlement on the flow stress at constant strains, and the fracture stress as influenced by testing temperatures. At a strain of 0.04 little difference in behavior is observed for both material conditions. This would be expected as it is well known that initial yielding is relatively unaffected by this type of embrittlement. At a larger strain of 0.19 a distinct difference in stress level is evident. For both grain sizes the stress level of the embrittled material decreases with increasing testing temperature at a greater rate than that of the unembrittled material. This apparent increase in the flow stress-temperature sensitivity of the embrittled 3140 could explain the increase in the fibrous transition temperature obtained by impact tests. Such an increase can be indicative of an increase in strain rate sensitivity, which is closely related to the flow stress-temperature sensitivity. The stress at fracture (Fig. 2) seems to be considerably lower for the embrittled material for both grain sizes.

Figure 3 illustrates the behavior of the strain at fracture and the strain hardening exponent, *n*, over the temperature range studied for both grain size materials. There is a tendency for the embrittled material to have a lower strain hardening exponent than the unembrittled material. An exception to this general behavior occurs at and above 100 C for the coarse grain material only. In this range of temperature (100 to 200 C), the strain hardening exponent is the same for both material conditions (Fig. 3). The strain at fracture for both materials, in both conditions, is maximum in the vicinity of room temperature and decreases with increasing or decreasing testing temperatures (Fig. 3). With one exception (coarse grain material tested at 100 C), the strain at fracture of the embrittled specimens is appreciably less than that of the unembrittled specimens tested at corresponding temperatures. From room temperature to −196 C the difference in fracture strains between the umbrittled and embrittled materials is greater for the coarse grain steel (Fig. 3).

The effect of temper brittleness on the stress at maximum load is illustrated in Fig. 4. With increasing testing temperature, a constantly larger decrease in stress occurs for the embrittled condition of both materials. This difference in stress becomes most pronounced at the highest testing temperature utilized, particularly in the region where strain aging is known to occur for the unembrittled case. Throughout the range of temperatures studied this difference in stress is more severe for the medium grain size material.

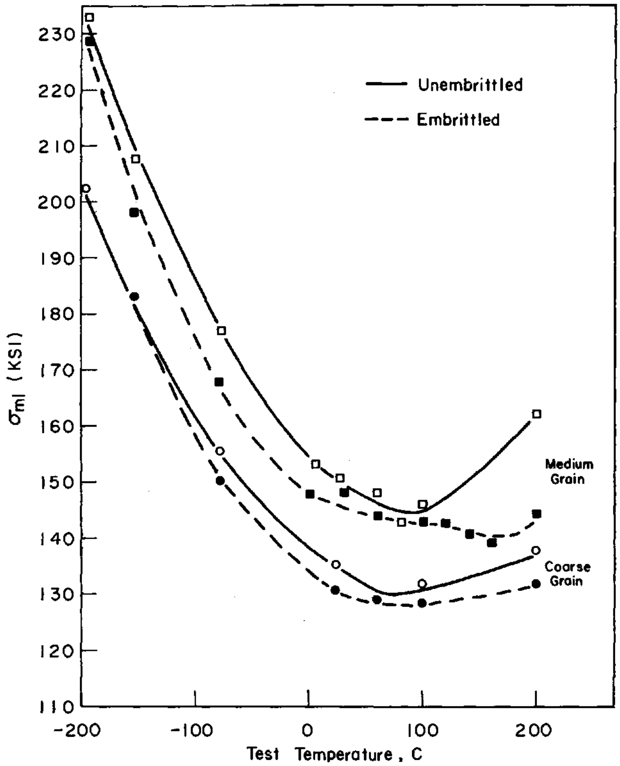

FIG. 4—*True stress at maximum load versus testing temperature—3140 steel.*

It is evident from the preceding data that there is a difference in the tensile flow and fracture behavior of unembrittled and temper embrittled steels. Such differences (which indicate a general deterioration of strength and ductility due to thermal embrittlement), have not been previously documented due to the lack of basic tensile flow and fracture data. As a convenient means for further differentiation between the relative amount of embrittlement as a function of testing temperature, the ratios of the stress at fracture of the embrittled to the unembrittled specimens $\sigma F_e/\sigma F_u$ are presented in Table 2 and Fig. 5. Similar ratios of the

TABLE 2—*Embrittled and unembrittled yield stress and fracture stress ratios* ($\sigma_{YS_e}/\sigma_{YS_u}$ and $\sigma_{F_e}/\sigma_{F_e}$)

Testing Temperature, deg C	Medium Grain Size		Coarse Grain Size	
	$\sigma_{YS_e}/\sigma_{YS_u}$	$\sigma_{F_e}/\sigma_{F_u}$	$\sigma_{YS_e}/\sigma_{YS_v}$	$\sigma_{F_e}/\sigma_{F_u}$
200	1.00	0.84	0.98	0.90
100	1.02	0.97	0.96	1.00
60	1.01	0.96	1.01	0.98
RT	1.00	0.96	0.98	0.94
−80	0.97	0.95	0.97	0.91
−155	1.02	0.98	1.00	0.83
−196	1.00	0.92	0.98	0.80

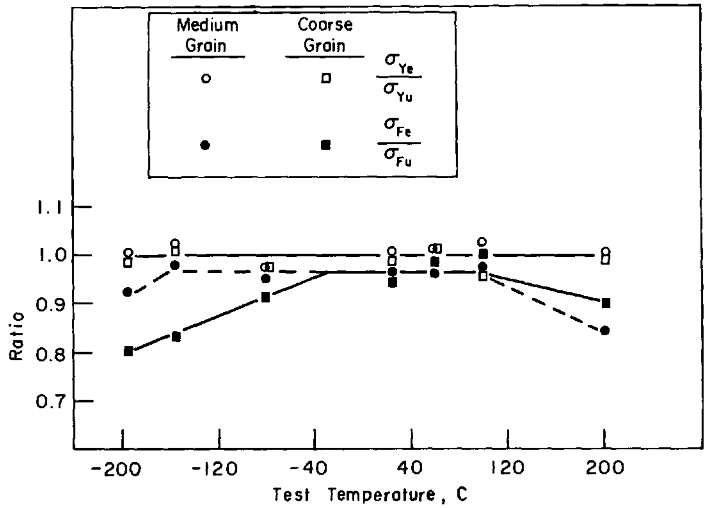

FIG. 5—*Fracture stress and yield stress ratios for unembrittled and embrittled 3140 steel.*

yield strengths $\sigma Y_e/\sigma Y_u$ are equal to unity within experimental error, and are also included in Table 2 and Fig. 5. The fracture stress-ratio parameter gives a qualitative picture of the relative decrease in toughness at various testing temperatures due to this amount of embrittlement. Comparison of these two fracture stress ratio curves (Fig. 5) for the range of testing temperatures which would preclude any strain aging effects, reveals a marked difference in the temperature at which a decrease occurs.

It is also obvious that the yield strength ratio of both materials gives no indication of such a decrease.

Fracture and Fracture Surface Topography

General

A cursory examination of the fracture surface topography revealed the following:

A pronounced difference in fracture appearance existed between the materials differing in grain size. For either of these materials, the difference between unembrittled and embrittled specimens was primarily transitional. Specimen geometry exerted some influence on the fracture surface configurations. Thus, the various types of fracture surface topography are segregated according to grain size and specimen geometry.

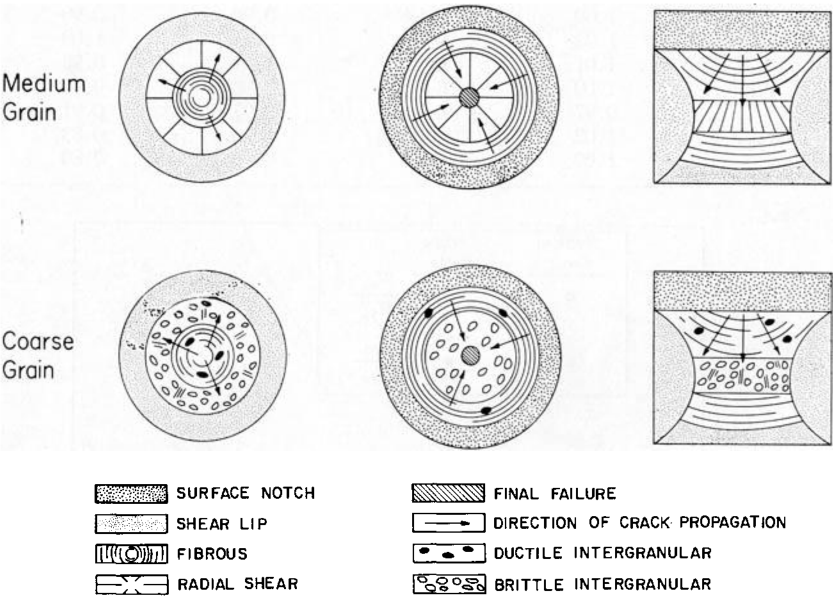

FIG. 6—*Fracture surface zones—schematic.*

Medium Grain Size Material

Considering first, only the medium grain size material in both conditions, the fracture surface topography, in general, was the same as that previously observed and reported for 4340 steel [*10–12*].

The zones of configurations observed on the fractured surfaces of this material are illustrated schematically in Fig. 6 and are summarized as follows:

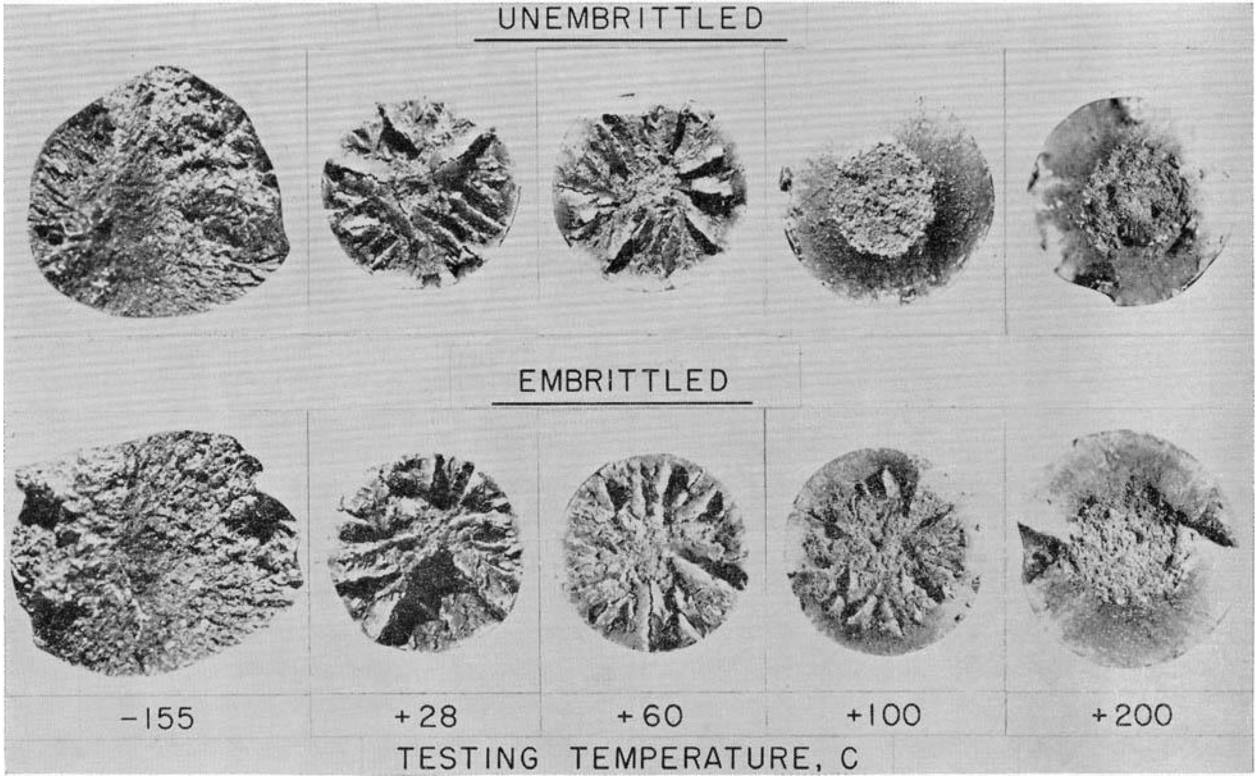

FIG. 7—*Tensile fractures of medium grain 3140 steel.*

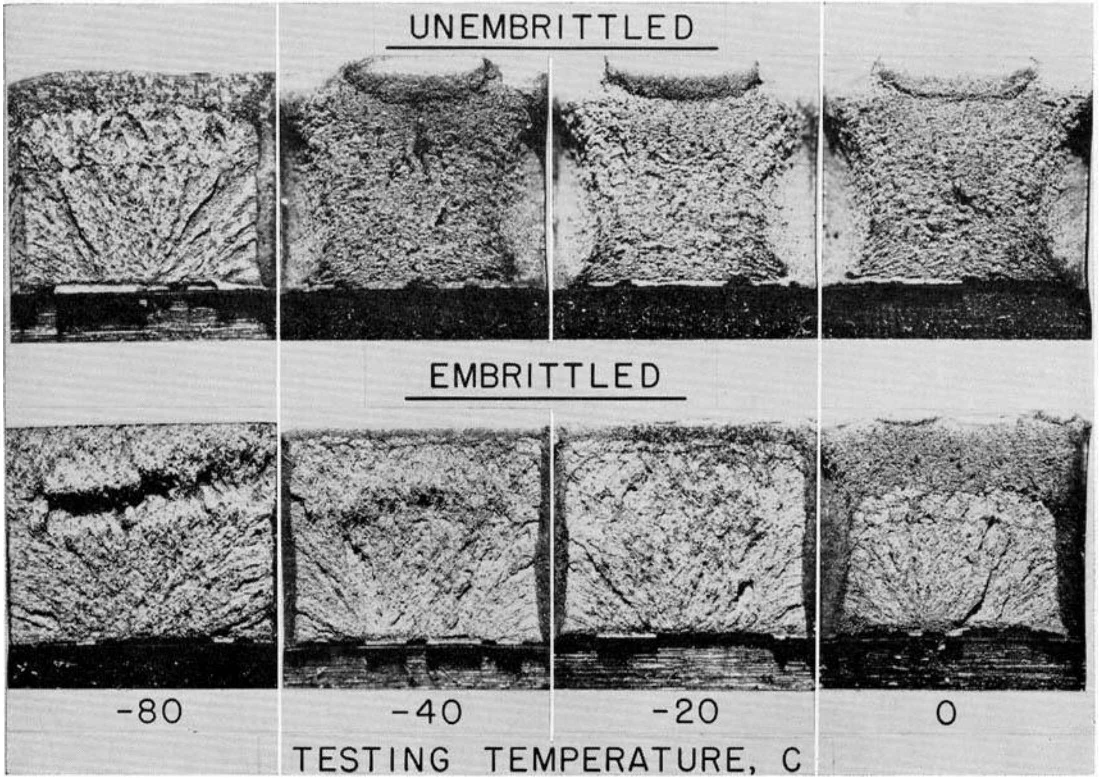

FIG. 8—*Charpy impact fractures of medium grain 3140 steel.*

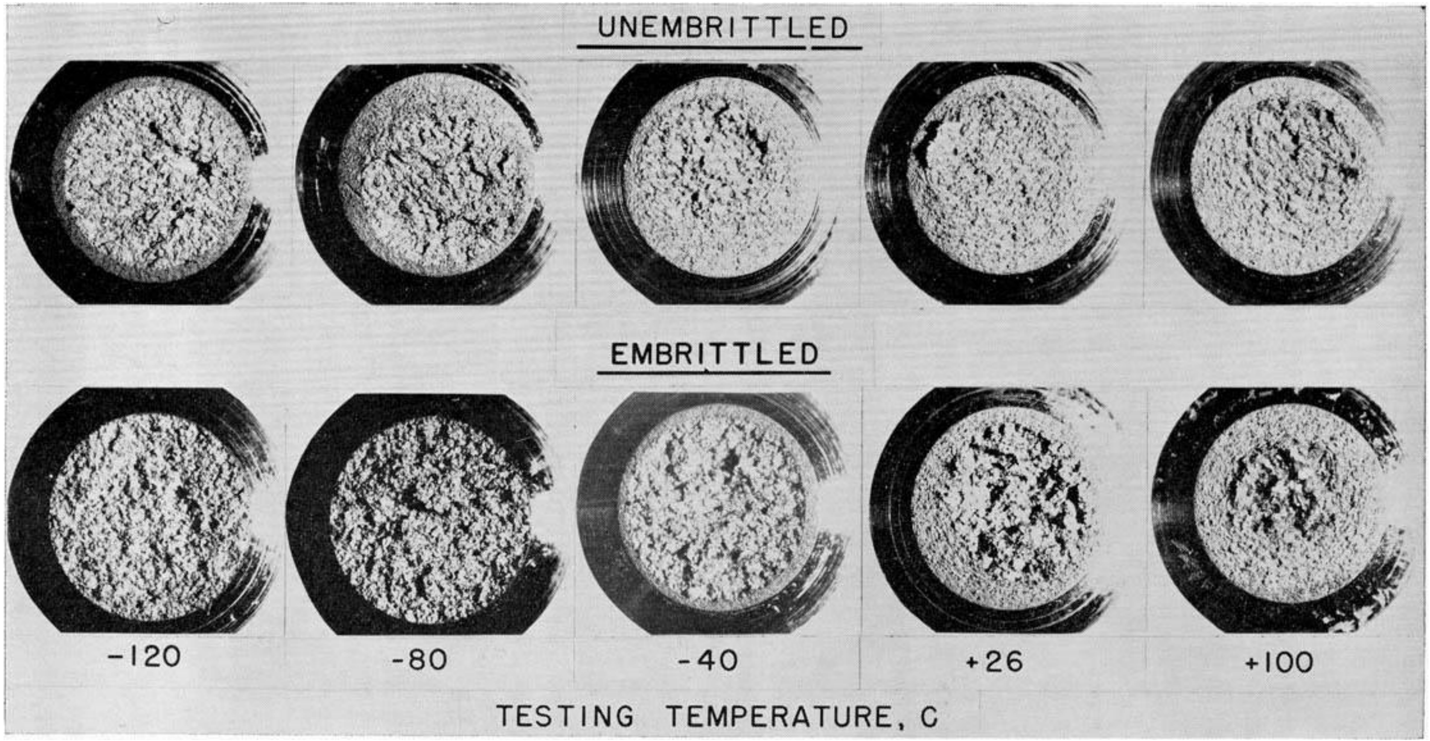

FIG. 9—*Notch tensile fractures of medium grain 3140 steel.*

Zone I—Fibrous—consisting of circumferential markings normal to the direction of crack propagation. These markings are indicative of relatively slow ductile crack extension requiring a relatively high amount of energy.

Zone II—Radial—consisting of radial marks coincident to the direction of crack propagation. These markings are indicative of relatively fast crack propagation requiring a relatively low amount of energy.

Zone III—Shear lip—a smooth element (macroshear) adjacent to the free surface or surfaces of the specimen.

The actual zones present and their respective size varied with testing temperature resulting in transitional behavior. This transitional behavior is illustrated, for the three types of specimens, in Figs, 7, 8, and 9 and followed one of three temperature transitional sequences. In the order of decreasing temperature these were:

1. Fibrous to shear lip.
2. Fibrous to radial to shear lip.
3. Radial to shear lip.

Due to the direction of cracks propagation in notch tension specimens, the shear lip zone was absent, and the transitional sequences of notch tension specimens were:

1. Fibrous.
2. Fibrous to radial.
3. Radial.

These temperature-transitional sequences explain the difference illustrated by Holloman [*2*] between the fracture appearance of embrittled and unembrittled tension specimens tested at the same temperature. A similar comparison is observable in Fig. 7 for specimens tested at +100 C. Comparisons similar to those reported by Bailey and Kies [*3*] can likewise be observed.

Examination of Figs. 7, 8, and 9 revealed a difference in the appearance of the radial zone, due to both specimen geometry and testing temperature. Similar to 4340 steel, the size of the markings (in relief) of this radial zone on the smooth tensile fractures depended on testing temperature. In contrast, the markings of this same zone (II) on impact and notch tensile fractures were relatively fine at all testing temperatures (Figs. 7, 8, and 9).

Whenever the radial zone of this material consisted of fine markings, there were numerous small areas of high reflectivity which caused this zone to have a lustre. As this appearance could be indicative of intergranular fracture, various specimens were plated, sectioned, and examined along the fracture path at high magnifications. These examinations revealed that within this radial zone (II), coarse markings (observed on fractures of smooth tension specimens) were indicative of transgranular fracture; while fine lustrous markings, observed on fractures of all three types of specimens, were indicative of bimodal fracture (transgranular and intergranular). This behavior was common for both material conditions.

Figure 10 illustrates the fractures of embrittled and unembrittled impact specimens. For this illustration, transitional differences are nearly neutralized by the choice of testing temperatures. It is evident, in the representative section at X1000, that qualitatively the modes of fracture are the same for both material conditions. Quantitative differentiation of these modes for these two specimens would be extremely difficult.

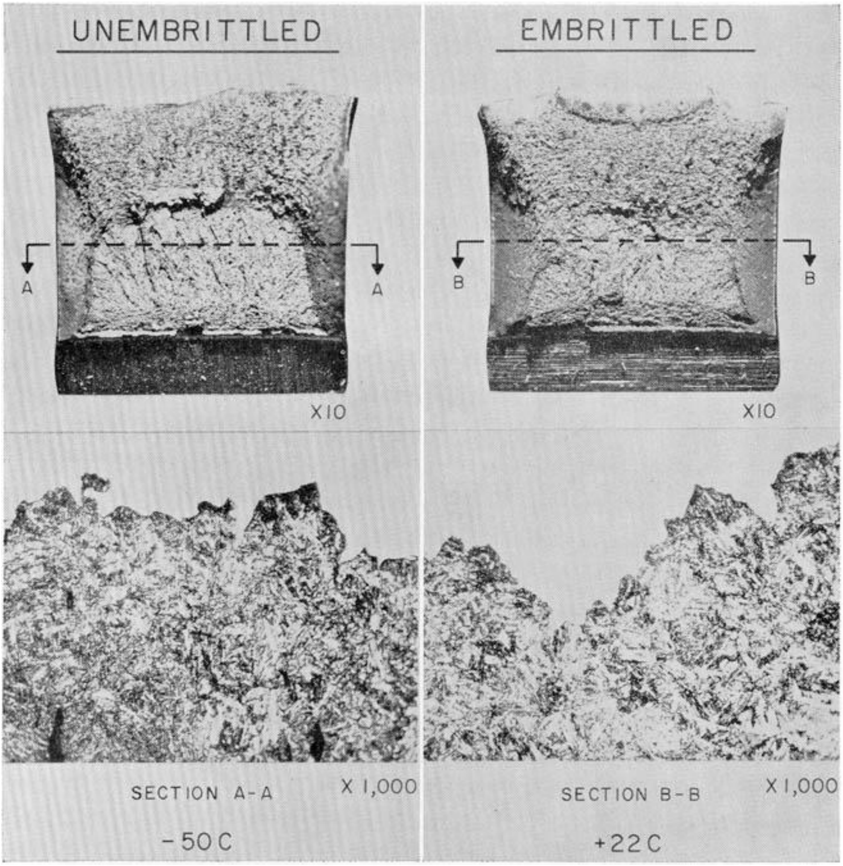

FIG. 10—*Impact fractures of unembrittled and embrittled medium grain 3140 steel.*

Thus, for smooth tension specimens of this material in either condition, crack extension which produced the radial zone could occur solely by transgranular separation, or in a bimodal manner depending on testing temperature. In contrast, crack extention in the radial zone for both

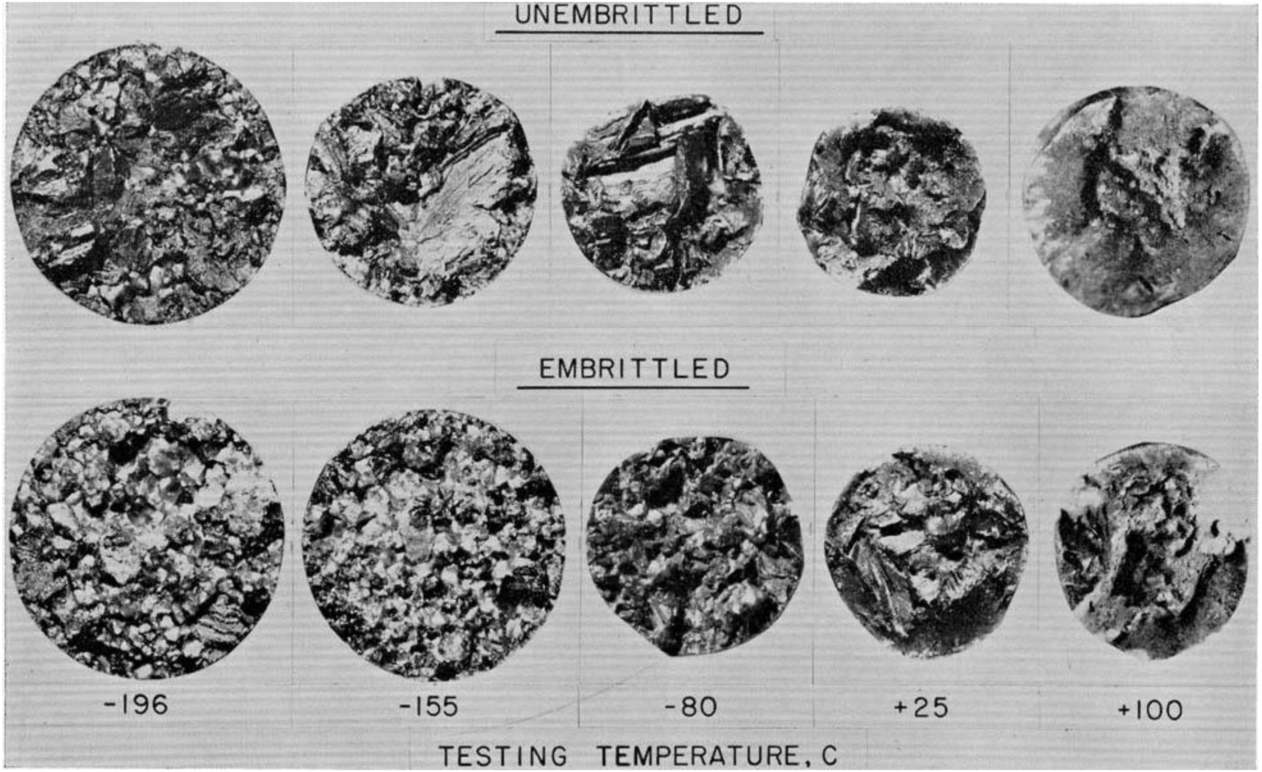

FIG. 11—*Tensile fracture of coarse grain 3140 steel.*

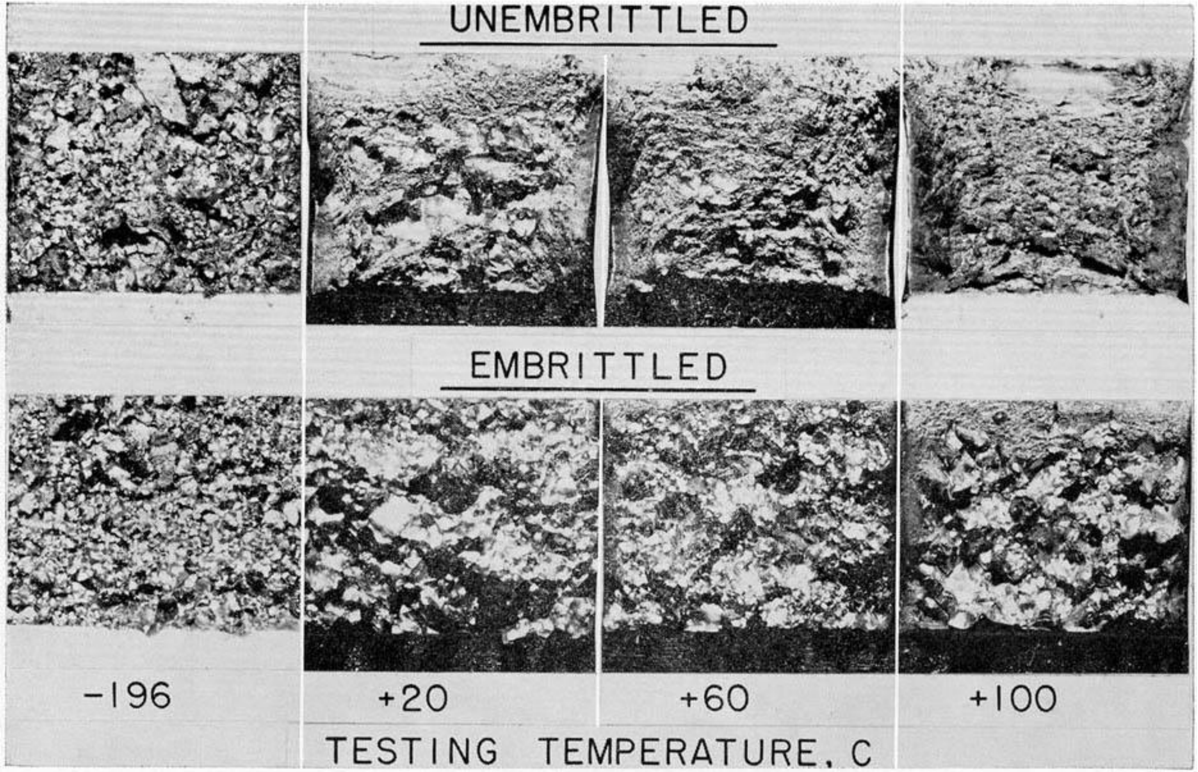

FIG. 12—*Charpy impact fractures of coarse grain 3140 steel.*

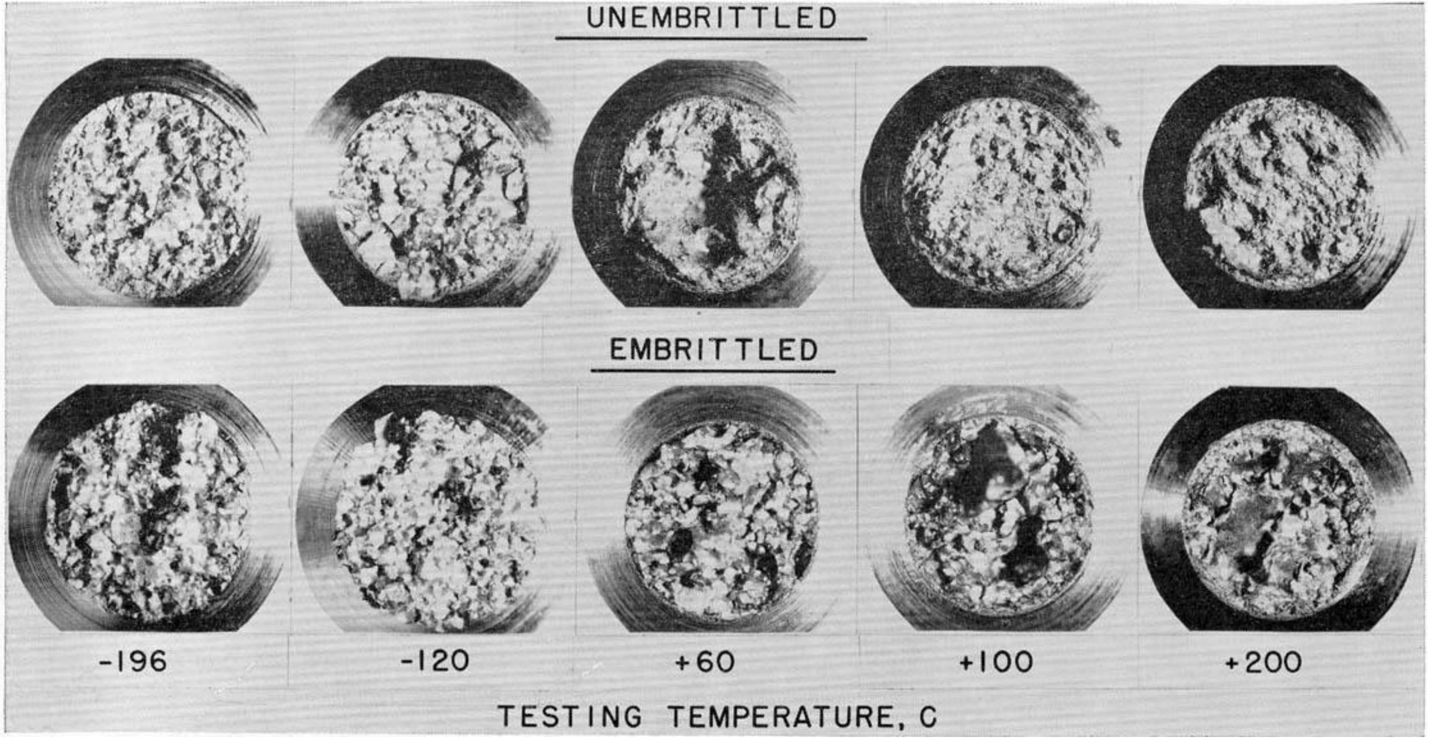

FIG. 13—*Notch tensile fractures of coarse grain 3140 steel.*

types of notch specimens occurred by bimodal separation regardless of testing temperature. These characteristic appearances of the markings of this radial zone (II) for this grain size delineates the mode or modes of fracture (Figs. 7, 8, and 9).

Deep longitudinal splits were also observed on the fractures of smooth tension specimens and were common to both material conditions. Such splits have generally been attributed to temper embrittlement [*1*]. The presence of such splits on both embrittled and unembrittled specimens would mean that either this association is not valid or that some degree of embrittlement developed during the initial temper. The recent study of Capus [*16*] indicates the latter to be correct; thus, the term "unembrittled" must be regarded as relative rather than absolute.

Coarse Grain Material

The fracture surface topography of this material in both the unembrittled and the embrittled condition is illustrated in Figs. 11, 12, and 13. This topography is also compared schematically with that of the medium grain material in Fig. 6. In general, only the shear lip zone (III) remained unmodified in appearance due to this increase in grain size of this steel.

Some intergranular fracture was observed in the otherwise fibrous zone (I) in decreasing amounts with increasing testing temperature. At low magnifications, this intergranular fracture had a different appearance than the intergranular fracture observed on specimens tested at lower temperatures, which was the type usually associated with low-energy, brittle fracture. This brittle type was granular and reflective. In contrast, the type observed in the fibrous zone on specimens tested at higher temperatures appeared less reflective, and the original granular shape was distorted apparently by plastic deformation. Both this deformation and the coexistence with fibrous markings suggested that this type of intergranular fracture might be relatively high energy and ductile. Based on fractographic studies utilizing the electron microscope, Warke and Elsea [*17*] suggested that some intergranular fracture might be termed "intergranular ductile fracture." Thus, for this coarse grain material, Zone I, which is believed to result from relatively high-energy crack extension, consists predominantly of fibrous markings with some ductile intergranular fracture.

With exceptions, which will be described later, the radial zone (II) consisted predominantly of intergranular fracture which had a brittle appearance compared to the type observed in the fibrous zone (I). There were some small areas of radial markings—which were actually river markings indicative of cleavage—and which had orientations that usually differed with each grain.

In general, this described topography was common to both material conditions. Except at low testing temperature difference in fracture behavior between embrittled and unembrittled specimens was transitional.

Below approximately −120 C, the fracture behavior of the unembrittled specimens changed. With decreasing testing temperature, there was an increase in the amount of cleavage fracture until the fracture surfaces at −155 and −196 C were predominantly transgranular fracture. This indicated that the well-known difference in fracture behavior at low testing temperatures between embrittled and unembrittled coarse grain steel was due to the peculiar fracture behavior of the unembrittled material. It also indicated that indiscriminate association of temper brittleness with intergranular fracture may result in error (Fig. 14).

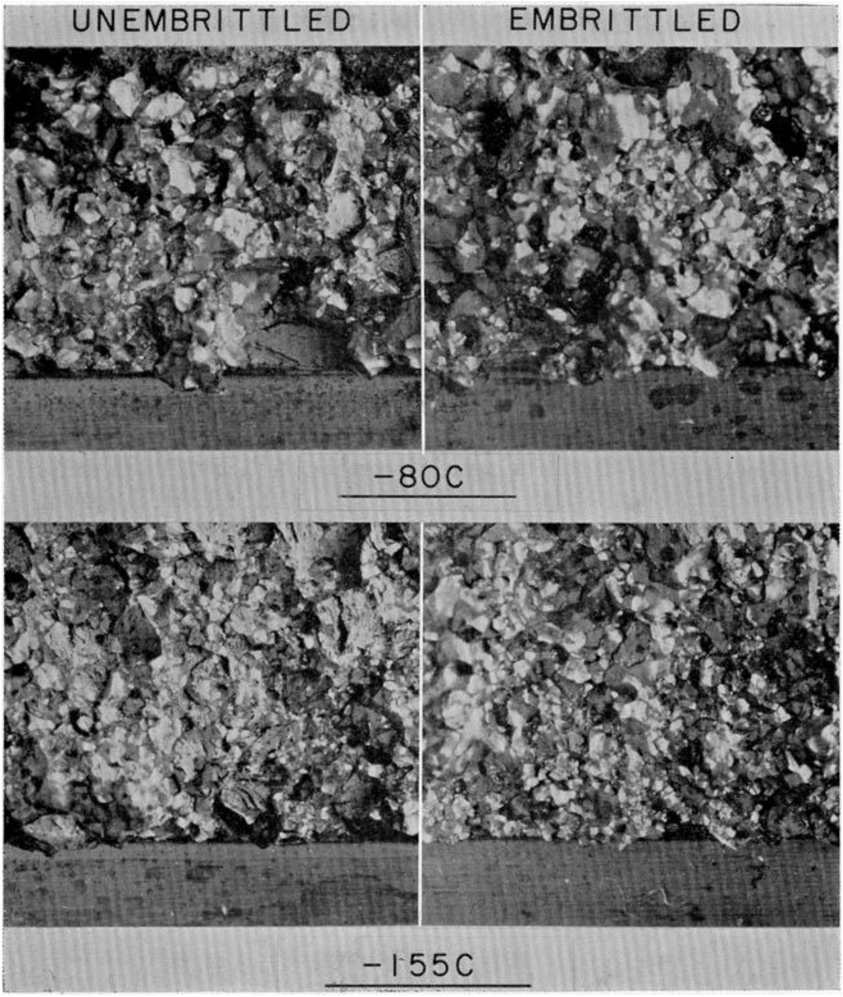

FIG. 14—*Fracture of coarse grain impact specimens at low temperatures.*

The various zones of fracture surface configurations of this coarse grain material may be summarized as follows:

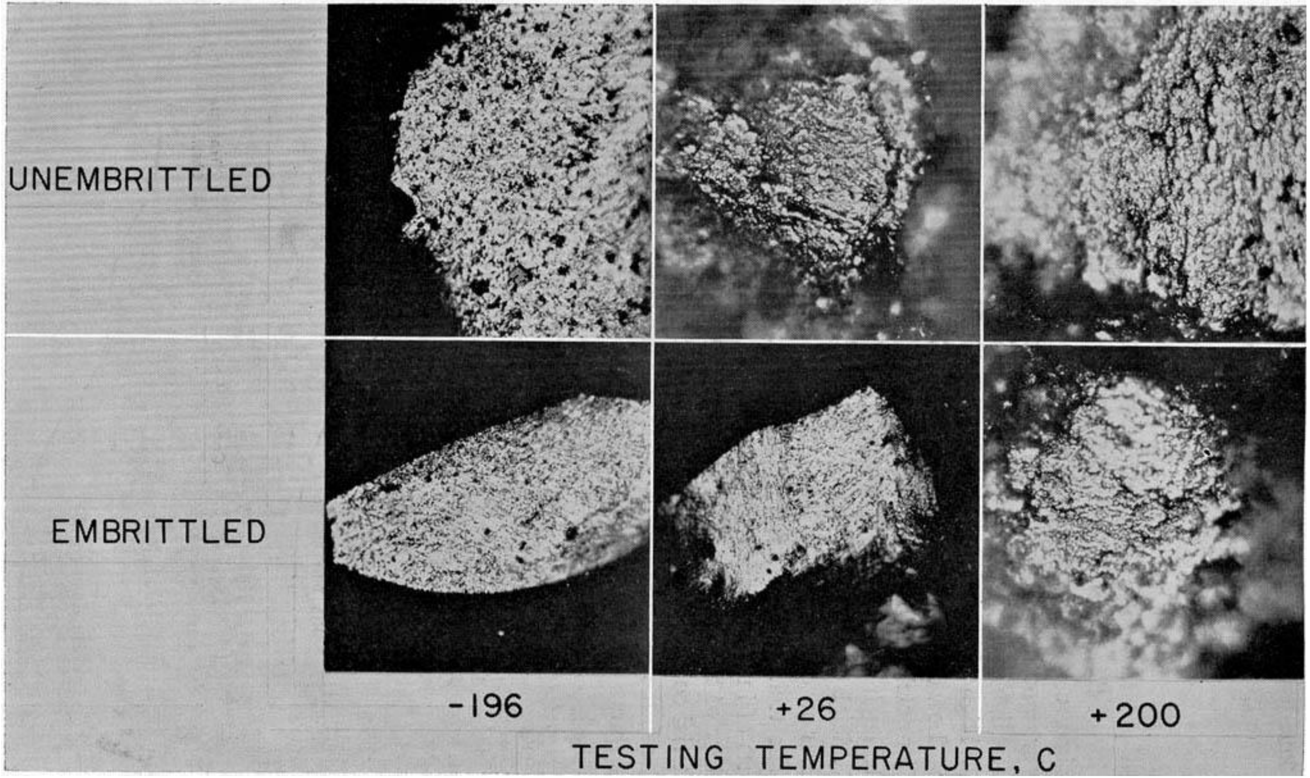

FIG. 15—*Texture of intergranular facets versus testing temperature.*

Zone I—High energy (fibrous and ductile intergranular).

Zone II—Low energy (brittle intergranular and areas of radial markings).

Zone III—Shear lip—a smooth shear element (macroshear) adjacent to the free surfaces of the specimen.

In order of decreasing temperature, the temperature-transitional behavior of this material, as indicated by the fracture surface topography, can be generalized according to specimen geometry as follows:

For smooth tension and Charpy V-notch impact specimens:

1. High energy to shear lip.
2. High energy to low energy to shear lip.
3. Low energy to shear lip.

For notch tension specimens:

1. High energy.
2. High energy to low energy.
3. Low energy.

The technique of Zapffe and Worden [*18*] was utilized to examine facets of intergranular fracture on notch tension specimens. The surface texture of these facets differed appreciably with testing temperature and material condition. This difference in texture is illustrated in Fig. 15. In general, the texture of facets on specimens tested at the higher temperature shows considerable deformation indicating ductility at this magnifi-

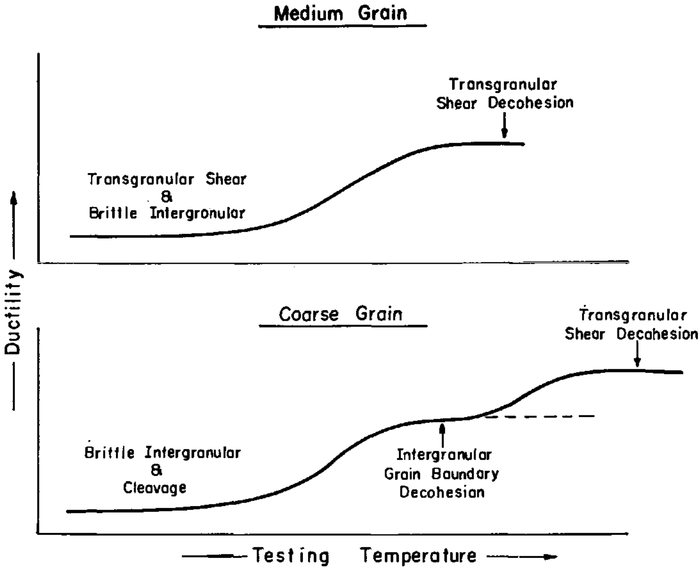

FIG. 16—*Ductility and modes of fracture versus testing temperature—schematic.*

cation. At lower testing temperatures, the texture of facets appears relatively undeformed, which suggests a difference in energies required for separation. Likewise, the difference in texture of facets on specimens tested at 26 C illustrates the difference in deformation due to material condition.

Voids and small conical projections estimated to be 0.2 to 0.5 mil diameter (at the base) were observed on facets having a relatively smooth texture. These had an appearance similar to inclusion mounds, described by Larson and Carr [*10*], but were about an order of magnitude smaller in size. There appeared to be a particle at the apex, but limitations of this technique precluded more extensive study for confirmation.

TABLE 3—*AISI 3140 steel tension specimens.*

Condition	Medium Grain				Coarse Grain			
	Testing Temperature, deg C	Fracture Surface Zones, in.			Testing Temperature, deg C	Fracture Surface Zones, in.		
		I	II	III		I	II	III
Unembrittled.....	+200	0.044	...	0.042	+200	0.039	...	0.061
	+100	0.043	...	0.043	+100	0.053	...	0.053
	+80	0.021	0.040	0.018	+60	0.060	...	0.030
	+60	0.017	0.045	0.015	+23	0.037	0.025	0.022
	+27	0.017	0.049	0.012	−80	0.009	0.068	0.010
	0	0.013	0.054	0.012	−120	...	0.091	0.006
	−80	...	0.073	0.009	−155	...	0.098	0.002
	−155	...	0.086	0.006	−196	...	0.112	0.001
	−196	...	0.096	0.004	...	...	...	...
Embrittled........	+200	0.047	0	0.043	+200	0.052	...	0.052
	+160	0.047	0.010	0.034	+100	0.058	...	0.030
	+140	0.024	0.026	0.034	+60	0.038	0.035	0.020
	+120	0.022	0.042	0.016	+23	0.026	0.051	0.016
	+100	0.017	0.046	0.018	−40	0.005	0.077	0.010
	+60	0.015	0.054	0.009	−80	...	0.092	0.004
	+28	0.011	0.056	0.010	−155	...	0.115	0.001
	0	0.010	0.058	0.010	−196	...	0.123	0.001
	−80	...	0.080	0.006	...	...	...	...
	−155	...	0.094	0.002	...	...	...	...
	−196	...	0.102	0.005	...	...	...	...

The combined macroscopic and microscopic studies of the fracture of this material indicated that intergranular fracture can occur with different degrees of energy required for separation. The type of intergranular fracture which apparently requires relatively high energy for separation appeared at ×500 to be grain boundary decohesion.

The fracture topography of all materials studied indicate that both high- and low-energy separation may occur by either the transgranular or the intergranular mode as illustrated schematically in Fig. 16.

TABLE 4—*AISI 3140 steel Charpy impact specimens.*

Condition	Testing Temperature, deg C	Fracture Surface Zones, in.			Impact Energy, ft·lb	Fibrous Fracture, %
		I	II	III		
		MEDIUM GRAIN				
Unembrittled.....	0	0.272	0	0.073	58.2	100
	−20	0.261	0	0.077	63.7	100
	−30	0.279	0	0.072	59.1	100
	−40	0.265	0	0.070	53.6	95
	−50	0.150	0.155	0.058	39.8	70
	−60	0.128	0.165	0.064	34.5	65
	−60	0.177	0.167	0.058	33.7	65
	−80	0.039	0.257	0.028	21.5	30
	−80	0.060	0.222	0.037	23.6	45
	−105	0	0.287	0.021	16.2	15
	−120	0	0.301	0.016	14.9	10
	−196	0	0.311	0.007	7.8	0
Embrittled........	+60	0.281	0	0.071	56.7	100
	+40	0.270	0	0.080	55.9	100
	+35	0.275	0	0.071	54.9	100
	+30	0.207	0.053	0.072	47.0	90
	+22	0.158	0.111	0.063	42.7	80
	+10	0.128	0.176	0.055	32.6	65
	0	0.103	0.186	0.043	26.8	55
	0	0.056	0.219	0.044	29.1	55
	−10	0.056	0.240	0.035	22.5	40
	−20	0.040	0.262	0.025	16.2	25
	−40	0.020	0.280	0.020	14.9	15
	−80	0	0.303	0.008	11.5	5
	−196	0	0.314	0.001	5.2	0
		COARSE GRAIN				
Unembrittled.....	+100	0.292	0	0.044	75.5	90
	+90	0.294	0	0.046	78.4	90
	+60	0.282	0.010	0.047	75.5	95
	+40	0.276	0.017	0.043	72.7	85
	+20	0.243	0.039	0.034	63.7	65
	0	0.212	0.080	0.029	53.1	70
	−20	0.184	0.107	0.020	50.9	50
	−40	0.114	0.179	0.029	34.5	45
	−60	0.066	0.227	0.026	28.0	35
	−80	0.038	0.254	0.010	15.8	15
	−80	0.052	0.261	0.019	14.9	35
	−120	0.025	0.281	0.011	10.9	5
	−120	0.012	0.300	0.006	7.8	5
	−130	0	0.316	NM[a]	8.4	5
	−155	0	0.316	NM[a]	7.3	0
	−196	0	0.312	0.002	4.0	0
	−196	0	0.316	NM[a]	5.0	0

TABLE 4—*Continued*

Condition	Testing Temperature, deg C	Fracture Surface Zones, in.			Impact Energy, ft·lb	Fibrous Fracture, %
		I	II	III		
COARSE GRAIN—*Continued*						
Embrittled........	+300	0.309	0	0.032	56.7	100
	+290	0.290	0	0.040	67.9	95
	+270	0.294	0	0.042	61.8	95
	+250	0.279	0.012	0.034	70.8	90
	+250	0.277	0.015	0.033	63.2	75
	+225	0.259	0.034	0.034	62.2	85
	+200	0.219	0.074	0.034	59.6	65
	+180	0.239	0.052	0.034	60.9	85
	+165	0.169	0.120	0.033	47.8	70
	+150	0.181	0.112	0.032	51.3	55
	+120	0.112	0.180	0.019	32.9	40
	+100	0.074	0.229	0.020	33.3	35
	+50	0.028	0.270	0.012	19.4	25
	+22	0.009	0.299	NM[a]	10.9	5
	−40	0	0.320	NM[a]	8.4	0
	−80	0	0.314	NM[a]	5.4	5
	−120	0	0.315	NM[a]	3.2	0
	−130	0	0.315	NM[a]	2.8	0
	−155	0	0.314	NM[a]	2.8	0
	−196	0	0.319	NM[a]	1.8	0
	−196	0	0.316	NM[a]	2.3	0

[a] NM = not measurable.

Transitional Behavior

Cognizance of the different fracture surface appearances, which suggested either high- or low-energy crack extension, enabled measurements to be made of the size of these fracture surface zones at low magnification. These data, together with the pertinent mechanical properties, are contained in Tables 3 to 5. The per cent fibrous fracture ratings of impact specimens obtained by the conventional method are included in Table 4.

Conventional Charpy V-notch impact transitional curves of these materials obtained from the data of Table 4 are illustrated in Fig. 17. Transition curves of these same specimens, obtained by plotting the respective zone sizes (in terms of the radius) as a function of testing temperature, are presented in Fig. 18. Similar fracture transition curves were obtained for both the smooth (Fig. 19) and the notch tension specimens (Fig. 20). Also illustrated are the various mechanical properties as a function of testing temperature.

These topographical-temperature curves (Figs. 18, 19, and 20 reflect both the transitional behavior and the effects of temper embrittlement for all three types of specimens. The actual transition temperatures

TABLE 5—*AISI 3140 steel notch tension specimens.*

Condition	Testing Temperature, deg C	Notch Tensile Strength, ksi	Ultimate Tensile Strength, ksi	Notch Strength Ratio	Fracture Surface Zones, in.	
					I	II
			MEDIUM GRAIN			
Unembrittled.....	+200	184.5	136.0	1.36	0.121	...
	+100	192.8	131.2	1.47	0.121	...
	+60	194.8	132.4	1.47	0.121	...
	+26	197.6	136.0	1.45	0.121	...
	0	203.2	139.6	1.46	0.122	...
	−40	208.0	142.8	1.46	0.051	0.071
	−60	211.2	...	...	0.048	0.075
	−80	214.7	154.8	1.39	0.027	0.097
	−120	229.3	...	...	0.016	0.109
	−155	241.4	174.8	1.38	...	0.126
	−196	239.0	197.6	1.21	...	0.126
Embrittled........	+200	181.7	129.2	1.41	0.122	...
	+160	181.3	125.2	1.45	0.122	...
	+100	188.4	128.0	1.47	0.065	0.057
	+60	195.2	129.2	1.51	0.038	0.084
	+26	196.4	132.8	1.48	0.030	0.092
	−40	204.0	145.2	1.41	0.015	0.110
	−60	206.8	...	...	0.014	0.110
	−80	203.2	150.4	1.35	...	0.126
	−120	204.8	...	...	...	0.126
	−155	206.0	176.8	1.17	...	0.126
	−196	127.2	196.4	0.65	...	0.126
			COARSE GRAIN			
Unembrittled.....	+200	174.3	121.6	1.43	0.120	...
	+100	175.7	120.8	1.45	0.119	...
	+60	181.0	118.6	1.53	0.119	...
	+26	184.4	123.6	1.49	0.105	0.026
	−40	194.4	...	...	0.015	0.106
	−80	204.4	137.2	1.49	0.008	0.116
	−120	213.3	147.2	1.45	0.007	0.117
	−155	218.6	160.4	1.36	...	0.125
	−196	226.7	177.6	1.28	...	0.126
Embrittled........	+200	165.6	115.0	1.44	0.054	0.068
	+160	170.3	...	...	0.032	0.093
	+100	173.7	115.8	1.50	0.013	0.108
	+60	177.0	117.6	1.51	0.006	0.117
	+26	181.0	118.0	1.53	0.004	0.120
	−40	191.5	127.0	1.51	0.004	0.120
	−80	179.6	132.8	1.35	...	0.127
	−120	177.7	...	...	...	0.127
	−155	159.1	157.0	1.01	...	0.126
	−196	132.5	167.0	0.79	...	0.126

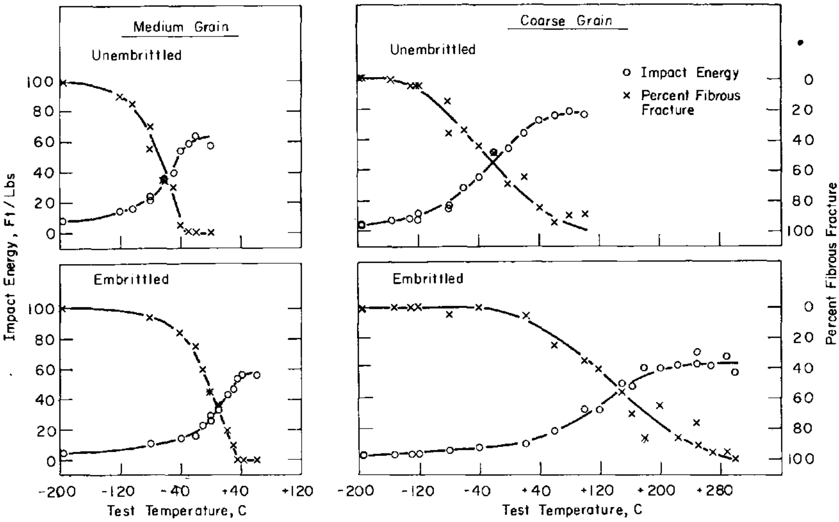

FIG. 17—*Conventional Charpy impact transition curves of 3140 steel.*

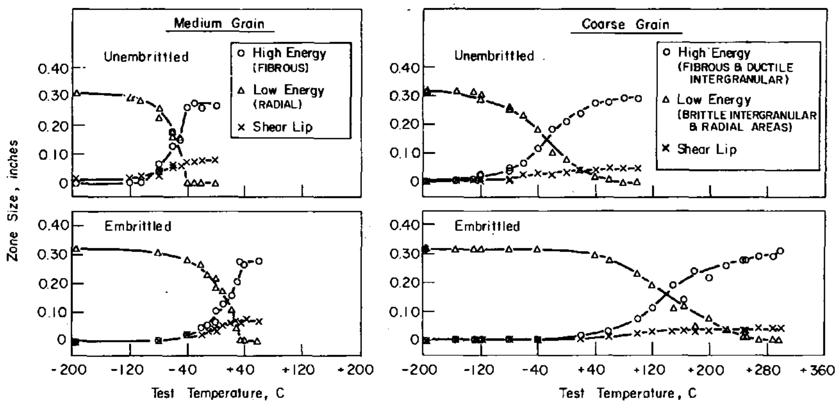

FIG. 18—*Fracture topography versus testing temperature for impact fractures of 3140 steel.*

based on several criteria varied according to grain size, material condition, and type of test. The criteria utilized were as follows:

Charpy Transition—the lowest testing temperature at which the fracture consisted entirely of the fibrous and shear lip zones (100 per cent fibrous).

High Energy—the lowest testing temperature at which the fracture contained no low-energy separation (Zone II) as indicated by the fracture surface topography.

Low Energy—The highest testing temperature at which the fracture

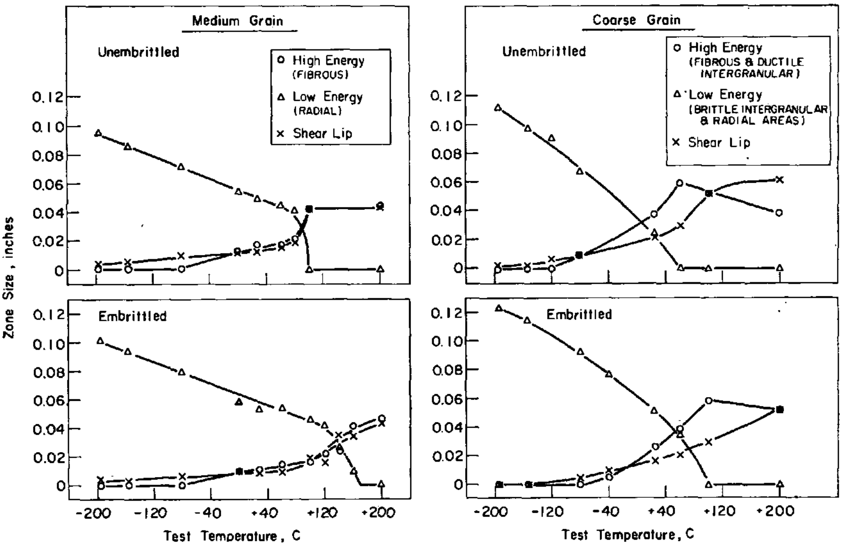

FIG. 19—*Fracture topography versus testing temperature for tensile fractures of 3140 steel.*

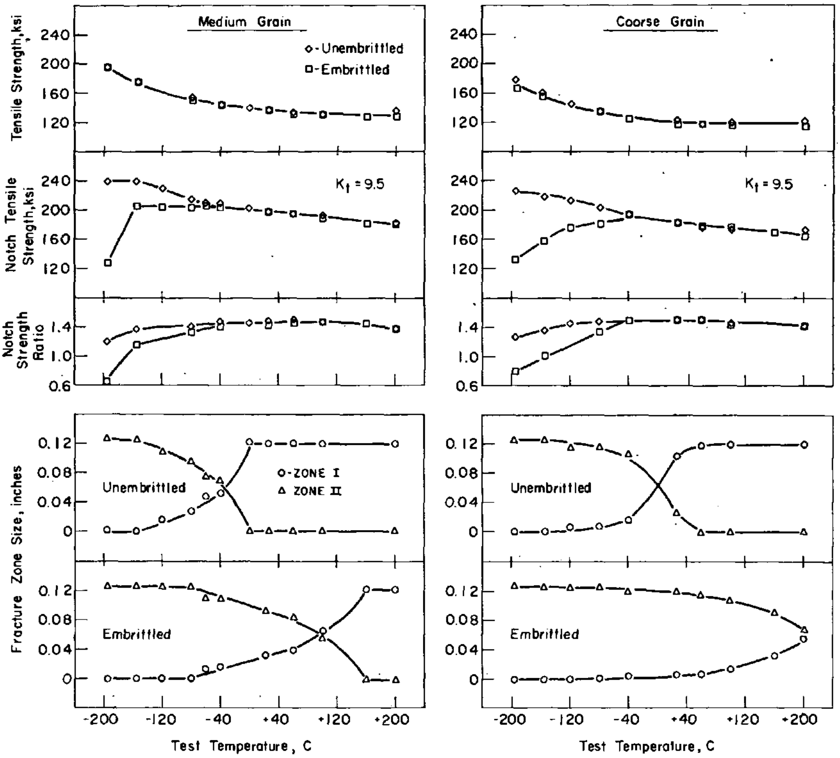

FIG. 20—*Notch tensile properties and fracture surface topography versus testing temperature—3140 steel.*

contained no high-energy separation (Zone I) as indicated by the fracture surface topography.

Shear Lip—the highest temperature at which there is an abrupt increase in the slope of this curve.

Based on these criteria, the transition temperatures obtained for these specimens are listed in degrees centigrade in the table herewith.

Charpy Impact

	Charpy Transition	High Energy	Low Energy	Shear Lip
	Medium Grain			
Unembrittled	−35	−40	−105	−40
Embrittled	+35	+35	−80	+35
Difference	70	75	25	75
	Coarse Grain			
Unembrittled	+120[a]	+80	−130	+80
Embrittled	+300	+270	0[a]	+300
Difference	200	190	130	220

	Tensile			Notch Tensile	
	High Energy	Low Energy	Shear Lip	High Energy	Low Energy
	Medium Grain				
Unembrittled	+100	−80[a]	+100	0	−155
Embrittled	+170	−80[a]	+200	+160	−80
Difference	70	0	100	160	75
	Coarse Grain				
Unembrittled	+60	−120	+60	+60	−155
Embrittled	+100	−80	+100	+240[a]	−50
Difference	40	40	40	180	105

[a] Approximate or estimated.

Differences in fracture behavior due to temper brittleness were indicated quantitatively by the high-energy criterion for all types of specimens utilized.

Good agreement is evident between the Charpy transition (100 percent fibrous) obtained by conventional methods and its counterpart. (high energy), obtained by fracture surface topography. The latter method has the advantage of applicability to specimens of different geometries subjected to different types of loading [*12*]. Differences in transition temperatures obtained by this criterion indicate that this method has about the same sensitivity for the detection of embrittlement for notch tension specimens as it has for impact specimens of these materials.

Fracture Behavior and Temper Brittleness

Excepting coarse grain specimens tested in the vicinity of −196 C, the fracture behavior of both the embrittled and unembrittled specimens were the same for the same grain size material. Qualitatively the mode or modes of fracture, as indicated by both the fracture surface topography and metallographic examination were, in general, the same for both conditions in each respective material. Quantitatively, embrittled specimens having the same respective grain size contained more intergranular fracture at corresponding testing temperatures due to transitional differences. The embrittling mechanism caused a decrease in the amount of high-energy crack propagation as indicated by the fracture surface topography. At testing temperatures which produced low-energy separation, considerable intergranular fracture was observed for both material conditions as well as both grain size materials. As noted previously, differentiation of material condition for the coarse grain specimens, tested in the vicinity of − 196 C, due to a change in the fracture behavior of the unembrittled material. Otherwise, the only difference in fracture surface appearance was transitional.

Confirming an earlier study [*19*] the Charpy impact test data indicate that an increase in the prior austenitic grain size reduces the toughness of the "as-tempered" material and enhances the effects of temper embrittlement. Capus [*16*] utilizing impact specimens from vacuum melted 3 percent nickel-chromium steels with controlled additions, attributed this described behavior to the presence of certain minor elements. These elements were reported to be the cause of two forms of embrittlement, temper brittleness [*20*], and the 500 F embrittlement [*21,22*].

The small projections (and voids) observed on the intergranular facets suggested the possible correctness of the grain boundary precipitate theory as the mechanism responsible for temper embrittlement. This merits further investigations as the presence of particles of another phase—whether this phase be carbides or intermetallic compounds—could serve as nucleation sites for grain boundary decohesion. The relative ductility of such a mode of fracture would depend greatly on the testing temperature similar to the behavior of the coarse grain material.

Summary

1. The tensile plastic flow and fracture behavior observed over a range of testing temperatures was shown to differ for unembrittled and embrittled materials.
2. Quantitative measurements of fracture surface configurations yield transitional curves which differentiate the fracture behavior for a constant amount of embrittlement.
3. Transition curves based on fracture surface configurations can be obtained for both smooth and notch tension specimens as well as Charpy impact specimens. Such curves obtained on Charpy impact specimens are in good agreement with the conventional fibrous transition curves.
4. Various facets of intergranular fracture on the coarse grain frac-

tures had different textures indicating different degrees of deformation, ductility, and energy required for separation.

5. Based on fracture surface configurations, temper brittleness reduces the amount of high-energy crack extension at a constant testing temperature.

6. In general, the mode or modes of fracture operative were the same for both embrittled and unembrittled specimens of these respective materials, within the testing temperature range studied. The one observed exception was due to a change in the fracture behavior of the unembrittled coarse grain material.

7. Small projections observed on intergranular facets suggested the possibility of an intergranular precipitate at grain boundaries.

References

[*1*] Lea, F. C. and Arnold, R. N., "The Embrittlement of Alloys Steels," *Proceedings*, Institution of Mechanical Engineers, Vol. 131, 1935, pp. 539–588.

[*2*] Hollomon, J. H., "Temper Brittleness," *Transactions*, American Society for Metals, Vol. 36, 1946, pp. 473–540.

[*3*] Bailey, E. F. and Kies, J. A., discussion on "Effect of Hardness on the Level of the Impact Energy Curve for Temper Brittle and Unembrittled Steel," *Transactions*, American Society for Metals, Vol. 45, 1953, pp. 736–740.

[*4*] Greaves, R. H., "Temper-Brittleness of Nickel-Chrome Steel," *Journal of the Iron and Steel Institute*, Vol. 100, No. 2, 1919, pp. 329–339.

[*5*] Greaves, R. H., Fell, M., and Hadfield, R., "Further Communication on Temper-Brittleness of Nickel-Chrome Steel," *Journal of the Iron and Steel Institute*, Vol. 100, No. 2, 1919, pp. 340–348.

[*6*] Entwisle, A. R., "Low-Temperature Fractures in Tempered Alloy Steels," *Journal of the Iron and Steel Institute*, Vol. 169, Sept. 1951, pp. 36–38.

[*7*] Jaffe, L. D. and Buffum, D. C., "Upper Nose Temper Embrittlement of a Ni-Cr Steel," *Transactions*, American Institute of Mining, Metallurgical, and Petroleum Engineers, *Welding Journal*, Vol. 35, No. 3, March 1955, pp. 141S–152S.

[*9*] Larson, F. R. and Nunes, J., "Low Temperature Plastic Flow and Fracture Tension Properties of Heat-Treated SAE 4340 Steel," U.S. Army Materials Research Agency, WAL TR 834.1/1, Dec. 1959; also *Transactions*, American Society for Metals, Vol. 53, 1961, pp. 663–682.

[*10*] Larson, F. R. and Carr, F. L., "Tensile Fracture Surface Configurations of a Heat-Treated Steel as Affected by Temperature," U.S. Army Materials Research Agency, WAL TR 320.1/5, July 1961; also *Transactions*, American Society for Metals, Vol. 55, No. 3, Sept. 1962, pp. 599–612.

[*11*] Larson, F. R. and Nunes, J., "Relationships Between Energy, Fibrosity, and Temperature in Charpy Impact Tests on AISI 4340 Steel," U.S. Army Materials Research Agency, WAL TR 834.2/3, Dec. 1961; also *Proceedings*, American Society for Testing and Materials, Vol. 62, 1962, pp. 1192–1205.

[*12*] Carr, F. L. and Larson, F. R., "Fracture Surface Configurations of AISI 4340 Steel as Affected by Temperature and Geometry," U.S. Army Materials Research Agency, WAL TR 320.1/10, Jan. 1963; also *Proceedings*, American Society for Testing and Materials, Vol. 2, 1962, pp. 1210–1222.

[*13*] Carr, F. L. et al, "Isothermal Temper Embrittlement of SAE 3140 Steel," U.S. Army Materials Research Agency, WAL 801/1–11, 27 May 1952; also *Transactions*, American Institute of Mining, Metallurgical, and Petroleum Engineers, Vol. 197, 1953, p. 998.

[*14*] Nunes, J. and Larson, F. R., "A Method for Determining the Plastic Flow Properties of Sheet and Round Tension Test Specimens," U.S. Army Mate-

rials Research Agency, WAL TR 111.1/1, March 1961; also *Proceedings*, American Society for Testing and Materials, Vol. 61, 1961, pp. 1349–1361.

[*15*] Carr, F. L. et al, "Effect of Hardness on the Level of the Impact Energy Curve for Temper Brittle and Unembrittled Steel," U.S. Army Materials Research Agency, WAL 801/1–10, 29 Jan. 1952; also *Transactions*, American Society for Metals, Vol. 45, 1953, pp. 732–736.

[*16*] Capus, J. M., "Austenite Grain Size and Temper Brittleleness," *Journal of the Iron and Steel Institute*, Vol. 200, Nov. 1962, pp. 922–927.

[*17*] Warke, W. R. and Elsea, A. R., "Electron Microscopic Fractrography," Battelle Memorial Institute, DMIC Memorandum No. 161, 21 Dec. 1962.

[*18*] Zapffe, C. A. and Worden, C. O., "Fractography as a Technique in Crystal Chemistry," *Acta Crystallographica*, Vol. 2, 1949, pp. 377–382.

[*19*] Jaffe, L. D., Carr, F. L., and Buffum, D. C., "Effect of Grain Size Upon Temper Brittleness," U.S. Army Materials Research Agency, WAL 801/1–3, 19 March 1952; also *Transactions*, American Institute Mining, Metallurgical, and Petroleum Engineers, *Journal of Metals*, Sept. 1953, pp. 1147–1148.

[*20*] Steven, W. and Balajiva, K., "The Influence of Minor Elements on the Isothermal Embrittlement of Steels," *Journal of the Iron and Steel Institute*, Vol. 193, Oct. 1959, pp. 141–147.

[*21*] Capus, J. M., "L'Influence D'Oligo-Elements sur la Resilience des Aciers Faiblement Allies, Trempes et Revenus," *Revue de Metallurgie*, Vol. 56, Aug.–Sept. 1959, pp. 181–189.

[*22*] Capus, J. M. and Mayer, G., "The Influence of Trace Elements on Embrittlement Phenomena in Low-Alloy Steels," *Metallurgia*, Vol. 61, Oct. 1960, pp. 133–318.

F. P. Byrne,[1] *R. J. Nadalin,*[1] *J. Penkrot,*[1]
J. S. Rudolph,[1] *and C. R. Wolfe*[1]

Analysis of Rotor Steels for Residual Elements

REFERENCE: Byrne, F. P., Nadalin, R. J., Penkrot, J., Rudolph, J. S., and Wolfe, C. R., "**Analysis of Rotor Steels for Residual Elements,**" *Temper Embrittlement in Steel, ASTM STP 407,* American Society for Testing and Materials, 1968, pp. 237–250.

ABSTRACT: The general approaches to the analysis of rotor steels for antimony, arsenic, tin, lead, bismuth, selenium, tellurium, aluminum, and copper at the 15 ppm level are evaluated. Chemical methods are in existence but are slow. Polarography, with some further development, would also provide usable techniques which would be slow. The instrumental methods optical emission, X-ray fluorescence and atomic absorption do not yield adequate results upon direct application to the specimen. However, with suitable concentration techniques, these methods show considerable promise for rapid analysis of rotor steels. A number of concentration techniques are discussed. Of these, acid precipitation of the sulfides appears to be the best approach. Spark source mass spectrometry, while quite sensitive, is not yet developed to the point of supplying rapid, precise, and accurate quantitative analyses.

KEY WORDS: analysis, rotating generators, steel constituents, residual, chemical analysis, polarography, optical emission, spectrochemical, X-ray fluorescence, atomic absorption, flame, mass spectrometry, spark source, concentration, ion-exchange, extraction

In approaching this problem of the determination of the amounts of residual elements in steel, four factors must be considered. First is the name of those elements that are considered residual, second is the concentration levels around which the various analytical methods will be built, third is the desired precision, and fourth is minimized time per analysis for a complete analysis. Once the first three factors are defined, it is possible to proceed to a consideration of the fourth and to the various analytical techniques that may be applied to minimize time.

The elements considered to be residual by the Task Force on Residual Elements are hydrogen, oxygen, nitrogen, phosphorus, sulfur, antimony,

---

[1] Manager, senior chemist, supervisor, and senior chemists, respectively, Analytical Chemistry Dept., Research and Development Center, Westinghouse Electric Corp., Pittsburgh, Pa. Dr. Byrne is a personal member ASTM.

arsenic, tin, lead, bismuth, selenium, tellurium, aluminum, and copper. Since methods for hydrogen, oxygen, nitrogen, phosphorus, and sulfur are well established, this discussion will be confined to the remaining elements. For these elements a concentration level of 15 ppm is arbitrarily selected as the point around which the final analytical method will be constructed. This does not mean that 15 ppm is to be the specification level, rather it is to be considered a kind of midpoint for the various calibration curves. For the third point it is hoped that a standard deviation near 5 to 10 per cent of the amount present can be achieved for a single determination. The fourth item—minimization of time per analysis—considering the equipment available is, it might be said, the underlying theme of the discussion which follows.

The techniques which can be applied are chemical, polarographic, spectrographic, or spectrochemical and spark source mass spectrometry. In chemical techniques the element is usually but not always separated and its amount measured by weighing, titrating with a standardized reagent or by measurement of a color intensity (absorbance or transmittancy) derived by reaction with a color-forming reagent.

Polarographic analysis involves a measurement of the potential and current generated when a drop of mercury is slowly formed at the end of a capillary immersed in a solution of the element of interest. A detailed discussion of the theory involved is given by Kolthoff and Lingane [*1*].[2]

Spectrographic analysis is considered here in a broad sense and involves the emission or absorption of electromagnetic energy. The wave length of the emitted energy is characteristic of the element, and its intensity is a measure of the amount of the element and is generally related to the amount by means of a previously prepared calibration curve. X-ray fluorescence analysis, flame photometry, and the classical optical spectroscopy are the emission techniques of interest for this discussion.

Another technique, which we classify under spectroscopy, is atomic absorption, a technique in which the neutral atoms of the element of interest absorb electromagnetic energy. In this case the quantity of energy absorbed is a measure of the amount of the element. Detailed discussions of the fundamentals of these techniques are discussed by Liebhafsky et al [*2*], Herrman et al [*3*], Harrison et al [*4*], and Robinson [*5*], respectively.

In spark source mass spectrometry the solid specimen is subjected to a high frequency, high voltage spark. A portion of the specimen is vaporized and the individual elements converted to ions. These are sorted according to the mass/charge ratio by a high resolution mass spectrometer and the individual ions collected on a photographic plate.

---

[2] The italic numbers in brackets refer to the list of references appended to this paper.

TABLE 1—*Summary of chemical methods.*

Element	Reference	Reagent	Applicable Range, ppm[a]	Coefficient Variation[b]	Comments
Al........	[6] p. 228	aluminon	0.1 to 25	2	separate by Hg cathode and cupferron
Al........	[7]	8-hydroxyquinoline	0.1 to 300	2	separation by Hg cathode or NaOH
Al........	[6] p. 154 [8]	eriochrome[d] cyanine-R	0.1 to 40	2	chelate the interferences
As........	[6] p. 289 [9]	molybdoarsenate[d]	0.1 to 20	2	distil from bromine-hydrazine solution
Sb........	[10]	crystal violet	0.1 to 25	2	toluene extraction
Sb........	[6] p. 258 [11,12]	rhodamine B	0.1 to 400	5	preliminary di-isopropyl ether extraction
Sb........	[6] p. 269 [13,14]	brilliant green	0.1 to 2.5	2	benzene extraction
Bi........	[6] p. 332	dithizone[d]	0.1 to 75	5	co-ppt[c] with hydrous manganous dioxide sulfide
Bi........	[6] p. 332 [15]	iodide	0.1 to 125	3	amyl acetate extraction
Bi........	[16]	molybdobismuthophosphate	0.005 to 0.01	1	bismuth enhances blue color of reduced molybdate
Cu........	[17]	neocuproine[d]	0.1 to 300	3	chloroform extraction
Cu........	[18]	*n*-acetylanabasine thiocyanate	0.1 to 1000	5	none
Cu........	[6] p. 443	Na diethyl dithiocarbamate	0.1 to 500	5	butyl acetate extraction
Pb........	[6] p. 560 [19,20]	dithiozone[d]	0.1 to 25	5	preliminary chloroform–dithiozone or chloroform–carbamate extract or sulfide ppt
Pb........	[21]	4-(2-pyridylazo) resorcinol	0.1 to 200	5	none
Se........	[22,23]	3,3′-diaminobenzidine[d]	0.1 to 20	5	toluene extract or ppt with arsenic collector
Te........	[23]	butylrhodamine B		3	preliminary separation as ppt with As and Se collector
Sn........	[24]	quercetin[d]	0.1 to 65	2	separate by distillation as $SnBr_4$
Sn........	[25,26]	pyrocatechol violet	0.1 to 40	3	extract as iodide
Sn........	[27]	8-quinolinol	0.1 to 20	4	none
Sn........	[27]	phenylfluorone	0.1 to 20	4	none
Sn........	[6] p. 854	dithiol	0.1 to 1250	5	sensitivity very low

[a] Applicable range based on a 1-g specimen.

[b] Coefficient variation = (standard deviation/ppm found) 100.

[c] ppt—precipitate.

[d] These methods or a modification thereof are in use regularly in our Westinghouse Research and Development Laboratories.

TABLE 2—*Application of polarography.*

Element	Reference	Applicable Range, ppm	Procedural Details	Comments
Al.....	[*28*]	8 to 10 000	differential cathode-ray polarograph	...
Sb.....	[*29*]	0.02 to 10 000	anodic stripping voltammetry	in high purity tin
As....	[*30*]	1 to 1 000	evolution as arsine followed by polarographic analysis	in biological material
Bi.....	[*31*]	1 to 10 000	oscillopolarographically in EDTA (pH 4.6)	preceded by extraction
	[*28*]	0.5 to 10 000	differential cathode-ray polarograph	...
Cu....	[*31*]	1 to 10 000	polarographically in NH_4Cl supporting electrolyte	preceded by extraction
	[*32*]	0.2 to 10 000	1 *M* ammonium acetate–1 *M* acetic acid–0.002 *M* EDTA supporting electrolyte	...
Pb....	[*33*]	0.1 to 1 000	cyclic stationary electrode polarography; formate buffer plus pyrogallol as supporting electrolyte	...
	[*31*]	1 to 10 000	oscillopolarographically in EDTA (pH 4.6)	preceded by extraction
Pb....	[*28*]	5 to 10 000	differential cathode-ray polarography	in stainless steel
	[*32*]	0.02 to 10 000	polarographically in 1 *M* ammonium acetate–1 *M* acetic acid–0.002 *M* EDTA supporting electrolyte	in selenium
	[*34*]	1 to 10 000	polarography in neutral fluoride solution	effect of 34 other elements discussed
Se.....	[*35*]	5 to 100	polarographed in HBr with tungsten-saturated calomel electrode system	can increase sensitivity by using 2 *N* HCl as supporting electrolyte
Te.....	[*32*]	0.0015 to 100	polarographically in 1 *M* ammonium acetate–1 *M* acetic acid–0.002 *M* EDTA	in selenium
	[*36*]	0.05 to 5	oscillopolarographically	separation by precipitation
Sn.....	[*33*]	0.1 to 1 000	cyclic stationary electrode polarography	
	[*28*]	1 to 10 000	differential cathode-ray polarography	in stainless steel

These are rather loose descriptions and purposely so. The basic purpose of this presentation is to emphasize what can be accomplished with the various analytical techniques, rather than the various procedural and precautionary details necessary for best results. Attention to these is the duty of the practicing analyst.

Chemical Methods

It was stated above that final measurement of the elements of interest after separation from its matrix is made by weighing, titrating, or by measurement of a color. At a level of 15 ppm the first two of these are insufficiently sensitive for a precise and accurate determination. Thus, all elements must be measured colorimetrically if a chemical procedure is to be used. In addition, each element will require a method for separation and a particular colorimetric reagent. The procedures are, in general, complicated, tedious, and time consuming. The most important methods for each of the residual elements are summarized, with their applicability ranges in Table 1. It is evident from Table 1 that any one of the methods tabulated is adequate for the problem we have defined. It will be noted that some methods are marked with the superscript *d*. These methods or a modification thereof are in regular use in our Laboratories and yield the coefficient of variation indicated in Table 1. The important point to be made here is that these methods require, in many cases, a high degree of skill to achieve proper results. However, such methods are essential to establish standard or reference specimens to be used in checking or standardizing spectrographic methods.

Polarography

In the application of polarography to actual specimens, an intrinsic part of the technique involves a separation. For example, in the version of polarography called stripping voltammetry, a very thin layer of mercury is placed on an electrode which is first operated as a cathode. In this mode of operation, it behaves as a mercury cathode—to be discussed in more detail—and the element of interest is plated into the mercury if present as a cation. If the element is present as an anion then the electrode is made the anode. Upon reversal of the "mercury" electrode polarity so that the system operates polarographically, a much higher signal is obtained by virtue of the concentration of the element in the mercury electrode.

Results that can be obtained are summarized in Table 2. Under procedural details the terms differential cathode-ray polarography, oscillopolarographically, and cyclic stationary electrode polarography are used in addition to anodic stripping voltammetry. These are modifications of the basic techniques and are explained in the references cited.

As is clearly evident in examining the various applicable ranges, polarography can be used. The difficulty in using polarographic techniques for all of the residual elements is the same as in colorimetry. An individual procedure must be established for each element; thus, an individual analysis must be made for each element. Thus, spectrographic methods appear to be more attractive because a number of elements may be determined on the same sample.

TABLE 3—*Direct application of X-ray fluorescence* [37].

Element	Applicable Range, ppm	Coefficient Variation
Cu	50 to 4700	2
Cu [*38*]	100 to 7000	5
Sb[a]	40 to 300	6
As	7 to 1400	...
Sn	40 to 660	...
Pb	40 to 200	...
Se	60 to 2000	...

[a] Based on results by R. Hullings, Westinghouse Electric Corp., Phila., Pa.

TABLE 4—*Direct application of optical emission* [38].

Element	Applicable Range, ppm	Coefficient Variation	Procedure
Al, soluble	100 to 20 000	5	spark analysis of solutions E-2 SM 9-27
Al, insoluble	20 to 200	8	
Al, total	50 to 15 000	8	direct spark analysis of solid specimens E-2 SM 9-13
As	100 to 2 000	10	
Cu	100 to 7 500	10	
Sn	50 to 1 000	10	
Al, total	10 to 500	3	spark analysis of pelletized chips or drillings E-2 SM 9-18
Cu	50 to 15 000	1.3	
Pb	10 to 4 000	8	
Se	...	...	
Sn	10 to 7 000	4.5	
Te	...	...	

Spectrographic Methods

X-ray fluorescence, flame photometry, and optical emission are well-known techniques and have a considerable literature. From this literature and from our own experience we have obtained data which are descriptive of what can be accomplished.

When X-ray fluorescence is applied directly, only copper, antimony, arsenic, tin, and lead are observable at relatively low levels as seen in Table 3. Of these only arsenic has a useable range around the 15 ppm level we have set as the swing point of our calibration range. The lower boundary for the applicable ranges of the other elements is above that of arsenic.

For the direct application of flame photometry, we are assuming that a 1-g specimen is dissolved in 25 ml of solution and aspirated into the flame. Such a technique lacks sufficient sensitivity for the analysis of rotor steels. For example, even with extraction, the range reported by Eshelman et al [*42*] for aluminum was 0.04 to 1.1 per cent, a range too high for this application. On the other hand, classical optical emission has long been known for its sensitivity. Results obtained by direct application of this technique are in Table 4. Here it is seen that only with aluminum, lead, and tin is there an applicable range that includes 15 ppm. Even the use of carrier distillation techniques, as described by Ellenburg et al [*41*], offers no improvement in detectability.

Atomic absorption is a relatively new technique first described by Walsh in 1955 [*40*]. In this process, as it is now practiced, the element of interest in solution is aspirated into a flame or heated zone where it reacts to yield neutral atoms in the ground state. In this state these neutral atoms will absorb the energy of their resonance spectral lines. This resonance energy is obtained from a hollow cathode lamp containing in the cathode in a substantial amount the element of interest. The cathode is energized to emit the desired resonance lines. The amount of energy absorbed by the atoms in the flame is a measure of their number and by suitable control of conditions a measure of the number of such atoms in the specimen.

TABLE 5—*Direct application of atomic absorption* [49].

Element	Detectability[a] or Range	Coefficient Variation
Al, total	40 to 2500	...
Sb	40 to 1250	...
As	500	...
Bi	1.7 to 1250	...
Cu	2.5 to 400	1
Pb	1.5 to 750	10
Se	1000	...
Sn	50 to 5000	...
Te	1000	...

[a] Detectability is defined as the lowest concentration that will yield a useable atomic absorption signal. It is designated by a single number. The range is designated by two numbers.

For direct application of this technique, we are assuming as in flame photometry that 1 g of specimen is dissolved in 25 ml of solution and aspirated into the flame. The response obtained with such solutions is taken as an evaluation of the direct application of the technique. Such an evaluation is presented in Table 5. Examination of the detectability column in Table 5 shows that for only bismuth, copper, and lead can a direct analysis be made at the 15 ppm level. Thus, for spectrographic analysis it can be said that direct application of any of these techniques will not provide a useable analysis for residual elements in rotor steels. Consequently, if these techniques are to be used—and their use can save time—then means must be established to concentrate the residual elements to such an extent that the amount isolated falls within the sensitivity of the instrument. Such a concentration is carried out by chemical methods, and we proceed now to a discussion of such methods and their usefulness for this problem.

Chemical Concentration

The objective of such techniques is to remove the residuals from the matrix materials so that the measuring technique will be used to measure a higher concentration of material than would be found if it were dispersed in the original matrix. In general there are two basic approaches to accomplishing this separation and concentration of the desired elements. The first is removal of the matrix elements, in this case iron, chromium, molybdenum, nickel, and manganese. The second is removal of the minor constituents from the matrix. The second sounds redundant, actually it is not, as will be apparent from the ensuing discussion.

General methods for the removal of the matrix components are precipitation, mercury cathode electrolysis, ion exchange, and selective extraction. For this problem removal of only the iron would permit sufficient concentration.

Precipitation for the removal of matrix elements is generally undesirable because of adsorption and coprecipitation of the impurity elements with the matrix and thus loss of accuracy.

Mercury cathode electrolysis is a frequently used separation technique, and for this problem a sulfuric acid solution of the specimen would be electrolyzed. According to Lundell and Hoffman [*43*], not only would the desired removal of the matrix elements be accomplished, the residual elements would for the most part be wholly or partially removed. In fact, only aluminum would not be removed. Thus, mercury cathode electrolysis would not accomplish our purpose.

There are two general types of ion exchangers, cation and anion. When rotor steel alloys are dissolved in dilute perchloric acid the pertinent elements are in solutions as follows:

Matrix Elements

Cations	Anions
Fe III	Cr VI
Ni II	Mo VII
Mn II	V VI

Residual Elements

Cation	Anion
Sn IV	Sb V
Pb II	As V
Cu II	Te VI
Bi III	Se VI
Al III	

Use of a cation exchanger would yield an iron-free solution containing antimony, arsenic, tellurium, and selenium with tin, lead, copper, bismuth, and aluminum left on the column with the iron, nickel, and manganese.

TABLE 6—*Absorptivity of selected ions in 12 N hydrochloric acid* [44].

Ion	D_v[a]	
Sb V	5.5	decreasing absorption ↓
Fe III	4.5	
Sn IV	3.5	
V V	3.0	
Mo VI	2.0	
Bi III	1.5	
Cr VI	1.0	
Mn II, Cu II, As V	0.5	
Al III, Ni II, Pb II	not absorbed	

NOTE—No datum is given for Te VI

[a] D_v = estimated log of distribution coefficient. Underlined elements are the residual elements of interest.

By using a strong hydrochloric acid solution and a strong anion exchange resin many of the elements will be absorbed as their anionic chloride complexes. Kraus and Nelson [*44*] present data, Table 6, to show the relative absorptivity of the elements of interest from 12 N hydrochloric acid on Dowex 1X10, a strong anion exchange resin.

By suitable control of the acidity of the solvent solution and the eluting solution, the less strongly absorbed elements of interest from bismuth III down could be eluted while the strongly absorbed elements tin IV, iron III, and antimony V would be retained. This would allow the determination of all of the trace elements except tin and .antimony.

These ion exchange techniques are not attractive for isolation of the residual elements as a group because only about half of the residuals are separated and two of these, bismuth III and chromium VI, would probably not be completely eluted from Dowex 1X10 ([*44*], Note to Table I, p. 41).

However, if the various elements could be individually resolved by proper selection of eluant and ion exchange resin, then monitoring of the effluent by a technique, such as square wave polarography as carried out by Buchanan and Baker [*45*], would provide a useable analysis. Such a system for the residual elements would require somewhat more investigation.

The last method for removal of the bulk of the matrix elements is selective extraction of the metal compounds into an immiscible solvent. Since iron is present in the largest amounts consideration was limited to the application of methods known to remove iron III as compiled by Freiser and Morrison [*46*].

There are two methods which show promise. The first, extraction of iron III from a 70 per cent hydrochloric acid solution by isopropyl ether, results in the simultaneous removal of only vanadium, molybdenum, arsenic, and antimony. This well-known method is attractive since large quantities of iron III are removed in a few extractions.

The use of 2-thenoyl trifluoracetone (TTA) in xylene as a selective extractant for iron III from strong nitric acid solutions is the second. Although it does not extract the elements of interest, we have found that an inconveniently large number of extractions are necessary to remove the iron III from 1 g of alloy. More work is needed to perfect the use of this reagent for this purpose.

General methods to be considered for the removal of the trace constituents from the matrix elements in rotor steel include: (1) selective extraction and (2) group precipitants.

Selective extraction methods that were considered [*46*] all failed to remove more than a few of the desired elements. Consecutive extractions to extract a group of the desired elements using several reagents is not considered feasible.

Lundell and Hoffman [*43*] list group reagents to precipitate selectively the desired trace elements. Of the 15 reagents considered, most precipitated iron III or did not precipitate the desired elements. Hydrogen sulfide in acid solution, however, was shown to precipitate all of the desired trace elements except aluminum. In addition, the molybdenum present in the specimen acts as a carrier to help to precipitate and to gather the precipitated sulfides. This technique was used by Balfour et al [*47*] for the analysis of mild steels. In this method at a pH of about 1 the insoluble sulfides precipitate with hydrogen sulfide. The filtered precipitate is ignited to give a mixture of oxides for emission spectroscopy or redissolved in nitric acid to give a solution suitable for atomic absorption. A small amount of iron is also found in the sulfide precipitate due to adsorption, but its concentration is sufficiently low so as not to interfere in subsequent operations. With an optical emission finish the results of Table 7 were obtained by Balfour et al. With the exception of arsenic, reasonable results were obtained for the elements determined. The use of atomic absorption or X-ray fluorescence instead of emission on the precipitate may be equally precise and accurate.

An interesting concentration technique for tellurium only is reported by Burke [7], who precipitate metallic tellurium with tin II, collect the precipitate on millipore filter paper, and measure its amount directly on the paper by X-ray fluorescence. A range of 1 to 200 ppm is covered with a coefficient of variation of 5.

Thus, it can be seen that it is possible to analyze rotor steels for residuals at the 15 ppm level by chemical and polarographic methods. Optical emission, X-ray fluorescence, and atomic absorption can also be applied to this analysis after a concentration step.

TABLE 7—*Optical emission concentration of elements* [47].

Element	Applicable Range, ppm	Coefficient Variation	Procedure
Sb	5 to 500	5 to 10	all elements coprecipitated with copper as sulfides and excited by d-c arc
As	50 to 1000	5 to 10	
Bi	1 to 250	5 to 10	
Pb	1 to 50	5 to 10	
Sn	1 to 50	5 to 10	

Spark Source Mass Spectrometry

This is a relatively new technique for the analysis of solids. It is not our purpose to discuss the procedural details for using this instrument. Rather we wish to assess its value today in providing accurate reproducible values for our analysis problem.

Certainly the technique provides adequate sensitivity. It will detect "nearly all elements under favorable conditions" according to Ahearn [48] at the parts per billion (ppb) level. This is accomplished on a very small specimen. This fact, paradoxically, while a strength is also a weakness because it is primarily a specimen taken from the surface and, unless special measures are taken, does not penetrate to the bulk of the specimen. Thus, it is an excellent tool for mapping the inhomogeneity of a specimen. According to this same author it is becoming clear that if accurate, precise, quantitative analyses are to be obtained by mass spectrometry then highly homogeneous analyzed standards are essential. In addition to this need, Ahearn discusses a number of other shortcomings and needs. He states "the accuracy and precision of the spark source technique at present is not adequate to characterize the role of trace impurities in the physics and chemistry of solids."

This was the position of optical emission spectroscopy some 30 years ago. It is expected that in the not too distant future with the development of adequate standards and with instrumental improvements spark source mass spectroscopy will provide at least adequate analyses for this and for other problems.

Using Analytical Values

One of the burdens the analytical chemist often bears is the misuse of the composition values he reports. This comes about in various ways, but perhaps the most common is the desire of the customer, in your case metallurgists—physicists, chemists, and analytical chemists are also guilty—to prove an hypothesis with the analytical results and to impute to these results a precision that is simply not there. To avoid this trap the customer should know or obtain the standard deviation of the method used, and with this very important parameter of the analytical method it is possible to decide if the analytical results obtained on two different specimens are significantly different. A convenient formula to use to evaluate this significance is

$$X_1 - X_2 \overline{>} k\,1.41\sigma$$

where X_1 and X_2 are the two analytical values in question, σ is the standard deviation or its estimate, and k is a factor to which various values may be assigned depending on the degree of confidence desired in the significance of the difference. For example, for 95 per cent confidence k would have the value of 2, for 99 per cent confidence the value of 3, etc.

Conclusions

1. Adequate chemical methods are available for each of the residual elements. However they are tedious and slow.
2. Polarographic techniques, with perhaps some development, would provide adequate methods.
3. Spectroscopic methods do not yield adequate results upon direct application; however, if preceded by a concentration step, then suitable, rapid methods are feasible.
4. It appears that precipitation of the residual elements as sulfides is the concentration method of choice.
5. Spark source mass spectrometry while providing sufficient sensitivity will require more development and adequate standards before it can be used for accurate precise quantitative analysis.

References

[1] Kolthoff, I. M. and Lingane, J. J. *Polarography*, Vol. 1, Interscience, New York, 1952.

[2] Liebhafsky, H. A. et al, *X-Ray Absorption and Emission in Analytical Chemistry*, Wiley, New York, 1960.

[3] Herrman, R. et al, *Flame Photometry*, Interscience, New York, 1963.

[4] Harrison, G. R. et al, *Practical Spectroscopy*, Prentice-Hall, New York, 1948.

[5] Robinson, J. W., *Atomic Absorption Spectroscopy*, Marcel Dekker, New York, 1966.

[6] Sandel, E. B., *Colorimetric Determination of Traces of Metals*, 3rd ed., Interscience, New York, 1959.

[7] Burke, K. E., "Spectrophotometric Determination of Aluminum in Nickel-, Iron-, and Copper-Base Alloys," *Analytical Chemistry*, Vol. 38, 1966, pp. 1608–1611.

[8] Hill, U. T., "New Direct Spectrophotometric Determination of Aluminum in Steel, Spelter, and Iron Ore," *Analytical Chemistry*, Vol. 38, 1966, pp. 654–656.

[9] Kovacs, E. and Guyer, H., "Determination of Arsenic in Cast Iron and Plain Steel," *Zeitschrift fuer Analytische Chemie*, Vol. 208, 1965, pp. 321–328.

[10] Penkrot, J., "The Photometric Determination of Antimony in Steels," paper presented at the 1962 Pittsburgh Conference on Analytical Chemistry and Applied Spectroscopy.

[11] Kedman, L. and Waite, C. B., "Determination of Antimony with Rhodamine-B," *Metallurgia*, Vol. 66, 1962, p. 143.

[12] Jeffrey, W. C., "Determination of Antimony in Steels," *Modern Castings*, Vol. 49, 1966, p. 85.

[13] Burke, R. W. and Menis, O., "Extraction-Spectrophotometric Determination of Antimony as a Ternary Complex," *Analytical Chemistry*, Vol. 38, 1966, pp. 1719–1722.

[14] Muller, J. C., "Determination of Antimony Using Brilliant Green," *Bulletin de la Societe Chimique de France*, Vol. 86, 1964, p. 293.

[15] Lazareva, V. I. and Lazarev, A. I., "Extraction-Photometric Determination of Bismuth in Cast Iron," *Zavodskaya Laboratoriya 31*, 1965, p. 1437.

[16] Guyou, J. C. and Cline, L. J., "Spectrophotometric Determination of Bismuth," *Analytical Chemistry*, Vol. 37, 1965, pp. 1778–1779.

[17] Luke, C. L., "Neocuproine-Carbamate Spectrophotometric Determination of Copper," *Analytica Chimica Acta*, Vol. 32, 1965, p. 286.

[18] Tolipov, Sh. et al, "Extractive Photometric Determination of Copper in Alloys as an N-Acetylanabasine Thiocyanate Complex," *Zavodskoya Laboratoriya*, Vol. 29, 1963, p. 804.

[19] Stobart, J. A., "The Colorimetric Determination of Traces in Heat-Resistant Nickel-Chromium Alloy Steel," *Analyst*, Vol. 90, 1965, pp. 278–282.

[20] Filipov, D. et al, "The Colorimetric Determination of Lead in Steels and Cast Irons," *Comptes Rendus de l'Academie Bulgare de Sciences*, Vol. 18, 1965, p. 813.

[21] Dagnall, R. M. et al, "Determination of Lead with 4-(2-Pyridylazo)-Resorcinol, *Talanta*, Vol. 12, 1965, pp. 583–558.

[22] Cheng, K. L., "Determination of Traces of Selenium," *Analytical Chemistry*, Vol. 28, 1956, pp. 1738–1742.

[23] Invanova, A. I. and Blyurn, I. A., "Separation and Determination of Small Amounts of Selenium and Tellurium," *Zavodkoya Laboratoriya*, Vol. 27, 1961, pp. 371–376.

[24] Penkrot, J., "Photometric Determination of Tin in Steels and High Temperature Alloys," paper presented at the 1960 Pittsburgh Conference on Analytical Chemistry and Applied Spectroscopy.

[25] Ross, W. J. and White, J. C., "Application of Pyrocatechol Violet as a Colorimetric Reagent for Tin," *Analytical Chemistry*, Vol. 33, 1961, pp. 421–424.

[26] Newman, E. S. and Jones, P. D., "Separation and Determination of Small Amounts of Tin," *Analyst*, Vol. 91, 1966, pp. 406–410.

[27] Pollock, E. N., and Zopotte, L. P., "Spectrophotometric Procedure for the Determination of Tin in Complex Materials Using γ-Quindinal and Phenylfluorone," *Analytical Chemistry*, Vol. 37, 1965, pp. 290–291.

[28] Rawlings, J. N. and Priest, D. A., "Polarographic Analysis for Trace Ele-

ments in Stainless Steels," *Iron and Steel*, London, Vol. 38, no. 12, 1965, pp. 554–556.

[*29*] Zaichko, L. F., Yankauskao, V. F., and Zakharov, M. S., "Rapid Determination of Antimony in High Purity Tin by Anodic-Stripping Voltammetry," *Fav. Lab.*, Vol. 31, no. 3, 1965, pp. 265–267.

[*30*] Bambach, K., "Polarographic Determination of Arsenic in Biological Material," *Industrial and Engineering Chemistry*, Analytical Edition, Vol. 14, 1942, pp. 265–267.

[*31*] Mukhina, Z. S., Kotova, G. S., and Kuz'micheva, R. A., "Determination of Lead, Copper, Bismuth and Cadmium in Refractory Alloys," *Zhurnal Analitcheskoi Khimii*, Vol. 20, no. 7, 1965, pp. 785–788.

[*32*] Bush, E. L., "The Polarographic Determination of Copper, Cadmium, Thallium, Lead, Tellurium and Iron in Selenium," *Analyst*, Vol. 88, 1963, pp. 614–617.

[*33*] Phillips, S. T., "Simultaneous Determination of Tin and Lead, Using Cyclic Stationary Electrode Polarography," *Analytical Chemistry*, Vol. 39, No. 4, 1967, pp. 536–537.

[*34*] Hamza, A. G. and Headridge, J. B., "Polarography in Neutrol Flouride Solution with Particular Reference to Lead," *Talanta*, Vol. 12, no. 11, 1965, pp. 1043–1046.

[*35*] Cervenka, R. and Korbova, M., "Determination of Se in Water," *Chemische Listy*, Vol. 49, 1955, p. 1158, through *Chemical Abstracts*, Vol. 49, 1955, p. 14566 b.

[*36*] Maienthal, E. J. and Taylor, J. K., "Determination of Te by Cathode-Ray Polarography," *Analytical Chemistry*, Vol. 37, No. 12, 1965, pp. 1516–1519.

[*37*] Michaelis, R. E. et al, "Determination of Minor Constituents in Low Alloy Steels by X-ray Spectroscopy," *Journal of Research*, Vol. 65C, No. 1, National Bureau of Standards, 1961, pp. 71–76.

[*38*] "Methods for Emission Spectrochemical Analysis," 4th ed., American Society for Testing and Materials, 1964.

[*39*] "Determination of Lead in Steels by Atomic Absorption Spectroscopy," Research Report B25, Hilger & Watts, London, 1966.

[*40*] Walsh, A., "The Application of Atomic Absorption Spectra to Chemical Analysis," *Spectrochemica Acta*, Vol. 7, 1955, pp. 108–117.

[*41*] Ellenburg, J., "Application of Carrier Distillation to the Spectrographic Determination of Tramp Elements in Cast Irons and Low Alloy Steels," *Analytical Chemistry*, Vol. 34, 1962, pp. 230–233.

[*42*] Eshelman, H. C. et al, "Extraction and Flame Spectrophotometric Determination of Aluminum," *Analytical Chemistry*, Vol. 31, 1959, pp. 183–187.

[*43*] Lundell, G. and Hoffman, J., *Outlines of Methods of Chemical Analysis*, Wiley, New York, 1938, p. 94.

[*44*] Kraus, K. and Nelson, F., *Ion Exchange and Chromatography in Analytical Chemistry, ASTM STP 195*, American Society for Testing and Materials, 195[illegible], p. 36.

[*45*] Buchanan, E. B., Jr., and Bacon, J. R., "Continuous Monitoring of Ion-Exchange Column Effluents with Square Wave Polarography," *Analytical Chemistry*, Vol. 39, 1967, pp. 615–620.

[*46*] Freiser, H. and Morrison, G., *Solvent Extraction in Analytical Chemistry*, Wiley, New York, 1957, pp. 212–214.

[*47*] Balfour, B. et al, "A Spectrochemical Method for the Determination of Trace Impurities in Metallurgical Materials," *Applied Spectroscopy*, Vol. 20, 1966, pp. 168–671.

[*48*] Ahearn, A. J., "Spark Source Mass Spectrometric Analysis of Solids," *Trace Characterization, Chemical and Physical*, U.S. Department of Commerce, National Bureau of Standards, Monograph 100, 1967, pp. 347–375.

[*49*] Beyer, M., "The Determination of Manganese, Copper, Chromium, Nickel, and Magnesium in Cast Iron and Steel," *Atomic Absorption Newsletter*, Vol. 4, 1965, pp. 212–223.

Foreword

The Symposium on Temper Embrittlement in Steel was held at ASTM Headquarters in Philadelphia, Pa., 3–4 Oct. 1967. The sponsor of this symposium was ASTM Special Task Force on Large Turbine and Generator Rotors, Subcommittee VI of Committee A-1 on Steel. D. L. Newhouse, General Electric Co., presided as symposium chairman.